Characteristics of Fixation in Infantile Nystagmus

A thesis submitted in fulfilment of the requirement for the degree of
Doctor of Philosophy (Vision Sciences)

Onyekachukwu Mary-Anne Amiebenomo

Research Unit for Nystagmus,
School of Optometry and Vision Sciences
Cardiff University

May 2023

Supervisors
Dr J Margaret Woodhouse, OBE
Professor Jonathan T Erichsen
Dr Lee McIlreavy

Advisor
Professor Jeremy Guggenheim

DECLARATION

STATEMENT 1
This thesis is being submitted in partial fulfilment of the requirements for the degree of PhD.

Signed _____
Date _____

STATEMENT 2
This work has not been submitted in substance for any other degree or award at this or any other university or place of learning, nor is it being submitted concurrently for any other degree or award (outside of any formal collaboration agreement between the University and a partner organisation).

Signed _____
Date _____

STATEMENT 3
I hereby give consent for my thesis, if accepted, to be available in the University's Open Access repository (or, where approved, to be available in the University's library and for inter-library loan), and for the title and summary to be made available to outside organisations, subject to the expiry of a University-approved bar on access if applicable.

Signed _____
Date _____

DECLARATION
This thesis is the result of my own independent work, except where otherwise stated, and the views expressed are my own. Other sources are acknowledged by explicit references. The thesis has not been edited by a third party beyond what is permitted by Cardiff University's Use of Third Party Editors by Research Degree Students Procedure.

Signed _____
Date _____

WORD COUNT _____
(Excluding summary, acknowledgements, declarations, contents pages, appendices, tables, diagrams and figures, references, bibliography, footnotes and endnotes).

ACKNOWLEDGEMENTS

I am indeed indebted to my supervisors for shaping me into what I am today. This research journey has been a memorable roller coaster ride and I feel very fortunate to have been under your meticulous tutelage. For your guidance and support, even beyond the PhD, I am deeply thankful. To my advisor, all members of the Research Unit for Nystagmus (RUN), Rod Woodhouse, Denley Slade and Stephen Mead, thank you for your input at one time or the other during the PhD research.

Special thanks to the charities and institutions who generously funded the PhD at various times during the studies namely: The British Federation of Women Graduates, Johnson and Johnson, Ameobi funds for international students, the Richard Stapley Educational Trust, Alan and Cyril Body Trust, Professionals Aid Guild, the Sidney Perry Foundation, Cardiff University. Your generous drops made this water flow and sparkle, and I am truly grateful.

To all participants who volunteered for the experiments, especially those with nystagmus some of whom had to travel very long distances, I say a big thank you for your time and effort. Without you this work wouldn't have been possible.

How far my OPTOM people!!! This PhD waka don finally end o... I would always cherish the times spent at the building, especially when I would hail 'how far!' and you'd answer 'I dey!' To Sasha, Sue - my OPTOM mom, the clinic staff, Rob, Gregg, Al, Pauline and other technical staff who helped at one time or the other towards the successful running of the PhD projects, thank you. I am also super grateful to all postgrad students, especially occupants of room 2.10 and 2.11, for their companionship throughout this journey; from tackling MATLAB to enjoying socials. Thank you Bader, Viktor, Kristian, K the Katherine for roughing the participant recruitment and testing times with me, after COVID struck. K the Krishna, how far! Thank you for accepting the challenge of learning my Nigerian lingua franca. I would throw it at you but you never failed to respond efficiently. Our conversations in the office, especially those in pidgin made me feel connected to home. You are my Cardiff-Naija sista, you do well! K the Khawlah, I deeply appreciate you for being a constant true friend especially when I needed a shoulder to rant and cry on, and of course for your unending supply of sweets when satisfying my sugar cravings tended to keep me sane. You never judged, thank you.

To the Orienos and all the parents, too numerous to mention, at St Monica's and at The Table, I am thankful for your frequent words of encouragement.

My heartfelt gratitude goes to my parents (Patricia and late Christopher Onyeogo), siblings (Uncle T, Dee and Coco) and other family members, who patiently coped with my very long disappearances when I needed to get work done. Daddy, to have lost you in the midst of all this is devastating, but the firm foundation you set in many areas of our lives was indeed the driving force to forge ahead.

To my husband and children, Hamzat, Asher, Nene* and Etse, we made it! I couldn't have done this without your constant love and support. This is indeed our victory. We have worked really hard. Now, what is left is to party!!!

For Patricia, Christopher and Hamzat. You nurtured the seed, set the ball rolling, and nourished it along the way. I cannot thank you enough!

kaka

* The Illustrations included on each chapter cover are inspired by Nene and her special gift of interpreting texts through pictures, as well as how she represents spoken words with her unique drawings. Each one has a nystagmus theme embedded in it and largely signifies what the chapter is all about.

ABSTRACT

Infantile nystagmus (IN) oscillations are known to be multiplanar in some cases however, eye movement assessment for treatment strategies are often done in one plane. Common forms of treatment include maximizing the patients preferred gaze and/or convergence null where the IN oscillation is expected to be least. The main purpose of experiments in this thesis was to evaluate, in *two-dimensions,* fixational eye movements during fixation at eccentric gaze and at different viewing distances. A probability density function method was used to analyse high speed eye tracking data wherein, the derived 68% isocontour of eye position samples were further analysed to quantify the accuracy and precision of fixation.

For the first experiment, data from 18 participants with IN, fixating nine horizontal gaze positions up to ±20°, were evaluated. To investigate further any changes in visual performance with eccentric gaze, experiments thereafter progressed to include psychophysical visual acuity testing at seven horizontal gaze positions up to ±45°, in 12 participants with IN and 14 typical participants. For the second aspect, a third experiment was designed using custom made automated occluder system, alongside eye tracking, to investigate fixational eye movement during convergence and when viewing distance was changed up to 25 cm.

Results highlight the idiosyncratic nature of IN between participants and suggests that a difference in waveform at each component of the horizontal plane may not necessarily drive fixation preference at the null. Nonetheless, the amount of IN oscillation, often found to reduce with convergence, was, for the first time, objectively quantified using the fixation precision measure. For typical participants, a preference for an eccentric or convergence position was not objectively found, suggesting that, just like in people with IN, a preference for the null point or primary position of gaze may be attributed to other inherent ocular phenomena.

TABLE OF CONTENTS

DECLARATION ii
ACKNOWLEDGEMENTS iii
ABSTRACT v
TABLE OF CONTENTS vi
LIST OF FIGURES x
LIST OF TABLES xiii
ABBREVIATIONS xiv
CHAPTER ONE 1
1 General introduction 1
1.1 Eye movements and the oculomotor system 2
1.1.1 Saccades 5
1.1.2 Fixation 6
1.1.3 Vergence 8
1.1.4 Focusing an image – the near triad 9
1.1.5 Eye positions and the laws of ocular motility 12
1.2 Infantile nystagmus 14
1.2.1 Fixation in infantile nystagmus 19
1.2.2 Null zones and the many ways they are defined 20
1.3 Summary and research objectives 28
1.4 Thesis structure 29
CHAPTER TWO 31
2 General methods 31
2.1 Materials 32
2.2 Ethics 34
2.3 Participants 34
2.3.1 Pre-examination and exclusion 34
2.4 Laboratory set up 36
2.5 Fixation stimuli 37
2.6 Eye movement recording 38
2.6.1 Calibration 38
2.7 Processing and analysing eye movement data 41

2.7.1 The EyeLink Data Viewer 41
2.7.2 Analysis using MATLAB 41
2.7.3 The bivariate Probability Density Function (bPDF) method for quantifying fixation performance 42
2.7.4 Statistical analysis 56
CHAPTER THREE 57
3 Fixation characteristics at eccentric gaze positions in infantile nystagmus 57
3.1 Introduction 58
3.1.1 The multiplanar nature of the IN waveform and its possible implications for null zone preference 58
3.1.2 Aim and objectives 60
3.1.3 Hypotheses 60
3.2 Methods 60
3.2.1 Participants 61
3.2.2 Laboratory set up 61
3.2.3 Procedure 62
3.3 Results 63
3.3.1 Participant information 63
3.3.2 Fixation performance at gaze positions 64
3.3.3 Horizontal and vertical axis range of data spread 69
3.3.4 Fixation performance and clinical VA 73
3.4 Discussion 74
CHAPTER FOUR 77
4 Fixation characteristics and uncorrected resolution thresholds at eccentric gaze positions in participants with infantile nystagmus and controls 77
4.1 Introduction 78
4.1.1 Visual resolution and fixation performance at eccentric gaze positions 78
4.1.2 Aim and objectives 83
4.1.3 Hypotheses 83
4.2 Methods 84
4.2.1 Participants 84
4.2.2 Laboratory set up 84
4.2.3 Procedure 86
4.2.4 Analysis 88

4.3 Results 90
4.3.1 Participants 90
4.3.2 Visual resolution at gaze positions 90
4.3.3 Fixation performance at gaze positions 96
4.3.4 The relationship between fixation performance and VA in participants with IN 106
4.4 Discussion 110
4.4.1 Visual resolution at gaze positions. 110
4.4.2 Fixation performance at gaze positions 111
CHAPTER FIVE 114
5 Fixation and dynamics of vergence with distance change in participants with infantile nystagmus and controls 114
5.1 Introduction 115
5.1.1 Aim and objectives 117
5.1.2 Hypotheses 117
5.2 Methods 118
5.2.1 Participants 118
5.2.2 Laboratory set up 118
5.2.3 Procedure 119
5.2.4 Validation of convergence accuracy 122
5.2.5 Analysis 123
5.3 Results 126
5.3.1 Participants 126
5.3.2 Quantifying convergence dampening in IN and determining its relationship with ocular deviation 126
5.3.3 The dynamics of achieving and maintaining vergence in IN 140
5.3.4 The effect of viewing distance on fixation performance, in typical observers 142
5.4 Discussion 146
CHAPTER SIX 149
6 General conclusions and future work 149
6.1 Overview 150
6.1.1 Chapter three 151
6.1.2 Chapter four 153

6.1.3 Chapter five 155
6.2 Summary 162
REFERENCES 165
7 165
APPENDICES 179
8 179
8.1 Participant details 180
8.2 Additional results 185
8.3 Research output 188

LIST OF FIGURES

Figure 1-1: Classifying eye movements 3
Figure 1-2: Scanning a visual scene (Source: Rucci and Poletti 2015) 4
Figure 1-3: Sample plot showing fixational eye movements in a typical participant 7
Figure 1-4: 2D sample fixational eye movements (Source: Alexiev and Vakarelski 2023). 8
Figure 1-5: State of the intraocular structures during accommodation and disaccommodation 10
Figure 1-6: Cross coupling model of vergence and accommodation (Source: Bharadwaj 2017). 11
Figure 1-7: Centre and axes of rotation of the eye including the equatorial plane (Source: von Noorden and Campos 2002) 12
Figure 1-8: The extraocular muscles (Source: Krauzlis 2013) 13
Figure 1-9: Classifying IN waveforms 17
Figure 1-10: Eye movements and the IN cycle 18
Figure 1-11: The PAN cycle (Source: Shallo-Hoffmann and Riordan-Eva 2002) 19
Figure 1-12: Eye position values and histogram plot of three consecutive IN cycles 23
Figure 1-13: Illustrating similar horizontal eye position frequencies but different amplitudes 24
Figure 1-14: Velocity samples for participant P031 while viewing at primary position 25
Figure 1-15: Illustrating the accuracy and precision of data points 28
Figure 2-1: EyeLink® 1000 plus desktop mount 32
Figure 2-2: The automated occluder system 33
Figure 2-3: Main instrumentation used for experiments. 36
Figure 2-4: Target size determination 37
Figure 2-5: Validation error increases with distance 39
Figure 2-6: Sample pursuit calibration output 40
Figure 2-7: Illustrating data accuracy and precision as a PDF 43
Figure 2-8: The 68% isoline and BCEA line (Source: Castet and Crossland 2012) 45
Figure 2-9: Output using two different bandwidths (Source: Castet and Crossland 2012) .. 49
Figure 2-10: Schematic 2D representation of the metrics used to quantify fixation 51
Figure 2-11: Illustrating the horizontal and vertical axis range 56

Figure 3-1: Laboratory set up 62
Figure 3-2: Representative eye position data and corresponding bPDF analysis output 65
Figure 3-3: Accuracy, contour area and contour shape at all fixation positions. 68
Figure 3-4: The isocontour area alongside the horizontal and vertical range at each gaze angle..... 71
Figure 3-5: The relationship between horizontal and vertical axis range, as a function of gaze angle 72
Figure 3-6: The relationship between fixation performance and entry VA 74
Figure 4-1: Summary of results obtained from pilot experiments 81
Figure 4-2: Laboratory set up..... 85
Figure 4-3: Schematic showing vanishing and regular Landolt C optotypes 86
Figure 4-4: Psychometric function curve from one typical participant..... 89
Figure 4-5: Visual resolution at gaze angles for participants with IN 91
Figure 4-6: Mean threshold vision for typical participants at gaze angles 93
Figure 4-7: Visual resolution threshold measured in emmetropes 94
Figure 4-8: Comparing clinical and psychometric visual resolution 95
Figure 4-9: Accuracy values at all fixation positions in participants with IN. 97
Figure 4-10: Contour shape values at all fixation positions in participants with IN. 99
Figure 4-11: Contour area, including the horizontal and vertical eye position range for participants with IN. 101
Figure 4-12: The horizontal and vertical axis range, as a function of gaze angle 102
Figure 4-13: Accuracy at eccentric gaze position in typical participants 104
Figure 4-14: Contour shape at eccentric gaze position in typical participants 105
Figure 4-15: Mean isocontour area alongside the horizontal and vertical eye position range 106
Figure 4-16: The relationship between fixation performance and entry VA in participants with IN 107
Figure 4-17: The relationship between psychometric threshold VA and fixation precision 109
Figure 5-1: Instrumentation for automated eye occlusion 119
Figure 5-2: Schematic representation of the occlusion process during experiment. 120
Figure 5-3: Initial results for fixation at different distance in typical participants 120

Figure 5-4: Horizontal and vertical eye position plot from participant IN16 while viewing at 25 cm. 125
Figure 5-5: Accuracy at all viewing distances in participants with IN. 128
Figure 5-6: Contour shape at different distances in participants with IN 130
Figure 5-7: Contour area at different distances in participants with IN 132
Figure 5-8: Horizontal and vertical axis range at different distances in people with IN 134
Figure 5-9: The relationship between ocular deviation and percentage change in fixation precision from 300 to 25 cm 139
Figure 5-10: Sample plots for three participants showing the first two 5 s periods of binocular fixation 142
Figure 5-11: Mean fixation accuracy at four distances. 143
Figure 5-12: Mean contour shape at four distances for typical participants 144
Figure 5-13: Mean contour area at four distances for typical participants 145
Figure 6-1: Device designed to measure head orientation 153
Figure 6-2: Experimental setup for off-gaze refraction measures 159
Figure 6-3: Mean refraction measured at different gaze positions, and with different lens induced. 160
Figure 6-4: Relationship between measured refraction and induced lens power for all gaze positions. 160
Figure 6-5: Simulated IN movement using OKN stimuli 161
Figure 6-6: Measuring accommodation and vergence (Source: Suryakumar et al. 2007) .. 162

LIST OF TABLES

Table 1-1: Forms of saccades 5
Table 2-1: Expected and measured on screen target size.....37
Table 2-2: Grading validation error 38
Table 2-3: A review of previous fixation studies 46
Table 2-4: A summary of the bootstrapping procedure carried on the four eye position distributions.....51
Table 2-5: A summary of the sample distributions for each of the metrics..... 52
Table 3-1: Participant clinical data 64
Table 3-2: Mean and standard deviation of fixation performance across gaze angles 73
Table 4-1: Design of pilot experiment 80
Table 4-2: Confirming the onscreen Landolt C gap size for targets presented..... 88
Table 4-3: Mean and standard deviation of accuracy and precision data for all participants across gaze angles 103
Table 4-4: Mean and standard deviation across all gaze position in typical participants... 104
Table 5-1: Amount of vergence induced at each test distance 122
Table 5-2: Change in accuracy and precision from distance to near in people with IN 136
Table 5-3: Mean ocular deviation objectively measured in participants with IN.....138
Table 8-1: Clinical details from 18 participants with IN..... 180
Table 8-2: Clinical details from 14 typical participants 183

ABBREVIATIONS

ANOVA	Analysis of variance
BES	Both eyes
bPDF	Bivariate probability density function
COVID	Coronavirus disease
CEMAS	Classification of eye movement abnormalities and strabismus
ETDRS	Early treatment diabetic retinopathy study
FMNS	Fusion maldevelopment nystagmus syndrome
IMU	Inertial measurement unit
IN	Infantile nystagmus
IPD	Interpupillary distance
IR	Infrared
LE	Left eye
logMAR	Logarithm of the minimum angle of resolution
min	Minute
OCT	Optical coherence tomography
OKN	Optokinetic nystagmus
PAN	Periodic alternating nystagmus
QTVI	Qualified teacher of the vision impaired
RE	Right eye
RUN	Research unit for nystagmus
SD	Standard deviation
s	Second
VOR	Vestibulo-ocular reflex
VA	Visual acuity
VDU	Visual display unit

CHAPTER ONE

1 General introduction

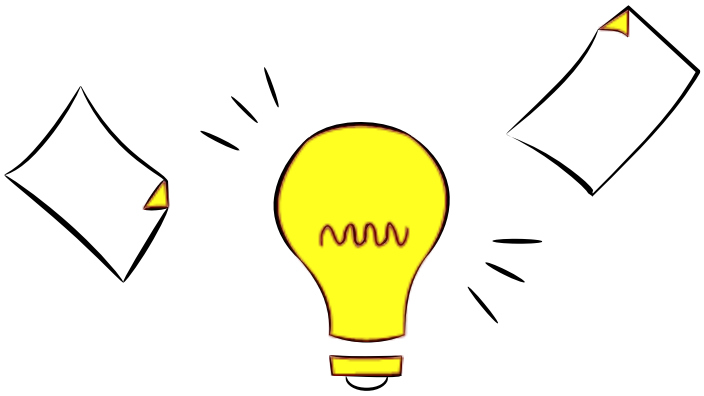

This thesis describes studies into the fixational eye movements of people with infantile nystagmus (IN) in terms of eye-in-orbit position. Much is known about fixational eye movements in humans. However, given the presence of IN oscillations in more than one component of the fixation plane, complete information is still lacking about the fixation performance in this condition; especially when the null zone is considered. The null zone, which is a position of gaze or range of gaze angles where the IN oscillation is usually reported to be at a minimum, is an important factor in IN. This reduced oscillation can also exist as a function of viewing distance, referred to as convergence null. From the individual's perspective, the null zone is a preferred eye/head position that the person chooses to adopt especially when concentrating on a task. In addition to reports of reduced eye movement intensity, an increase in visual acuity could be responsible for improved visual performance at the null zone. The null is important because common management strategies of IN are often aimed at maximizing the patient's gaze and/or viewing distance null (Serra et al. 2006). Moreover, why people with IN prefer to use their null is not well enough understood, and hence this is the principal motivation for this study. Using experiments designed to objectively measure visual performance (fixational eye stability and visual acuity), the overarching aim was to study the two-dimensional components of the IN waveform as a function of horizontal gaze positions, as well as viewing distance.

This general introductory chapter will begin with an overview of the oculomotor system and specific eye movements, including fixation and vergence. This will lay the foundation for further discussion in the subsequent chapters focused on the atypical eye movement – IN, highlighting fixation and convergence in this condition.

1.1 Eye movements and the oculomotor system

In humans, the frequent movement of the eyes enables us to scan a visual scene, direct gaze on to a target, follow a target and in some cases remain fixated on the target. These eye movements could either be voluntary or involuntary. Broadly, typical eye movements can be grouped as conjugate and disconjugate (Dell'osso and Daroff 1990). In the oculomotor system, the version subsystem consists of fast and slow conjugate eye movements in which both eyes move together in the same direction. These kinds of eye

movements include saccades, smooth pursuit, and the physiological eye movement responses: vestibulo-ocular reflex (VOR) and optokinetic nystagmus (OKN). In addition, there are other types of eye movements that may remain unnoticed clinically. These occur during fixation as the eyes are not precisely fixating steadily at a point of focus, but are continuously making small eye movements (see Section 1.1.2). These small eye movements, known to be largely conjugate (Otero-Millan, Macknik and Martinez-Conde 2014), have been identified as microsaccades, ocular drifts and tremors (Ditchburn and Ginsborg 1953). The other aspect of the oculomotor system, the vergence subsystem, is responsible for all disconjugate eye movements in which the eyes can move in opposite directions, as can be seen during vergence, i.e. when fixating objects at different distances. Vergence comprises convergence and divergence eye movements which happen during accommodation and disaccommodation, respectively; these processes occur together with pupil and lens changes to focus on a target of interest. A diagrammatic representation of eye movement types is given in Figure 1-1.

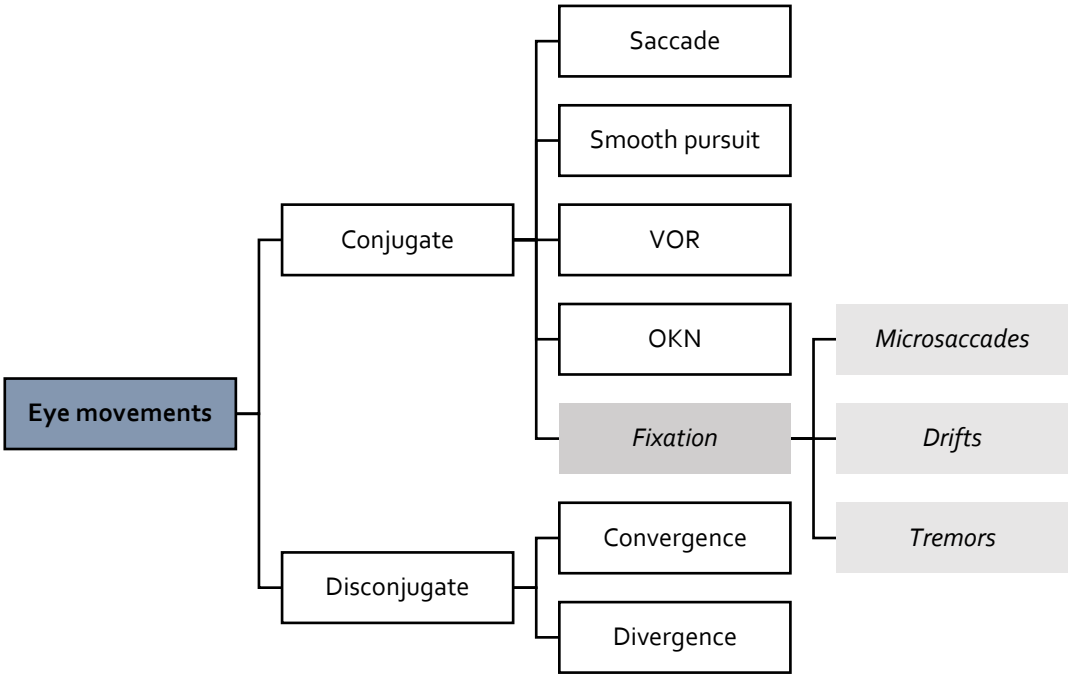

Figure 1-1: Classifying eye movements
Fixational eye movements are known to be largely conjugate.

The classification of eye movements described above highlights their mechanism of movement. But, in describing their functional roles, eye movements can be classified into those used to redirect gaze or to stabilize gaze (Büttner and Büttner-Ennever 2006; Krauzlis

2013). The process of gaze redirection occurs when humans scan their visual surroundings and shift the line of sight to different areas of interest. For this role, saccadic, smooth pursuit and vergence eye movements come into play. Gaze-stabilizing eye movements are crucial to keep an object of interest on the portion of the retina where visual acuity is best (the fovea), while producing minimal retinal slips; this occurs especially when the head is in motion. To achieve this, the VOR and OKN responses are important. At gaze movement intervals, the eyes become actively held on to the target of interest by fixation and fixational eye movements (Krauzlis 2013).

The review by Rucci and Poletti (2015) explains succinctly how eye movements occur when scanning a visual scene. A diagram explaining this can be found in Figure 1-2. When examining objects of interest, fast gaze shifts known as saccades happen about two to three times per second. In the intervals that occur between those movements, visual information is acquired and targets for the next saccadic motion selected. At the selected gaze positions where fixation is taking place, continuous fixational eye movements (microsaccades, ocular drifts and tremors) occurs. These authors have also identified that fixational eye movements are not separately defined as they are classified, especially ocular drifts and tremors, this is due to their ability to present with small amplitudes and indistinct frequency bandwidth (Eizenman, Hallett and Frecker 1985). As a result of this, movements happening in between microsaccades can be collectively referred to as inter-saccadic movements.

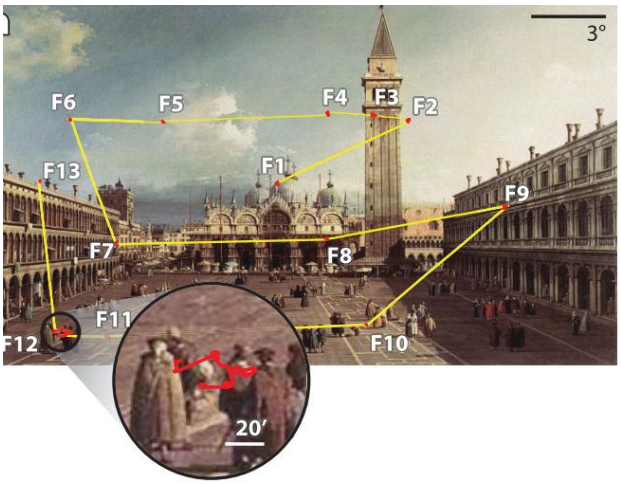

Figure 1-2: Scanning a visual scene (Source: Rucci and Poletti 2015)
Eye tracking recording of a visual scene shows portions labelled F1 to F12, which are consecutive points of fixation. Fast saccades occur in between (yellow lines). At point F12 (enlarged), where fixation is taking place, small fixational eye movements (red) are seen to occur.

Small saccades of refixation (microsaccades) occurring during fixational eye movements have been called a miniature replica of the fast gaze shifts (saccades) seen in the visual scene described above (Rucci and Poletti 2015). Research has shown that microsaccades and the fast phases of the VOR, OKN and pathologic IN are also examples of saccadic eye movements that share the same physiologic characteristics (Dell'osso and Daroff 1990; Harrison et al. 2015). Because of this similarity between microsaccades and saccades, a brief description of saccades is given followed by a review of fixation.

1.1.1 Saccades

Saccades are fast conjugate eye movements which take place to change the point of fixation. This visual action could be instigated in a finely controlled manner and not necessarily voluntarily, for example, when scanning a visual scene or in response to a command requiring a change in fixation. Saccades could also occur in response to the sudden appearance of an object in the peripheral visual space or from the presence of a unexpected sound or touch (Leigh and Zee 2015). When this happens naturally outside of a controlled laboratory environment, the saccadic eye movement will occur together with a head movement in the same direction (Dell'osso and Daroff 1990). Apart from saccades being intentional or reflexive, saccadic eye movements could also exist in other forms. These are briefly explained in Table 1-1.

Table 1-1: Forms of saccades
Adapted from Büttner and Büttner-Ennever (2006)

Saccade type	Description
Intentional saccade	occurring as a result of one's free will
Reflexive saccades	happens in response to an unexpected visual, auditory or tactile stimuli
Antisaccades	happens when asked to look in the opposite direction of an unexpected stimulus
Express saccades	very short latency saccade, occurring in response to a new stimulus, after the fixation stimulus has been removed
Memory-guided saccades	occurring in response to an absent target previously present
Predictive saccades	anticipatory eye movement directed to a given location
Microsaccades	small saccades that occurs during fixation and helps to position the retinal image within the foveola (Ko, Poletti and Rucci 2010)

Saccades have a latency period of between 200 and 380 ms (Dell'osso and Daroff 1974; McSorley, Gilchrist and McCloy 2019a; McSorley, Gilchrist and McCloy 2019b), often increasing when there is less information about the target location (McSorley, Gilchrist and McCloy 2019b).

1.1.2 Fixation

Fixation is the state in which the eyes are foveating a stationary target. But during fixation, when the eyes are supposedly locked onto a stationary target, our eyes constantly move. These relatively microscopic eye movements are together known as fixational eye movements and include the fast microsaccades, slow drifts and rapid high frequency oscillatory tremors. These small eye movements often remain unnoticed, clinically. However, the resultant effect is that visual information is shifted across many photoreceptors during its acquisition, and the resultant acuity depends mainly on the action of ocular drift. Research has shown that lower acuity thresholds are associated with larger ocular drifts diffusion constant (Clark et al. 2022). It has been shown also that, fine spatial vision decreases progressively from a region of five to 15 arcmins away from central gaze (Poletti, Listorti and Rucci 2013) and when this happens, fixational eye movements help to constantly reposition the image of the target onto the fovea (Rucci and Poletti 2015; Bowers et al. 2021), and result in further processing of visual information. The visual processing functions of fixational eye movements could include: image fade prevention (Martinez-Conde et al. 2006; Collewijn and Kowler 2008), discrimination enhancement of fine spatial details (Rucci 2008; Ko, Poletti and Rucci 2010; Rucci et al. 2007), and enriching visual information sent to the brain to provide high acuity vision (Ratnam et al. 2017; Anderson et al. 2020). The positional eye movements that occur during fixation can be quantified to determine the stability of the eyes i.e. fixation performance. For this, the term *fixational eye stability* is used in this thesis.

To illustrate these fixational eye movements, an enlarged eye position plot from one typical participant during the experiment described in Chapter four is shown in Figure 1-3. Two episodes of microsaccades can be seen occurring, within a second, in the horizontal eye position trace. Before and after these microsaccades are inter-saccadic movements. During the initial second, the horizontal eye position drifts up (rightwards) from about -0.15 to

-0.25° and ends with a microsaccade of about 0.35° amplitude. This is then followed with another period of drift down (leftwards), and a similar amplitude of microsaccade. Tremors can be seen interspersed within drifts.

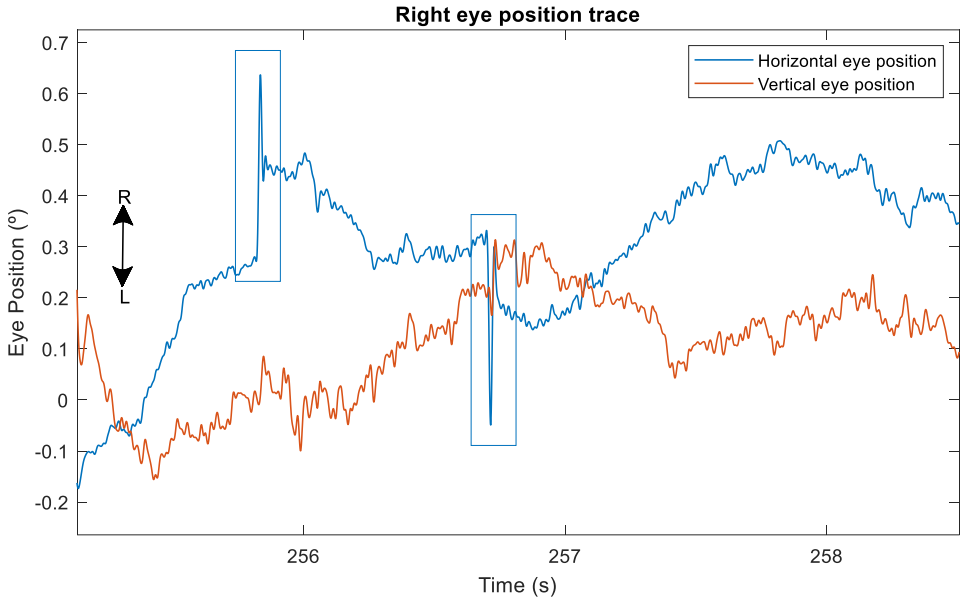

Figure 1-3: Sample plot showing fixational eye movements in a typical participant
Diagram shows a 3.5 s window of fixation, at primary position, for one typical participant (Co1). Microsaccades are enclosed in **blue** rectangle while other eye position traces are periods of drifts interspersed with tremors. R and L on the black arrow indicate that the right eye moved rightwards and leftward, respectively.

In addition, from two-dimensional eye position traces, Alexiev and Vakarelski (2023) have extracted each component of fixational eye position data with the intention of using microsaccades as a potential biomarker over the other two types of fixational eye movements (i.e. drifts and tremors). This is presented in Figure 1-4. Extracted plots of each fixational eye movement component show the degree of amplitude based on how data points are spread.

Of all the three fixational eye movements, tremors have the least amplitude and highest frequency; ranging from about 25 – 100 Hz (Steinman et al. 1973; Spauschus et al. 1999). Drifts have a frequency of 0 – 40 Hz, whereas periods of drifts could have an amplitude change of about 1.5 - 4 angular minutes (0.025 - 0.07°), the amplitudes of microsaccades in humans are usually in the range of 1 - 12 angular minutes (0.02 - 0.2°) (Collewijn and Kowler 2008; Krauzlis 2013). They also have a frequency of one to two times per second (Rucci and

Poletti 2015). In summary, fixational eye movements exhibit remarkable fine oculomotor control while contributing to improved spatial vision. Across the central fovea, vision is carefully regulated by these minute eye movements.

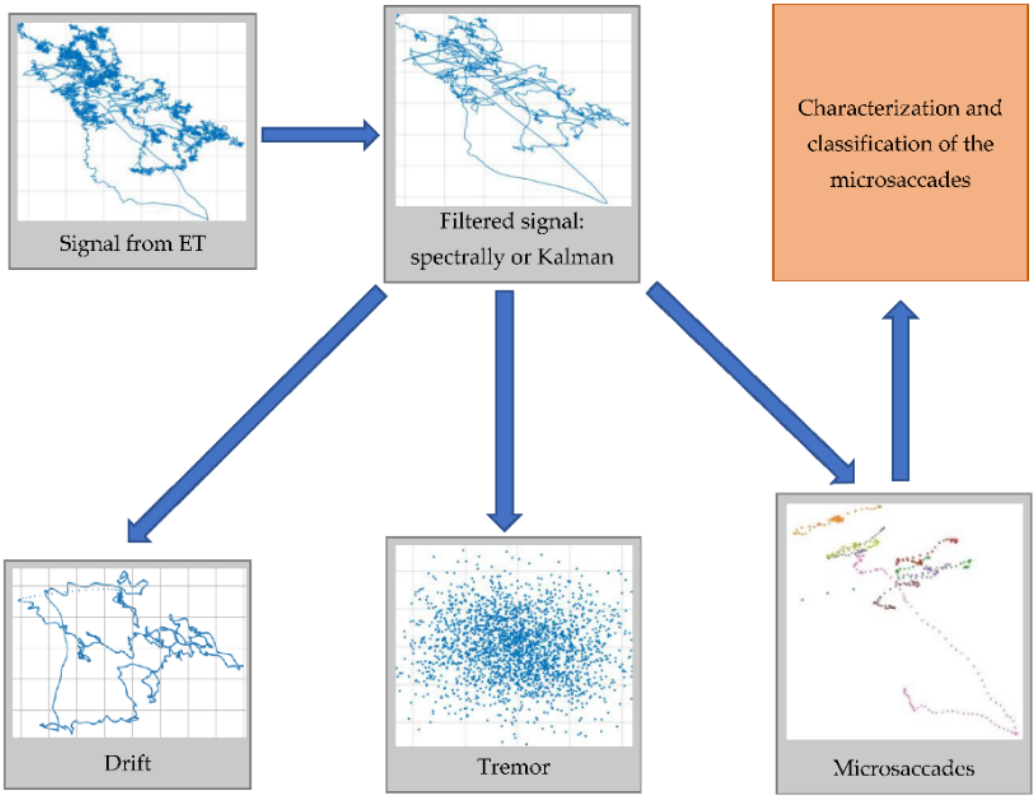

Figure 1-4: 2D sample fixational eye movements (Source: Alexiev and Vakarelski 2023).
Diagram shows 2D eye tracker (ET) signal in top panels. In the bottom panels, two-dimensional samples of drifts, tremor and microsaccades, extracted from the eye tracker recording, are illustrated with dots. These were detected and separated based on predefined frequency cut-offs.

1.1.3 Vergence

Vergence is the ability to move both eyes together, simultaneously, in an opposite direction to enable us to focus on objects at different distances, in a 3D world. When there is a change in focus from distance to near both eyes move nasally towards each other, a process known as convergence. A change in focus from near to distance will require both eyes to move temporarily, away from each other. This is called divergence. Vergence eye movements can be fusional or accommodative. A disparity between the image location on the two retinas will give rise to fusional vergence, while in the presence of retinal blur,

accommodative vergence is stimulated. In a normal situation, vergence eye movement arises from an interaction between blur and disparity signals, in which the vergence system responds to retinal disparity signals as a closed loop system and to retinal blur as an open loop system (Dell'osso and Daroff 1990; Büttner and Büttner-Ennever 2006; Del Águila-Carrasco et al. 2017b). However, fusional vergence and accommodative vergence can be studied separately. Vergence eye movements have a latency of about 160 ms, and a maximum velocity of 20°/s. Convergence movements are often quicker than divergence movements, and therefore the vergence system is termed asymmetric (Dell'osso and Daroff 1990) this is because convergence and divergence movements have different latencies. Studies have shown varied results, with some finding a longer latency for convergence (Krishnan, Farazian and Stark 1973; Yang, Bucci and Kapoula 2002) and others a longer latency for the divergence response (Semmlow and Wetzel 1979; Hung, Zhu and Ciuffreda 1997).

1.1.4 Focusing an image – the near triad

Extensive studies in humans have given us an in depth understanding of how the eye works to focus images; a process involving three physiological functions closely knit together in its neural pathways. The near triad, consisting of pupillary constriction, convergence and accommodation, is invaluable for the eye to focus images at closer distances. The main goal of the mechanisms of the near triad, which is broadly classified as *ocular accommodation*, is to change the optical power of the eye to reduce disparity and increase the depth of focus in order to bring into focus images on the retina (Bharadwaj 2017) with less accommodative effort.

One of many researchers who have contributed immensely to the study of accommodation and whose theory has been widely accepted is Helmholtz (Southall and von Helmholts 1925). Helmholtz observed that the pupil constricts for accommodation and dilates when looking at far. The anterior surface of the lens becomes more convex for near vision and less for far. This is manifested as the pupillary margin of the iris and the centre of the anterior surface of the lens moving forward slightly when accommodation begins (Figure 1-5). Recent research has now made more acceptable the use of the term "disaccommodation" (Kasthurirangan and Glasser 2005; Anderson et al. 2011; Bharadwaj

2017; Del Águila-Carrasco et al. 2017a; Labhishetty, Bobier and Lakshminarayanan 2019). During disaccommodation, the opposite of what takes place in accommodation occurs; the optical power of the eye decreases in order to focus objects at a farther distance. In addition, there will be divergence and pupillary dilatation during this process.

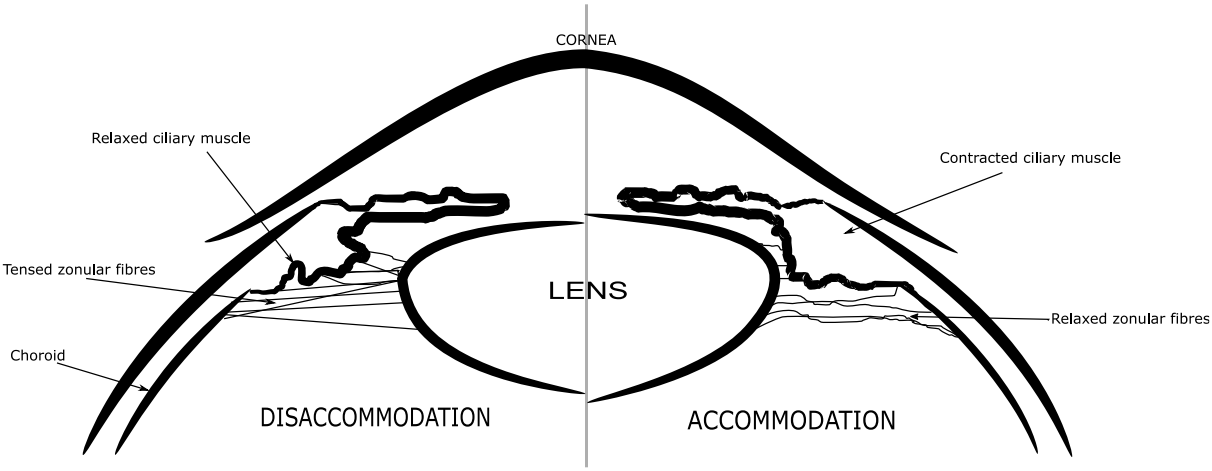

Figure 1-5: State of the intraocular structures during accommodation and disaccommodation

Cues for accommodation

Accommodation is driven by two main cues, namely, blur and disparity. Proximal cues, e.g. looming also play a passive role to drive accommodation (Horwood and Riddell 2008). Each cue are described by Morgan (1980) as part of the four Maddox components of accommodation. The fourth component known as tonic accommodation, is the amount of accommodation present at baseline, when there is no stimulus to accommodate, such as in complete darkness. At this tonic accommodative state, values of about 0.5 - 1.5D are usually obtained (Glasser 2011). Since image blur and disparity use the eye as a reference and proximity cues use the body as a reference, these cues to accommodation can be classified as retinotopic and spatiotopic, respectively. The effect of the retinotopic and spatiotopic cues supplement each other, thereby leading to an improved accommodative response (Bharadwaj 2017).

Viewing objects that vary in depth requires that the lens focusing power and the position of both eyes will be adjusted at the same time through a feedback control system to bring about accommodation and convergence. Disparity and blur cues drive the accommodative and vergence systems, however various ideas exist as to which is the main cue. Studies

(Bharadwaj and Candy 2008; Horwood and Riddell 2008) have shown that, in children and young adults, disparity is the primary stimulus to the accommodation and vergence system followed by blur and then proximity. The proximal cue contributes significantly when blur and disparity is absent (open-loop conditions), but its role when blur and disparity cues are present (closed-loop condition), is not clear (Fogt, Toole and Rogers 2016).

Under binocular conditions, the accommodation and vergence system do not work separately. In fact, both systems interact by receiving neural signals from each other to produce the changes in the lens and eye position (Hung and Semmlow 1980). During the process, blur-stimulated accommodation will give rise to a vergence eye movement known as accommodative convergence, and disparity alone will also initiate a lens response called convergence accommodation. This feedback mechanism and interconnection between the two systems, as proposed by Schor (1992), is simply illustrated by Bharadwaj, in the diagram presented in Figure 1-6. The relationship between the accommodative and vergence system is known clinically as the accommodative-convergence to accommodation (AC/A) ratio and the convergence-accommodation to convergence (CA/C) ratio. It is known that the ability to accommodate decreases with age (Mordi and Ciuffreda 1998), however there is no effect of age on vergence (Yang, Le and Kapoula 2009).

This image has been removed by the author for copyright reasons

Figure 1-6: Cross coupling model of vergence and accommodation (Source: Bharadwaj 2017).
Accommodation and vergence responses are stimulated by retinal blur and disparity. The phasic and tonic controllers act on these cues to feed the necessary biomechanical plant, which in turn generate the accommodative and vergence response. The controllers have a gain element and time constant. The phasic controllers from their large gain, generate large and rapid step changes in motor response and end by initiating a steady state. The tonic controllers thereafter respond slowly to these step changes and helps to maintain the steady state. Signals are further processed in a negative feedback loop until both cues fall below the limits of depth of focus and Panum's fusional area. See figure 24.3, page 336 in referenced publication.

1.1.5 Eye positions and the laws of ocular motility

To ensure that images from both eyes are brought onto a corresponding area on the retina, the action of the extraocular muscles are needed. Extraocular muscles help to *rotate* the eye around one of three axes (x, y and z), with a hypothetical fixed centre of rotation (Figure 1-7). Rotation in these three axes produces a three-dimensional eye movement of yaw (left to right), pitch (up to down) and roll (clockwise and anticlockwise). The x (yaw) and z (pitch) axis are both perpendicular to the line of fixation and are the horizontal and vertical axes, respectively, while the anterior-posterior y-axis (responsible for roll) coincides with the line of fixation (von Noorden and Campos 2002). In primary position, the individual is looking straight ahead, with head erect, and the x and z planes are said to coincide with the equatorial or Listing's plane. At this position, the equatorial plane passes through the centre of rotation and globe equator. In secondary positions, the eye is either abducted (outwards), adducted (inwards), elevated or depressed, while tertiary positions involve torsional movements, e.g. gaze directed to an 'up and right' position.

Figure 1-7: Centre and axes of rotation of the eye including the equatorial plane (Source: von Noorden and Campos 2002)
See figure 4-1, page 53 in referenced publication.

The six extraocular muscles responsible for eye movements within the orbit are shown in Figure 1-8. These are four recti and two oblique muscles. The medial and lateral recti muscles have only one action each of adducting and abducting the eye, respectively. This is necessary to produce horizontal eye rotations in the yaw, i.e. movement from side to side. This is the movement mainly employed for experiments in this thesis. The other four recti and oblique muscles have primary, secondary and tertiary rotatory actions. A number of

studies have provided details about these muscles, their central control, and how they can be assessed (Shaunak, O'Sullivan and Kennard 1995; von Noorden and Campos 2002).

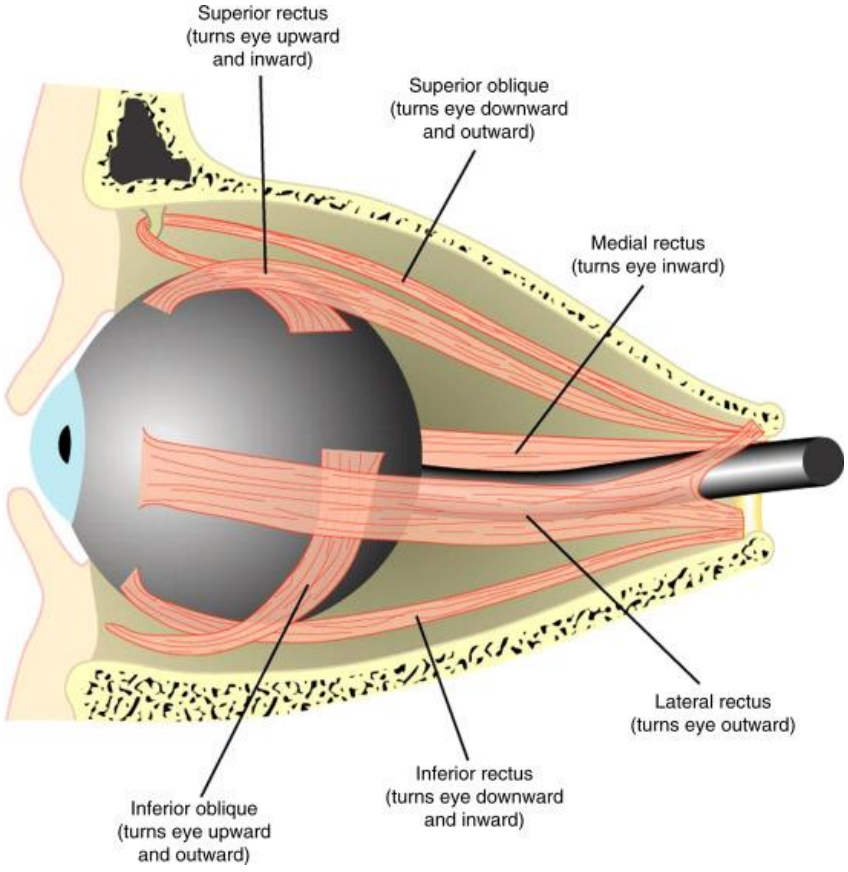

Figure 1-8: The extraocular muscles (Source: Krauzlis 2013)
Diagram shows a lateral view of the eye in the orbit. The attachments of the extraocular muscles and their main actions are indicated.

We have seen earlier that the eye rotates in three-dimensions. However, the visual image is projected onto the retina in two-dimensions, using only vertical and horizontal movements. The typical oculomotor system compensates for the degree of rotations in the roll by constraining the position of the eye to zero torsion (Klier, Meng and Angelaki 2011). Two fundamental laws that explain this physiological phenomenon is Donder's and Listing's law. **Donder's law** states that, despite the eye's ability to rotate to various roll positions on the y-axis, the globe always assumes the same orientation when fixating at a given direction. **Listings' law** further highlights the three dimensional orientations needed for fixating a given direction and provides justification for such a movement (Simonsz and Den Tonkelaar 1990). His law states that the axes required to move the globe in accordance with Donders

law are restricted to a single plane known as the Listing's or equatorial plane (shown in Figure 1-7).

The two dimensions of eye movement, which occur as the eye moves in each plane, are for the purpose of this thesis referred to as the horizontal and vertical *components.* Unlike in previous times, modern eye tracking technology like the Eyelink 1000 allows eye movements trace to be recorded simultaneously for both (i.e. X and Y) components. And in IN, where oscillations can exist in both components, this is invaluable. However, in evaluating eye movements during fixation, most studies use only the horizontal component.

In the subsequent sections, IN, which is a pathological condition, is discussed. This will be followed by evidence highlighting a need for a shift in traditional IN waveform evaluation, and a justification for the thesis aims.

1.2 Infantile nystagmus

IN is a pathologic involuntary movement of the eyes present at birth or developing within six months after birth. The IN eye movements are in most cases conjugate, symmetrical and have primarily a horizontal component (Abadi and Dickinson 1986; Abadi and Bjerre 2002). In a few cases, however, a vertical or torsional waveform component can exist (Averbuch-Heller et al. 2002; Hertle and Dell'Osso 1999; Collewijn, Apkarian and Spekreijse 1985; Shawkat et al. 2000). According to the Classification of Eye Movement Abnormalities and Strabismus (CEMAS) report (CEMAS 2001), which gives an exhaustive description of oculomotor disorders, pathological involuntary eye movements comprise IN. Where the term 'infantile' replaces its previous terms namely, congenital, oculomotor and sensory nystagmus. IN is a relatively rare condition. In a wide nystagmus survey conducted in Leicestershire and Rutland, the prevalence of IN was estimated to be 1.4 per 1,000 (Sarvananthan et al. 2009). In their study, Fusion Maldevelopment Nystagmus Syndrome (FMNS) and spasmus nutans, which are other forms of pathologic nystagmus were included. This may have resulted in a higher prevalence than would be true for just IN. Other studies however, have shown an estimated prevalence of IN ranging from 1 in 821 in

the Northern America (Nash, Diehl and Mohney 2017) to 0.61 per 1,000 live births in Denmark (Hvid et al. 2020).

IN can occur on its own, otherwise known as idiopathic nystagmus, or alongside other sensory or neurological causes (Bertsch et al. 2017; Suppiej et al. 2022). Sensory disorders such as cataract, retinal and optic nerve disease, corneal opacity, albinism or achromatopsia are often commonly associated with IN. Neurological conditions may include a variety of developmental syndromes such as Down's syndrome (Zahidi 2019), cases of brain malformations and metabolic disorders, and some cases of IN could involve mixed neurological and sensory causes (Suppiej et al. 2022). Research findings indicate that IN occurring with ocular diseases and idiopathic IN are the most prevalent forms of IN (Hvid et al. 2020; Nash, Diehl and Mohney 2017). Moreover, one study has found that albinism is the condition most commonly associated with IN (19%) in the 202 clinical records (cases present before six months of age) sampled (Bertsch et al. 2017). IN is associated with reduced VA (Abadi and Bjerre 2002; Abadi and Pascal 1991; Simmers, Gray and Winn 1999). Research has shown that the involuntary constant oscillations can greatly affect foveation periods (i.e. the period when the image is on the fovea and eye velocity is reduced) (Abadi and Pascal 1991; Cesarelli et al. 2000; Dai, Cham and Abel 2021), and when this happens, VA, a measure of visual impairment, is affected.

Recent advances in the identification of genetic mutations associated with IN have enhanced our understanding of its aetiology (Gottlob and Proudlock 2014). The first gene found to be associated with idiopathic IN is the FRMD7 located on chromosome Xq26 (Tarpey et al. 2006). Since then, other mutations have been found (Galvez-Ruiz, Galindo-Ferreiro and Lehner 2021). In fact, the resulting changes in cellular function that occur in most IN types manifest as possible defects in the afferent visual pathway, oculomotor system and the extraocular muscles, including proprioceptive feedback, and these defects have been identified to have their source in genetic mutations (Gottlob and Proudlock 2014). Apart from genetic testing, diagnosing IN may go beyond the usual clinical observations (which often reveal an obvious continuous eye movement). In some cases, a detailed evaluation of oculomotor performance using high speed eye tracking methods is invaluable (Clark et al. 2019). In addition, high resolution ocular scans, such as optical

coherence tomography (OCT) and other internal examinations of the ocular structures, are important to give information on ocular defects that may aid diagnosis.

During eye movement recording, the output shows the eye position recorded against time. The to and fro oscillation of the IN eye movement results in a *waveform* of eye position. This waveform is characterized by its amplitude and frequency, which together make up the eye movement intensity (or average velocity). The characteristic feature of all IN waveform is an increasing velocity slow phase (just like a microdrift) which takes the target away from the fovea. This is then followed by a variable fast phase (or less commonly, another slow phase) which brings the target back to the fovea, ending with a foveation period of lowest velocity but with variable duration.

Although another approach to classifying IN waveforms exists (Harris, Waddington and Erichsen 2012), IN waveforms are more commonly identified to present in at least 12 different types (Theodorou and Clement 2016; Dell'osso and Daroff 1975; Abadi and Pascal 1995), broadly classified into three classes: pendular, jerk and dual. Velocity traces of an eye movement waveform facilitate categorization. As the fast phases are 'corrective movements' made to counteract the drift slow phase error, nystagmus types are also named according to the direction of movement of the fast phase. These waveform types are shown in Figure 1-9, and a detailed explanation can be found in the paper by Dell'osso and Daroff (1975). Briefly, **pendular** waveforms occur in a wavelike manner. They are characterized by slow smooth eye movements away and back to the point of fixation (Abadi and Bjerre 2002). The **jerk** eye movement, on the other hand, is characterized by either an accelerating, decelerating or linear/constant velocity eye movement drifts, away from the fixation point, followed by a quick phase or saccadic intrusion (Hertle and Dell'Osso 1999) necessary to bring the fovea back towards the point of fixation. In the jerk form of nystagmus, the directionality of the saccade is taken into consideration. Where there are two saccades in a cycle, both in a refoveating direction, it is called bidirectional jerk. These are often short lived and hence have little or no foveation. In the other type of jerk nystagmus, unidirectional jerk, the only saccade in the cycle indicates the nystagmus direction, and this is always in a refoveating direction. Lastly, **dual** waveform types are made up of a combination of jerk and pendular nystagmus, featuring a quick sinusoidal oscillation (with small amplitude) superimposed on a large amplitude jerk nystagmus.

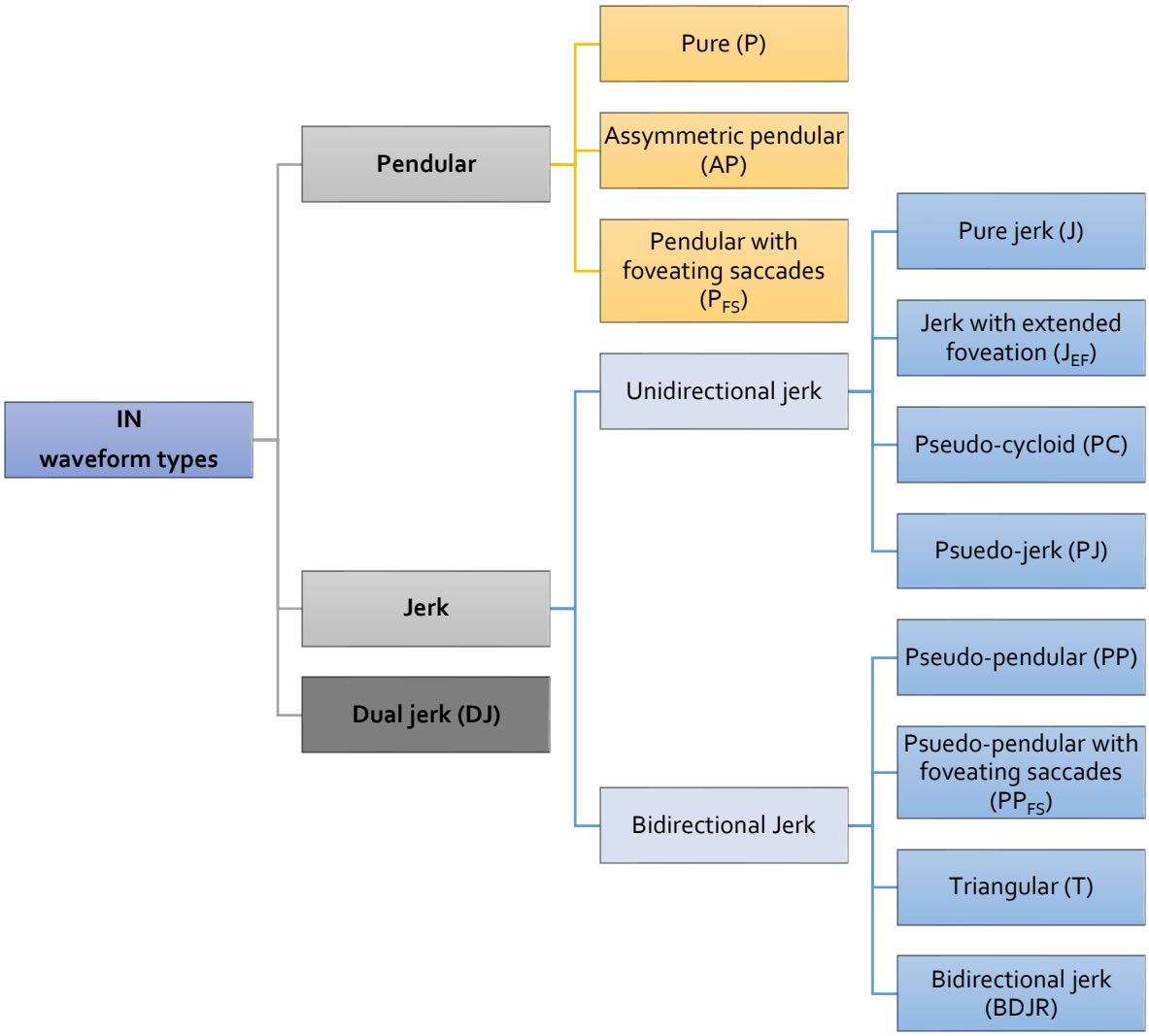

Figure 1-9: Classifying IN waveforms

It is important to note that these waveform types were originally classified using only the horizontal component of eye movement trace whereas oscillations could also have a vertical component. A typical example of a waveform recorded for one participant, during the experiment presented in Chapter five, is presented in Figure 1-10. This eye movement trace shows oscillations present in both the horizontal and vertical components of both eyes, further highlighting the two-dimensional nature of IN. The traces also indicate the slow and fast (or quick) phases as well as the foveation period that together make up a cycle. IN waveforms can have an amplitude ranging from 0.3 – 15.7° and frequencies from 0.5 – 8 Hz (Abadi and Bjerre 2002). These parameters can vary within and between people with IN (Abadi and Dickinson 1986). Foveations, as indicated by the sections enclosed in the green rectangle (Figure 1-10), are defined as periods when the image of the target is on the

fovea, and velocity is at a minimum. For individuals with IN, as well as those with typical vision, it is expected that, during the foveation period, the gaze direction (of the fovea) and target position coincide, retinal image slip velocity is reduced and therefore VA increased (Dell'Osso et al. 1992b).

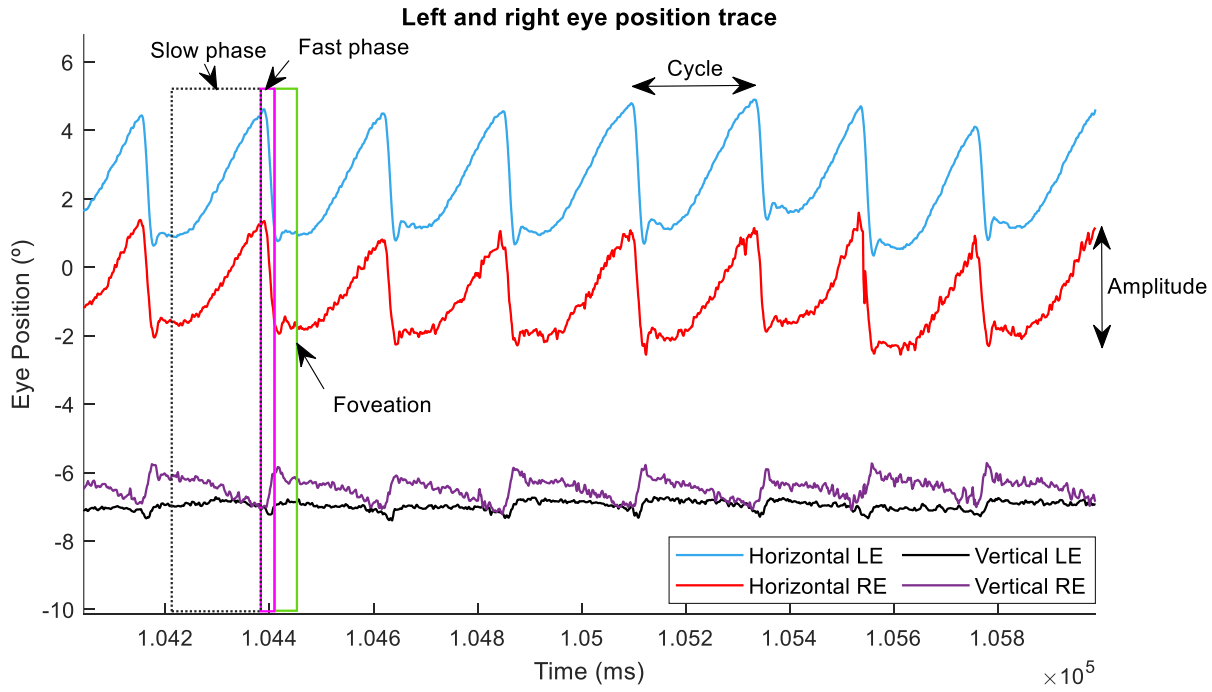

Figure 1-10: Eye movements and the IN cycle
Diagram of a section of the horizontal and vertical eye movement traces for participant IN02 while fixating binocularly at 100 cm. This participant has a jerk waveform type present in two-dimensions, as can be seen in both the horizontal and vertical components of the eye movement trace. The distance from one peak to the next indicates one cycle. The number of cycles present in one second (frequency) x range of eye movement excursion (amplitude) gives a measure of intensity. LE = Left eye, RE = right eye.

Worthy of mention is Periodic Alternating Nystagmus (PAN), a form of IN in which the waveform changes with time (Abadi and Dickinson 1986). Identifying PAN requires eye movement recording lasting about three minutes or more (Shallo-Hoffmann and Riordan-Eva 2001) and this is relevant for the experiment presented in Chapter four, which lasted for a period of over three minutes. This condition was previously thought to be rare, however, more recent research has found a prevalence of five to 39% in both albinos (Abadi and Pascal 1994) and others with and without a sensory defect (Shallo-Hoffmann, Faldon and Tusa 1999; Gradstein et al. 1997). The characteristic presenting waveform of PAN will generally have periods of active and intermediate quiet (or transition) phases, with a

complete cycle (of phases) found to last about one to seven minutes. Diagram representing PAN in a participant with IN is shown in Figure 1-11. A full cycle usually manifests as a pure unidirectional jerk (left or right beating) waveform during the active phases. In the quiet phase, intensity can be completely dampened or present as very minimal jerk or pendular waveforms, often bi-directional (Shallo-Hoffmann, Faldon and Tusa 1999; Robb 1972).

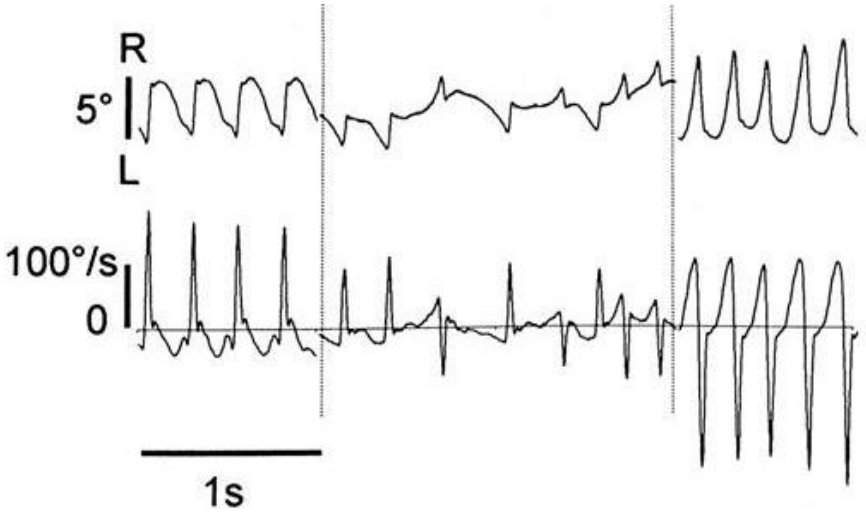

Figure 1-11: The PAN cycle (Source: Shallo-Hoffmann and Riordan-Eva 2002)
Diagram shows section of eye movement trace from each phase of the PAN cycle. The eye position plot is presented above while velocity trace is shown below. From the eye position plot, it can be seen that the cycle starts with an active right beating phase, breaks with a quiet phase (shown in between) and then ends with a left beating accelerating one. R and L = right and left, respectively. Figure reprinted by permission of Informa UK Limited, trading as Taylor & Taylor & Francis Group, http://www.tandfonline.com

1.2.1 Fixation in infantile nystagmus

Previously, IN was thought of as a fixation anomaly whereby a disruption of the fixation process causes eye movements away from, and then back to the fixation target. However, research has shown that, during each IN cycle, there is a period when the target remains foveated and the process of achieving and maintaining foveation of a target is not very different from the fixation eye movements seen in typical individuals (Dell'Osso et al. 1992). Indeed, if we look at the fixation process in typical participants whereby fixational eye movements drift the eye away, and microsaccades bring it back on to the target, we can generally say that fixation in both typical participants and those with IN present with the same basic characteristics. The eye movement trace in Figure 1-10 shows similarities with

that from the typical participant presented in Figure 1-3, this is because both have periods of drifts (and tremors occurring during the drift episode) punctuated by saccades which help to redirect the eye back to the target. However, the drifts and saccades in both might differ in especially amplitude as well as direction and frequency. Therefore, the IN waveform could be said to be a fairly organised fixational eye movement trace because of the characteristic pattern of the waveforms, which is absent in fixational eye movement patterns for typical participants. The only difference in fixation between people with IN and typical participants may be that, with typical participants, there is no evidence of change in fixation parameters with gaze angle whereas, with IN, there is a clearly defined null zone in some cases (Dell'Osso et al. 1992b). The IN waveform at different viewing positions, and its characteristic null zone will now be considered. This discussion will further lay a foundation for justifying the methods used in this thesis to evaluate fixational eye stability and quantify fixation performance.

1.2.2 Null zones and the many ways they are defined

As illustrated in the Section 1.2, the IN waveform is made up of slow and fast phases which together manifest as oscillations. Fixating a stimulus at a range of gaze angles has been associated with reports of subjective and objective changes in the IN eye movements. Subjectively, patients report better visual function especially with treatment (Hertle et al. 2003; McLean et al. 2007). Objectively, eye movement recording research has shown that the IN waveform can be significantly altered at different times and conditions, especially during eye movement recording (Abadi and Dickinson 1986). This change in waveform can also occur as a result of shift in gaze angle, viewing distance (Dell'Osso et al. 1972), including other psychophysical conditions of the subject such as fatigue, stress and/or state of attention (Abadi and Dickinson 1986; Kraft and Irving 2004; Dunn et al. 2017; Jones et al. 2013). Also, visual task difficulty which may translate to increased concentration or fixation effort (Harris 1995), or to a prolonged time-to-see (manifesting as an increased target acquisition time, and attributed to an increased saccade latency towards peripherally presented targets) (Wang and Dell'Osso 2007) could also change the waveform. A particular range of eye positions can, in most cases, manifest as a region of gaze in which the intensity of the waveform oscillation is minimal (Abadi and Bjerre 2002). This region is

called the **null zone**. In individuals who do not have an alternating component, the null zone is termed a *static null* this is because it becomes entirely a function of gaze angle. In others with an alternating component, the null zone is *dynamic* (Dell'Osso et al. 1992b). The null can also manifest as a reduced waveform oscillation associated with near viewing. This condition is known as convergence dampening, and individuals who have it are said to have a **convergence null**. Additionally, it has even been reported that more than one null zone may be present at different viewing distances (Kraft and Irving 2004). More information on the convergence null is presented in Chapter five but in continuing discussions here, centered on quantifying fixation performance, the null zone at gaze angles will be the focus.

While viewing at the null zone, the oscillations are found to be less frequent and/or the amplitude of eye movements is less, and as a consequence the subsequent intensity measure (amplitude x frequency) of the IN oscillation can reduce significantly. Where the null zone is at an eccentric gaze position, a compensatory head posture may develop, presumably in order to produce this less intense oscillation and facilitate the processing of visual information. Null zones are found in more than 60% of people with IN (Abadi and Bjerre 2002; Hertle and Dell'Osso 1999; Dunn et al. 2017). In a large study evaluating the characteristics of IN (Abadi and Bjerre 2002), null zones were mostly found to be at primary position or within ±10° of primary position (73% of 143 subjects), while for about 27% of their subjects, a null zone at ±20° and beyond (up to ±40°) accompanied with a compensatory head posture was found. Also, the previous study by Abadi and Dickinson (1986) reported that the preferred head postures of 69% of their 16 participants was within ±20° of the primary position.

The null zone is such an important characteristic of IN that measures of IN treatment often rely on finding and shifting this position to central gaze, through surgical or optical means (Thurtell and Leigh 2012; Chang et al. 2023; Serra et al. 2006; Dell'osso 2002), or by maximally utilizing it through a procedure known as 'null zone training' (Fadzil et al. 2019; Fitzmaurice and Lesley 1987). This is because, at the null zone, VA has been shown to be slightly better and retinal slip minimised (Dell'Osso et al. 1992b; Vieira da Costa et al. 2014), with one study finding a marginal but significant improvement in VA of 0.08 logMAR at the null zone (Dunn et al. 2017). In addition, one or more of the other waveform parameters

used to determine fixation performance, such as the amplitude and frequency as well as the foveation duration and accuracy, are known to significantly improve at the null zone (Wiggins et al. 2007; Dell'osso and Daroff 1975; Dell'Osso et al. 1992b; Dunn et al. 2017).

A generally accepted approach to defining the IN null zone does not exist. Clinically, the null zone can be evaluated by direct observation of the IN eye oscillations at different gaze angles (Self et al. 2020), and noting where there is a reduction in the amplitude of the eye movement oscillation. Various objective means of defining the IN null zone have also existed for many years. This is traditionally done by quantifying one or more of the features of the IN waveform; specifically, the amplitude, frequency, and/or the resulting intensities, as well as slow phase velocities and foveation duration (Abadi and Bjerre 2002; Abadi and Whittle 1991; Dell'Osso 1973; Dell'Osso et al. 1972; Dell'Osso et al. 1992b; Jones et al. 2013; Wiggins et al. 2007; Collewijn, Apkarian and Spekreijse 1985; Thomas et al. 2011; Bedell, White and Abplanalp 1989). Any one of these methods for evaluating IN eye movements, however, may not give a truly comprehensive picture of the IN waveform oscillations, and the reasons are outlined for each parameter in the following sections.

Amplitude

Amplitude is a measure of eye position range. For example, if we consider the fact that the slow phase of the IN waveform is accelerating, then the crucial information concerning the eye position spread during that phase is missed. This is because more of the eye position samples in a given IN cycle will be present around/near foveation than away from it (i.e. at the point where the eyes begin to drift away from the target, before they become refixated by the fast phase; see Figure 1-10). A histogram plot of three consecutive cycles drawn from the horizontal eye movement position of one participant is presented in Figure 1-12. Results show how skewed data samples are towards zero, which is the foveation position. Therefore, we could conclude that although the amplitude provides a measure of the degree of excursion of the eye, this parameter does not account for the uneven spread of eye positions in a given cycle.

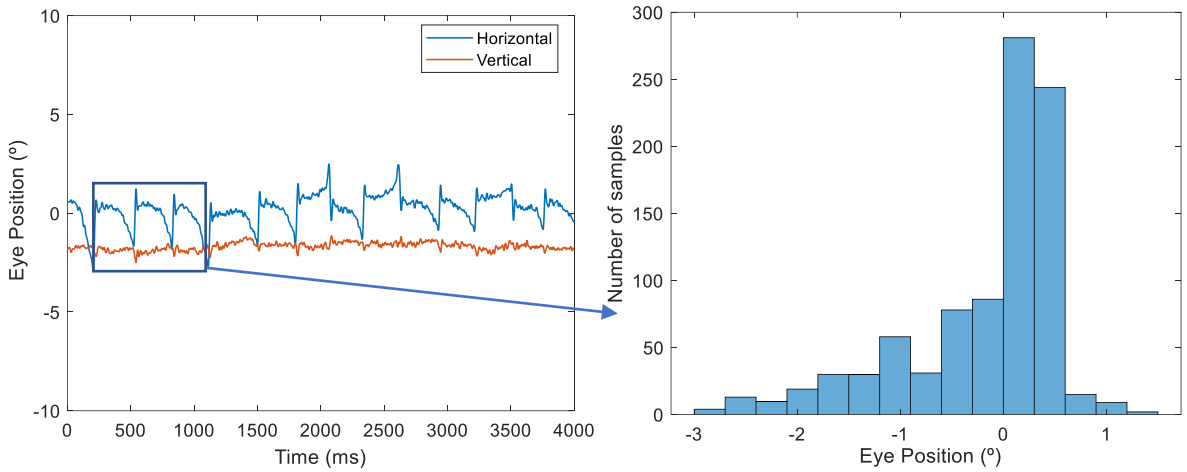

Figure 1-12: Eye position values and histogram plot of three consecutive IN cycles
Diagram shows eye position trace for participant P031 while viewing at primary position. The figure on the left includes a section in rectangle. **Horizontal** eye position data points from this rectangle were plotted to produce the figure on the right. In the histogram on the right, the majority of eye position samples are found at or near the primary position, which is the region of foveation.

Frequency

The frequency of an IN waveform is a parameter used to describe the number of slow phase/fast phase cycles per second but does not include the position of samples in the waveform oscillation. Due to the fact that the IN waveform could be influenced by various factors, including gaze angle (Abadi and Whittle 1991), the amplitude may vary within an individual. Therefore, a measure of frequency will not necessarily correlate with the magnitude of the waveform oscillation. Two eye position waveform plots are shown from participant P023 while fixating at two left eccentric (-15 and -10°) positions in Figure 1-13. It can be seen in the plots that, although both have similar frequencies, their amplitudes differ. Equally, waveforms with similar amplitudes may have quite different frequencies. In other words, a measure of frequency does not give the complete picture of the IN waveform oscillation.

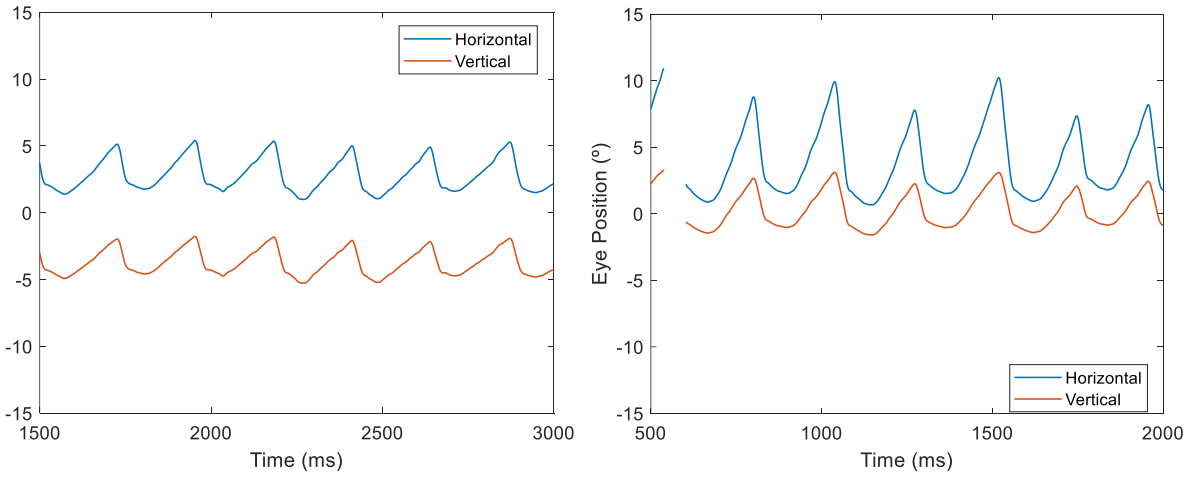

Figure 1-13: Illustrating similar horizontal eye position frequencies but different amplitudes
Both diagrams comprise a 1.5 s eye position trace, while viewing left at -15° (left) and -10° (right) positions. Notice the increase in horizontal waveform amplitude with the change in eccentric gaze angle.

Intensity

The intensity measure gives an overall description of the severity of IN waveform oscillation. Traditionally, this value is calculated as the product of amplitude and frequency, which is equivalent to the average velocity of the eye movements (Abadi and Dickinson 1986). Perhaps due to the inherent flaws that can arise from using each of the two underlying metrics, both are frequently combined to give a measure of intensity. However, as can be seen in the description above, the intensity value will clearly suffer the same drawbacks and will not reveal the underlying distribution of eye velocities in a slow phase of the IN waveform. As an example, the velocity derived from the same participant's (P028) eye position in Figure 1-12 is plotted as a histogram in Figure 1-14. It can be seen that the graph is again skewed towards the central foveation position where more eye velocity samples can be found, i.e. there was only a very minimal eye position change from one point to another (for most of the samples) while foveating at the central position, highlighting the non-uniformity of eye velocity throughout the IN waveform.

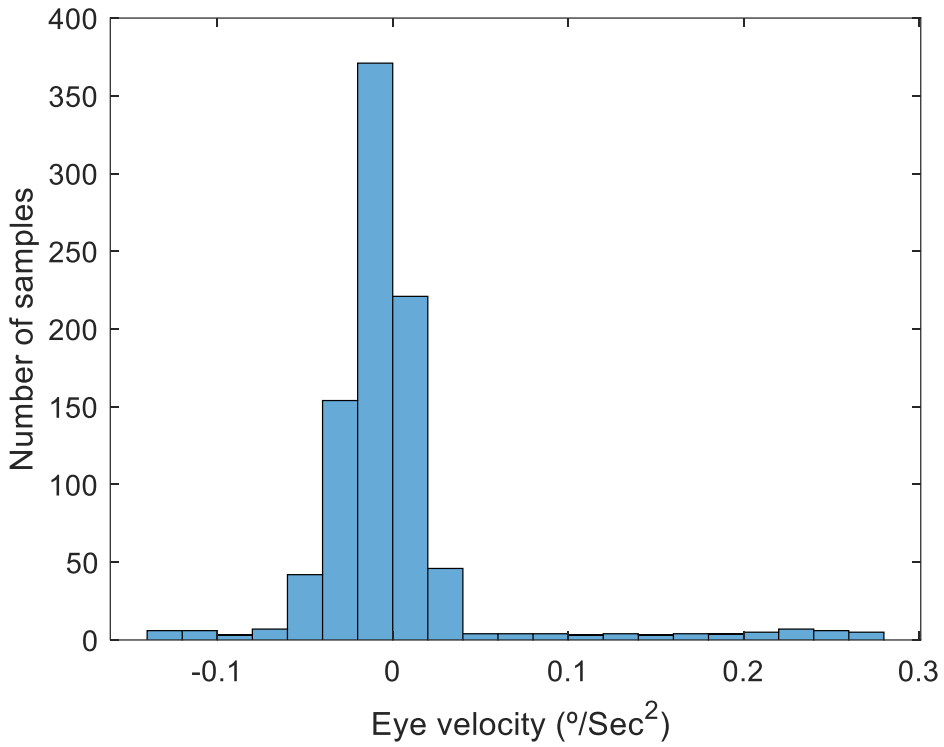

Figure 1-14: Velocity samples for participant P031 while viewing at primary position
Figure shows that even while viewing at a target, the displacement of eye position is not uniform throughout the IN waveform oscillation. Eye position is displaced less from the fovea for more samples (where velocity is about 0) indicating the eyes stay longer, or in other words are foveating longer at a given position.

Foveation duration

As illustrated above, a measure of the time spent foveating a target in each nystagmus cycle, which often manifests as periods of a reduction in velocity, is an important factor for determining the visual performance of people with IN (Chung and Bedell 1996). One issue with this metric is that its definition is somewhat arbitrary. Prior studies have used different methods to analyze the IN cycle and determine the foveation duration, either using a fixed velocity threshold criterion or one that is automatically determined (Dunn et al. 2019). In using a fixed threshold criteria, some studies define the foveation duration using a velocity criterion and a set velocity threshold of, for example, 4°/s and a duration longer than 7 ms (Dell'Osso et al. 1992b; Jones et al. 2013; Bifulco et al. 2003) while some others additionally use a positional criterion, such that all detected foveations must be within a certain positional range of the fixation target for it to be accepted as a foveation period (Dell'Osso et al. 1992b; Felius et al. 2011; Dell'Osso and Jacobs 2002).

The problem with these methods is that, firstly, the chosen criteria are applied to all participants in a study whereas, a wide range of waveform types could exists between and within individuals (Abadi and Dickinson 1986). Secondly, the foveation velocity threshold can also change for each IN cycle depending on the methods used for determining this threshold, i.e. either a fixed threshold or one arrived at automatically (using relative changes in velocity). With the varied methods of classifying foveation duration that exists, it is possible that, when the foveation duration is used to determine null zone, the end result could differ even within an individual.

To eliminate the incomplete representation of the IN waveform oscillation, inconsistencies arising from using a one size fits all set of criteria, and the potential source of error due to the wide variety of waveform oscillations, a unifying method is required. This is because segmenting the waveform to obtain individual values of one or more of the waveform amplitude, frequency, or velocity of the slow phase cannot give an all-encompassing metric for the characteristic waveform. Moreover, where waveform segmentation is required to produce a metric, a comprehensive segmentation algorithm may not work for all waveform types. For example, in the study by Abadi and Whittle (1991), although intensity was a better match to preferred position of gaze than other measures of amplitude and frequency, this was the case in only six out of nine subjects. Therefore, this suggests that, for the remaining 33% of subjects, other factors may be contributing to a choice of this null zone. Given that VA may marginally improve at the null zone and the various components of the waveform will not completely explain this gaze angle preference, it is imperative that more comprehensive metrics representing fixation, such as the accuracy and precision of fixational eye stability, are explored.

Quantifying the stability of ocular fixation

As discussed above, the predominant methods for evaluating IN eye movements will involve analysing one or more aspects of the eye movement trace, and this could be misleading. Another inherent flaw with IN eye movement analysis is the fact that, most of the time, only the horizontal component of the eye movement trace is investigated (Dell'Osso et al. 2020; Abadi and Dickinson 1986; Abadi et al. 1989; Dell'Osso and Flynn 1979; Dell'Osso, Flynn and Daroff 1974; Felius et al. 2011; Gresty, Page and Barratt 1984;

Jones et al. 2013; Ukwade and Bedell 1992; Abadi and Whittle 1991; Dell'Osso et al. 1992b; Dunn et al. 2017). This may partly be because the IN oscillation is predominantly horizontal or, previously existing instruments that were popularly used allows only one component to be measured at a time (e.g. see: Dell'Osso et al. 2020). Although a few studies presented both horizontal and vertical components simultaneously (Thomas et al. 2011; Bedell, White and Abplanalp 1989; Collewijn, Apkarian and Spekreijse 1985), these data still miss information on how these components relate within an individual, especially when gaze angles and viewing distance are considered. Modern eye tracking technology (e.g. the EyeLink 1000) allows recording of both horizontal and vertical components of eye movements, and therefore, this gives an excellent opportunity for a simultaneous analysis of both components of eye movement within a participant.

The method used in this thesis to analyse fixational eye stability and quantify fixation performance is a Kernel Density Estimation (KDE) for two-dimensional bivariate Probability Density Function (bPDF) of eye position data. The analysis will involve both the horizontal and vertical components of the eye movements at a specified gaze direction, irrespective of the type of waveform present (Dell'osso and Daroff 1975). The bPDF method is an established method of analysing eye movement traces and has been used in recent studies for both typical participants (Cherici et al. 2012; Wooding et al. 2023) and those with IN (McIlreavy, Freeman and Erichsen 2019; McIlreavy, Freeman and Erichsen 2020; Zahidi 2019). It has also been shown that, bPDF measures of eye velocity are reasonably well correlated with traditional measures of intensity (amplitude x frequency), using the velocity of eye movement (McIlreavy 2016). Since eye velocity is a first derivative of the eye position waveform, it is expected that a similar correlation exists between measure of eye position intensity and the bPDF results of eye position.

Briefly, what the bPDF method entails is a two dimensional evaluation of relative eye position, to determine the accuracy and precision of fixation, from the derived non-uniform isocontour (i.e. the highest 68% density) of the entire set of eye position points recorded (Castet and Crossland 2012). Accuracy in this case is how near the contour centre (centre of mass or mean) of the recorded data points are to the fixation point, while precision is the variability of recorded eye position data points or its standard deviation (i.e. the contour

area. Both can both be likened to the validity and reliability of results, respectively (Hessels and Hooge 2019).

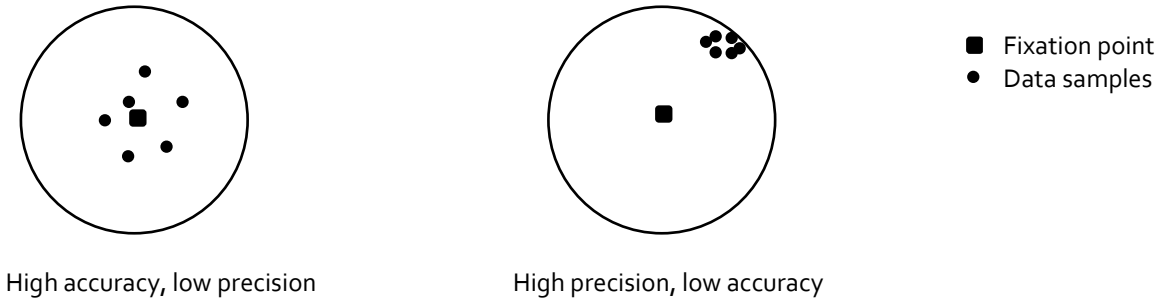

Figure 1-15: Illustrating the accuracy and precision of data points

This description of accuracy and precision is illustrated by the example in Figure 1-15 where it is seen that a data set can be accurate but imprecise or inaccurate but precise. In one study (Cesarelli et al. 2000), the standard deviation of eye position during foveation was identified to fit patients' clinical VA better than measures of increased foveation time. Therefore, eye position variability (obtained from the precision metrics of the bPDF analysis) could provide a better means of analysing eye position data. For this thesis, analysis using the bPDF method goes beyond a single evaluation of each component trace, and also provides a measure of the comprehensive relationship between the horizontal and vertical component at each fixation position. More information about this method is given in Chapter two.

1.3 Summary and research objectives

A review of the human oculomotor system has been given, highlighting the fixation characteristics in typical participants and those with IN, in order to lay a foundation for the experimental research presented in this thesis. Much like every day viewing conditions, fixation at different gaze angles and distances will be investigated as the main aim of the experiments in this thesis. For the first time, the results will provide a comprehensive assessment of the contributions of the horizontal and vertical components of eye movements to fixation performance in those with IN by using the bPDF method. Obtaining findings relating to any possible pattern of change in fixation performance at fixation

positions, both at eccentric gaze positions and at different viewing distances, could provide a potential explanation for null zone preference. This may in turn help better understand why people with IN adopt a preferred head position. Each experimental chapter delves more deeply into the topics of discussion. A summary of the thesis content is given in the next section.

1.4 Thesis structure

This thesis consists of six chapters, including this introductory chapter. **Chapter two** provides a general overview of the materials and methods used for the experiments presented in this thesis. The materials section also provides a brief introduction into instrumentation used for automated eye occlusion. This is relevant to the experiment in Chapter five that involves convergence. Chapter two also includes a section on the use of pursuit analysis for calibrating IN eye movement data. Most importantly, a comprehensive review of the bPDF method for analysing fixational eye movement data is included. In addition, more details about the horizontal and vertical components of eye movements are given.

Chapter three concerns an investigation of the fixation characteristics at eccentric horizontal gaze positions in IN. This chapter includes results from existing IN data obtained from Dr Matt Dunn of the Research Unit for Nystagmus at Cardiff University (as experiments during the COVID-19 pandemic were not permitted), that have been analysed using the bPDF method. The aim of this chapter is to determine if fixation performance differs at the horizontal gaze positions tested (with respect to the clinical null zones).

Chapter four, using slightly different experimental conditions, comprises an investigation of fixation characteristics at eccentric gaze positions (up to ±45°). These results include bPDF analysis and psychophysical VA testing at these eccentric gaze positions. The aim of this chapter is to evaluate any changes in fixational eye stability and provide more information about visual performance at horizontal eccentric gaze positions. This information also provides a basis for comparing the performance of the typical oculomotor system when viewing straight ahead and at other horizontal gaze positions with that of people with IN when viewing at the null zone and away from the null zone. These

experiments will therefore provide information about the intrinsic properties of the oculomotor system, particularly the stability of fixation, at different gaze directions in people with IN as well as in typical participants.

In **Chapter five**, fixation at different distances is evaluated as a function of convergence. Here, fixation was quantified (using the bPDF method) in an experiment where participants with IN and typical participants performed a fixation task and a simultaneous automated cover test procedure. The use of the automated covers was necessary to evaluate the dynamics of achieving and maintaining vergence in IN, i.e. when each eye moves fixation away from the target, and takes up fixation, at each distance. Fixational eye movements at different distances is analysed in both groups of participants. This experiment is also aimed at determining the effect of convergence on fixational eye movements. In addition, in people with IN, quantifying fixational eye stability at difference distances provides novel findings of the typical amount of reduction in intensity that occurs with convergence (convergence dampening).

Lastly, a general discussion of findings and a highlight of potential future work is given in **Chapter six**. This chapter summarises all of the experimental findings concerning fixation, and how this relates to eye-in-orbit position, in typical participants and those with IN. Regarding convergence, future work relating to accommodation is considered. An abstract of an initial pilot study, conducted to evaluate the off-axis performance of the PowerRef3 for measurements in IN, is available in the Journal of Perception (Amiebenomo et al. 2020).

CHAPTER TWO

2 General methods

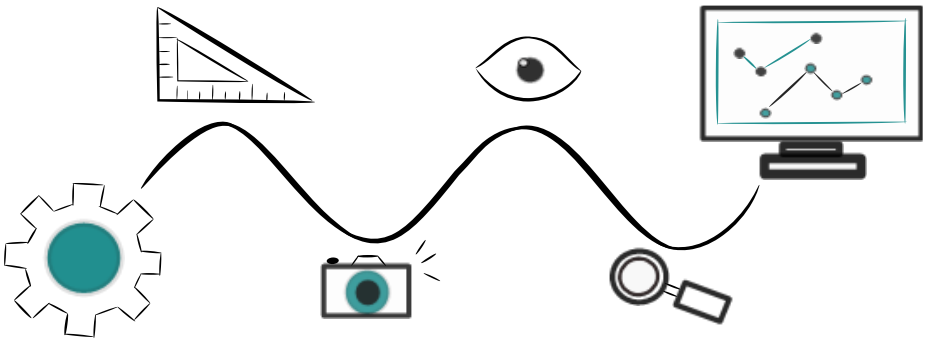

2.1 Materials

The following items of equipment were used for the experiments in this thesis:

1. *Eye tracker and head support unit*

For all experiments in this thesis, the EyeLink® 1000 plus eye tracker (SR Research Ltd., Ottawa, Canada), at a sampling rate of 1000 Hz, was used to record eye movements. This instrument projects infra-red (IR) light into the eye and predicts eye position through the light reflected off the cornea and pupil position. In other words, the eye tracker determines eye position by judging the position of the cornea light reflex relative to the pupil centre.

The EyeLink® 1000 plus can be set in five configurations described by its camera mounting options: Desktop, Tower, Arm, Primate and Long-range mounts. Desktop and tower mount are mostly used for research involving adults humans. However, for experiments presented in this thesis, the Eyelink® was configured with a desktop mount. This configuration was chosen in order to allow for eye tracking while participants viewed targets at a close distance of up to 25 cm and to accommodate an additional device (the occluder system discussed in Chapter five) which was installed up close to the participant. In addition, avoiding an extra barrier (i.e. the mirror system present with the tower mount) for IR passage during recording was crucial in order to reduce reflections and produce good data (Holmqvist et al. 2011). A combination of the Tower mount's IR reflective mirror, alongside the automated occluders and participants glasses, would have made recording difficult.

Figure 2-1: EyeLink® 1000 plus desktop mount
(source: https://www.sr-research.com/eyelink-1000-plus/)

The EyeLink® 1000 plus eye tracker has a typical accuracy of 0.25 to 0.50°, and a real-time data access of 2.2 ± 0.3 ms at 1000 Hz. In desktop mode, a trackable range of at most 32° is possible allowing the maximum viewing angle of a monitor display to be 32° horizontally and 25° vertically. The SR research head support (shown in Figure 2-3) enabled comfortable positioning of participants in front of the instrument. It consists of a head and chin rest, securely attached to a moveable table.

Other items of equipment included:

2. *Monitor screens.*

Different monitors were used depending upon the observer's viewing distance. This was necessary to allow the stimulus to be shown, at closer distances, without obstructing the eye tracker. For viewing distances of 100, 300 and 400 cm, a single moveable monitor (Hanns.G, model HE225DPB) measuring 47.5 cm (horizontal) was used to present the targets. At 25 and 50 cm, however, smaller screens (Lilliput, 869GL) measuring 15.2 cm were attached to a monitor mount (see Figure 2-3). All screens had a resolution of 1080 x 1920 pixels and a refresh rate of 60 Hz.

3. *Eye patch for occluding the nondominant eye during experiment.*
4. ***ETDRS** LogMAR VA chart*
5. *Automated occluder system, including IR pass occluders (Optolite®)*

The automated eye occlusion unit (Figure 2-2), as the name implies, is instrumentation designed to automatically cover the participants left or right eye during the experiment discussed in Chapter five. More details about the device and set up can be found in Section 5.2.2.

Figure 2-2: The automated occluder system

2.2 Ethics

Ethical approval was obtained from the School of Optometry and Vision Sciences Research Ethics Audit Committee (Project number – 1499). In addition, all participants gave their informed consent in writing before the experiment commenced. Participant recruitment, general conduct as well as the experiments were performed in accordance with the tenets of the Declaration of Helsinki.

2.3 Participants

Participants with IN were recruited from the existing research cohort of the Research Unit for Nystagmus (RUN) and were reimbursed in an amount of up to £50 for travel costs. Many new members recently joined this cohort using online forms. Therefore, this warranted a thorough pre-examination to confirm each participant's reported condition (see next section). Those examined as typical participants were recruited from the staff and student population of the School of Optometry and Vision Sciences, here at Cardiff University. The minimum number of participants planned to be seen for each experiment was 12. This is in line with previous studies which had a cohort of eight (Dunn et al. 2017), 11 (Wiggins et al. 2007) and 12 (McIlreavy, Freeman and Erichsen 2020).

Chapter three includes previous data collected from 18 participants with IN generously provided by Dr Matt Dunn, a member of the RUN, for analysis during the COVID-19 pandemic period. These participants were also recruited from the exciting RUN research cohort, and examined in the period between May 2014 to July 2015.

2.3.1 Pre-examination and exclusion

Prior to commencing the experiments, a diagnosis of IN, as reported by the participant or ophthalmologist (through written documents), was confirmed after a detailed history, slit lamp examination, optical coherence tomography (OCT) and high-speed eye movement recording. Using a 90 D lens, internal eye examination with a slit lamp was performed to examine the macular region and note any presence of hypoplasia. The presence of iris transillumination was also noted, as it is typical of participants with nystagmus and

albinism. The Spectralis OCT (Heidelberg engineering – HEUK01737) was also used to examine participants fundi. Foveal hypoplasia, if present, was also an indication of nystagmus being congenital (Bertsch et al. 2017). Other clinical test conducted for all participants include measurements of visual acuity at distance (using the EDTRS logMAR acuity chart) and near (using the N notation card), ocular alignment with the cover test, ocular motility, ocular dominance test (using the hole-in-card procedure) and interpupillary distance (IPD) measurement. Where a participant had a spectacle correction, the lens power was determined using a manual focimeter (Topcon lensmeter LM-8). Clinical ocular examination was performed alongside another member of RUN (Miss Katherine Ward). The following exclusion criteria were selected to minimise factors that may confound the results of the experiments.

1. Individuals under the age of 18
2. Those known to be pregnant, because of the possibility of the tasks being onerous.
3. Those who are considered vulnerable, or who are unable to give informed consent
4. Any history of eye disease or trauma that might affect visual performance (not including IN or congenital conditions associated with IN)
5. Any systemic disease and/or medications that may affect visual performance (not including any taken for congenital conditions associated with IN)

Inclusion criteria

For participants with nystagmus:

1. A clinical diagnosis of IN by the hospital eye service
2. Corrected VA of 1.6 logMAR (6/240 Snellen) or better.

For typical participants:

1. No previous clinical diagnosis of nystagmus or other history of eye movement disorders
2. Corrected VA of 0.0 logMAR (6/6 Snellen) or better.

2.4 Laboratory set up

The desktop mount eyetracker was positioned 50 to 60 cm from each participant (SR Research Ltd. 2014) on an adjustable height table. Monitor screens were also placed at the required distance for each experiment. Two small display screens, included in the set up for viewing at 25 and 50 cm, were mounted on a monitor mount such that, when not in use, they can be swung out of the way. The larger display was secured on a moveable table for use at 100, 300 and 400 cm. Figure 2-3 shows the laboratory main set up. All three displays were connected to one PC, while another host PC was exclusively allocated to data collection. An ethernet connection therefore allowed the sharing of EyeLink camera images (between both PCs) during patient set up, eye events and gaze position recordings. The room illumination was set to maximum, and this corresponded to 199 Lux at the chin and head rest.

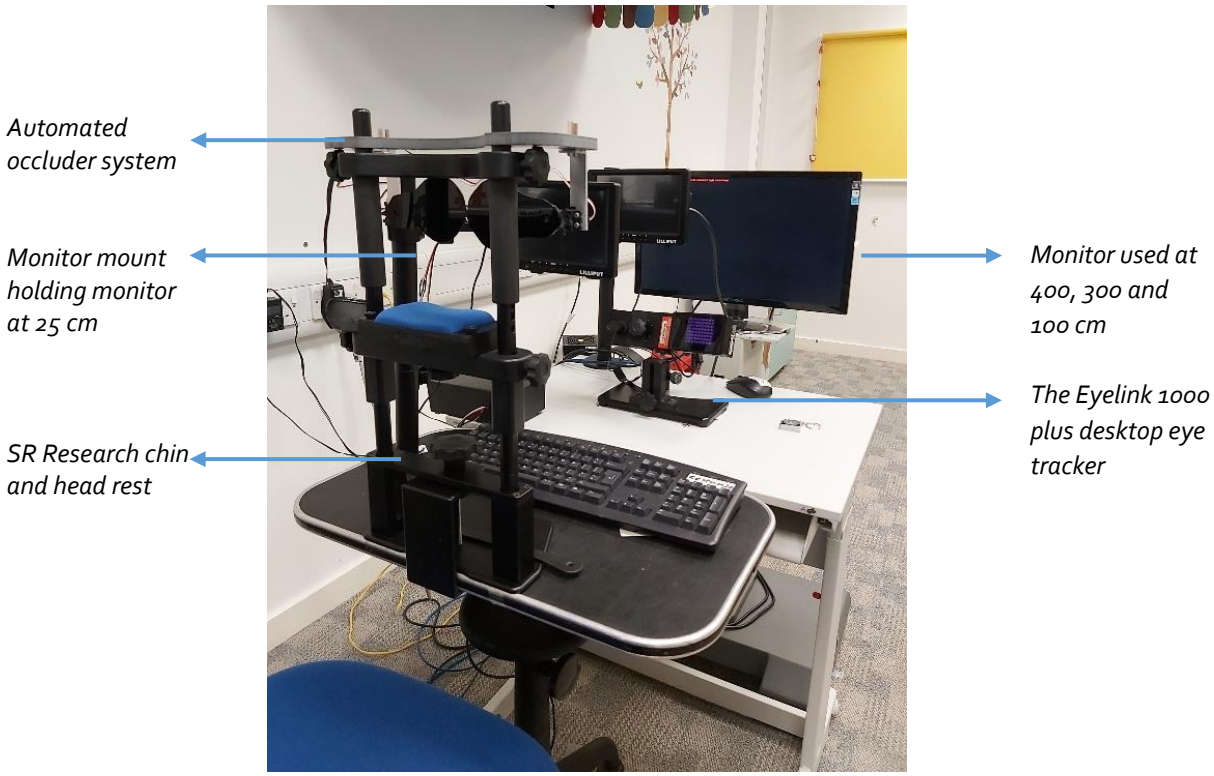

Figure 2-3: Main instrumentation used for experiments.
Diagram of the complete instrument setup with automated occluders included. Displays are shown placed at 25, 50 and 100 cm from the SR research head support.

2.5 Fixation stimuli

The test stimulus of a single 0.4° dot was programmed and presented in MATLAB (version R2016b; MathWorks, Natick, MA, USA), using the Psychophysics toolbox (Version 3.0.16). This 0.4° white dot was presented on a black background at the centre of each screen. A non-accommodative dot target was chosen because research has shown that in order not to intensify IN and avoid anxiety, the effort-to-see needs to be reduced. Therefore, by providing a target that does not necessarily have to be identified, the anxieties related to identification can be eliminated (Dell'Osso and Flynn 1979). Moreover, this same target type has been used successfully in a previous study involving fixation (McIlreavy, Freeman and Erichsen 2019).

The resulting dot size for each test distance was derived using the horizontal screen dimension and distance to the screen. Thus, irrespective of the viewing distance, the stimulus subtended the same angle. This is illustrated in Figure 2-4. Table 2-1 also shows screen size as well as expected and measured target size for each screen. During fixation, participants were instructed to look at the centre of this white dot.

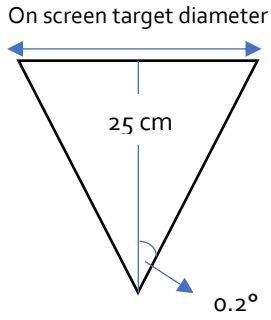

For example, at 25 cm test distance,
Target should subtend 0.4°, half of that will be 0.2°.
Therefore,
Half on-screen target diameter = tan (0.2°) x 25 cm = 0.087
On screen target (dot) diameter = 0.087 x 2
= 0.17 cm

Figure 2-4: Target size determination

Table 2-1: Expected and measured on screen target size

Test distance (cm)	Screen size (cm)	Expected (calculated) dot diameter (cm)	Measured on-screen dot diameter (cm)	Pixels per degree
25	15.2	0.17	0.25	56.77
50	15.2	0.35	0.50	111.08
100	47.5	0.70	0.70	71.86
300	47.5	2.09	2.05	212.09
400	47.5	2.79	2.75	282.52

2.6 Eye movement recording

2.6.1 Calibration

Prior to eye movement recording, a calibration is required. For typical participants, the eye tracker can be calibrated for measurements using calibration points arranged in a grid. In this case, participants were asked to serially fixate the 3 x 3 grid of calibration stimuli as each dot appeared randomly on the screen. Gaze at each calibration point was manually accepted by the participant by pressing the space bar or the enter key on the display keyboard. The calibration points were thereafter validated by re-presenting nine points in the same locations. Validation is necessary to confirm and show the gaze position accuracy obtained by the most recent calibration fitting. This is typical with recent eye-tracker vendor software, which reports accuracy after each calibration (Holmqvist et al. 2022). The further the validation error value (gaze position in degrees) is from zero (which represents the point where the target is presented), the more inaccurate was the calibration. Based on these calculations, the EyeLink software (SR Research Ltd. 2014) produces on-screen numerical outputs (representing accuracy) for 'Good', 'Fair' and 'Poor' calibration. In cases where accuracy was not sufficient, calibration was repeated so as to select one with the best accuracy during the validation test. Only the validations that were judged as 'Good' were accepted. A summary of the criteria the EyeLink software uses to judge validation is shown in Table 2-2.

Table 2-2: Grading validation error
Source: https://www.sr-research.com/support/thread-244.html?highlight=poor+calibration

Criteria	Worst point error	Average error
Good	< 1.5°	< 1.0°
Fair	between 1.5° and 2.0°	between 1.0° and 1.5°
Poor	> 2.0°	>1.5°

From initial pilot experiments, calibration and subsequent validation proved difficult with increasing distances up to 4 m. To demonstrate this, one 39 year old emmetrope was examined. Results from mean calibration errors (averaged over three recordings) are shown

in Figure 2-5. Findings indicate that, during the main experiments, calibration was going to prove difficult at distances of about 300 cm or more.

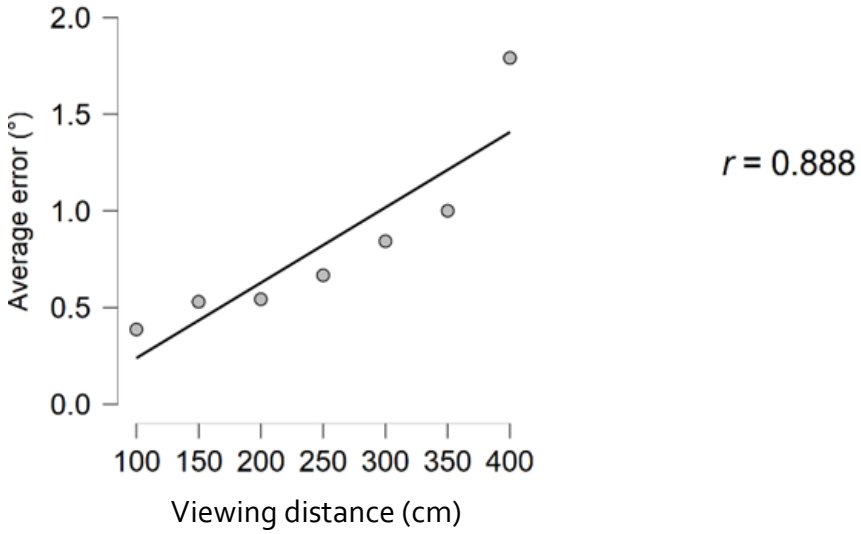

Figure 2-5: Validation error increases with distance

In addition, for participants with IN, a typical calibration procedure will not be easily achieved as a result of the continuous eye movements, and the inability to maintain fixation on the calibration targets. Therefore for an easier, more accurate and reliable calibration process, and to achieve a data set comparable with that obtained from people with IN, it was decided that a smooth pursuit calibration would be more appropriate for all participants during the main experiment. Smooth pursuit calibration has been used in previous studies (Drewes, Pfeuffer and Alt 2019; Blignaut 2017). With this method, attention is easily maintained, many points can be sampled, and it is time efficient.

Retrospective calibration using pursuit eye movement analysis

During a smooth pursuit calibration, the participant is required to follow a target as it moves across the screen. Thereafter, sampled points can be regressed with stimulus position. The regression coefficient obtained can then be applied retrospectively to calibrate other data from the same participant. For studies in this thesis, a typical 9-point calibration was performed by typical participants at 100 cm, followed by horizontal and vertical pursuit eye movement using a 0.4° dot target, similar in size to the dot used in the main experiment. This calibration target, also presented at 100 cm, moved at a speed of

4°/sec and amplitude of 12°, both horizontally and vertically. For participants with IN, the researcher performed a typical 9-point calibration on themselves so as to ensure eye movement recording obtained will be reasonable. Afterwards, at the onset of the experiment, the participant with IN is then asked to follow the pursuit target for calibration. Although previous research indicates that the accuracy of data is likely to be slightly reduced when calibration is done on a person other than the actual participant (Harrar et al. 2018) or using an artificial eye (Holmqvist and Blignaut 2020), one study found that data quality was improved for their 'difficult to calibrate' infant participants by calibrating on adults first (Kulke 2015). Based on their findings, it was recommended that, where calibration proves difficult, for example when testing people who are blind or visually impaired, using a single stand-in is a preferrable alternative which should only cause a small decrease in accuracy (Harrar et al. 2018).

In Figure 2-6, a sample pursuit calibration output for one participant with IN is shown. The eye movement output is seen to match that for target motion. As an example, during the vertical pursuit of the target (where the eye movements is seen to be less intense than in the horizontal eye movement graph presented on the left), the vertical eye movement output differed slightly from the actual position of the pursuit target. Retrospective calibration ensured that these eye movements are adjusted to their correct position, alongside the target movement as indicated by the arrows. The amplitude of pursuit target is seen to span ±6°, making a total of 12° each for four sweeps.

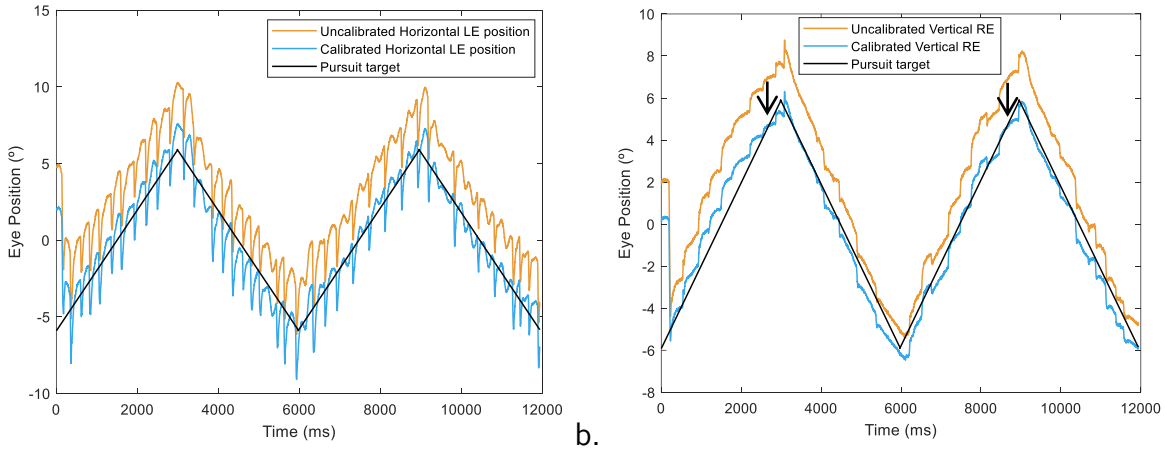

a. b.

Figure 2-6: Sample pursuit calibration output
These outputs show calibrated and uncalibrated data points from the left and right eye of participant IN08. (a) pursuit target moving horizontally across the screen; (b) pursuit target moving vertically across the screen. Notice the shift in eye position trace after the calibration regression coefficient was applied.

2.7 Processing and analysing eye movement data

2.7.1 The EyeLink Data Viewer

The EyeLink Data Viewer (SR Research Ltd., version 3.2.1) is the ideal data analysis tool that was specifically designed to enable interactive display, data processing and extraction of EyeLink Data File (EDF) data. After eye movement recording, data files were first inspected for consistency using the EyeLink Data Viewer. For the purpose of analysis, in the EyeLink Data Viewer, eye movement patterns during a fixation task consists of three major events namely: *blinks*, *saccades* having different spatial directions and temporal durations, and periods of actual *fixation* having different durations (Anantrasirichai, Gilchrist and Bull 2016). Blinks are detected as periods when the pupil size is very small or cannot be seen in the captured image of the eye. Eye position data 100 ms before and after identified blinks were also excluded in order to eliminate blink-related artefacts or blink saccades. In a previous study (Davies and Freeman 2011), 83 ms eye position data was removed from either side of a blink. To remove most artifacts, however, it is recommended to discard 100 ms of data before and after blinks (SR Research Ltd. 2014), therefore for studies in this thesis, ±100 ms of eye position data recorded before and after blinks were grouped together as blinks and later removed during analysis at the MATLAB interface.

The saccadic detection process of the EyeLink Data Viewer works by using both a velocity and acceleration criterion to detect a saccadic event. Saccades were detected using the default software threshold of velocity ≥ 22°/s; acceleration ≥ 3800(°/s)^2. Using more than one criterion is known to increase the chances of accurately detecting a saccade (Holmqvist et al. 2011). With the pixel per degree value for the test distance in which calibration was performed (100 cm), data were then reparsed and saved (in pixel values) for analysis offline using MATLAB (version R2019b; MathWorks, Natick, MA, USA).

2.7.2 Analysis using MATLAB

Prior to quantifying fixational eye movement in MATLAB, the correlation coefficient obtained from calibrating each participant's eye movement at 100 cm is first applied to the data collected during the experiment. Eye position data were then converted from pixels to degrees, drift corrected and then smoothed. Small body adjustments, such as head-mount

slippage when using head-worn eye trackers, pupil size changes and changes in the hardware and software setup are known to reduce the accuracy of measurement during the experiment when compared to the true gaze location, and this is called *drift* (Holmqvist et al. 2022). Since calibration was performed only at 100 cm, a drift correction for fixation stimulus was needed at all other positions in which experiment was carried out. This was necessary to know what represents the centre of the screen, as the screen was either moved from one point to another or interchanged during the experiment.

The Eyelink data viewer has built-in functions available to drift correct data points during experiments. This process however relies on the ability of participants to fixate stationary targets presented on the screen. As this is likely to prove difficult for participants with IN, a customised drift correction method was chosen given that people with IN may not be able to fixate steadily on the dots presented during the typical drift correction for the EyeLink. For this, a steady 0.4° white dot was presented at the centre of the screen (black) for 10 s; enough time to collect sufficient data representing about 40 fast phases from those with IN. The centroid X and Y values for output data were then subtracted from the eye position data to calculate the correction to be applied. In the case of data from participants with IN, the end of the saccades (fast phases of the nystagmus cycle, see Figure 1-10 in introduction) was used to derive the centroid X and Y data, given that data points from the saccade end points are known to represent target fixation (Hertle et al. 2002).

After calibrating data in MATLAB, blinks and other eye movements associated with blinks were excluded. Eye position (in degrees) was then smoothed using a low pass 4th order Butterworth low pass filter, at a cut-off frequency of 60 Hz (Mack, Belfanti and Schwarz 2017; Butterworth 1930). Due to the high sampling frequency of the eye tracker, some level of noise is introduced during the accurate tracking process. Therefore, smoothing is a necessary step (Liu et al. 2018), but it is important that the data are not overly modified, and hence the choice of a low pass filter.

2.7.3 The bivariate Probability Density Function (bPDF) method for quantifying fixation performance

As a result of the small eye movements associated with fixating a steady stimuli, it is often necessary to quantify fixation. In Chapter one, a detailed explanation of the inherent flaws

involved in analysing IN data using individual waveform components was given. In order to provide a more comprehensive assessment of fixational eye stability, as well as to allow the simultaneous evaluation of the horizontal and vertical components of the recorded eye movement trace, the bPDF method was chosen.

Probability density function is a statistical expression used to define the likelihood of an outcome (much like a probability distribution). A PDF represented graphically will have an area under the curve indicating the intervals in which measured values fall. This area under the curve can be further truncated at the tail ends of both sides to represent a certain percentage of the highest data points e.g. 95 or 68%. A normal or Gaussian distribution is an example of a PDF in which data is symmetric about the mean. In eye movement research, a bivariate PDF analysis which involves combining the horizontal and vertical components (variables) of recorded eye movement trace is an excellent way of evaluating accuracy and precision of recorded data. However, the methods of computing the resulting PDF may be an issue especially when the data in question are not normally distributed; as has been reported with fixational eye movement data (Castet and Crossland 2012).

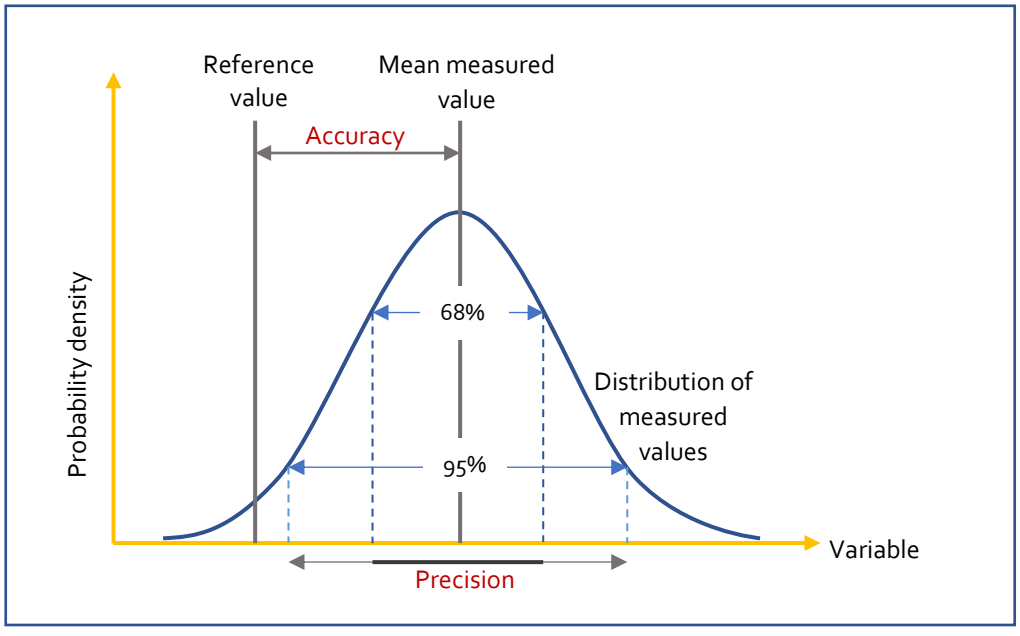

Figure 2-7: Illustrating data accuracy and precision as a PDF
Accuracy is represented by the distance between the mean measured value and the reference value (e.g. fixation point). Precision is the distribution area of measured values defined by the percentage number of highest data points. The larger the area, the farther away from the mean and hence less precise.

Recall the simple illustration of fixational eye movement data accuracy and precision described in Figure 1-15. This can be represented in the form of a PDF graph as shown in Figure 2-7, which also illustrates that data precision can change depending on the percentage level of highest data points chosen. Considering that, for people with IN, during fixation more data points are clustered towards the period of foveation (as illustrated in Chapter one: Figure 1-12), precision is better represented by 68% of the highest data points. This value is analogous to ±1 SD away from the mean.

Combining variables

A bivariate PDF of fixational eye movement can be computed using two distinct methods. The review by Castet and Crossland (2012) identifies the resulting span of fixation points from these two methods: the Bivariate Contour Ellipse Area (BCEA), and the isoline or contour line. The BCEA or what is otherwise known as the confidence ellipsoid (Steinman 1965; Skavenski and Steinman 1970; Raveendran, Bobier and Thompson 2019; Raveendran et al. 2020) is derived from the correlation between the horizontal and vertical components of the eye movement data. This BCEA represents the fixation span that comprise a certain proportion of the data points assuming these data points arose from an estimated bivariate Gaussian distribution. Therefore, this means that, for a BCEA analysis, the data are assumed to be normally distributed even though they may not be.

The less common, but more appropriate, method fit for fixational eye movement data analysis, is the non-parametric alternative, which does not make any assumption of data normality (Whittaker, Budd and Cummings 1988; Cherici et al. 2012; McIlreavy, Freeman and Erichsen 2019; McIlreavy, Freeman and Erichsen 2020). For this method, an isoline or contour line representing the highest data points is mapped out from an estimated PDF equating the bivariate data set. Figure 2-8 shows sample data points enclosed in the 68% and 95% isoline, as well as the 68% BCEA line (broken line). A comparison between the 68% isoline and BCEA lines indicate how the isoline better represents the region containing the highest density of data points.

This image has been removed by the author for copyright reasons

Figure 2-8: The 68% isoline and BCEA line (Source: Castet and Crossland 2012)
Figure shows a bivariate PDF represented by a two-dimensional surface. Data are 100 random points drawn from a bivariate normal distribution. X and Y are the horizontal and vertical eye positions, respectively. The two irregular full lines which surrounds the data points represent the 95% and 68% contour lines. The oval broken line represents the 68% BCEA. See figure 1, page 454 in referenced publication.

For this thesis, fixational eye movement was analysed using isolines or contour lines. However, going forward, the derived span of fixational eye movement data is referred to as an *isocontour.* Isocontours were derived from the horizontal target-relative eye position (one variable) and the vertical target-relative eye position (another variable). In addition, 68% was chosen as the preferred isocontour proportion as this is analogous to taking mean ±1 SD and will exclude extreme fixational eye movement values or outliers, and thus will not include the full range of IN eye movements. A comprehensive review of previous studies and what proportion was chosen is given in Table 2-3.

Table 2-3: A review of previous fixation studies

S/N	Study	Title	n	Age of participants (years)	Instrument	Target	Test distance (cm)	Fixation duration (s)	Level chosen for fixation data (%)
1	Crossland and Rubin (2002)	The use of an infrared eyetracker to measure fixation stability	6	< 40 years	Gazetracker using Eyelink software (version 2.04) at 250 Hz	Red cross of height 2.5°	50	10 (3 trials)	68
2	Crossland, Culham and Rubin (2004)	Fixation stability and reading speed in patients with newly developed macular disease.	25	-	Gazetracker using Eyelink software (version 2.04) at 250 Hz	3° diameter round black target with an 18′ (0.3°) central white part	50	10	68
3	González et al. (2006)	Fixation stability using radial gratings in patients with age-related macular degeneration	18	72 - 92 (case) 23 - 72 (control)	Video based corneal reflection eye tracker at 60 Hz	A 9-cycle square-wave radial grating measuring 5° in diameter and a white 0.5° disc	100	6-7	63.2
4	Cherici et al. (2012)	Precision of sustained fixation in trained and untrained observers	14	20 - 40	Generation 6 Dual Purkinje Image (DPI) eye tracker at 1000 Hz	4′ (0.07°) dot on a black background	125	5	75

S/N	Study	Title	n	Age of participants (years)	Instrument	Target	Test distance (cm)	Fixation duration (s)	Level chosen for fixation data (%)
5	González et al. (2012)	Eye position stability in amblyopia and in normal binocular vision	31	31.5 ± 10.7 (case) 30 ± 12.7 (control)	EyeLink 1000, at 250 Hz	3° red cross on a white background	60	15	68.2
6	Kumar and Chung (2014)	Characteristics of fixational eye movements in people with macular disease	30	48 - 89 (case) 62 - 77 (control)	Scanning laser ophthalmoscope (SLO) at 30 Hz. Eye movement extracted from recorded video at 540 Hz.	1° fixation cross (2° for those with VA <0.7 logMAR	-	Trials of 30 s each	68
7	Shirama et al. (2016)	Ocular fixation abnormality in patients with autism spectrum disorder	32	26.3 ± 1.9 (case) 27.7 ± 2.1 (control)	Remote type eye tracker (model: ViewPoint MHU03, Arrington Research), 220 Hz.	Black cross subtending 0.81°	57	15	68.3
10	Raveendran, Bobier and Thompson (2019)	Binocular vision and fixational eye movements	11	27 ± 4	EyeLink-II, at 500 Hz	1° fixation cross on a grey background.	40	4 trials of 30 s each	68.2
11	Bhattarai et al. (2019)	Fixation stability with Bessel beams	16	18 - 42	Eye Tribe tracker at 30 Hz	7 random targets per trial	50	20 per trial	68.2

Deriving isocontours using bPDF analysis

During the bPDF analysis process, the probability density function which corresponds to a given bivariate data set was estimated using kernel density estimation. This reflects the area of eye movement. Kernel density estimation has been identified as the most popular nonparametric method for density estimation (Botev, Grotowski and Kroese 2010). An open source function – kde2d (Botev 2015), specifically designed to estimate kernel density in MATLAB, was utilized. A detailed explanation of this method is available (McIlreavy 2016) but as a summary, the basic steps involved include:

1. Bounding box specification and PDF calculation – The bPDF data were computed on the X and Y distribution of relative eye positions. In order to construct the bivariate PDF, an area with margins is first set. The resulting bounding box and margins were customised to fit each data set by utilizing the maximum and minimum horizontal (x) and vertical (y) target-relative eye movement data (see formulas below). Specifying this bounding box ensures that isocontours for all data points, including the one for the least probable data, are completely enclosed. A default mesh resolution (factor which corresponds to the bin size of a bivariate histogram) of 256 x 256 grid was made to spread equally over the derived bounding box and used to calculate the PDF.

$$(x_{lower}, y_{lower}) = \left(\left(x_{min} - \frac{x_{range}}{4}\right), \left(y_{min} - \frac{y_{range}}{4}\right)\right)$$

$$(x_{upper}, y_{upper}) = \left(\left(x_{max} - \frac{x_{range}}{4}\right), \left(y_{max} - \frac{y_{range}}{4}\right)\right)$$

2. Smoothing the bivariate PDF (or area of eye movement) is another necessary step to account for differences in individual data and produce more accurate data. Just like the individual bin width used for histograms, a bandwidth or window width is used for the bPDF analysis to represent the standard deviation of the Gaussian kernel. Variation in constructing the bPDF can arise through different values for the kernel bandwidth. In simple terms, the kernel bandwidth is a smoothing factor. A

smaller kernel bandwidth will result in 'finer' bPDF whereas a larger kernel bandwidth will result in a 'coarser' bPDF. It is important to choose an appropriate bandwidth, and bootstrapping (Faraway and Jhun 1990) may be one approach to finding the optimal bandwidth. However, to determine the most appropriate bandwidth for ocular data, it has been suggested that the kernel bandwidth value should not be less than the eye tracker's accuracy (Castet and Crossland 2012). Since the EyeLink 1000 plus that was used for this study has an accuracy of at least 0.25°, the kde2d function was modified to produce data points with the fixed minimal bandwidth of 0.25. An example is shown in Figure 2-9 of how the peak density (accuracy) of fixational eye movement data differ when the bandwidth is changed.

This image has been removed by the author for copyright reasons

Figure 2-9: Output using two different bandwidths (Source: Castet and Crossland 2012)
Two- dimensional Isocontours (68 and 95%) and 68% BCEAs (broken lines) are highlighted for a sample of 100 points taken from a bivariate non-Gaussian random variable. Notice the difference in estimation of highest density points for the isocontour and BCEA method. Diagram on the left was plotted using a bandwidth of x = 0.21 and y = 0.44, and the resulting peak density was 0.089. For the diagram on the right, a bandwidth of 1 was chosen for x and y axis, and the resulting peak density was 0.061. See figure 2 (top right and top left), page 455 in referenced publication.

3. Selecting the 68% isocontours and quantifying fixation performance: The isocontour which surrounds 68% of data points was extracted using the *contour* function available in MATLAB®. Sometimes, recorded data points could exists as multiple islands of data or holes of data points embedded in other data. In these cases, multiple 68% isocontours were corrected for and computed as a single

isocontour. To establish the relationship of multiple contours and produce a contiguous image, an open source function – *contour2area* (Sundqvist 2010), available in MATLAB® was utilized. Furthermore, the contour data were extracted from the contour matrix of plots (using an open-source function called *contourdata* (Hanselman 2012)), and finally, using the extracted contour data, the *ContourMetrics* function written by McIlreavy (2016) was utilized to calculate the isocontour centroid, total area, as well as the ratio and orientation of its major and minor axes (McIlreavy, Freeman and Erichsen 2019; McIlreavy, Freeman and Erichsen 2020); values of which inform the accuracy and precision of the fixational eye movement data.

Further depictions of the extracted isocontour that encircles the gaze positions with the highest 68% density are presented in Figure 2-10. *Accuracy*, represented by accuracy rho, was computed as the length of the vector from the centre of the isocontour to the target, wherein the closer the value is to zero the more accurate the measured data. *Precision* on the other hand was determined by the total area, as well as the shape factor of the isocontour. A larger isocontour area would indicate relative eye positions are largely spread, and hence less precise. The shape factor, which provides more information on the isocontour symmetry, is obtained from the ratio of the minor to major axes. Whereby the minor axis indicated the position of least spread in eye positions and the major axis the position of greatest spread in eye position; signifying more imprecision. Values close to one indicate an almost equal distribution of eye position along both axes, which therefore means that the isocontour was more nearly circular. Furthermore, the orientation of the isocontour major axis was determined. This orientation is an indication of the direction of imprecision, with respect to the horizontal plane. In other words, this signifies the direction of the major axis of imperfection.

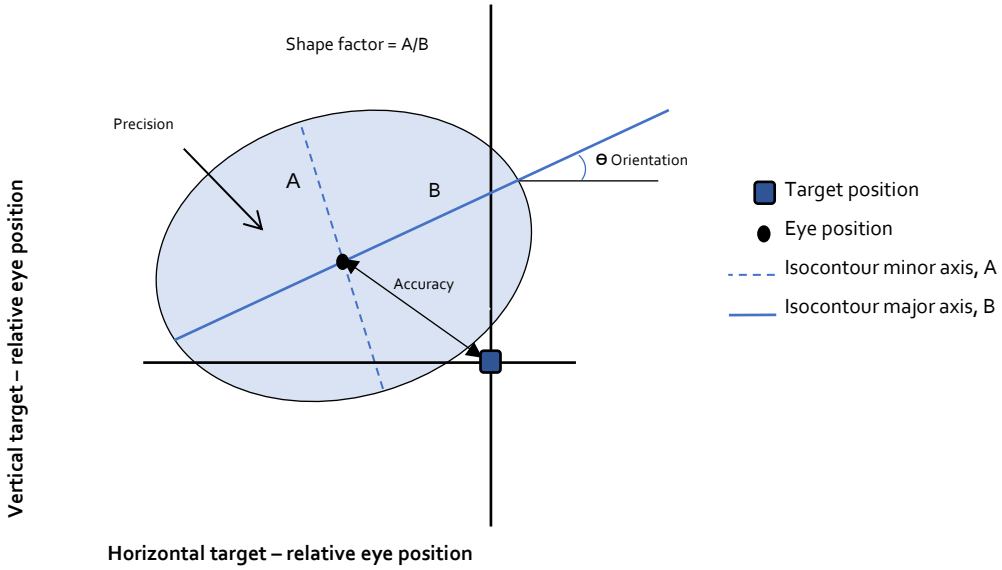

Figure 2-10: Schematic 2D representation of the metrics used to quantify fixation.
The blue oval represents the contour with 68% of highest density data points. The major axis (solid blue line) represents the region of greatest imprecision, and the angle which this axis makes with the horizontal plane gives a measure of orientation.

Validity of the bPDF construction

Following notes from page 48 (item 2), the variability within the data was determined using bootstrapping. The two-dimensional eye position distributions for two participants (one control participant and one participant with nystagmus) at two gaze angles (primary position i.e. 0° and 45°) was resampled with replacement (i.e., bootstrapped). A thousand iterations of the bootstrapping procedure per eye position distribution was performed. For clarity, the number of samples in each eye position distribution, the number of resamples with replacement per iteration, and the number of iterations is tabulated in Table 2-4.

Table 2-4: A summary of the bootstrapping procedure carried on the four eye position distributions.
Two gaze angles were chosen for this analysis, 0° and 45°. The analysis includes data from one control participant (C01) and one participant with IN (IN16).

	Control		IN	
	0°	45°	0°	45°
Number of samples in eye position distribution	336,574	308,364	646,521	604,065
Number of resamples with replacement per iteration	336,574	308,364	646,521	604,065
Number of iterations	1,000	1,000	1,000	1,000

For each iteration, the 68% isocontour was then computed along with accuracy (the vector distance and angle of the centroid of the isocontour relative to the target), the isocontour centroid x and y coordinates, precision (the area of the isocontour) and shape factor.

Note that for brevity, a drift correction (a correction for the x and y offset of gaze position) was not performed prior to the analysis. However, it is important to emphasise that this would not affect the results for variability. E.g., consider a distribution with a mean of 4 and standard deviation of 2.5. Adding or subtracting a constant to all values would alter only the mean not the standard deviation.

After having derived the metrics, it was anticipated to plot the sampling distribution (i.e., a histogram of calculated outputs) for each metric, for each gaze position and for each participant. From these distributions it was intended (assuming normality) to take the 25th and 975th ranked values as the 95% confidence intervals. However, because the results were truncated to 4 decimal places, and the variability within the results so small, it was not possible to construct a histogram. Therefore, to estimate the variability, the mean and standard deviations of the sampling distributions for each metric was computed and summarised in Table 2-5. These findings, therefore, indicate that with a fixed minimal bandwidth of 0.25 our results show no meaningful variability in the PDF construction.

Table 2-5: A summary of the sample distributions for each of the metrics.
Data are the mean and standard from one control participant (C01) and one participant with IN (IN16).

	Control		IN	
	0°	45°	0°	45°
Accuracy rho (°)	5.0277 ± 0.0003	4.8473 ±0.0004	4.2343 ± 0.0011	1.4697 ± 0.0010
Accuracy theta (radians)	-1.7549 ± 0.0001	-1.8129±0.0002	2.4365 ± 0.0002	2.3526 ± 0.0010
Centroid x coordinate (°)	-0.9208 ± 0.0006	-1.1623 ± 0.0010	-3.2248 ± 0.0009	-1.0355 ± 0.0012
Centroid y coordinate (°)	-4.9427 ± 0.0004	-4.7059 ± 0.0004	2.7441 ± 0.0011	1.0430 ± 0.0013
Precision $(°)^2$	0.5702 ± 0.0008	0.5663 ± 0.0014	2.3449 ± 0.0053	2.0493 ± 0.0082
Shape factor	0.6895 ± 0.0015	0.7277 ± 0.0020	0.9585 ± 0.0022	0.7120 ± 0.0019

Horizontal and vertical axis range of data spread

In line with one of the main aims of this thesis, a knowledge of the spread of imprecision along the vertical and horizontal isocontour axis, and not accuracy, will provide a better evaluation of the horizontal and vertical components of eye movement trace. This is because accuracy, which is basically a measure of the mean of the distribution, could be the same for very different degrees of precision. Furthermore, the ratio of the major and minor axes of the isocontour (shape factor) will also not tell the true value of the degree of imprecision. Therefore, it was necessary to compute the precision along the individual minor and major axis, respectively; otherwise known as the eye position range about the isocontour or the magnitude of spread. Recall that the IN eye movement may not always be horizontal only, and in most cases the isocontour axes are usually somewhat tilted. Therefore, the orientation of the isocontour major axis (i.e. the angle between the major axis and the horizontal plane) together with the precision values of contour area and contour shape become useful to derive the horizontal and vertical axis range of the isocontour. This was necessary to account for cases where the major and minor axis were oblique.

For example, assuming for a particular gaze angle the derived isocontour metrics of contour area, contour shape and major axis orientation were 1.56(°)², 0.72 and 21.91°, respectively. Formulas to obtain the maximum horizontal and vertical span of the isocontour can be obtained from that used to obtain the corresponding major (x range) and minor (y range) radius length if it were an ellipse. In this case,

$$\text{x range} = \sqrt{[(\text{major AL}/2)^2 \times \cos^{\circ}(\text{major AO})^2 + (\text{minor AL}/2)^2 \times \sin^{\circ}(\text{major AO})^2]}$$

$$\text{y range} = \sqrt{[(\text{major AL}/2)^2 \times \sin^{\circ}(\text{major AO})^2 + (\text{minor AL}/2)^2 \times \cos^{\circ}(\text{major AO})^2]}$$

AL = Axis length, AO = Axis orientation

To derive the major and minor axis lengths used in the formular above, recall that a shape factor 0.72 was obtained from a ratio of the minor and major isocontour axes as described in Section 2.7.3 and Figure 2-10.

If a = half the minor axis and b = half the major axis,

$$\text{Shape factor } (a/b) = 0.72$$

$$a = b \times 0.72$$

since area (precision, in the case of the isocontour) of an ellipse is:

$$\pi \times r \times r$$

therefore,

$$\text{area} = \pi \times (b \times 0.72) \times b$$

$$b \times b = \frac{\text{area}/\pi}{0.72}$$

$$b^2 = \frac{\text{precision}/\pi}{0.72}$$

$$b = \sqrt{\frac{1.56/\pi}{0.72}} \quad \text{and} \quad a = \sqrt{\frac{1.56/\pi}{0.72}} \times 0.72$$

Major axis length = 2 x b
Minor axis length = 2 x a

Substituting into the initial enclosed formulas above, the horizontal (x) axis range and vertical (y) axis range obtained will be 1.60° and 1.37°, respectively.

Recall that the 68% isocontour is derived excluding outliers or data points with lower density. To illustrate the effect of truncating the data points on the resulting x and y axis range, sample fixation data (shown in Figure 2-11) are analysed from one participant during fixation at two different gaze angles. For this participant, the IN oscillations had a greater intensity in the horizontal component. Using simple histograms to estimate the position of highest density, we can see that, for example, while fixating at the -45° position, the amplitudes of eye position in the horizontal and vertical eye position trace were at least 5° and 0.5°, respectively (considering the whole six minutes eye position trace during task). However the resulting isocontour range along the x and y axis were computed as 6.63° and 1.11°

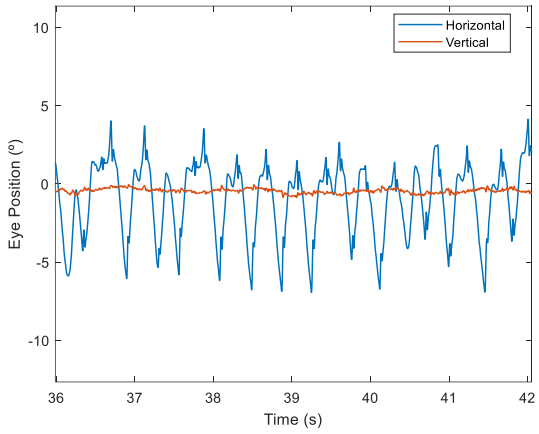

a(i)

Isocontour H range = 6.63°

Isocontour V range = 1.11°

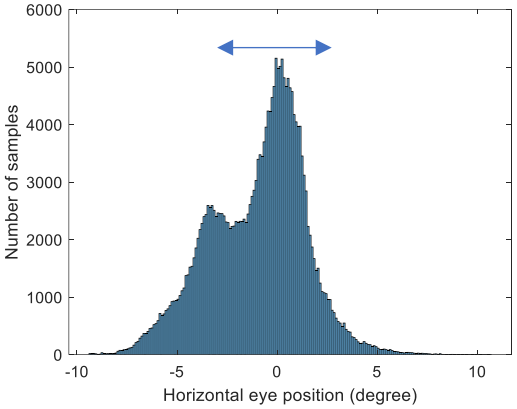

a(ii)

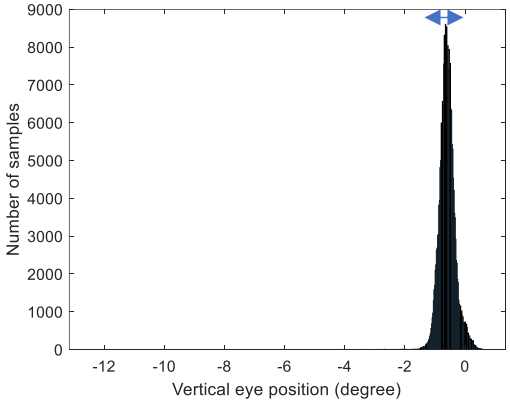

a(iii)

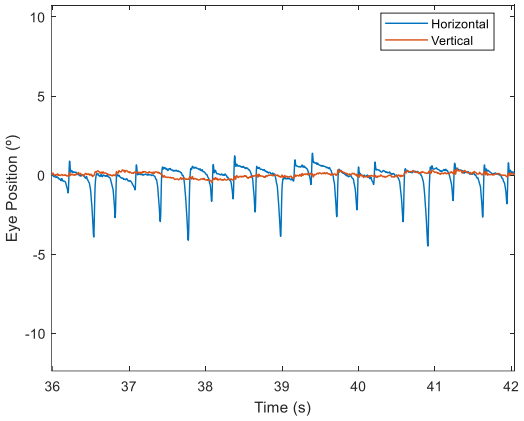

b(i)

Isocontour H range = 1.60°

Isocontour V range = 1.25°

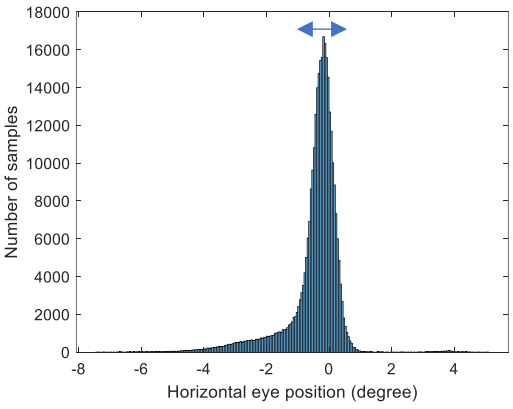

b(ii)

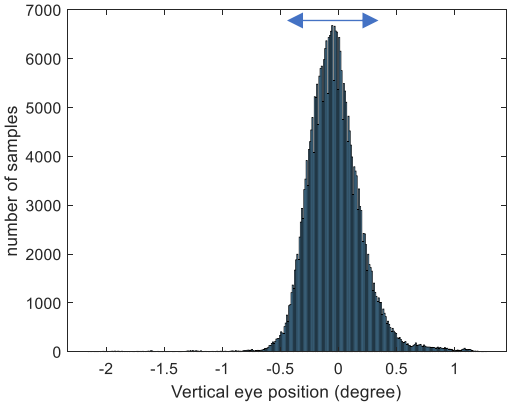

b(iii)

Figure 2-11: Illustrating the horizontal and vertical axis range
Section of eye position trace are shown for participant IN06 while fixating monocularly at two extreme gaze angles (a) at -45° and (b) at 45°. Alongside the 6 s section of eye movement trace is the derived horizontal (ii) and vertical (iii) eye position histogram plot for the entire duration of the fixation task which lasted about 6 min. The x-axis of the histogram plots represents the wide spread of recorded data points. Peak density can be found at the highest point of the histogram. An estimate 68% isocontour would be derived from the blue double arrowed lines across the top of the histograms. Recall that this horizontal and vertical range computation also takes into consideration the major axis orientation and the shape factor. H = horizontal, V = vertical.

The illustrations given above have implications for the analysis presented in the rest of the thesis. Despite the fact that the x and y axis ranges are restricted to 68% of the highest density data points, computed data presented in the subsequent chapters reveal that any modifications in waveform amplitude occurring as a result of a change in fixation position is still reflected in the computed axis ranges. Moreover, the data presented above have demonstrated that this difference in the X and Y component trace is adequately accounted for.

2.7.4 Statistical analysis

All data including the bPDF metrics of accuracy and precision were analysed using Microsoft Excel (version 2304) and JASP (version 0.16.1.0) (Love et al. 2019), at an alpha of 0.05. At the JASP interphase, a one-way or repeated measure analysis of variance (ANOVA) were used to find difference among group(s) of means depending on the number of independent variables. While computing the ANOVAS, the Mauchly's test was used to validate the repeated measures ANOVA. Where Mauchly's test indicated assumption of sphericity was violated, the Greenhouse-Geisser correction was then used to produce more accurate results. In addition, Pearson's correlation analysis were also used to determine relationships between variables.

CHAPTER THREE

3 Fixation characteristics at eccentric gaze positions in infantile nystagmus

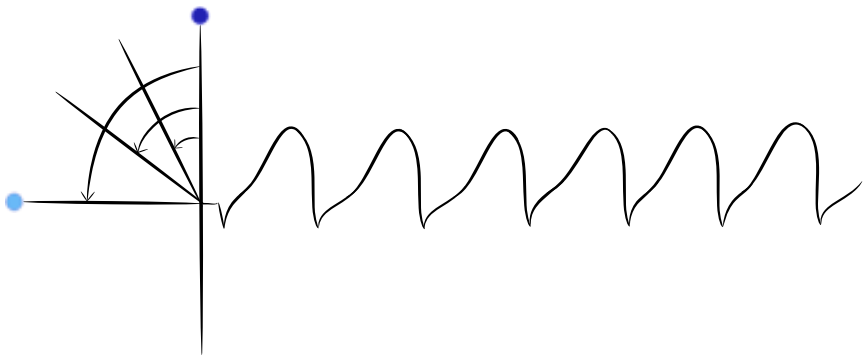

3.1 Introduction

Many people with infantile nystagmus (IN) are known to prefer using their null zone, but why they do so has remained elusive. Various objective factors are known to influence the choice of the null zone but do not adequately explain why there is a preferred, often eccentric gaze angle. In this chapter, quantifying the inevitable small fixational eye movement at different angle of gaze and the potential use of measures of their accuracy and precision, to describe fixation performance, is explored to provide a better understanding of the basis for null zone preference.

3.1.1 The multiplanar nature of the IN waveform and its possible implications for null zone preference

Following from discussions in Chapter one, the IN waveform could also have some torsional and/or vertical components, which were found to be present in 22% of 224 subjects (Abadi and Bjerre 2002). The clinical detection of the torsional component is difficult because the horizontal and torsional component may be phase locked (Averbuch-Heller et al. 2002) however, and requires high sampling eye tracking methods (Clark et al. 2019). One inherent flaw in current methods of evaluating the null zone is the fact that computation is done using only the horizontal eye recordings. Therefore, the contributions of any vertical eye component or its relationship with the horizontal eye position as a function of gaze angle remain unknown.

The bPDF analysis evaluates both the vertical and horizontal components of the eye movements, including the calculated metrics for the direction of inaccuracy and the orientation of imprecision (indirectly accounting for the plane of IN oscillation) (McIlreavy, Freeman and Erichsen 2019; McIlreavy, Freeman and Erichsen 2020). Therefore, this suggests that quantifying fixational eye movement stability using all of the relative eye positions (entire waveform) as well as both the relative horizontal and vertical components may be a better way to evaluate the eye movements during fixation at different gaze angles.

With IN, when the image of the target is on the fovea (foveation), retinal image slip velocity is reduced and therefore VA increased (Dell'Osso et al. 1992). As mentioned previously, the

oscillations of each eye during fixation will differ with gaze angle and have been particularly found to be unequal, in one subject, for a range of ±30° gaze angle (Dell'Osso 1973). Other studies, which evaluated fixation in IN at different gaze angles also used an analysis of one or more of the IN waveform parameters, or a section of the eye movement waveform (slow phase velocity or foveation) in one component (Dell'Osso et al. 1992b; Abadi and Bjerre 2002; Abadi and Whittle 1991; Abadi and Dickinson 1986). Only a few have utilized an analysis of the PDF of eye position data, which invariably will include the amplitude, frequency and all of the slow and fast phases (accounting for all waveform types) of IN data (Cherici et al. 2012; Zahidi 2019).

If we liken viewing at the null zone to viewing at primary position in typical participants, and the role of the neural integrator to stabilize eye position at eccentric gaze, turning ones gaze to an eccentric position will require the action of the neural integrator to keep it in place (Leigh and Zee 2015). Therefore, a preference for the null zone (which could be exhibited by more stable fixational eye movement or better fixation performance) could show that it is indeed the intrinsic property of the oculomotor system to become unstable at other gaze positions besides the null. These findings of fixation performance, quantified using the accuracy and precision of eye position data, could in turn give added information to why people with IN prefer to use their null zones. However, while viewing at 'eccentric gaze' positions, the question becomes whether the vertical component of eye position changes alongside the horizontal component as a function of gaze angle. It is therefore crucial to know if it is just the horizontal eye movement component or both a horizontal and vertical eye movement components which contribute to fixation preference for a given range of horizontal gaze angles.

Furthermore, due to the importance of eye examinations during IN treatment regimens, findings from this experiment will also help us to better understand the implications of 'eccentric gaze' and its role in fixation performance during clinical tests such as fundus photography, OCT scans or microperimetry.

3.1.2 Aim and objectives

The aim of this chapter is to provide novel measurements of fixational eye movement performance as a function of eccentric gaze, using the bPDF method in participants with IN.

Specific objectives include:

1. To quantify the accuracy and precision of fixation at eccentric gaze positions
2. To evaluate the contributions of the vertical as well as horizontal components of eye movements to fixation performance at eccentric gaze positions.

3.1.3 Hypotheses

Investigations carried out were to determine whether the gaze angles had impact on either the accuracy and/or the precision of fixational eye movements, and whether there was a difference between the horizontal and vertical components during fixation. Therefore, the null hypotheses are:

1. The accuracy and precision of fixational eye movements do not change at all gaze directions in people with IN.
2. The horizontal and vertical eye movement components contribute equally to fixation performance at gaze angles.

3.2 Methods

The data presented in this chapter were generously provided by Dr Matt J. Dunn of the Cardiff University Research Unit for Nystagmus (RUN) for the present analysis. This was necessary because, during the COVID-19 pandemic in the lockdown period spanning from 2019 to 2021, participants with IN could not be invited into the lab. The experimental set up and methods differ slightly from those previously presented in Chapter two (General methods). Any differences will be noted and explained.

3.2.1 Participants

Data from 18 participants with IN, recruited from an existing participant cohort of the RUN, at Cardiff University, were analysed for this study. Ethical approval was obtained from the School of Optometry and Vision Sciences Research Ethics Audit Committee (Project number: 1380). All participants gave their informed consent in writing before the study commenced. Prior to commencing the experiment, a diagnosis of nystagmus as reported by the participant or ophthalmologist, was confirmed by an optometrist after a detailed history, slit lamp examination, OCT, and high-speed eye movement recording.

3.2.2 Laboratory set up

The EyeLink® 1000 plus eye tracker (SR Research Ltd., Ottawa, Canada) was set, in desktop configuration, to record eye position while the participant viewed a large display screen from a distance of 100 cm. It is presumed that at this 1m distance, the likelihood of convergence dampening affecting the results is minimal and the results should be similar to distance viewing. To explain this further, if we assume the typical interpupillary distance of an adult is 63 mm (Murphy and Laskin 1990), each eye would then converge by an angle of 1.80°; a value considerably less than 4° (or 7^{Δ} base out) previously found to induce convergence dampening (Serra et al. 2006). Using a CRT projector (Christie DS+26), stimuli were rear projected onto a dual display projector screen setup. This display screen had a resolution of 1280 × 1024 pixels and a width of 1.43m. Figure 3-1 illustrates the set up for this experiment.

Calibration was performed by detection of foveations. Participants directed their gaze to 45 different positions spanning ±20° in each axis (nine equal steps horizontally and five steps vertically; each fixated twice, for 5 s each time). An algorithm (Dunn et al. 2019) was used to isolate only the times when the eyes were foveating for 10% of the total slow phase period in each IN cycle. The regression coefficient model derived was subsequently applied, using MATLAB version R2019b (The MathWorks Natick, MA, USA), to calibrate the raw eyetracker signal.

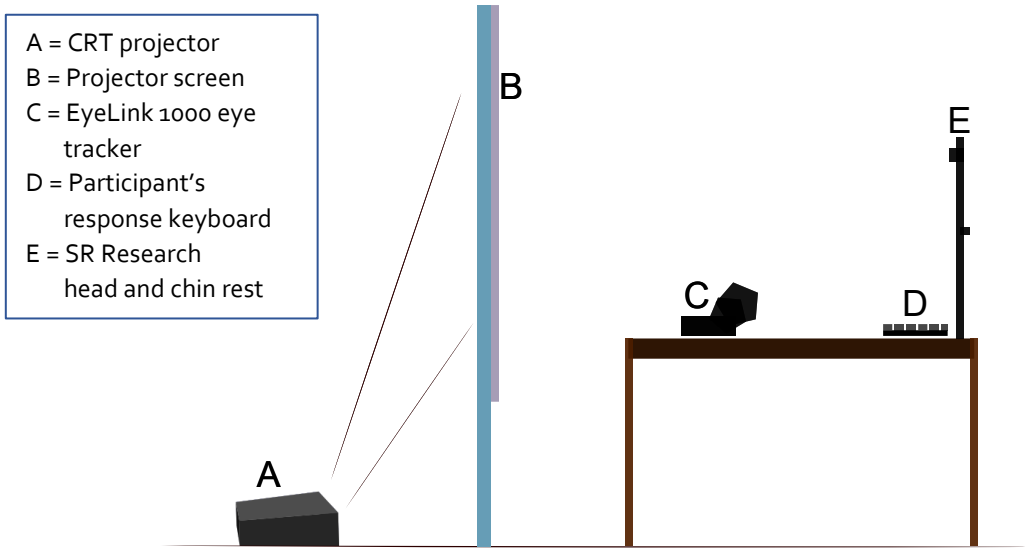

Figure 3-1: Laboratory set up

3.2.3 Procedure

Participants were comfortably stabilized in the SR Research chin and forehead rest after which measurements were obtained while fixating a 1° target (Thaler et al. 2013) rear-projected onto the screen, at nine horizontal positions spanning ±20° (at 5° intervals) and five vertical positions. Room lighting was turned off during the experiment. The room lighting being on or off is not likely to affect eye tracking performance because the EyeLink camera does not operate in the visible light spectrum (SR Research Ltd. 2014).

During recording, each position was tested twice in a pseudorandom order, to compensate for any time-based changes in the waveform that may have resulted from the likely discomfort arising from using positions of gaze not in their null zone. Eye movements were recorded monocularly, from each eye, and binocularly. However, analysis for this chapter was limited to using data from the nine positions across the midline (i.e. y = 0) and from the eye with the better VA. Where both eyes had equal VA, the right eye was chosen.

Eye movement data processing

Data files were first visually inspected to ensure successful eye movement recording using EyeLink Data Viewer (SR Research Ltd., version 3.2.1). Eye movements associated with

blinks were identified to be excluded, as described in section 2.7. Saved data were thereafter analyzed using MATLAB (version R2019b; MathWorks, Natick, MA, USA).

Each trial for a given stimulus position consisted of 5,031 ms of data. Of these, the initial 800 ms of eye position data from each stimulus position were removed to allow participants sufficient time to move their gaze toward the new target. Since data were obtained twice from each stimulus position, both sets of data were concatenated. Therefore, after removing the initial 800 ms of data in each case, a total of about 8.4 s of data were left to analyze for each stimulus position. The filtered eye position data were thereafter subjected to a bPDF analysis as described in Section 2.7.3 (McIlreavy 2016) to determine the accuracy and precision with which participants fixated.

3.3 Results

3.3.1 Participant information

The clinical data for all participants are represented in Table 3-1. Twelve females and six male participants were seen, aged 18 to 72 years (mean and SD: 43.4 ± 16.4 years).

Table 3-1: Participant clinical data

Participant	Age/sex	Diagnosis	Eye examined	VA (logMAR)	*Clinical null
P010	53/F	Idiopathic	Left	0.48	Left gaze
P012	65/M	Achromatopsia	Right	0.98	Right gaze
P016	30/M	Idiopathic	Right	0.50	Up gaze; Nystagmus greater in right gaze
P018	47/M	Unknown macular defect	Right	0.32	Left gaze
P019	72/M	Idiopathic	Right	0.30	PP; nystagmus greater in left gaze
P020	23/F	Idiopathic	Left	0.02	Right gaze
P021	49/F	Albinism	Right	1.36	Nystagmus greater in left gaze
P022	28/F	Albinism	Right	0.32	PP and right gaze
P023	25/F	Albinism	Left	1.10	Left gaze
P024	31/F	FMNS, Achromatopsia	Left	0.80	Not applicable
P025	43/F	Idiopathic	Right	0.60	Right gaze
P026	61/M	Albinism	Left	0.52	Right gaze
P027	45/F	Optic atrophy	Right	-0.06	PP; Nystagmus greater in right gaze
P028	57/F	Idiopathic	Right	0.56	PP; Nystagmus equal in left and right gaze
P030	54/F	Optic atrophy	Right	0.80	Right gaze
P031	24/F	Idiopathic	Right	0.32	Left gaze
P033	18/F	Aniridia	Right	1.30	PP; Nystagmus greater in right gaze
P034	57/M	Idiopathic	Left	0.02	PP; nystagmus greater in right gaze

*Clinical null was determined by asking participant to look at a pen torch presented at near in three positions, left, right and straight ahead, and observing the eye movements. PP = Primary position.

3.3.2 Fixation performance at gaze positions

Measures of accuracy and precision were used to quantify fixation performance at gaze positions. A sample of a participant's eye position and bPDF analysis at three gaze positions is shown in Figure 3-2. Data obtained from all participants are further represented in Figure 3-3. It is interesting to note that, in sample eye position plots, a significant amount of

vertical component is found (especially when viewing at the -20° position). If an evaluation of horizontal eye movement amplitude or intensity were done, this vertical eye position information would be left uncaptured. It can also be seen how varied the IN waveform is while viewing at the three different fixation positions.

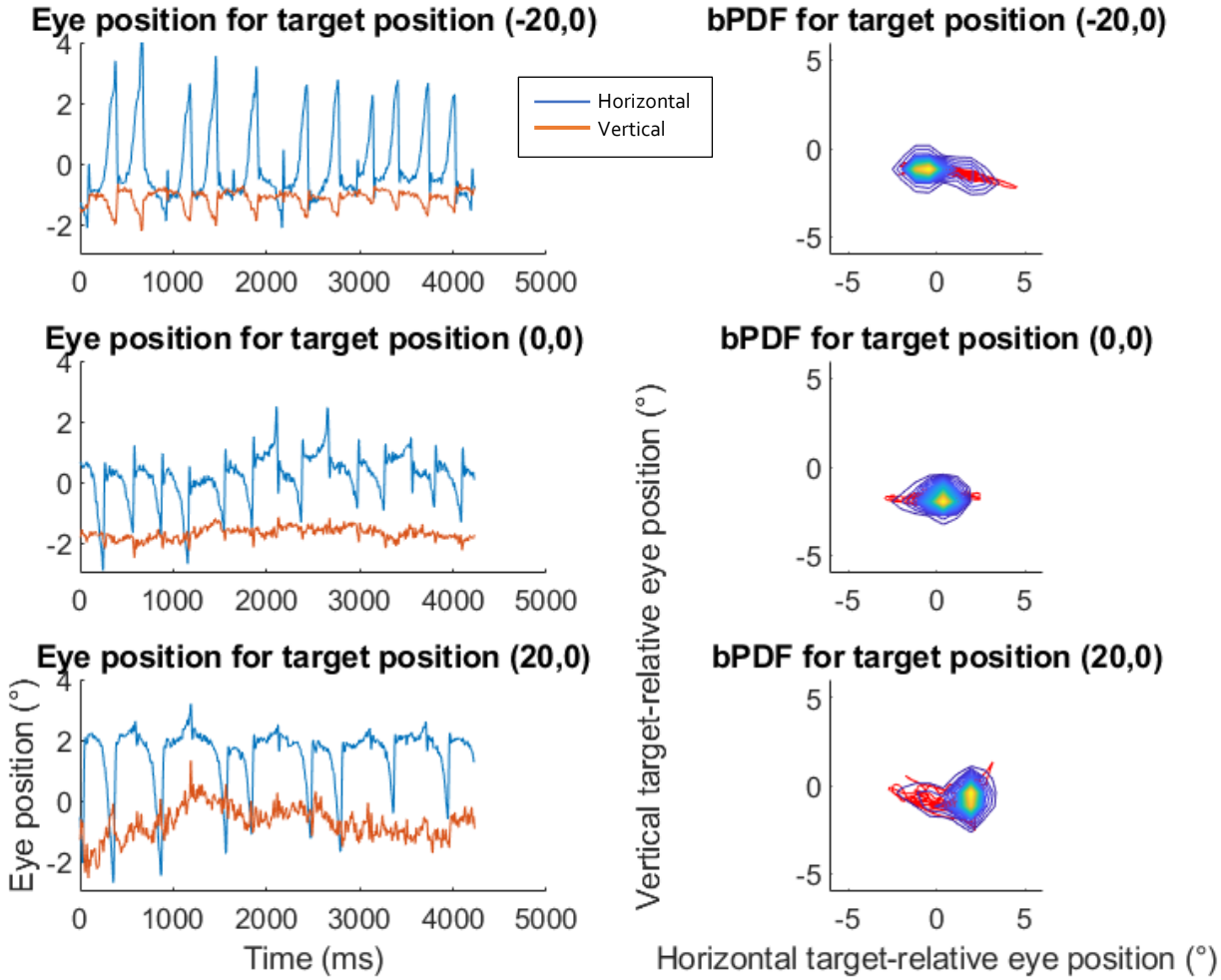

Figure 3-2: Representative eye position data and corresponding bPDF analysis output
Diagram obtained from eye movement trace for participant P028 while fixation horizontally at -20° (top), central (middle) and +20° (bottom) gaze angles. On the eye position images situated on the left hand side, a deflection towards the plus position on the vertical axis indicates a rightward eye movement. The (-20,0) position is for target situated 20° on the left of participants visual field while the (20,0) position is towards the right. The plots of eye movement traces presented here are relative to the target. Diagrams show a significant vertical component of IN waveform which neither intensity nor amplitude can capture in a traditional waveform analysis, unless performed for horizontal or vertical eye movement trace differently. The red blob underneath the isocontours (images on the right hand side) is a plot of all data points, warmer colors in the isocontour indicating higher probability density. It is the isocontour surrounding the gaze positions with the highest 68% density that was further analysed to give measures of fixational eye stability.

The accuracy, contour area and shape factor (contour shape) derived from the isocontour, at each gaze angle, are plotted for all participants in Figure 3-3. As described in Section 2.7.3, page 50, the accuracy of eye position was quantified using the length of the vector extending from the isocontour centroid to the point of fixation. Recall that points on this isocontour are expressed relative to target position. Therefore, smaller values of the deviation from the target will reflect a greater accuracy. Larger contour areas indicate a larger spread of eye positions and hence a greater imprecision or in other words could reflect a larger 'relative' waveform amplitude. The imprecision could be equally spread along the major and the minor axis thereby producing a value close to one for the shape factor (min/max isocontour axes) metrics.

Individual plots show that at horizontal gaze positions, the points of best fixation accuracy, best precision and most symmetric isocontour (i.e. highest shape factor) do not always correspond, as well as match with the clinically measured null zones. An exception was seen in P018, P022, P025, P030 and P033. The isocontour shape factor appeared to vary more across eccentric gaze positions than other measured parameters. Although higher isocontour symmetry only highlights an almost equal horizontal and vertical isocontour axis ranges, as seen in the plots, this finding may not always signify better fixation performance in terms of accuracy and precision.

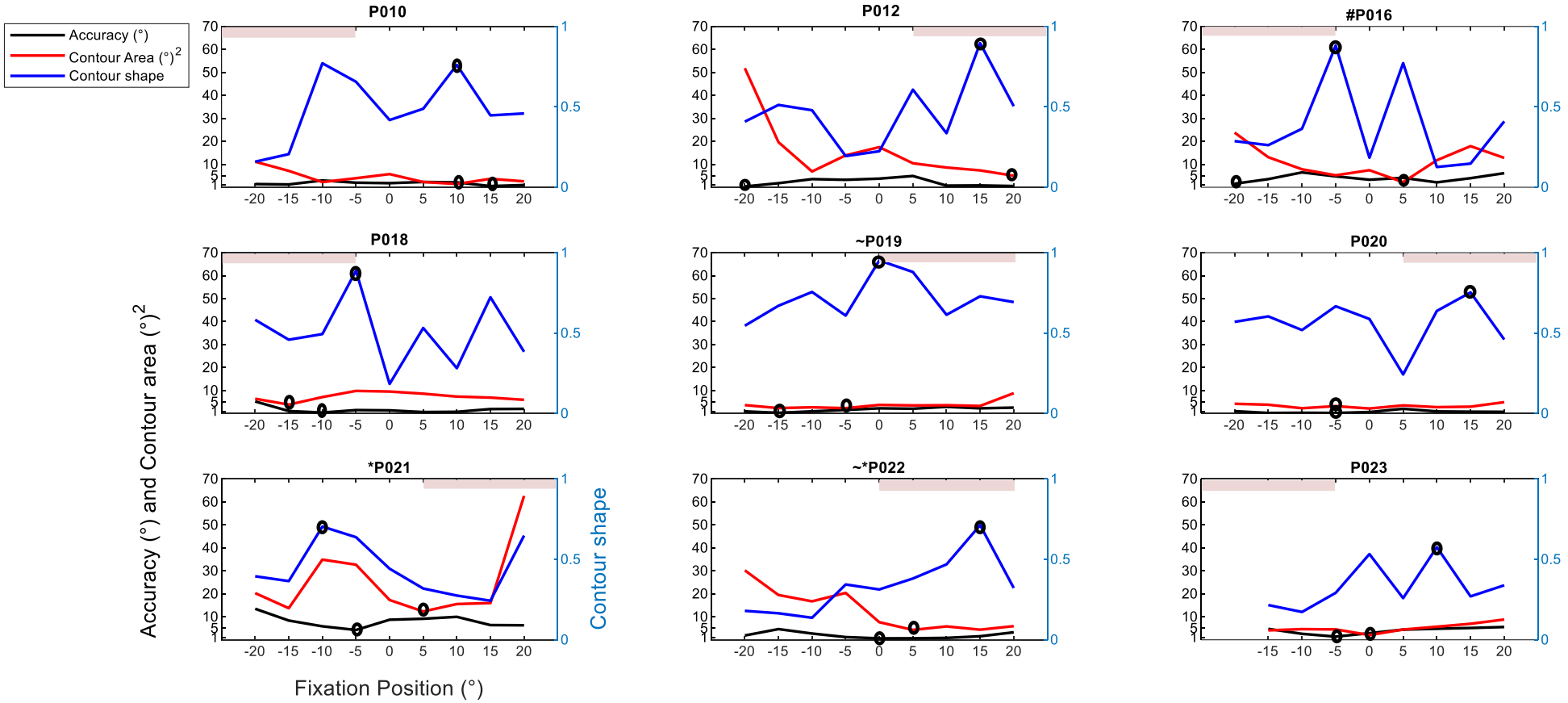
Accuracy (°)
Contour Area (°)2
Contour shape
P010
P012
#P016
P018
~P019
P020
*P021
~*P022
P023
Accuracy (°) and Contour area (°)2
Contour shape
Fixation Position (°)

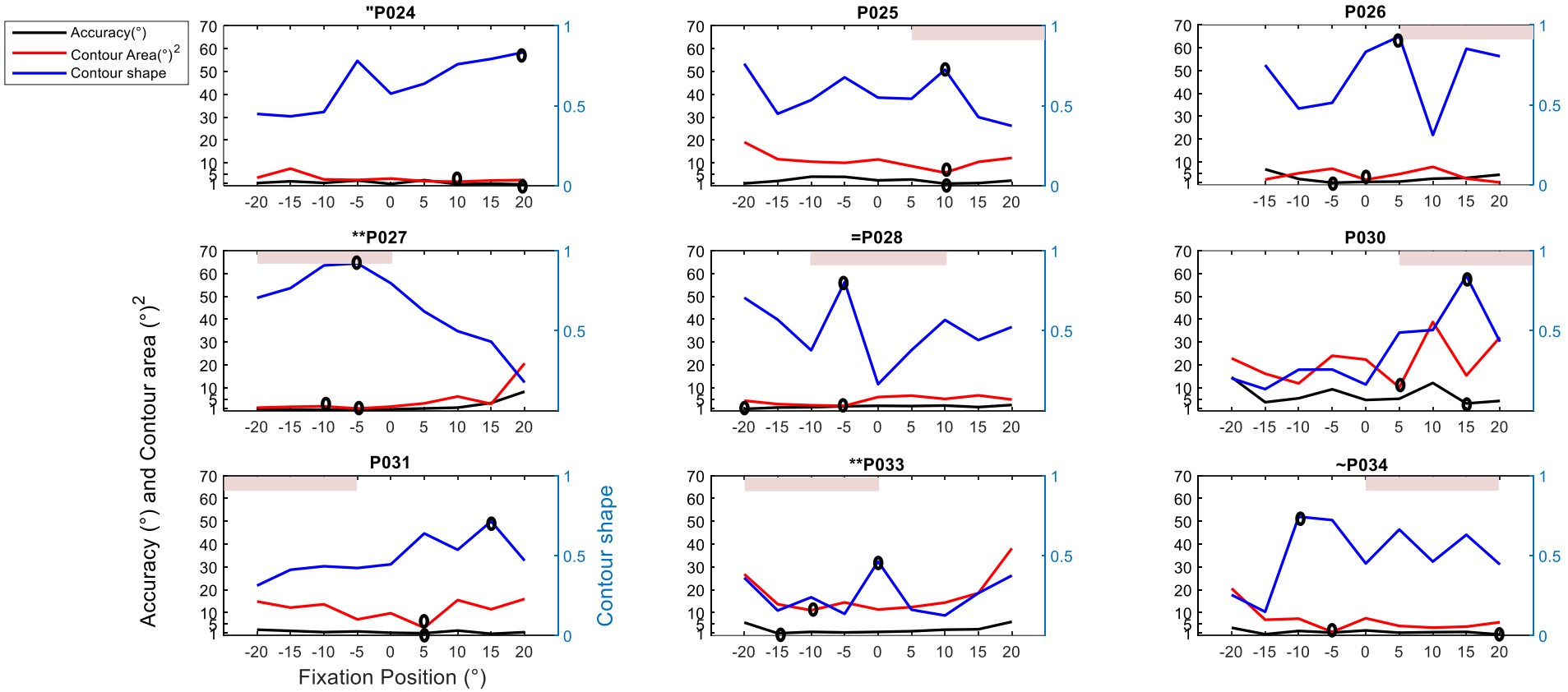

Figure 3-3: Accuracy, contour area and contour shape at all fixation positions.

The small ovals in each plot indicate points of high accuracy (shortest vector length to the target position) and precision (smallest contour area) including the point of eccentric gaze where contour shape is closest to 1; indicating that data spread on the horizontal and vertical isocontour axis are near symmetrical and the IN waveform oscillation in both components have remained almost equivalent in magnitude (considering the 68% of the highest density points). Where there is a dissimilarity in the data spread in both waveform components, as shown by these participants, it is indicative of a change in the IN waveform within each participant across the gaze angles. The pink shaded portions above each subplot show the region of measured clinical null, where positions to the right indicate nystagmus null during right gaze while shaded regions on the left indicate nystagmus null during left gaze. Other clinical null zones found are as follows: #up gaze, nystagmus greater in right gaze; ~Primary position (PP), nystagmus greater in left gaze; *Nystagmus greater in left gaze; ~*PP and right gaze; "Not applicable; **PP, nystagmus greater in right gaze; =PP, nystagmus in right gaze equal to left gaze.

3.3.3 Horizontal and vertical axis range of data spread

The major and minor axes of the isocontour, representing the horizontal and vertical axis range were computed using a custom function in MATLAB as described in Chapter two (Section 2.7.2). Results obtained were plotted as a function of gaze angle and are presented in Figure 3-4. Findings show similar values for each component measure, among all participants. Using repeated measures ANOVA, the horizontal and vertical axis range between participants did not differ [$F_{(1, 15)} = 0.58$, $p = 0.46$]. However, there was a significant main effect of gaze angles on the horizontal and vertical axis range [$F_{(3.43, 51.38)} = 3.44$, **$p = 0.02$**], and a significant effect of the interaction between gaze angle and axis range [$F_{(4.24, 63.53)} = 2.55$, **$p = 0.05$**]. For these last two results, assumption of sphericity was violated therefore, the sphericity correction results using Greenhouse-Geisser have been reported rather than the expected degrees of freedom of the residuals which is $F_{(8.00, 120.00)}$.

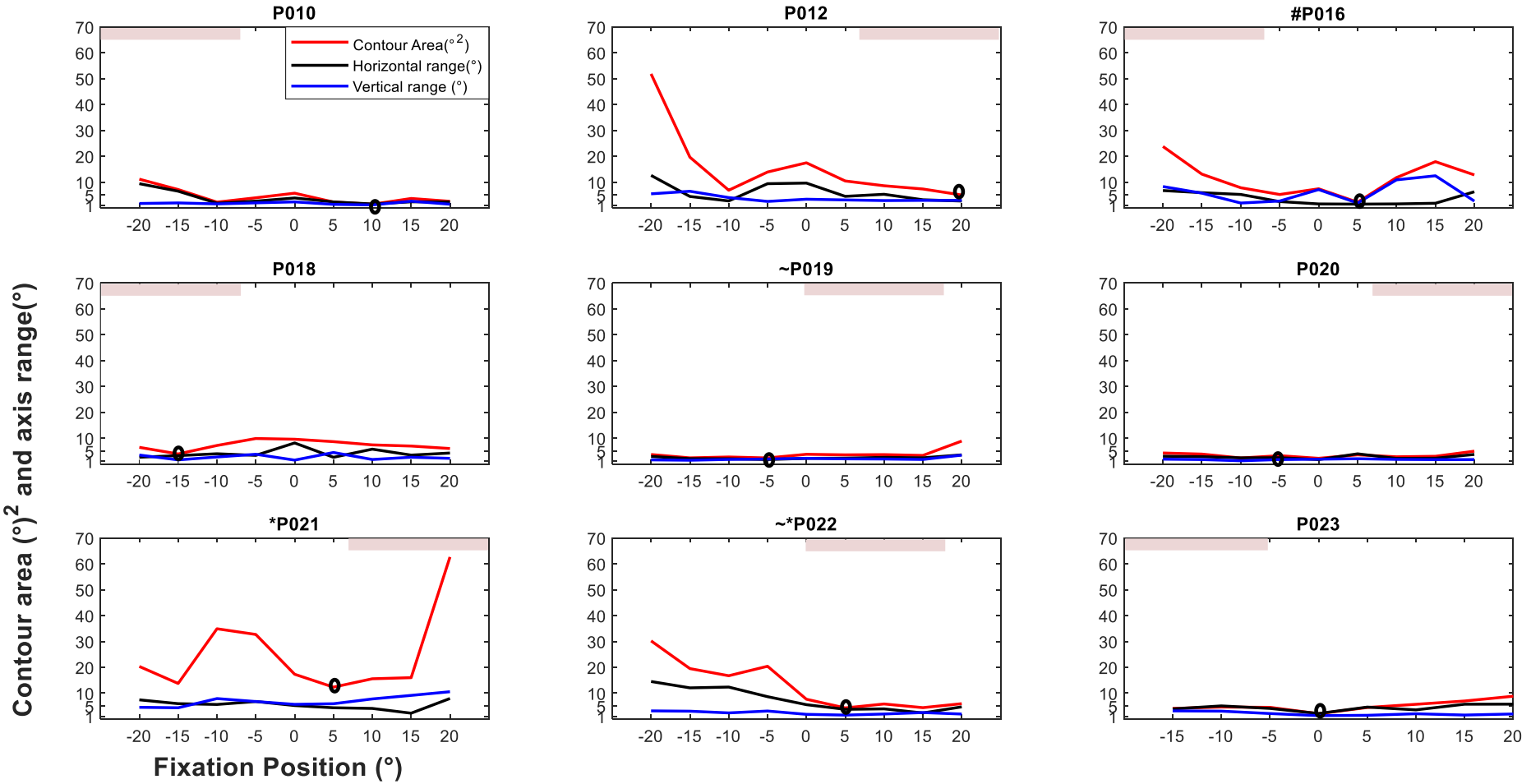
P010
P012
#P016
P018
~P019
P020
*P021
~*P022
P023
Contour Area(°2)
Horizontal range(°)
Vertical range (°)
Contour area (°)2 and axis range(°)
Fixation Position (°)

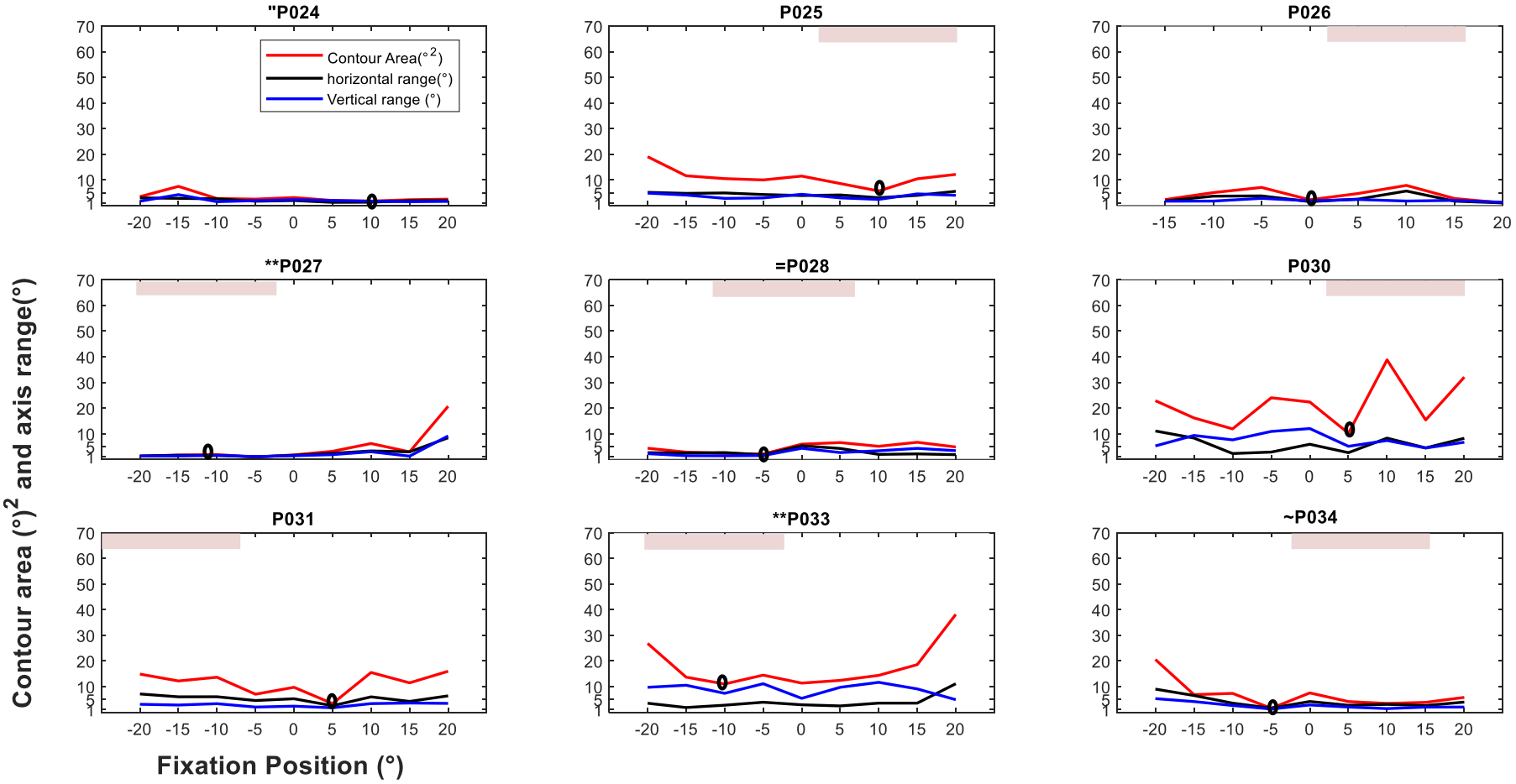

Figure 3-4: The isocontour area alongside the horizontal and vertical range at each gaze angle

Figures for all 18 participants showing the contour area and derived horizontal and vertical axis range. **Black** ovals indicate the point of lowest contour area value where the eye positions spread less. Shaded region in pink, above each subplot, indicates where the participants clinical null is located, where positions to the right indicate nystagmus null during right gaze while shaded regions on the left indicate nystagmus null during left gaze. Other clinical null zones found are as follows: #up gaze, nystagmus greater in right gaze; ~Primary position (PP), nystagmus greater in left gaze; *Nystagmus greater in left gaze; ~*PP and right gaze; "Not applicable; **PP, nystagmus greater in right gaze; =PP, nystagmus in right gaze equal to left gaze.

To evaluate how much these values varied across the nine gaze positions, a Pearson's correlation analysis was performed between the vertical and horizontal axis range, and some of these are presented in Figure 3-5. Result indicate that for most participants, there was a corresponding increase in the vertical axis range (indicating less precision) when the horizontal axis range increased; this was significant for participants P022 ($p = 0.03$), P027 ($p<0.001$) and P034 ($p<0.001$). For five other participants, there was a negative relationship, indicating that the vertical axis range increased even when the horizontal range decreased, but this was only significant in one participant (P018 ; $P = 0.043$).

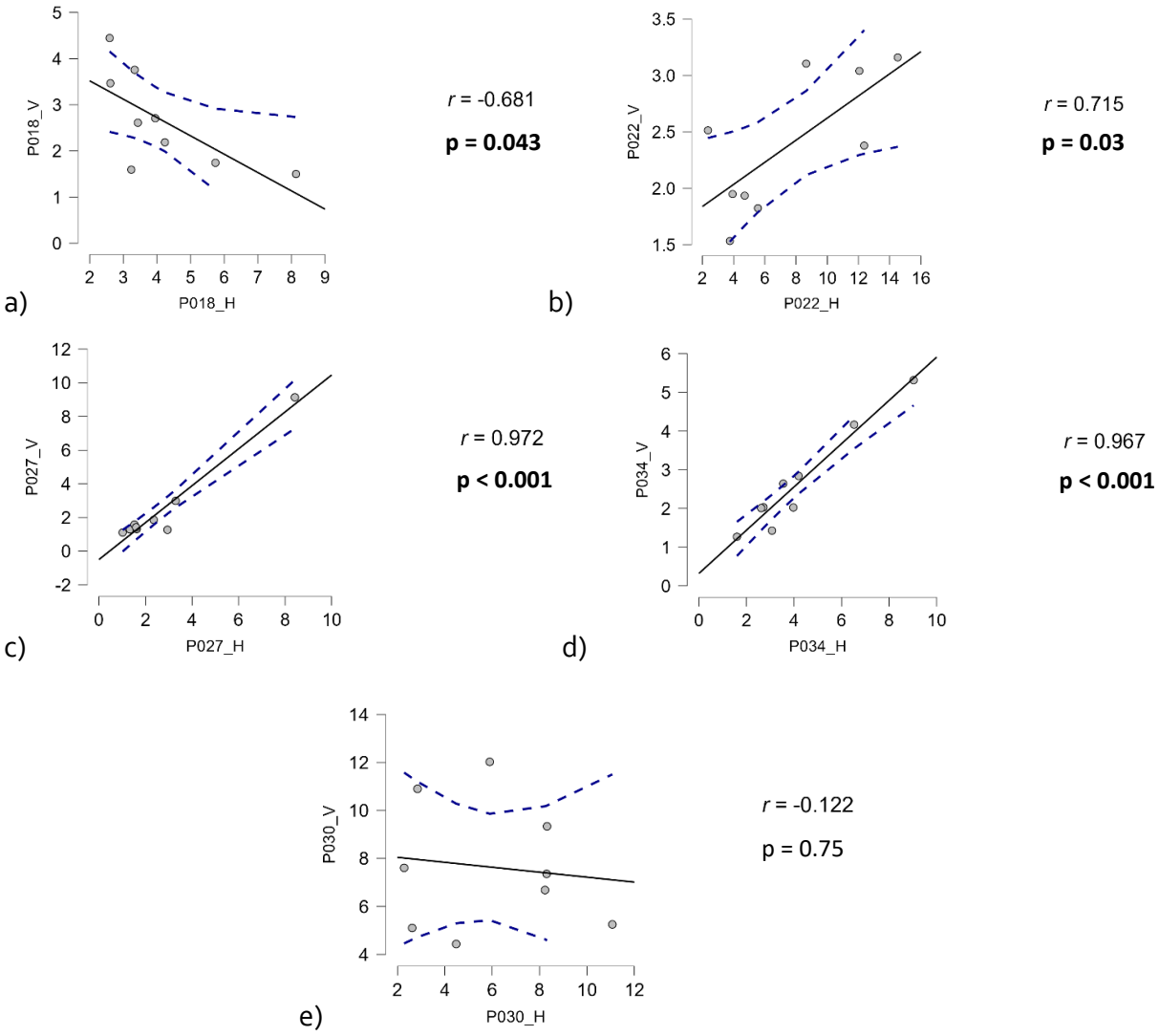

Figure 3-5: The relationship between horizontal and vertical axis range, as a function of gaze angle
Correlation plots are presented for significant relationships (a, b, c and d) and for participant with the worst r value (e). The vertical meridians are indicated by the participant's identity and V, representing vertical axis range. Horizontal meridians represent the horizontal axis range. Significant P values are included beside each individual participant's plot. Dotted lines represent the 95% confidence interval. A change in the horizontal range but not in vertical range will produce a more horizontal trend line, while one with a change in vertical range but not in the horizontal range will produce a more vertical trend line. In cases where an increase or

decrease in the horizontal range values corresponds to those in the vertical range, the trend line will be more diagonal.

In order to summarise the obvious variation in the amplitude (range) of IN waveform across participants, the relationships between the amplitude of vertical and horizontal eye positions, as well as other computed parameters are presented in Table 3-2. The results indicate that for those in which the horizontal and vertical axis ranges were almost equal, the isocontours were more circular (shape factor close to 1). For example, this can be seen in P019 and P026. In others where isocontours were less circular (shape factor closer to 0), e.g. P023 and P033, the horizontal and vertical axis ranges differed, indicating a difference in the vertical spread of data from the horizontal. Other values of accuracy and precision, show variability among participants and within participants, at different gaze angles.

Table 3-2: Mean and standard deviation of fixation performance across gaze angles
The correlation coefficient and P values apply to analysis performed using the horizontal and vertical axis ranges at each gaze position. These were in turn derived from contour area, contour shape and the major axis orientation, at each gaze position.

Participant	Accuracy (°)	Contour shape	Contour area (°)²	*Horizontal axis range (°)*	*Vertical axis range (°)*	*Correlation coefficient r =*	*P value*
P010	1.70 ± 0.75	0.49 ± 0.22	4.47 ± 3.09	3.65 ± 2.62	1.81 ± 0.47	0.17	0.67
P012	2.18 ± 1.70	0.46 ± 0.21	15.68 ± 14.44	6.05 ± 3.59	3.75 ± 1.34	0.19	0.62
P016	3.99 ± 1.63	0.38 ± 0.27	11.34 ± 6.63	3.68 ± 2.29	5.96 ± 3.99	-0.27	0.47
P018	1.68 ± 1.46	0.50 ± 0.22	7.32 ± 1.86	4.14 ± 1.78	2.67 ± 1.04	-0.68	**0.04**
P019	1.77 ± 0.87	0.72 ± 0.13	3.80 ± 1.98	2.41 ± 0.54	2.01 ± 0.57	0.66	0.05
P020	0.79 ± 0.56	0.56 ± 0.15	3.34 ± 0.90	2.71 ± 0.73	1.74 ± 0.22	0.34	0.38
P021	8.07 ± 2.74	0.45 ± 0.17	25.06 ± 16.25	5.52 ± 1.78	6.96 ± 2.08	-0.13	0.74
P022	1.93 ± 1.38	0.34 ± 0.18	12.78 ± 9.26	7.55 ± 4.47	2.38 ± 0.61	0.72	**0.03**
P023	3.95 ± 1.47	0.33 ± 0.15	5.17 ± 2.03	4.37 ± 1.21	2.08 ± 0.70	0.15	0.72
P024	1.32 ± 0.72	0.64 ± 0.16	3.10 ± 1.74	2.06 ± 0.62	2.06 ± 0.86	0.35	0.36
P025	2.25 ± 1.13	0.56 ± 0.14	11.06 ± 3.58	4.42 ± 0.76	3.68 ± 0.89	0.41	0.27
P026	2.89 ± 1.95	0.68 ± 0.22	4.14 ± 2.45	2.72 ± 1.55	1.95 ± 0.47	0.29	0.48
P027	1.84 ± 2.59	0.65 ± 0.24	4.49 ± 6.28	2.68 ± 2.28	2.44 ± 2.57	0.97	**<0.001**
P028	1.75 ± 0.53	0.50 ± 0.19	4.52 ± 1.76	2.78 ± 1.21	2.74 ± 1.18	0.32	0.40
P030	6.92 ± 4.10	0.36 ± 0.23	21.53 ± 9.40	6.01 ± 3.14	7.63 ± 2.65	-0.12	0.75
P031	1.59 ± 0.58	0.49 ± 0.12	11.54 ± 4.20	5.36 ± 1.39	2.87 ± 0.67	0.63	0.07
P033	2.69 ± 1.87	0.25 ± 0.12	17.88 ± 9.03	3.96 ± 2.76	8.84 ± 2.42	-0.55	0.12
P034	1.56 ± 0.90	0.50 ± 0.20	6.79 ± 5.55	4.14 ± 2.29	2.64 ± 1.32	0.97	**<0.001**

Significant correlations in bold

3.3.4 Fixation performance and clinical VA

As a follow up to data from Table 3-2, the mean accuracy and precision values obtained within each participant were correlated with their entry clinical VA. The graphs in Figure 3-6

illustrate these findings. Results indicate a positive correlation between mean accuracy and VA [r=0.618, **p=0.006**; (95%CI: 0.212, 0.842)] as well as mean precision and VA (r=0.617, **p=0.006**; (95%CI: 0.210, 0.841)]. In other words, as the accuracy score of fixational eye position and the mean contour area of the eye position isocontour increases across participants, the logMAR VA value of the participants also increased i.e. acuity worsened.

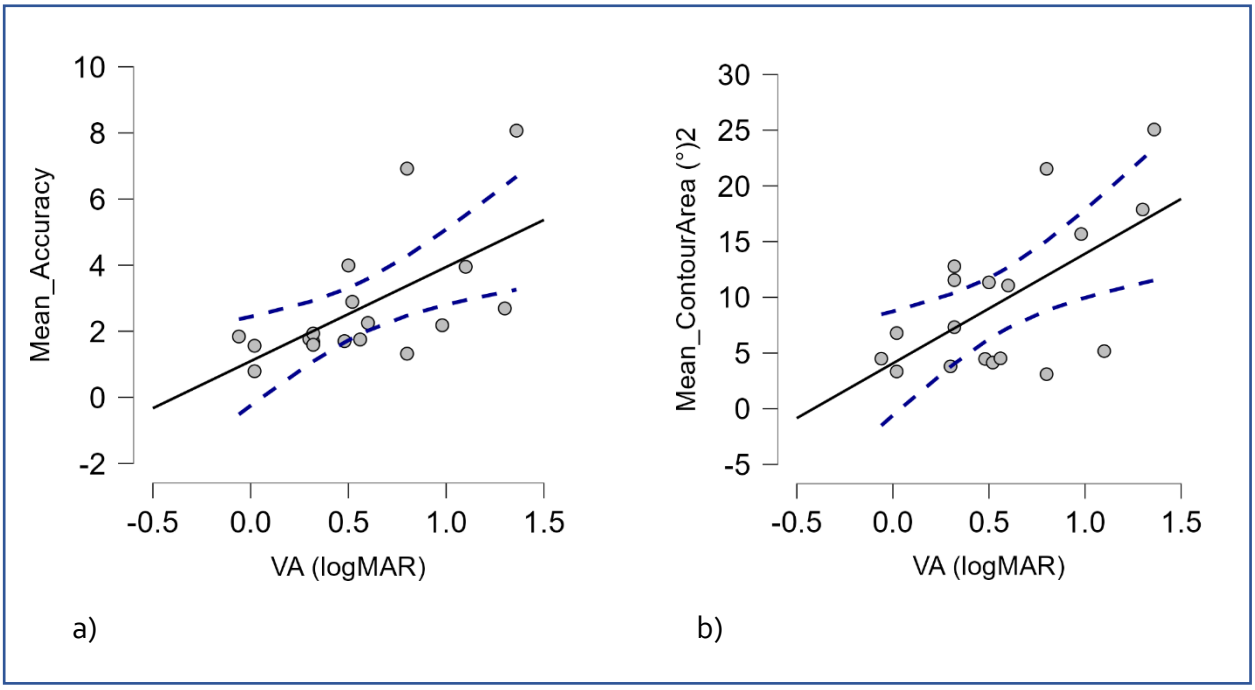

Figure 3-6: The relationship between fixation performance and entry VA
(a) shows data obtained from the mean accuracy across gaze positions, in each participant while (b) represents the mean contour area (precision) across all gaze positions for each participant. Blue dotted lines indicate the 95% confident interval region. A greater logMAR VA value depicts poorer VA.

3.4 Discussion

This study aimed to evaluate the characteristics of fixation at horizontal gaze angles using bPDF, and compare imprecision along the horizontal and vertical axis of the derived isocontour. Generally, our findings indicate a high variability in the derived data among participants and within participants, when fixating at different gaze angles. This was also evident in the null zones for these participants. If we were to identify the objective null zone using the accuracy and precision data, a conclusion would be difficult to reach because, in almost all participants, except P020, P025 and P031, the most accurate (shortest distance of isocontour to fixation point) gaze angle was not the most precise (smallest isocontour

area) gaze angle. Since the area comprises both horizontal and vertical eye position spread, the vertical eye position must make a significant contribution to fixational eye stability for people with IN; driving home the point that traditional methods which evaluate only the horizontal eye movement trace to characterize the null zone may be missing out vital information.

An attempt to tease out the contributions of the vertical component is complicated by the fact that findings from this experiment do not provide a clear cut pattern of how the vertical components contribute to best accuracy and precision. In some cases, the horizontal and vertical components change together. In many other participants, the vertical range is largely unaffected by the degree of horizontal eye movement, while in a couple of people there is a dramatic effect. Although participants were comfortably seated using a head and chin rest and could not possibly use a vertical head tilt even if they wanted to, these discrepancies in values could normally drive a head tilt, and could explain why some people with IN have head tilts to compensate for unstable fixation. There is evidence that a head tilt (chin elevation/depression) can be used to achieve null zones in IN, therefore it can be argued that it is not exclusively a 'horizontal only' phenomenon (Maybodi 2003; Abadi and Bjerre 2002; Abadi and Whittle 1991). Moreover, because video-based eye tracking, cannot measure any torsional component to the oscillation, a complete picture of the null zone remains to be determined, but these findings have undoubtedly added to current knowledge.

In addition, findings from Table 3-2 indicate that the contour area is more likely to vary across participants, when gaze angle changes, whereas shape and accuracy are much less affected. This finding may have resulted from the fact that the IN waveform could switch from a right beating to a left beating oscillation at any given position of gaze (e.g. see Figure 3-2, where target position is at (0,0). Therefore, the contour area metrics capture this relative eye position spread as it is; even in cases where the resulting amplitude increases due to changes in beat direction of the waveform. Unlike the traditional amplitude metrics which would only provide values for the average amplitude regardless of whether it was left or right beating. In addition, varied contour area values also further highlight the contributions of the vertical component to make the isocontour (i.e. eye position spread) either more vertically or horizontally oriented.

The relevance of visual resolution to predict an efficient fixation performance can be explained by the diagrams in Figure 3-6. The fact that, across subjects, VA correlates significantly with fixation accuracy and precision is in line with the common knowledge that the visual threshold gets poorer when the intensity of nystagmus gets worse (Dunn et al. 2017; Wiggins et al. 2007). However, it is worth noting that data compared here may not necessarily mean that, for any given patient with IN, if the nystagmus intensity were to be reduced by any form of treatment or remedy the VA may in turn become better. In order to probe further the effects of waveform changes and the null zone on visual resolution, it will be necessary to examine how visual resolution changes with gaze angles. This is addressed in the next chapter.

The findings of fixation performance and its relationship with VA are indeed useful for clinicians and researchers. This in turn relates to an ability to judge IN eye movement intensity clinically, and the benefits to predict VA. Given that there is no evidence that nystagmus characteristics change throughout lifetime, for younger patients, information regarding predicted VA could be suggestive of what their likely final VA will be before they can even begin to read. It is recommended that this information, about their predicted level of vision, can be used to provide, for example, Qualified Teachers of Visually Impaired (QTVI's) and other early schooling support that is appropriate for their level of vision, and which may be beneficial throughout their learning process.

One limitation of this experiment is that during calibration, the calibration area used was the same size as the stimulus area. This may give rise to a potential source of error that could make eye movement seem more unstable in more eccentric locations i.e. if the nystagmus oscillation takes the participants fixation outside the calibration area. Nonetheless, this experiment has highlighted how significant the vertical component of IN waveform oscillation might be for fixation preference, and why future research needs to pay more attention to this. Perhaps, where other methods [e.g. the cervical range of motion device used for testing abnormal head postures (Kushner 2000; Hertle and Ahmad 2019)], other than the video-based eye tracking, are used alone or alongside eye tracking to evaluate all planes of the IN eye movement trace (including torsion), then null zones can be better identified for treatment interventions (Dunn et al. 2017).

CHAPTER FOUR

4 Fixation characteristics and uncorrected resolution thresholds at eccentric gaze positions in participants with infantile nystagmus and controls

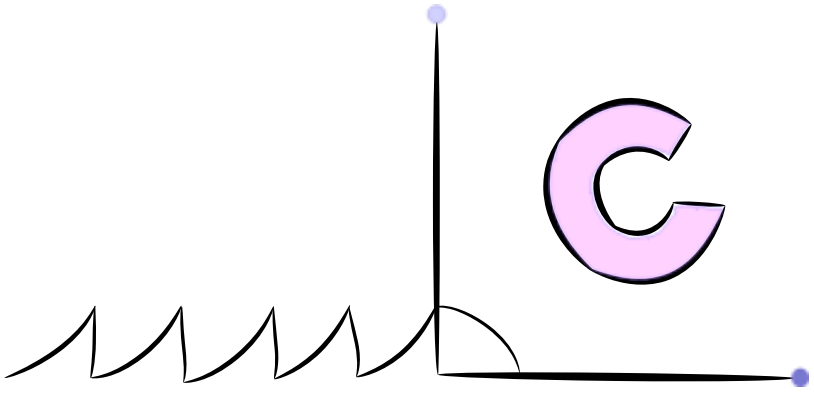

4.1 Introduction

In the previous chapter, fixation performance and how each directional component of the IN waveform oscillation relates to fixational eye stability at eccentric gaze were evaluated. Given that, with IN, there is no clearly defined pattern concerning the null zone and its association with fixation performance, visual resolution as another factor is explored here. For this chapter, the fixation performance of typical participants and those with IN will be evaluated during a visual resolution task. Here also, the relationship between visual resolution and threshold target (which was designed to measure bidirectionally in both horizontal and vertical planes) is evaluated.

4.1.1 Visual resolution and fixation performance at eccentric gaze positions

Until recently, the general assumption was that visual acuity (VA) of people with IN improves when viewing a target at the null zone. Although not a complete measure, VA is a well-established tool to measure the functional ability of the visual system. Foveation indicates a period of minimal eye velocity (and hence retinal slip), and thus, it is expected that, during foveation, VA is optimal. The relationship between VA and foveation duration was explored in simulated nystagmus (Chung and Bedell 1996). Their findings showed that when foveation duration increased, VA was better. Similarly, Wiggins et al. (2007) established that at the null zone when the visual task is more demanding, foveation period increases as resolution threshold is reached. One would reasonably expect a corresponding improvement in VA since the other waveform parameters of intensity, amplitude, and frequency reduce, and foveation duration increases. However, the marginal VA improvement at the null zone of only 0.08 logMAR (less than one line difference), which was reported in the study by Dunn and colleagues (Dunn et al. 2017), raises questions as to what other factors influence the choice of the null zone.

To achieve movements to eccentric gaze positions, the extraocular muscles send and receive signals from the higher centres of the brain. In the oculomotor system, eye movements are controlled by separate neural pathways which come together at the level of the motoneuron (Robinson 1981). These neurons, collectively known as the neural integrators, play a crucial role of holding the eyes still and stabilizing the image on the

fovea, despite orbital forces which tend to pull the eye back to primary position (Sanchez and Rowe 2018; Leigh and Zee 2015). Neural integrators act by mediating the visual process to convert eye velocity signals (or pulse commands) to eye position signals. In other words, when there is a neural command for a saccadic movement for example, or in the case of eccentric viewing, the neural integrator generates a step innervation for a position command to provide the extraocular muscles adequate neural activity needed to hold the eyes in its new eccentric position in the orbit, while opposing the elastic forces that could rotate the eyes back to the midline position.

The neural integrator relies on a visual feedback mechanism to refine its function (Shaikh et al. 2013). Position signals decay with time allowing the elastic forces of the orbit to rotate the eyes back to the central position. This decay in position signals, manifests as an inability of the extraocular muscles to sustain eccentric gaze and result in gaze evoked nystagmus; whereby fixation becomes unstable and the gaze holding system (neural integrator) works harder to sustain this gaze position (Abadi 2002). This physiological oscillation in typical subjects is called end-point nystagmus (Abel et al. 1978). In the experiment by Abel and colleagues, end-point nystagmus was seen in seven out of 12 participants at eccentric horizontal gaze positions up to 40°. Gaze positions above 40° could not be examined because of the limits of their test instrument. Furthermore, when there is a functional defect or unstable neural integrator, the eccentric eye positions will be difficult to attain and maintain, thereby producing irregular eye movements and visual disturbance. A comprehensive review of clinical disorders associated with neural integrator defect is beyond the scope of this thesis, but the interested reader can find more information here: Sanchez and Rowe (2018).

Furthermore, In typical participants, the extent to which the eye can sustain fixation in eccentric gaze was also investigated in one early study in which both authors fixated a target, when visible and in the dark, for gaze angles up to ±10° (Skavenski and Steinman 1970). From their study, eye position area increased by close to 50%, i.e. precision became worse, in both subjects while fixating (not in the dark) eccentrically. Fixation range of eye positions during fixation (i.e. while viewing straight ahead) has also been shown to increase significantly in the absence of a fixation target compared to when it was visible (Cherici et al. 2012). In other words, when the target was removed, fixation was more variable. More

recently, Raveendran and colleagues (Raveendran et al. 2020) also showed larger bivariate contour ellipse area (BCEA) (indicating poorer fixational eye stability) using both crowded and uncrowded peripheral stimuli, for gaze positions up to 10°. Their study also indicated that crowded stimuli result in significantly poorer fixation at eccentric gaze.

To further investigate the impact of eccentric gaze on visual resolution and its role in fixation performance, pilot studies were carried out by third year optometry students here at the School of Optometry and Vision Sciences, Cardiff University (Sherill Sim, Mohammed Anwar & David Roper, unpublished data, 2020). Three independent experiments were performed among typical participants, and results from two out of the three showed that VA decreased at extreme gaze positions, i.e. away from central gaze, up to ±30°. A summary of these studies and findings are given in Table 4-1 and Figure 4-1, respectively. For studies one and two, two mirrors were used in the test room to give rise to a 12m testing distance. This was necessary to prevent a floor effect and ensure that VA was not underestimated.

Table 4-1: Design of pilot experiment

	Study one (n=11)	Study two (n=12)	Study three (n=6)
Angles examined	0 and 30°	0, 10, 20 and 30°	0 and ±30°. No significant difference between VA found at +30 and -30° eccentricity (P=0.695)
Test distance	12m	12m	4m
VA chart	Thompson digital	Thompson digital	EDTRS illuminated

For studies one and three, statistical significance was found using the paired sample t-test, indicating that, as eccentricity increased, VA was poorer. It can also be seen from study two that there was a gradual reduction in VA (poorer visual resolution) as gaze angle increased to 30°; however this was not significant using ANOVA.

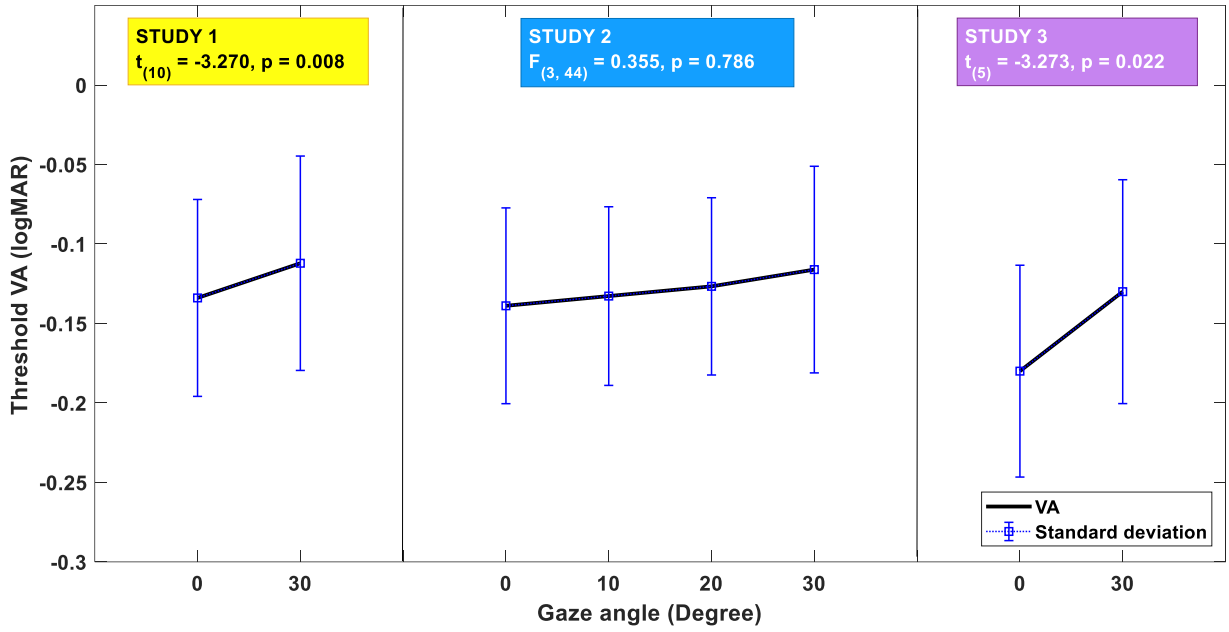

Figure 4-1: Summary of results obtained from pilot experiments
Findings from statistical analysis are included in the coloured boxes.

These research projects, however, did not include eye tracking for eye movement recording, and therefore missed out vital information on how fixation accuracy and precision relates to such changes in visual resolution. It has been proposed that, in order for studies evaluating visual resolution in IN to make a significant contribution, the relationship between eye movements and VA is better evaluated if they are recorded simultaneously, i.e. at the point when the effort to see is maximum (Wiggins et al. 2007). This is because of the changes that occur in the waveform due to visual demand. Moreover, it is only natural for both fixation at a target and visual resolution of that target to go hand in hand in real life scenarios, therefore highlighting further the importance of evaluating fixation performance and visual resolution simultaneously.

For the purpose of the present study, we have likened fixation in IN at the null position to fixation at primary position in typical participants, so that vision away from this fixation position are considered eccentric gaze. Considering the studies reviewed above, this chapter will aim to provide additional information on the relationship between visual resolution and fixation performance at eccentric gaze positions, in people with IN and controls, using the bPDF of eye position; an established method for determining fixation accuracy and precision from eye movement recordings (McIlreavy, Freeman and Erichsen 2019).

Determining the most suitable target to assess visual resolution

In measuring visual resolution, it is important to utilize targets that provide optimal end point measures; especially when target orientation is considered. Studies have shown that visual resolution threshold differs in people with IN when target orientation is changed. With horizontal gratings, significant improvement in VA has been reported (Dunn et al. 2014; Meiusi, Lavoie and Summers 1993) and this has been attributed to the IN oscillation being largely horizontal. To explain further, if we imagine the IN waveform oscillating horizontally from left to right in the presence of a horizontally oriented luminance grating, as the eye moves across the pattern, the retinal image would stay the same. However, for vertically orientated gratings, as the eye moves left and right, the retinal image would repeatedly change as the eyes move across the bars.

In typical participants however, the directionality of gratings does not affect the threshold for VA. A previous study (Jones 2011) reported no significant difference in VA measures using gratings in typical subjects ($P = 0.747$). In this study also, other stimulus types such as the Landolt C and tumbling E did not provide a significant difference in VA threshold measure in those with IN. However, the tumbling E gave better VA when oriented vertically ($P<0.001$) in typical participants. If gratings and the tumbling E are likely to produce variable resolution thresholds (in different orientations) for people with IN and typical participants, it is therefore logical to utilize a visual target, such as the Landolt C, which should not produce any bias to vision threshold measures based on target anisotropy. Target anisotropy in this case would mean different threshold measures resulting from a change in target direction.

A psychophysical adaptive procedure of VA measurement allows for two or more alternative forced choice (AFC) staircase procedures, wherein visual resolution can be determined for horizontal and vertical stimuli simultaneously as Landolt C targets are presented on the computer screen. Since there should be no bias in threshold as a result of target orientation (Jones 2011), a measure of visual resolution using the Landolt C targets appears to be a more effective way of determining visual resolution.

For some of the studies discussed above where visual performance was evaluated, visual resolution was being measured while simultaneously evaluating eye movements. However,

these studies concentrated on the horizontal eye movement alone (ignoring any vertical component), and this may potentially mask the true picture of the relationship between eye movements and visual performance at the specified gaze direction. In Chapter one, we have established the inconsistencies which exist from using a one-size-fits-all criterion to represent IN waveform oscillations. Given that there is a wide variety of waveform oscillations among individuals with IN, and the horizontal eye movement oscillation may not necessarily be solely responsible for gaze angle fixation preference, the bPDF method has been shown to provide a more complete measure of eye movements. In addition, since no specific pattern was found in the accuracy and precision of fixation across gaze angles (see Chapter three), but there was a positive correlation with clinical VA, by utilizing the bPDF method to determine the relationship between eye movements and visual resolution, it is more likely that visual performance at eccentric positions will be better investigated.

4.1.2 Aim and objectives

The aim of this chapter is to determine the effect of eccentric gaze viewing on visual performance in those with IN and typical participants.

Specific objectives include:

1. Evaluate the psychometric VA measured at eccentric gaze positions
2. Quantify fixation performance at eccentric gaze positions up to ±45°
3. Determine the contributions of the horizontal and vertical eye movement components to fixation performance at different gaze angles.

4.1.3 Hypotheses

For this chapter, it was investigated whether gaze angles had an impact on psychometric VA, as well as the accuracy and/or the precision of fixational eye movements and whether there was a difference between the horizontal and vertical eye movement components during fixation. The null hypotheses therefore are:

1. The psychometric VA measured at eccentric gaze position does not differ from that measured at primary position, in people with IN and typical participants .

2. The accuracy and precision of fixational eye movements do not change at all gaze directions in people with IN and typical participants.
3. The horizontal and vertical eye movement components contribute equally to fixation performance at gaze angles.

4.2 Methods

4.2.1 Participants

Each participant was pre-examined to determine their suitability for the experiment, and when they did not meet the exclusion criteria outlined in section 2.3.1, they were excluded.

Null zone determination

Null zones of participants with IN were determined subjectively during pre-examination. They were asked to fixate a pen torch that was presented at 40 cm, at 9 gaze positions on the visual field: straight ahead, top, bottom, left, right, top left and right, and bottom left and right. During the process, changes in the intensity of eye movement were estimated.

4.2.2 Laboratory set up

The larger monitor screen (described in Section 2-1), was used at 4 m. Because an electronic device was used to present the target, it is likely that at some distance, targets presented on the screen will become pixelated. However, the test distance of 4 m was preferred to 6 m this is because, the test room was not long enough to achieve a distance of 6 m except mirrors were utilized. Using a mirror could result to anomalous ghosting of very detailed stimuli, and the keyboard buttons may get reversed when selecting the Landolt C's therefore becoming confusing for the participant. The laboratory set up is presented in Figure 4-2.

Figure 4-2: Laboratory set up
Gaze angles were achieved by rotating the chinrest table to pre-marked positions (±45°; 15° apart) on the ground.

Stimuli

Based on previous literature (Jones 2011), the Landolt C target was chosen to be presented on the computer screen. Visual targets could be high contrast i.e. black on a white background or be presented as vanishing optotypes. Vanishing optotypes are targets that are of a high-pass design and cause the letters to vanish when the threshold is reached (Shah et al. 2011). It is designed such that the resulting output of mean luminance of the target is the same as the background. Figure 4-3 illustrates a vanishing and a regular Landolt C optotype. As no luminance cues are given in the vanishing optotype target, similar detection and resolution acuity are obtained (Anderson and Ennis 1999). For example, this can be illustrated using a black C on a white background wherein the gap may appear brighter to an observer, indicating the orientation of the C, even if they cannot resolve the gap. But with vanishing optotypes, it becomes much more difficult to resolve the gap in the letter as a result of it blending with the grey background, and therefore, a more precise threshold is reached.

1.  3. 

2.  4. 

Horizontal orientations
1 = staircase 1_0°; 3 = staircase 3_180°

Vertical orientations
2 = staircase 2_90°; 4 = staircase 4_270°

Figure 4-3: Schematic showing vanishing and regular Landolt C optotypes
The stimuli used for this experiment were like the one on the top left but presented in the four orientations as shown below (1-4). As a comparison, regular optotypes on the top right are shown for all horizontal and vertical orientations.

4.2.3 Procedure

Resolution threshold was determined using psychophysical methods. During the process, vanishing optotype Landolt C target sizes were presented at the centre of the screen while participants indicated the orientation of the gap in the C by a click on the keyboard (using the up, down, left and right arrow keys to specify orientation). This test stimulus was programmed by Dr McIlreavy, in MATLAB (version R2016b; MathWorks, Natick, MA, USA), using the Psychophysics toolbox. In addition, eye position during the fixation task (of resolving the targets) was continuously recorded monocularly for gaze angles up to ±45°, at 15° apart, therefore making a total of seven positions.

Since this experiment was conducted at different gaze angles, it is likely that some degree of prismatic effect will be induced at eccentric viewing in participants wearing spectacle correction. With spectacle wear, image could be degraded by transverse chromatic aberrations or other forms of axis aberrations like oblique astigmatism. All of these optical aberrations will result in poorer acuity at eccentric gaze positions. Therefore, resolution thresholds were measured uncorrected, but a few participants with IN who had their contact lenses, wore them for the experiment. Also, given that this experiment involved people with IN, only one eye was examined. This is because a previous study found that the

monocular and binocular eye positions during fixation (Dell'Osso et al. 1972) could differ, and the presence of a squint can also prevent one eye from taking up fixation. Therefore, to eliminate any effect of a squint, the dominant eye was chosen for this experiment. Eye dominance was determined using a distance hole-in-the card procedure (Rice et al. 2008; Li et al. 2010). Unlike the previous chapter where gaze angles was achieved by moving the fixation target, in this chapter gaze angles were achieved by changing the seating position. Recording began from the 45° seating position to the far left (participants turned gaze to the right), and ended at the 45° seating position to the far right.

Task

In order to measure the visual threshold, targets were presented sequentially for the participant to identify, until a point was reached where these targets could no longer be resolved by the visual system. In the case of vanishing optotypes, it is expected that the target would blend into the background and be unidentifiable. Visual threshold was determined using a psychophysical adaptive procedure, which means that the size of the next stimulus to be presented (i.e. larger or smaller) is determined by the previous stimulus and the accuracy of the participants response (Levitt 1971).

Visual performance was measured monocularly, as a function of stimulus orientation, using a four alternative forced choice (4-AFC) transformed up-down staircase procedure. Although 4-AFC procedures are generally more cognitively demanding, they have been found to be statistically more efficient than 2-AFC (Schlauch and Rose 1990; Vancleef et al. 2018), thus providing a more precise threshold. The four independent staircases ran one for each group of stimuli and were programmed to stop automatically after 12 reversals or a total of 80 presentations. The presentation was designed such that, if a staircase terminated, dummy trials were inserted so as to prevent the remaining staircases running alone; otherwise, the participant would notice and input the keyboard function for only the staircase(s) that was/were left running.

Stimulus size was selected using the 3-down 1-up staircase method whereby the next stimulus size will depend on performance of the previous trials. In this case, stimulus size becomes smaller (more difficult) after three correct consecutive responses, and larger (easier) after one incorrect response. At threshold, the Landolt C pixel value should be an

estimate of a value that has the probability of getting three consecutive correct targets equal to 1/2. For each participant, a starting size optotype of two logMAR lines above their clinical VA was selected. Because, in those with IN, VA may cover a very wide range, this value was chosen so that gap identification would start reasonably close to their clinical visual resolution threshold without being too difficult. From this start size, subsequent targets changed with a step size of 0.95 pixels (as a percent), meaning 5% smaller or bigger than the previous stimulus depending on the correctness of the response.

To ensure that the expected Landolt C gap size was projected on the screen for each pixel gap, the gap size in cm was physically measured after presenting a series of gaps. This validation of stimuli size was necessary to guarantee that the output resolution measures were correct. The results are presented in Table 4-2.

Table 4-2: Confirming the onscreen Landolt C gap size for targets presented

	Dimension (Pixels)	Dimension (cm)	Pixels per cm	cm per pixels
Horizontal screen	1920	47.5	40.42	0.025
Vertical screen	1080	26.7	40.45	0.025

**Expected gap size (cm) = Gap size (Pixels)*cm per pixel*

Landolt C Gap size (Pixels)	Expected gap size (cm)	Measured on screen gap size (cm)
1000	24.70	24.70
900	22.23	22.30
800	19.76	19.80
700	17.29	17.30
600	14.82	14.85
500	12.35	12.40
400	9.88	9.90
300	7.41	7.40
200	4.94	4.90
100	2.47	2.45

4.2.4 Analysis

Fitting the psychometric function and determining vision threshold

The probability of obtaining a positive response at any given level of stimulus presentation is called a psychometric function or a response curve, where the percent positive response is represented on the y axis and the level of the stimulus is represented on the x axis (Wetherill and Levitt 1965; Levitt 1971). All data obtained from the experiment were pooled

and fit using an open source function, Psignifit (https://github.com/wichmann-lab/psignifit/wiki/Plot-Functions). Since this was a 3-down 1-up procedure, the threshold determination was set to 79.4% of the derived curves. The value of 79.4% denotes the level at which the percent of positive response is 79.4, which was necessary to reflect the expected performance target (Leek 2001). To further explain this: If the probability of a down sequence must equal that of an up sequence (i.e. 0.5), for a 3-down 1-up procedure, the probability of a down sequence (p) must equal 3x the probability of an up sequence, p^3, and is derived from the cube root of 0.5 (Leek 2001; Levitt 1971). Thus, the threshold estimate or performance target will be the level at which the percent of positive response is:

$$\sqrt[3]{0.50} = 0.794$$

A sample psychometric function curve is presented in Figure 4-4. Resolution threshold is estimated to be at 7.02 pixels which when converted to logMAR will be 0.17 logMAR.

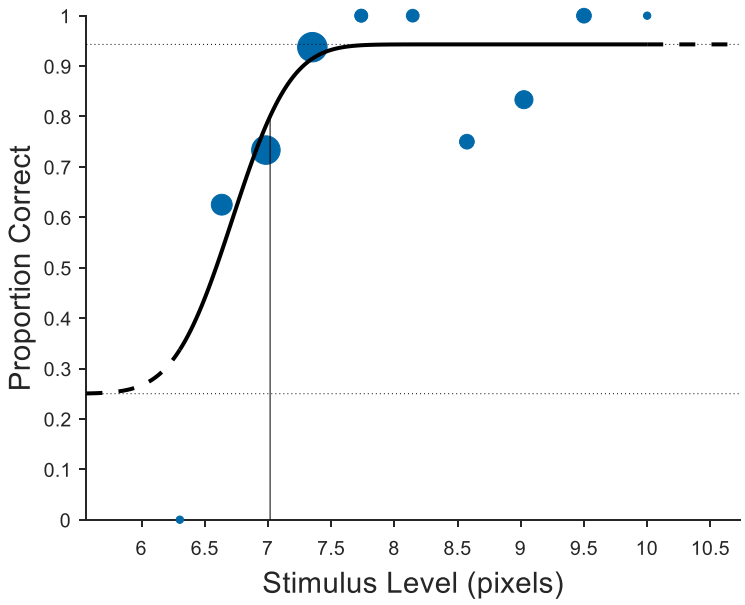

Figure 4-4: Psychometric function curve from one typical participant
Result is shown for a participant viewing the Landolt C target oriented horizontally at 0 degree, while at 15° eccentric position. Diagram shows the proportion of correct Landolt C gap identifications (blue circles) as a function of stimulus level or size, where the larger the circle the more correct entries for that pixel size. As the stimulus level decreases, the chance of getting a correct response drops while as the stimulus level increases, the chance of getting a correct response is greater. On a scale of 0 to 1, the 2.5 proportion correct identifies the level at which guessing is a chance of 1 in 4 (0.25), a value which equals the reciprocal of available alternatives in a 4AFC task. The upper 0.95 horizontal broken line represents the lapse rate, or the lapses produced from an incorrect response when a correct one was expected. When lapses occur, the function curve then asymptotes to a value close to 1. The threshold point indicated by the thin continuous vertical line is an estimate of the value that has the probability of getting three consecutive correct targets equal to half (following a 3-down, 1-up rule).

To achieve a standardised data format, accuracy and precision data were normalised within participants and presented in graphs. For data normalization raw data were rescaled to produce values between 0 and 1. This was done by subtracting the minimum value from each given value, and dividing by the range.

4.3 Results

4.3.1 Participants

Twelve participants with IN (5 females; age range 29 – 69 years; mean age 48.5) and 14 typical participants (9 females; age range 20 – 39 years; mean age 26.2) were examined for this experiment. Details of other clinical data are shown in Table 8-1 and Table 8-2 in the Appendix. An experiment was not performed for participant IN21 at the extreme left position of 45° (i.e. 45° right gaze) because they could not turn their gaze that far due to a previously performed squint surgery.

4.3.2 Visual resolution at gaze positions

A. Target orientation

Participants with IN: The mean visual resolution thresholds obtained for the horizontal (0 and 180°) and vertical (90 and 270°) Landolt 'C' orientation are presented individually, in Figure 4-5. Results show that the resolution threshold obtained when target was oriented vertically were, at most gaze angles, only slightly poorer (higher in value) for six out of 12 participants (IN03, IN05, IN07, IN09, IN11, and IN21). For two others (IN10 and IN13), visual resolution thresholds obtained using the vertical oriented Landolt C's were better, and for the other four they appeared the same. Furthermore, the gaze angles at which visual resolution threshold was lowest corresponds for both horizontal and vertical target orientation in only a quarter of all participants. In all other participants, the different thresholds obtained using either horizontal or vertical C orientations are close in value. Statistical analysis further showed that the within subjects mean threshold obtained using the vertical oriented Landolt C (mean = 0.995 ± 0.32 logMAR) was slightly larger than with horizontal oriented targets (mean = 0.991 ± 0.34 logMAR). The paired sample t-test show these values were not statistically significant [t = -0.16 (11), P = 0.88].

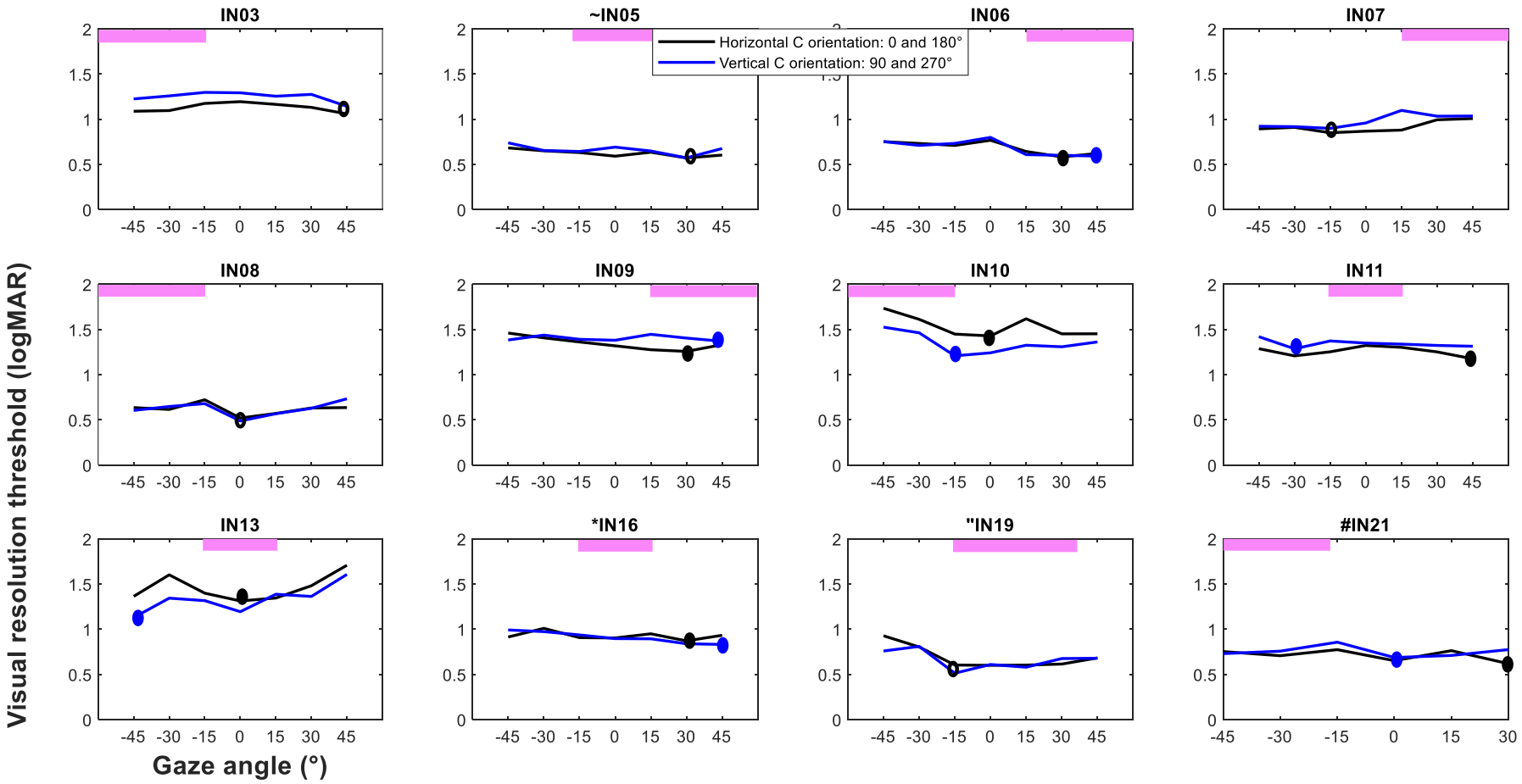

Figure 4-5: Visual resolution at gaze angles for participants with IN

Data presented are the mean threshold values obtained for both horizontal (0 and 180°) and vertical (90 and 270°) Landolt C orientations. Gaze angle of -45° represents left gaze while gaze angle of 45° represents right gaze. Violet shaded portion, above each subplot, indicates region of clinical null. Where it is on the far left, it represents left gaze, while for those on the far right it indicates the null is in the right gaze. For null zone at primary position (PP), shaded region is at the central position. ~IN05 = null gaze in PP and up gaze. *IN16 = PP, right equals left gaze. "IN19 = slightly right in PP. #IN21 = central to left gaze. Hollow **black** ovals represents points on the graph in which threshold was lowest whilst using the horizontal and vertical Landolt C targets. Where this differs, it is indicated by solid **black** (lowest threshold for Horizontal Landolt C target) and **blue** ovals (lowest threshold for vertical Landolt C threshold). Lower logMAR value = better vision.

Typical participants: The mean visual resolution thresholds obtained for all typical participants, at the seven gaze positions, are presented in Figure 4-6. Results obtained for the four Landolt C target orientation are presented separately. The graph reveals slightly more variable data, obtained using four different target orientations, for measurements at -45 and 30°. These results, however, show no significant main effect of target orientation [$F_{(3, 39)} = 0.80$, $p = 0.50$]. Given that there was no significant difference in data values, results from the left and right eccentric gaze positions were combined and presented in Figure 4-6b. Statistical analysis also revealed no significant difference when the Landolt C orientation was either horizontal or vertical [$F_{(1.83, 39)} = 0.67$, $p = 0.51$].

B. Effect of gaze angle

Participants with IN: As seen in Figure 4-5, visual resolution threshold varies slightly across gaze angles. The participants' best threshold corresponded with their clinical null zone in about a quarter of the participants (IN06, IN09, IN10, IN13, IN19). For some other participants, threshold at the null zone differs slightly from that obtained at other eccentric gaze positions. For example for participant IN03, the threshold measured at null zone (-30° eccentricity) is 1.10 logMAR using the horizontal Landolt C and 1.26 logMAR using the vertical Landolt C, while that at the lowest point (45°eccentricity) is 1.06 logMAR using the horizontal Landolt C and 1.14 logMAR using the vertical Landolt C targets.

Typical participants: The mean visual thresholds obtained for all typical participants, at the seven gaze positions, are presented in Figure 4-6. Statistical analysis indicated no significant difference in the vision threshold across gaze angles [$F_{(6, 78)} = 0.76$, $p = 0.60$]. Again, the left and right eccentric gaze positions were merged and presented in Figure 4-6b below. From this figure, the mean value obtained at primary position was only slightly better than at the extreme 45° eccentric gaze for when the Landolt C was oriented horizontally at 180°. Further analysis also indicated no significant difference in the visual threshold across gaze angles [$F_{(1.94, 39)} = 0.26$, $p = 0.77$].

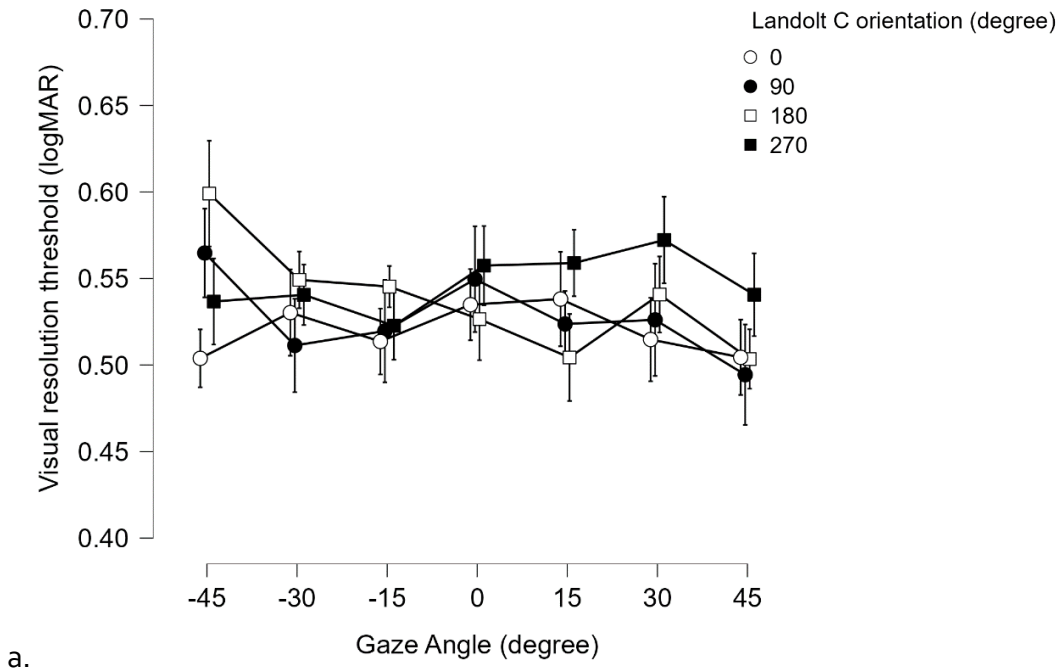

a.

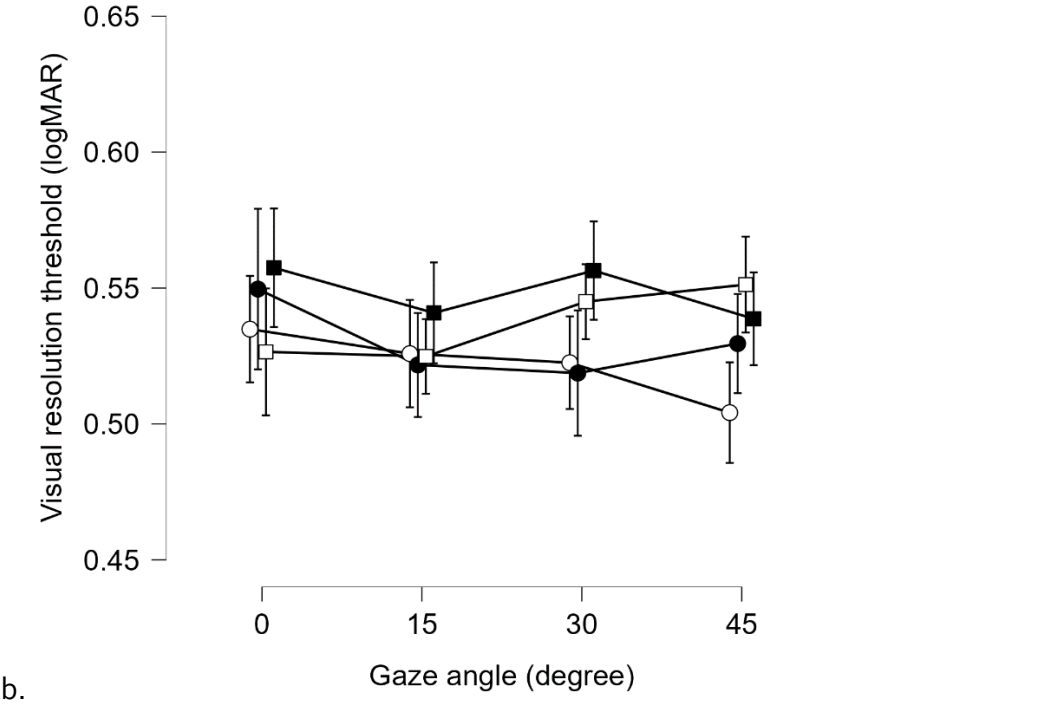

b.

Figure 4-6: Mean threshold vision for typical participants at gaze angles
Data obtained from all seven gaze positions are presented in (a) while that obtained from merging eccentric positions are presented in (b). Error bars = Standard error of mean.
Higher logMAR values indicate poorer vision.

C. Visual resolution threshold at eccentric gaze positions in emmetropes

Data from nine typical participants without significant refractive error (emmetropes) and presenting with VA better or less than 0.0 logMAR are given in Figure 4-7. As seen in the

graph, measured VA was about an average of 0.2 logMAR, a value poorer than their entry clinical VA. A more consistent threshold was found at the 45° right eccentric gaze position when the target was oriented in the four directions. Also, threshold obtained when the target was oriented 90° vertically appeared consistently better than when oriented vertically at 270°. Statistical analysis however, showed no significant difference in the mean threshold obtained at different gaze angles [$F_{(6, 48)} = 0.22$, $p = 0.97$] and while using differently oriented Landolt C targets [$F_{(3, 24)} = 2.33$, $p = 0.10$].

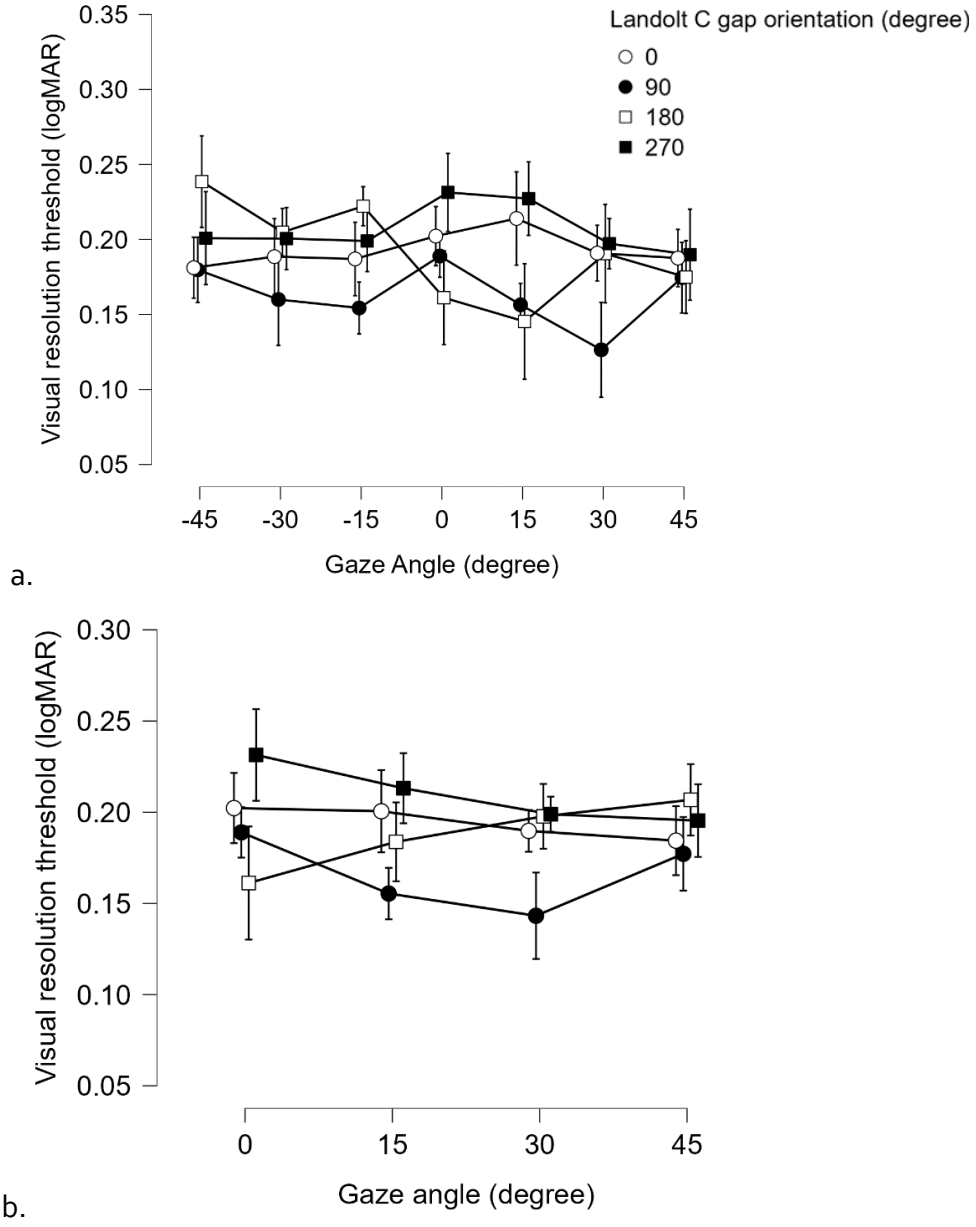

Figure 4-7: Visual resolution threshold measured in emmetropes
Data obtained from all seven gaze positions are presented in (a) while that obtained from merging eccentric positions are presented in (b). Error bars = Standard error of mean.
Higher logMAR values indicate poorer vision.

The left and right data sets were merged by finding the mean threshold obtained for each corresponding (i.e. left/right) position. Statistical results also indicate no significant difference in the mean values obtained at eccentric gaze viewing [$F_{(3,24)} = 0.21$, $p = 0.89$] and when the target orientation was changed [$F_{(3,24)} = 1.98$, $p = 0.14$].

To ensure that the data set was more comparable with that performed in the pilot study (discussed in section 4.1), a paired sample t-test was run for mean threshold values obtained at primary position and those obtained at the 30° and 45° gaze eccentric gaze positions, respectively. Results also show that there was no significant difference at 30° [$t_{(8)} = 0.90$, $p = 0.39$] and 45° [$t_{(8)} = 0.21$, $p = 0.84$] gaze positions.

D. Visual resolution threshold and Clinical VA

The VA measured clinically was correlated with resolution threshold obtained using the psychophysical mean from this experiment. Results are presented for both groups of participants in Figure 4-8. Correlation output was: participants with IN [r = 0.67, **p = 0.02**; (95% CI: 0.16, 0.90)] and typical participants [r = 0.97, **p<0.001**; (95% CI: 0.91, 0.99)]. Generally, it can be seen that visual resolution in participants with IN was poorer and varied more.

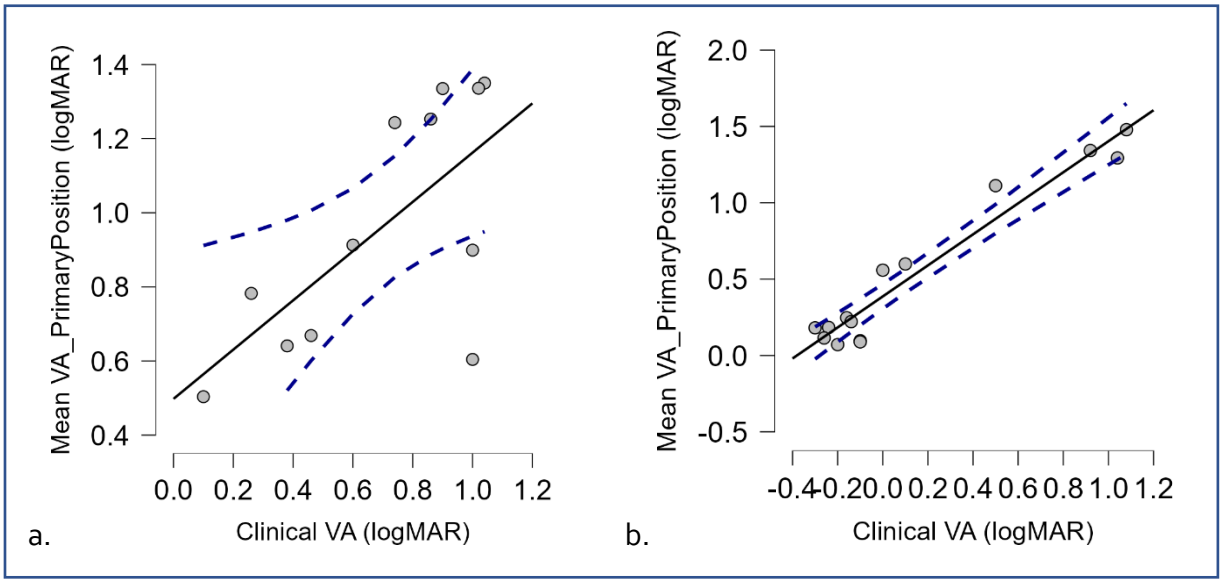

Figure 4-8: Comparing clinical and psychometric visual resolution
Figure (a) shows data obtained from participants with IN while figure (b) represents data obtained for typical participants. Blue dotted lines indicate the 95% confident interval region.
A greater logMAR VA value depicts poorer VA.

Figure 4-8 also indicates that, although the psychophysical procedure gave rise to much poorer resolution threshold (especially for those with IN), there was a significant positive correlation indicating that the resolution threshold obtained was reasonably consistent with clinical VA; although there appears to be a consistent offset between both measures.

4.3.3 Fixation performance at gaze positions

A. Participants with IN

Using the bPDF analysis described in Chapter two, metrics for fixation performance at eccentric gaze positions were derived, producing quantitative measures of accuracy and precision of fixation. Values for the accuracy and precision of eye movement while fixating eccentrically at seven gaze position spanning ±45° are presented in Figure 4-9 and 4-10. Also included are the horizontal and vertical range of eye position spread and contour area of each participant in Figure 4-11. Recall that, the lower the accuracy value, the closer the fixational data points are to the point of fixation, and therefore the more accurate the fixation at the gaze angle considered. The precision of eye movement was determined using the total area of the 68% isocontour. This value together with the shape factor and orientation of the major axis of this isocontour were used to determine the horizontal and vertical spread of eye movement data as described in section 2.7.3.

Accuracy: Generally, plots in Figure 4-9 show a variability in the accuracy of fixational eye movement across gaze angles, within and between participants. The fixation point of best accuracy corresponded with the null zone of close to half of the participants (IN06, IN09, IN11, IN19 and IN21). It can also be seen that from the point of best accuracy (i.e. position of lowest accuracy value), the pattern in which values increase to other fixation positions is not consistent.

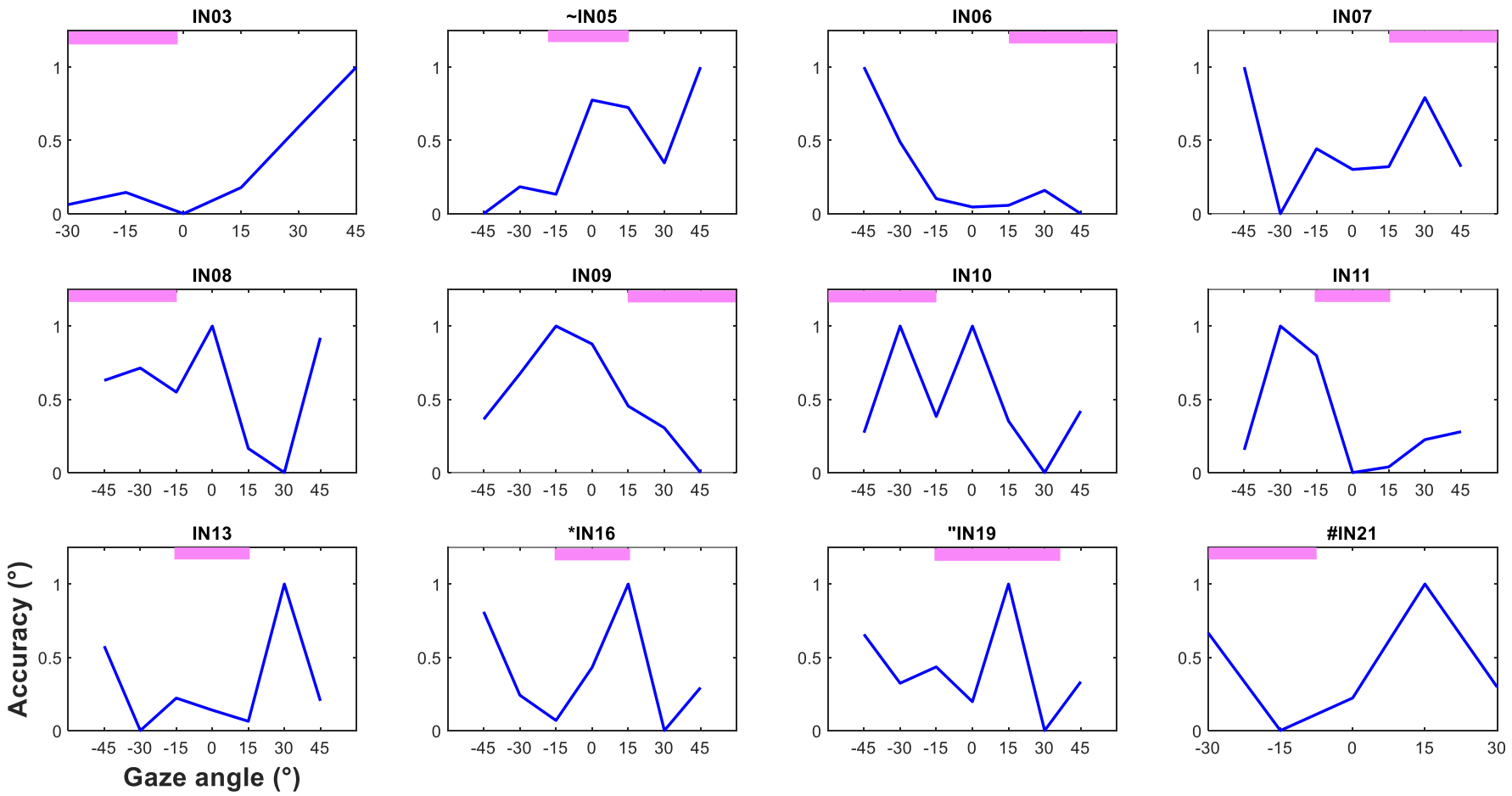

Figure 4-9: Accuracy values at all fixation positions in participants with IN.

Data presented are **normalised** for values between 0 and 1. Gaze angle of -45° represents left gaze while gaze angle of 45° represents right gaze.
Violet shaded portion, above each subplot, indicates region of clinical null. Where it is on the far left, it represents left gaze, while for those on the far right it indicates the null is in the right gaze. For null zone at primary position (PP), shaded region is at the central position. ~IN05=null gaze in PP and up gaze. *IN16=PP, right equals left gaze. "IN19= slightly right in PP. #IN21=central to left gaze. The lowest point in each plot (0°, on the vertical scale) indicate points of high accuracy i.e. the shortest isocontour vector length to the target position.

Contour shape: As seen in Figure 4-10, the ratio of the isocontour minor and major axes (contour shape or shape factor) were mostly nearer one than zero. Where it is close to one, it shows there is an almost equal spread of data in the maximum and minimum lengths of the derived isocontour, which also represent the horizontal and vertical planes of eye movement data. The points where shape factor is closest to one (i.e. where shape factor is highest), does not correspond with the null zones of all participants. This may not necessarily be the case because at the participants null zone, it is possible the horizontal spread of eye movement data is more than the vertical spread, or vice versa. Whichever is the case only highlights the nature of the IN eye movement oscillation present for that participant; if it exists more in the horizontal or the vertical plane.

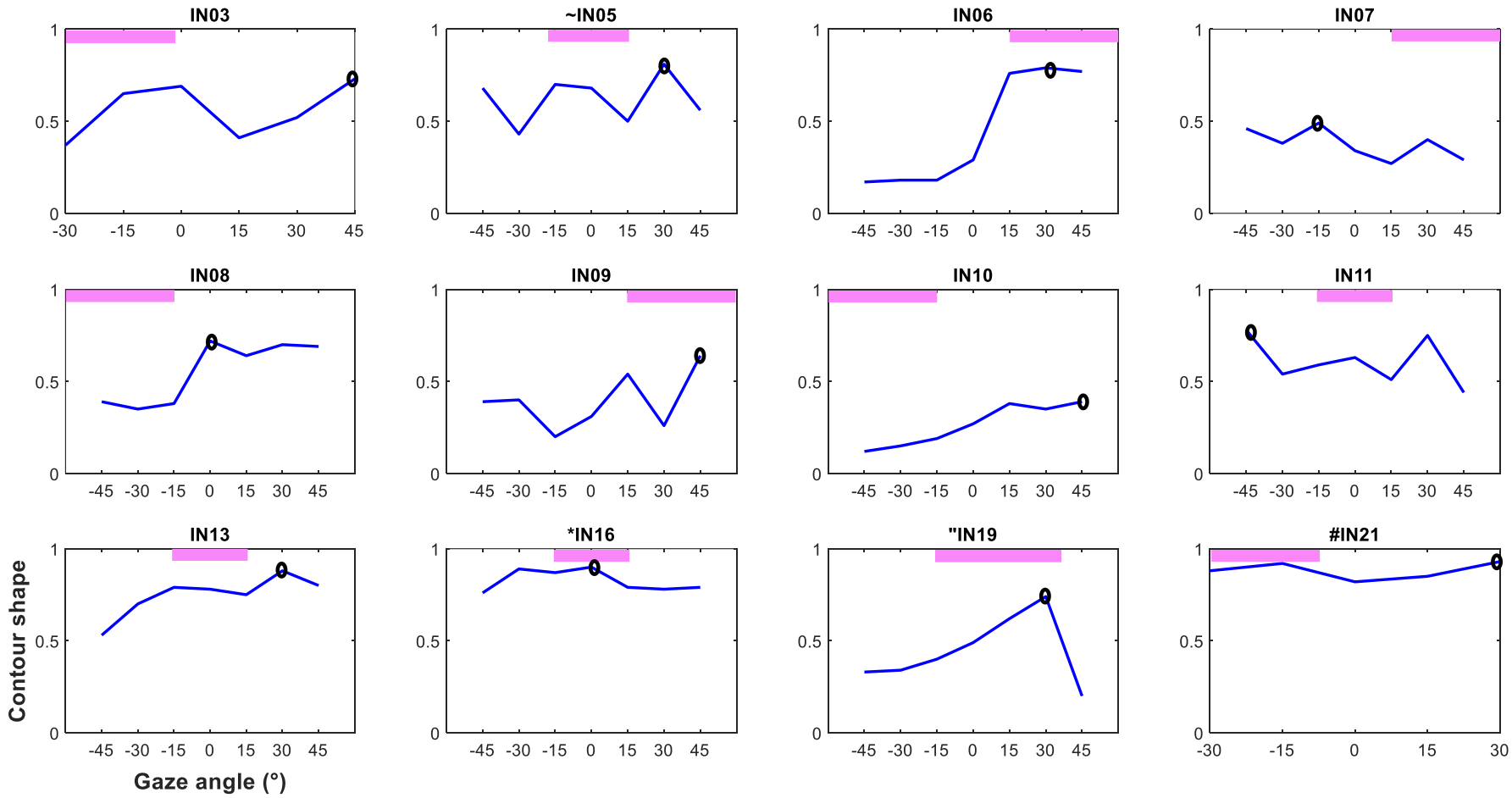

Figure 4-10: Contour shape values at all fixation positions in participants with IN.

The -45° gaze angle represents left gaze while gaze angle of 45° represents right gaze. Since shape factor is the product of a ratio, values fall within 0 and 1 therefore these were not normalised. Violet shaded portion, above each subplot, indicates region of clinical null. Where it is on the far left, it represents left gaze, while for those on the far right it indicates the null is in the right gaze. For null zone at primary position (PP), shaded region is at the central position. ~IN05=null gaze in PP and up gaze. *IN16=PP, right equals left gaze. "IN19= slightly right in PP. #IN21=central to left gaze. The small **black** ovals in each plot are used to mark the point of eccentric gaze where contour shape is closest to 1; indicating that data spread on the horizontal and vertical plane are more symmetrical or more uniformly spread.

Nonetheless, it can be seen that the derived isocontour is more symmetrical at the null zones for a quarter of the participants (IN06, IN09, IN16 and IN19). To understand further the contributions of each eye movements components at each fixation point, the range of eye movement spread was derived, using the contour shape as one of its parameter (see Section 2.7.3), and presented alongside the contour area in the next figure (Figure 4-11).

Contour area and the relationship between isocontour major and minor axis: Figure 4-11 shows that Isocontour area values were also very variable across gaze angles, in each participant. In more than half of the participants (IN03, IN06, IN09, IN10, IN11, IN13 and IN19) the point of best precision (i.e. smallest isocontour area) coincided with the null zone. In one (IN05) out of the remaining five, the value at the point of best precision was almost the same as that at the null zone [$(2.08°)^2$ vs $(2.56°)^2$, real values].

Just like a circle, each contour area point at gaze angles, will have two radii (represented by the horizontal and vertical eye position data spread) that make up this value. These are represented as the horizontal and vertical range in each plot, and can be seen to follow quite closely the contour area. Since these were normalised data, it is possible that the real values of horizontal and vertical range at the point of best precision will differ. However, gaze positions where the vertical range was higher than the horizontal range have been indicated in the figure.

Looking closely, it can be seen that at the points of best precision, the horizontal and vertical range of data are equally lowest in normalised value for only half of the participants (IN07, IN08, IN11, IN13, IN16 and IN21), indicating a uniform reduction in vertical and horizontal range of the isocontour at that gaze angle. In a quarter of the participants (IN03, IN05 and IN06), the range of data spread on the vertical axis was slightly larger at the point of best precision compared to other gaze angles, and that on the horizontal axis remained lowest. While for the rest of the participants (IN09, IN10 and IN19), at the point of best precision the horizontal spread of eye movement data increased remarkably compared to findings at other gaze angles (much more in participant IN09 and IN19), and that on the vertical axis remained lowest.

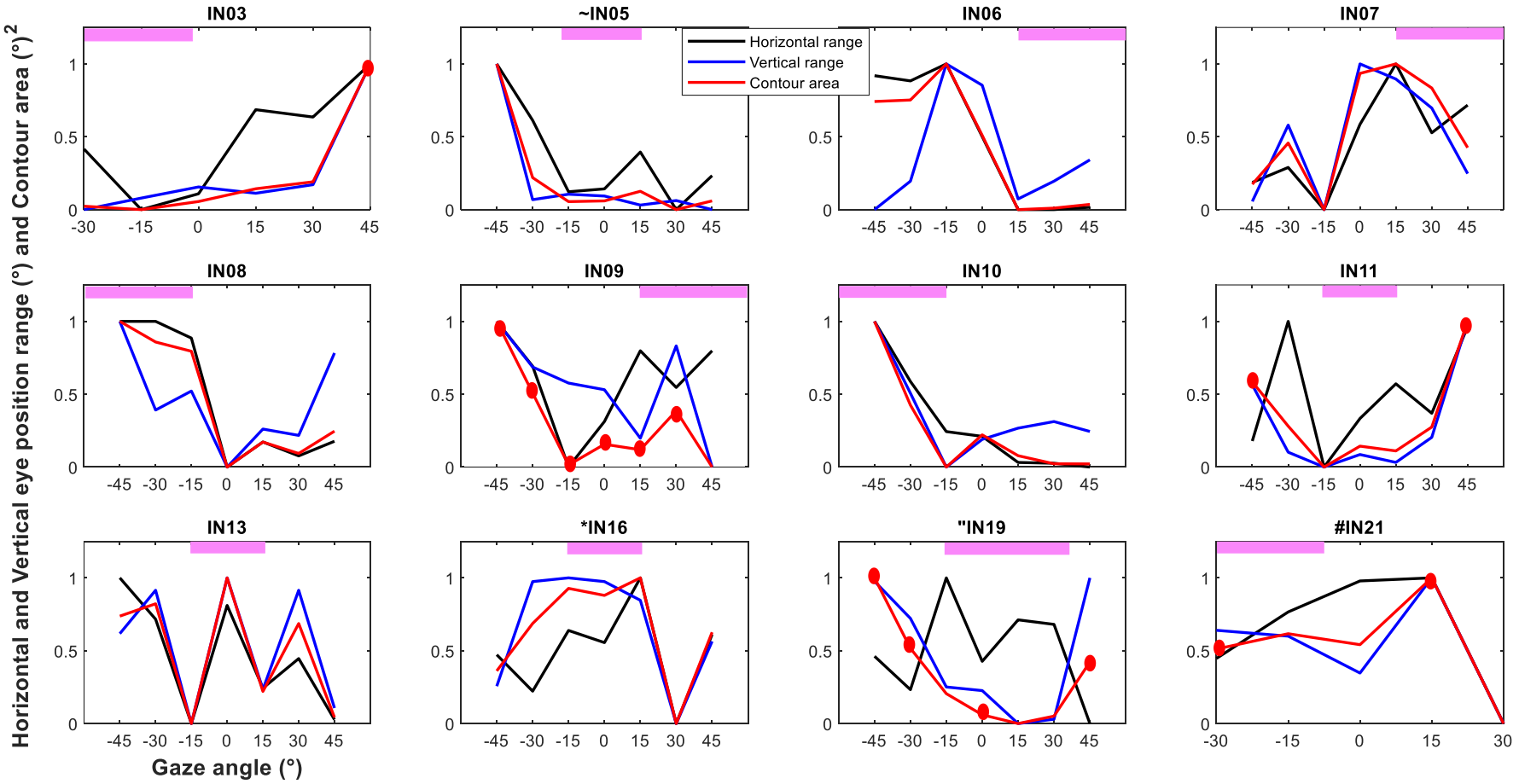

Figure 4-11: Contour area, including the horizontal and vertical eye position range for participants with IN.

For each parameter, data presented are **normalised** to produce values between 0 and 1. Gaze angle of -45° represents left gaze while gaze angle of 45° represents right gaze. Violet shaded portion indicates region of clinical null. Where it is on the far left, it represents left gaze, while for those on the far right it indicates the null is in the right gaze. For null zone at primary position (PP), shaded region is at the central position. ~IN05=null gaze in PP and up gaze. *IN16=PP, right equals left gaze. "IN19= slightly right in PP. #IN21=central to left gaze; this participant has the same normalised values at gaze positions 30° and 15° hence, the overlap in trace.

The lowest point in each plot (0°, on the vertical scale) indicate points of high precision where the contour area is smallest. The **red** ovals in some plots indicates gaze angles where the real values of the isocontour vertical range was wider than the horizontal range. In all other positions of gaze, the horizontal range were wider.

The relationship between the isocontour major and minor axes was also found using the Pearson's correlation graphs, some of which are presented in Figure 4-12. In 10 out of the 12 participants, there was a positive relationship between both parameters which means that as the horizontal eye position spread increases, the vertical data spread also increases. This relationship was only significant in participants IN05, IN10 and IN13. For the other two participants (IN09 and IN19), as the horizontal data spread increases the vertical data spread decreases, and vice versa. This negative relationship was however not statistically significant. The variability in data spread between participants is also evident from the correlation plots presented. Insignificant associations can be found in the appendix.

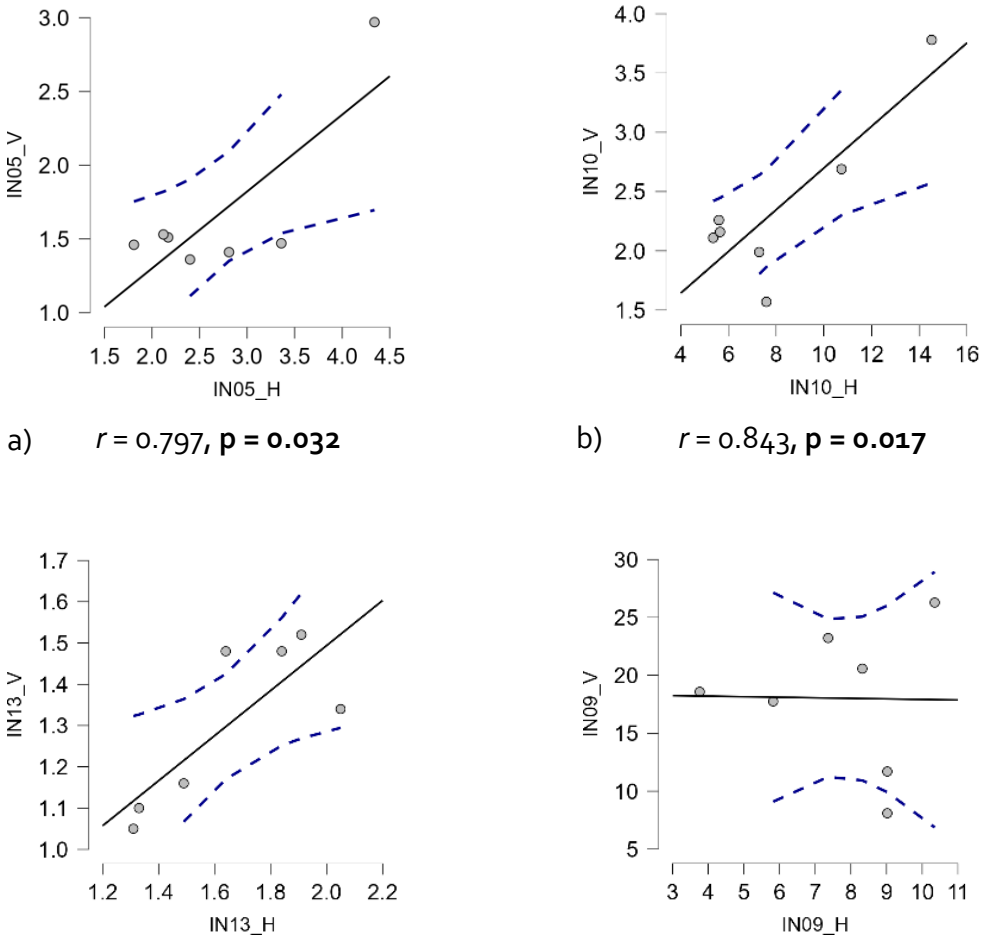

a) $r = 0.797$, **p = 0.032**

b) $r = 0.843$, **p = 0.017**

c) $r = 0.799$, **p = 0.031**

d) $r = -0.017$, p = 0.972

Figure 4-12: The horizontal and vertical axis range, as a function of gaze angle
Correlation plots are presented for significant relationships (a, b and c) and for participant with the worst r value (d). Both axes are indicated by the participants identity. V on the y axis indicates the vertical axis range while H on the x axis represent the horizontal axis range. Significant P values are included below individual participants plot. Dotted lines represent 95% CI. A change in the horizontal range but not in vertical range will produce a more horizontal trend line, while one with a change in vertical range but not in the horizontal range will produce a more vertical trend line. In cases where an increase or decrease in the horizontal range values corresponds to those in the vertical range, the trend line will be more diagonal.

Data representing the mean and standard deviation of fixation performance obtained from all participants are presented in Table 4-3. A further analysis of the contour area, shape factor and main axis orientation gave rise to the horizontal and vertical axis range. Correlation values for analysis between these variables are also presented in the table. It can be seen that raw values for fixation performance span a wide range between participants. Among the three parameters, contour area values showed more variability. Where the contour shape is lowest, the horizontal and vertical range of data is expected to differ widely in value. This is seen with participant IN10 who had the lowest contour shape factor. For cases of higher contour shape factor, this difference is expected to reduce, as seen in participant IN21 who had the highest contour shape value where both mean horizontal and vertical data range were similar.

Table 4-3: Mean and standard deviation of accuracy and precision data for all participants across gaze angles
The correlation coefficient and P values apply to analysis performed using the horizontal and vertical axis ranges at each gaze position. These were in turn derived from contour area, contour shape and the major axis orientation, at each gaze position. ▭ = *Statistical outlier*

Participant	Accuracy (°)	Contour shape	Contour area (°)²	*Horizontal axis range (°)*	*Vertical axis range (°)*	*Correlation coefficient r =*	*P value*
IN03	2.22 ± 0.94	0.56 ± 0.15	18.20 ± 17.61	5.58 ± 1.56	3.91 ± 2.58	0.69	0.13
IN05	0.73 ± 0.37	0.62 ± 0.13	3.82 ± 2.83	2.72 ± 0.88	1.67 ± 0.57	0.80	**0.03**
IN06	0.48 ± 0.32	0.45 ± 0.31	3.92 ±2.46	4.15 ± 2.59	1.27 ± 0.16	0.32	0.49
IN07	1.19 ± 0.36	0.38 ± 0.08	8.46 ± 2.67	4.47 ± 1.06	3.64 ± 0.93	0.69	0.09
IN08	1.27 ± 0.79	0.55 ± 0.17	2.79 ± 1.11	2.65 ± 0.97	1.33 ± 0.08	0.58	0.18
IN09	21.03 ± 7.67	0.39 ± 0.16	102.49 ± 57.46	7.66 ± 2.24	18.03 ± 6.33	-0.017	0.97
IN10	2.21 ± 1.09	0.26 ± 0.11	11.74 ± 4.51	8.11 ± 3.39	2.37 ± 0.71	0.84	**0.02**
IN11	1.24 ± 0.5	0.61 ± 0.12	5.01 ± 2.21	2.88 ± 0.32	2.35 ± 1.16	0.38	0.40
IN13	0.59 ± 0.56	0.75 ± 0.11	1.68 ± 0.48	1.65 ± 0.29	1.30 ± 0.20	0.80	**0.03**
IN16	0.32 ± 0.22	0.83 ± 0.06	2.08 ± 0.30	1.77 ± 0.12	1.5 ± 0.16	0.52	0.23
IN19	1.42 ± 0.64	0.45 ± 0.19	18.89 ± 7.79	4.15 ± 0.95	7.05 ± 3.50	-0.73	0.07
IN21	0.33 ± 0.11	0.88 ± 0.05	1.69 ± 0.48	1.46 ± 0.20	1.46 ± 0.28	0.70	0.19

Significant correlations in bold

B. Typical participants

A summary of mean and standard deviation of fixation performance in typical participants is presented in Table 4-4. These data indicate a decrease in fixation accuracy from the primary position to the extreme 45° gaze angle. Contour shape value also decreased at the extreme 45° gaze angle (less symmetry in major and minor axis data spread). For contour area, the change across gaze angle was not regular, and this is also reflected in the horizontal and vertical eye position data spread that was derived. These data, which were

statistically analysed and showed no significant difference between them, are presented as charts in the sections below.

Table 4-4: Mean and standard deviation across all gaze position in typical participants
Values are presented for 14 typical participants and merged with data from the corresponding gaze angles on the opposite side of the visual field.

Gaze angle (°)	Accuracy (°)	Contour shape	Contour area (°)²	*Horizontal axis range (°)*	*Vertical axis range (°)*
0	0.42 ± 0.16	0.84 ± 0.09	1.34 ± 0.78	1.23 ± 0.37	1.31 ± 0.40
15	0.63 ± 0.42	0.84 ± 0.12	1.09 ± 0.50	1.17 ± 0.26	1.18 ± 0.32
30	0.59 ± 0.30	0.77 ± 0.15	1.17 ± 0.50	1.20 ± 0.23	1.29 ± 0.47
45	0.69 ± 0.47	0.75 ± 0.13	1.16 ± 0.49	1.27 ± 0.27	1.23 ± 0.31

Accuracy: For typical participants, no significant difference was found across gaze angles [$F_{(6,91)} = 1.53$, $p = 0.18$]. Therefore, the data were combined for eccentric gaze positions of left and right and presented in Figure 4-13b. Values obtained for accuracy showed a mean increase at far eccentric positions; which means fixation was more inaccurate. Data were most variable at the 45° eccentric gaze position and were least variable at the primary position. Analyses however indicate no significant difference in fixation accuracy at eccentric gaze positions [$F_{(3, 52)} = 1.44$, $p = 0.24$].

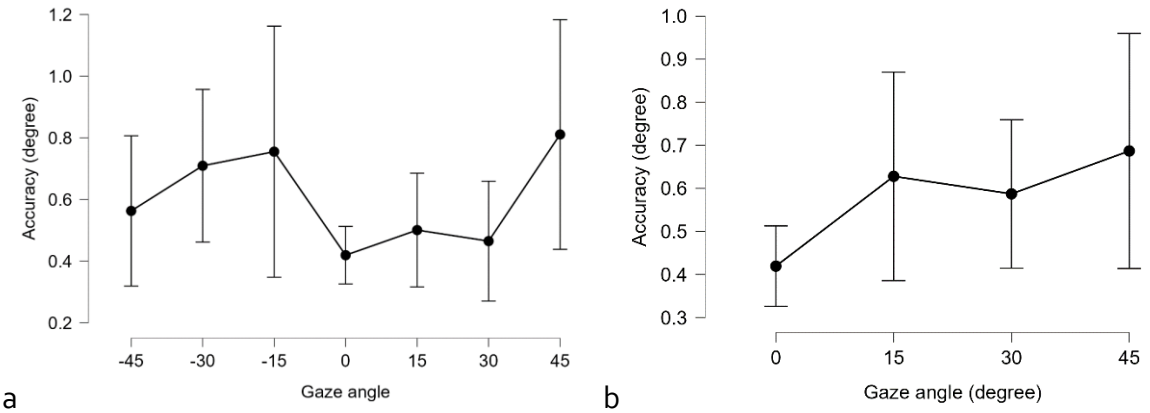

Figure 4-13: Accuracy at eccentric gaze position in typical participants
In figure (a) data is presented for all 7 eccentric gaze positions, while in (b) corresponding gaze positions on either side were merged. Error bars = 95%CI

Contour shape factor: Similarly, Figure 4-14b shows a reduced contour shape at increased gaze angle, with data at 45 and 30° showing more variability in data spread. However, data collected across all gaze angles were not statistically significant $F_{(6, 91)} = 1.67$, $p = 0.14$. When the results were merged for eccentric left and right gaze positions, there was also no significant difference in fixational eye movement contour shape factor at eccentric gaze positions [$F_{(3, 52)} = 2.26$, $p = 0.09$].

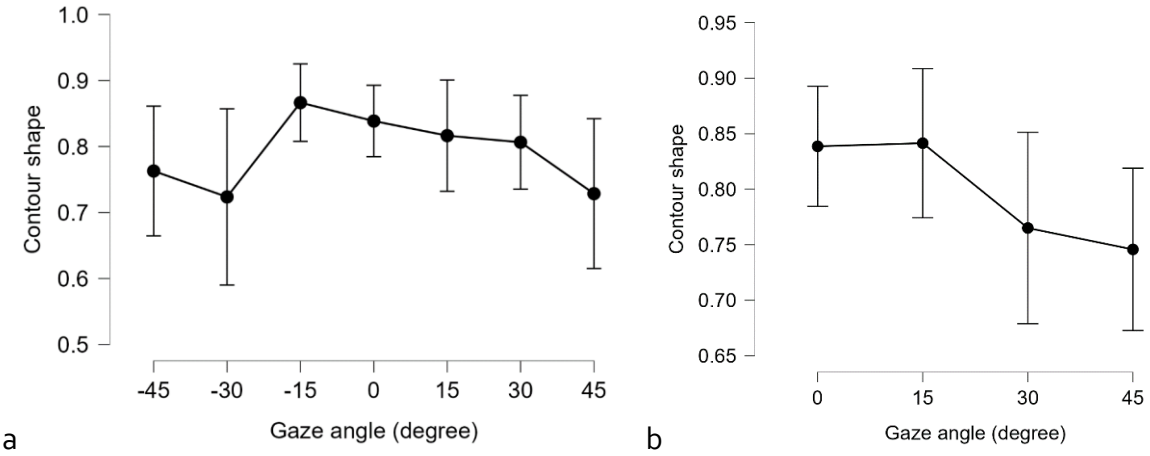

Figure 4-14: Contour shape at eccentric gaze position in typical participants
In figure (a) data is presented for all 7 eccentric gaze positions, while in (b) corresponding gaze positions on either side were merged. Error bars = 95%CI

Contour area including horizontal and vertical range: Mean values for the contour area as well as the horizontal and vertical data spread are presented in Figure 4-15. The diagram indicates that contour area was largest at primary position and showed a little more variability. Once again, however, this difference across gaze angles was not significant. When combined, each of the three parameters also do not show a significant change across all gaze angles [$F_{(1.81, 39)} = 0.93$, $p = 0.40$].

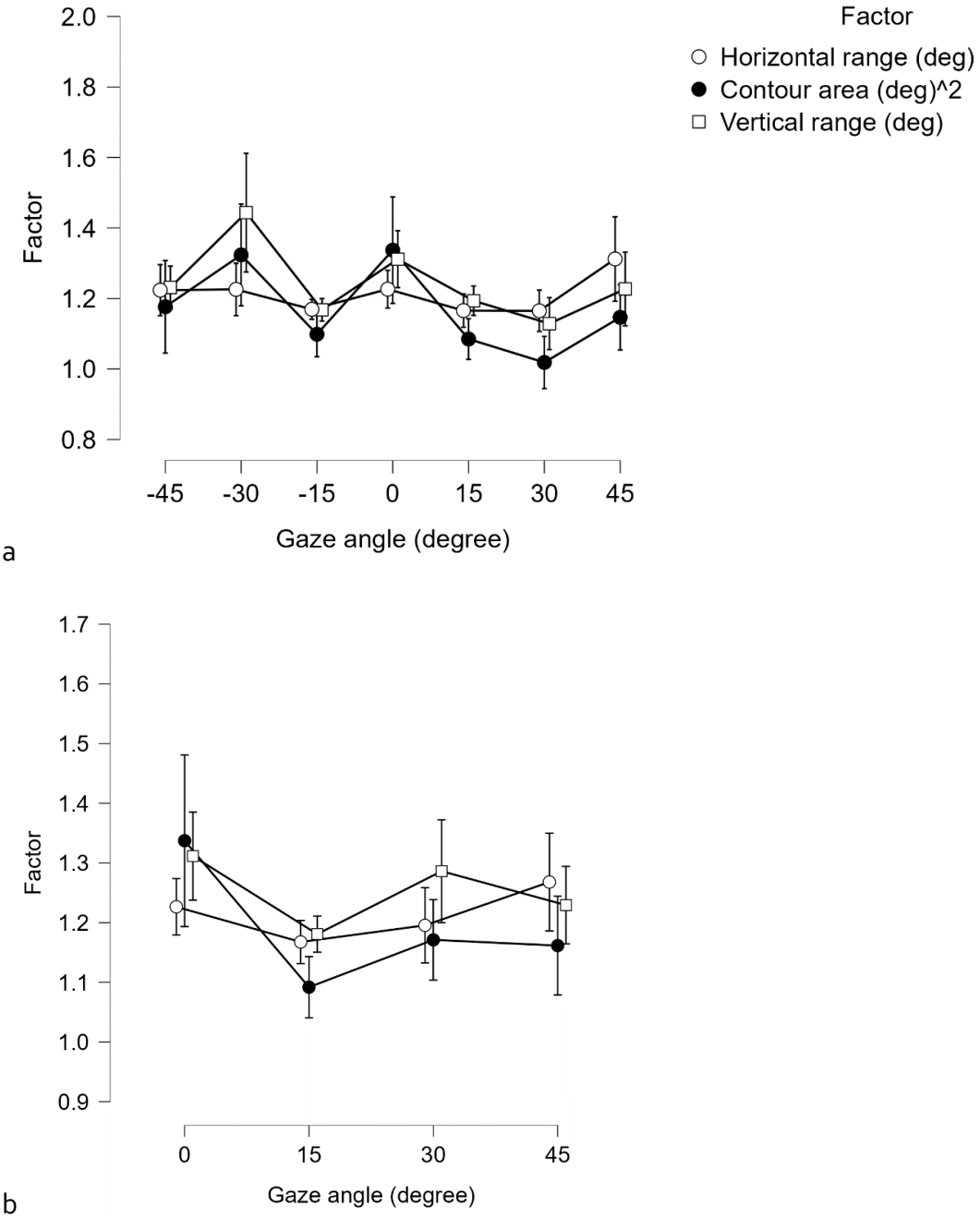

Figure 4-15: Mean isocontour area alongside the horizontal and vertical eye position range
In figure (a) data is presented for all 7 eccentric gaze positions, while in (b) corresponding gaze positions on either side were merged. Errors bars = Standard error of mean

4.3.4 The relationship between fixation performance and VA in participants with IN

A. Fixation performance and clinical VA

The mean accuracy and precision values obtained within each participant were correlated with their clinical VA. The graphs in Figure 4-16a illustrate these findings. From the plots it

can be seen that there is a gradual increase in mean fixation performance value in those with poorer VA. Statistical analysis however, showed no significant relationship between mean accuracy and VA [r = 0.25, p = 0.46; (95% CI: -0.41, 0.74)] as well as mean precision and VA [r = 0.39, p = 0.24; (95% CI: -0.28, 0.80)]. The outlier seen in both graphs was not included in the calculations, but since values of accuracy and contour area appear to be at or near an unrealistic value of 0, graphs were replotted without the outlier value included. This is shown in Figure 4-16b.

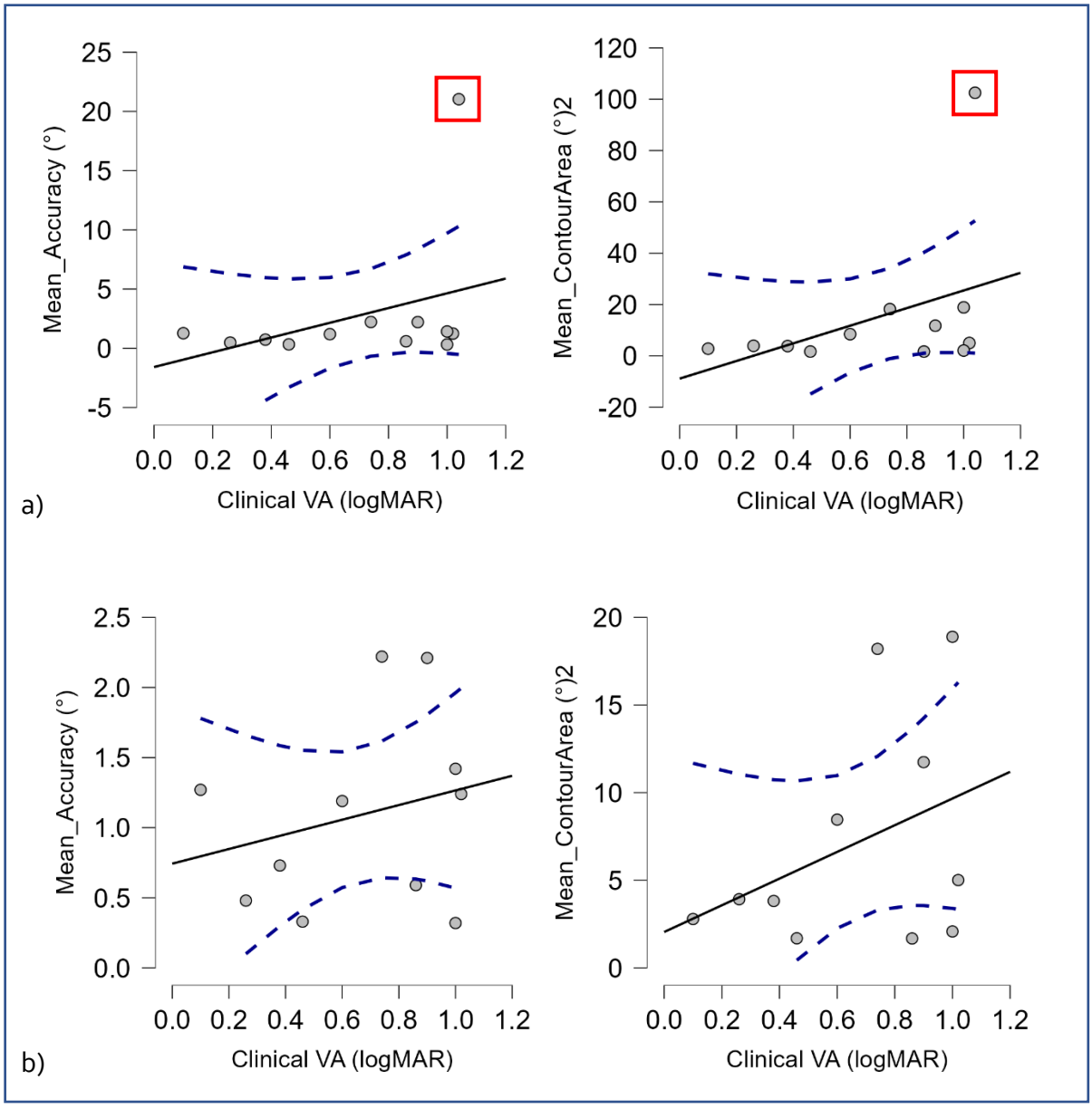

Figure 4-16: The relationship between fixation performance and entry VA in participants with IN
In figure (a) plots were produced with the outlier (enclosed in red squares) values included. Figure on the left show data obtained from the mean accuracy across gaze positions, while figure on the right represents the mean contour area (precision) across all gaze positions for each participant. In figures below (b), same

correlation plots were produced without the outlier values present. Blue dotted lines indicate the 95% confident interval region. A greater logMAR VA value depicts poorer VA.

B. Fixation performance and psychometric VA

Clinical visual resolution was measured at primary position hence it was correlated with measured psychometric VA at primary position as shown in Figure 4-8. However, the presence of the null zone necessitates finding a relationship between psychometric VA and fixation performance at eccentric gaze position. In order to do this, plot of measured VA (Figure 4-5) was reproduced in Figure 4-17, but with the position of best precision (fixational eye movement span) included. It can be seen from Figure 4-17 that, in two-third of the participants (IN05, IN07, IN08, IN09, IN10, IN13, IN16, IN21) fixation precision and visual threshold is best at the same gaze position.

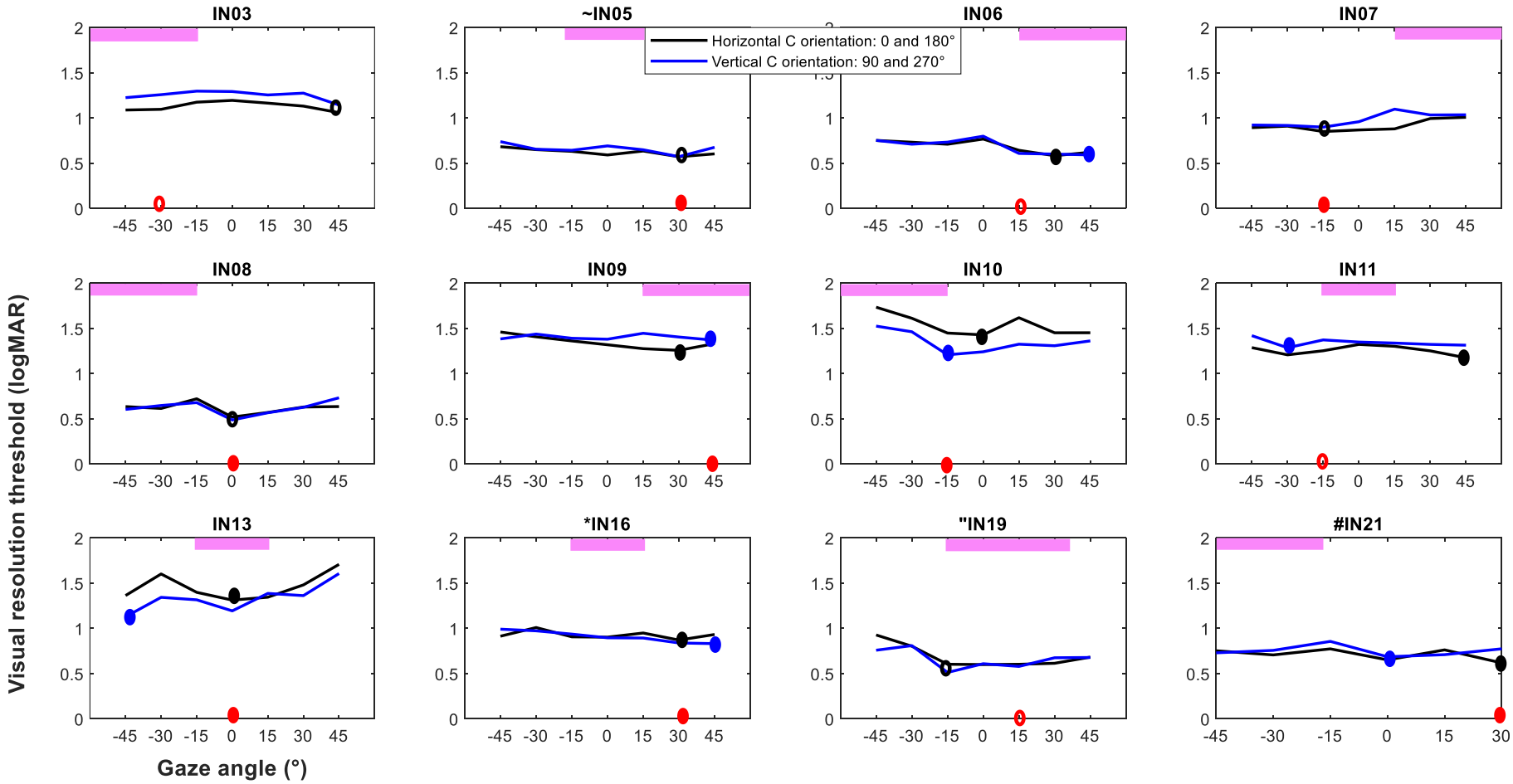

Figure 4-17: The relationship between psychometric threshold VA and fixation precision

Plot of measured threshold VA obtained at eccentric gaze positions reproduced with fixation precision included. Violet shaded portion, above each subplot, indicates region of clinical null. **Red** ovals indicate gaze position with the best fixation precision. Where it corresponds with gaze position of best VA (either with the horizontal or vertical oriented Landolt C), it is represented with a solid red oval. Hollow **black** ovals represents points on the graph in which threshold was lowest whilst using the horizontal and vertical Landolt C targets. Where this differs, it is indicated by solid **black** (lowest threshold for Horizontal Landolt C target) and **blue** ovals (lowest threshold for vertical Landolt C threshold). Lower logMAR value = better vision.

4.4 Discussion

Results obtained from this study have highlighted further the variable nature of VA and eye movements in people with IN. It can be seen repeatedly from the data presented in this chapter that the clinically measured null zones do not always correspond with indicators of best visual resolution threshold and fixation performance. As it is traditionally done, the determination of clinical null requires a subjective judgement of eye movement intensity during fixation at different gaze directions, usually at distances up close to the patient. Because of this, the influence of convergence null (Dell'Osso et al. 1972; Abadi and Dickinson 1986; Ukwade and Bedell 1992; Abadi and Bjerre 2002) on IN eye movement intensity, may have influenced the null zone findings presented here. Nonetheless, the objective threshold measures defining best visual resolution and fixation performance at gaze angles, are being considered and discussed as follows:

4.4.1 Visual resolution at gaze positions.

Consistent with previous literature (Jones 2011), the visual resolution thresholds obtained using horizontal and vertical Landolt C targets were quite similar in all participants. Individual data from those with IN only reveal a slight change in the horizontal and vertical thresholds for few participants where this difference was not clinically significant. Across gaze angles, the thresholds obtained in people with IN were not all uniform suggesting that fixation at eccentric gaze position may influence visual resolution. The presence of the null zone is one contributory factor for this difference in visual resolution across eccentric gaze position, however, as seen earlier in the introduction section, the small change in VA (Dunn et al. 2017) does not fully explain the choice of the null zone. It may be that an inability to detect a significant result from this current study was because of the methods used to determine visual resolution. Dunn and colleagues used the 2-AFC method and Landolt C target which was not a vanishing optotype, their study characteristics may have caused an easier identification of the targets and less precise VA threshold (Schlauch and Rose 1990; Vancleef et al. 2018; Anderson and Ennis 1999). These difference in tests conditions may have resulted in the inconsistent findings.

In typical participants, a similar finding is obtained where visual resolution differs across gaze angles but not significantly. In addition, the findings from the emmetropes who volunteered for this experiment do not agree with those obtained from the pilot study discussed in the Introduction. The dissimilarity in methodology of this study and the pilot experiments may have accounted for this finding. The fact that an accompanying task of eye movement recording and keyboard press to identify target orientation were involved for this study may have greatly influenced the results obtained. From this study, ocular stress which is expected to arise from a strain on the extraocular muscles and the neural integrator to maintain gaze at eccentric position do not cause a significant effect on the visual resolution measured. The findings from all participants are similar to that obtained from a previous study (Dunn et al. 2017), which found only a small change in VA to fixation preference at the null zone. It therefore means that, for people with IN or typical participants alike, fixation at the null zone (in the case of people with IN) or at primary position (in the case of typical participants) may feel more comfortable but the greater discomfort at a more eccentric gaze angle may not necessarily result in a significant change in VA threshold. These findings still leave our main question unanswered, as to what could really be the major influencing factor for null zone preference.

4.4.2 Fixation performance at gaze positions

Apart from the fact that all parameters of accuracy and precision measured across gaze angles varied considerably, the contour area metric (precision) was more consistent with measured clinical null than the others. The accuracy of fixation as described in chapter 3, may not necessarily give a true picture of fixation performance as it relates to gaze angle. This is because it is a measure of the mean of data points from the fixation position, and this mean value may remain consistent even though gaze direction changes. To get a true measure of fixation performance as a function of gaze angle, the horizontal and vertical spread of eye position changes is important. From this study it can be seen that for some of the participants with IN, the range of data spread was more in the vertical than horizontal axis. While this may be a true finding, it is different from the normal. However, it can be seen that in those who exhibited this trend, the finding was more in the extreme gaze angles and away from the identified null zones. We could conclude that a shift in gaze to

the far eccentric position was responsible for producing more eye movement oscillation in the vertical component of the eye position trace. Furthermore, the presence of a convergence null may have triggered this abnormal reaction while fixating at distance, as seen in three out of the five participants (IN09, IN11 and IN19 – see participants clinical information in Appendix) who present with a wider vertical range. Therefore, it is not in all participants with IN that we find a reduced intensity translated as a reduced horizontal eye movement component trace at null zone. Some of them may indeed have their vertical eye movement component intensity reduced (or even increased) alongside the horizontal.

The correlation plots in participants with IN have further shown that a corresponding change in the horizontal and vertical component is a common factor despite only being significant in a quarter of them. This finding further explains that, for most participants with IN, the null is a combination of a horizontal and vertical null and at the fixation point of best preference, it is possible that the retinal slip is reduced (or fixation is more stable) in both the horizontal and vertical components of the eye movement trace in order to enable the best possible quality of vision. In a few cases where the vertical component does not give a corresponding change alongside the horizontal component, it is possible that the null is horizontal only and the vertical component might also impair vision even when the individual uses their null. This further indicates the importance of evaluating the horizontal and vertical components of IN eye movement to understand fixation at eccentric gaze. However, it is important to note here that null zones for this study were determined subjectively. This limitation could have flawed judgement of fixation performance at gaze positions. It is therefore crucial that for future studies, an objective assessment of the null should be utilized in order to adequately determine findings of fixation preference at eccentric gaze.

In participants with IN, the findings of mean accuracy and precision were found to increase slightly with poorer clinical VA, although this corresponding change was not significant. This result differs from that reported in the previous chapter and may have resulted from the fact that the experiment in this chapter ran for a much longer time and fixation targets were designed for four independent staircases. During the experiment, it is possible that there were cases where, for example, a smaller Landolt 'C' would be testing a leftward gap and a larger 'C' an upward gap. So, it is expected that participants looked around more

(within the stimulus) during the task as compared to the cross target which was used in the previous chapter.

In typical participants, the mean accuracy was seen to worsen at the extreme gaze angles and the contour shape was less symmetrical as eccentricity increased, even though this change was not significant. Similarly, one recent study (McIlreavy, Nedelchev and Ennis 2022) has shown that eye velocity is biased towards primary position in typical participants, from gaze angles spanning ±16°. In the current study, contrary to what was expected, the mean precision value reduced slightly from the primary position to the extreme gaze positions, but this change was insignificant. Also, precision values obtained from this study [about 1.2(°)^2] were higher i.e. worse than that recorded from the mean contour area of fixation obtained from 14 typical participants in a previous study (Cherici et al. 2012): [0.1(°)^2]. The dissimilarity in fixation task and experiment methodology may have accounted for this difference in values obtained.

In summary, results from the experiment described in this chapter have demonstrated that VA alone will not completely explain the choice of the null zone or fixation in primary position. Rather, the fixation performance in both the horizontal and vertical components of eye movements will give more revealing findings. This therefore means that, in participants with IN, an ability to evaluate the eye movement dynamics in each component is crucial to understanding the implications of eccentric viewing. Convergence is an important factor to consider when evaluating a visual scene for fixation performance. For example, in a classroom environment, a shift in gaze for a participant with IN may involve changes in fixation performance and null zone across gaze angles and with distance. In order to get a more complete picture of a visual scene, fixation performance will need to be explored as a function of convergence, and this is what the next chapter addresses.

CHAPTER FIVE

5 Fixation and dynamics of vergence with distance change in participants with infantile nystagmus and controls

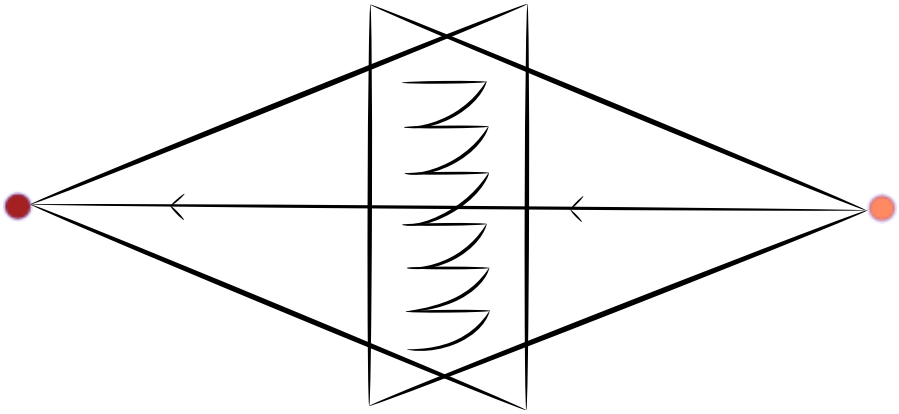

5.1 Introduction

In the preceding chapters, the fixation characteristics while viewing targets at horizontal eccentric gaze positions was evaluated and related to participants' null zone. Recall that the overall aim of this thesis is to investigate fixational eye movements with regards to eye-in-orbit position, when viewing eccentric positions and at different distances. Such eye movements are typical in the course of everyday life, e.g. in a classroom environment. This chapter will look at fixational eye movements as a function of change in viewing distance and therefore vergence.

In people with IN, the waveform intensity has been reported to change with viewing distance. In about 8 to 72% the characteristics of the horizontal IN waveform intensity improve, becoming lower at shorter working distances (Dell'Osso et al. 1972; Abadi and Dickinson 1986; Abadi and Bjerre 2002), while in others the characteristics of the IN waveform have been reported to worsen (Ukwade and Bedell 1992). This phenomenon where waveform intensity reduces is referred to as *convergence dampening* and people with IN who exhibit this are said to have a *convergence null*. In 1972, a case report of a single participant with IN reported a dampening of the oscillation when the eyes were first placed in the null position, and then converged (Dell'Osso et al., 1972). In the largest study which also reported this finding (Abadi and Bjerre 2002), the authors indicate that among 117 subjects, close to half of them (44%) showed a decrease in waveform intensity at a distance of 33 cm, and an even greater reduction in intensity for a distance of up to 25 cm. The measure used to judge this decrease in waveform oscillation was the amplitude and intensity of eye movement in the horizontal plane, as seen clinically. However, both studies (Dell'Osso et al. 1972; Abadi and Bjerre 2002) did not provide any objective evidence of the dampened oscillation. In addition, as seen in the study by Abadi and Bjerre, the proportion of those exhibiting convergence dampening may seem particularly low, but perhaps not when the ocular alignment of the participants is considered. In their study, 136 (64%) of the 213 participants examined had strabismus (manifest ocular deviation); consistent with a 7.8 to 71.2% prevalence of strabismus found in IN, in existing literature (Brodsky and Fray 1997; Kumar et al. 2011). The findings from their study (Abadi and Bjerre 2002) raises the question as to whether it was only those participants without a strabismus (36%) that can experience convergence dampening (44%), suggesting it may not simply be a matter of

eye-in-orbit position at near, but the vergence mechanism interacting with the IN oscillation.

Another question that has remained unanswered is how vergence is achieved and maintained in IN. During vergence, the phase of the nystagmus eye movement (either slow phase or quick phase) responsible for initiating or placing the eye in convergence is not known. While viewing at distance, the IN oscillation is regarded as conjugate, where both eyes oscillate simultaneously in the same direction. However, vergence is a disconjugate eye movement, often requiring the eyes to move in opposite directions. Consequently, when moving from distance to near in the presence of a horizontal oscillation, one eye will be moving (accelerating) in the correct direction (towards the nose), the other eye will be moving (accelerating) in the incorrect direction (away from the nose). How the eyes then arrive at the correct vergence position is unclear. Furthermore, once the vergence position has been achieved, information on how this position is maintained is not known. If we presume that the oscillation returns to being conjugate, in which case the eyes drift away from the point of regard, it remains unclear how the vergence system is affected.

Regarding typical observers, it is also unknown whether they have more stable fixation at near than distance. Studies of fixation experiments in typical individuals have only examined responses at intermediate (typical VDU) or longer distances (see Table 2-3 in Section 2.7.3). Hence, information is lacking as to whether more stable fixation is achieved at near (or conversely, less stable fixation at distance), as is reported in some people with IN. In particular, how the accuracy and/or precision of fixational eye movement change at near viewing is not known. This study was therefore designed to better quantify and understand any relative change in nystagmus waveform and fixation stability associated with near viewing, in all participants.

In the absence of fusional vergence, the eyes deviate into a phoric state. Previous studies have attempted to measure heterophoria using automated means (Barnard and Thomson 1995; Han et al. 2010; Mestre et al. 2018). Automated cover testing provides an objective and repeatable measure of heterophoria, allowing the movement of both the occluded and fixing eye to be evaluated (Mestre et al. 2018). Eye movement during the recovery phase has been found to be quite complex, often involving a saccadic as well as vergence movement of the occluded and fixing eyes, and sometimes a version eye movement at

nearer distances (Barnard and Thomson 1995). In the study by Barnard and Thomson (1995) analysing eye movements in emmetropes during an automated cover test, the amplitude of phorias measured between both eyes was not significantly different. In addition, the latency of recovery during distance (340 cm) viewing was 250 ms, while it was mostly <150 ms at near (40 cm). It was also found to be shorter in exophoric than esophoric deviation, for the initial period of deviation.

To assess ocular deviation, the response amplitude or deviation present in each eye was evaluated. Then, looking critically at eye position plots from participants with IN, the nystagmus eye movement cycle during vergence deviation and re-fixation was analysed to provide novel information on how vergence is achieved and maintained in people with IN.

5.1.1 Aim and objectives

While evaluating fixation as a function of viewing distance, other specific objectives include:

1. To quantify the typical reduction (if any) in IN intensity that occurs with convergence.
2. To find any relationship between convergence dampening and ocular deviation.
3. To evaluate the dynamics of achieving and maintaining vergence in participants with IN.
4. To determine if fixation performance is influenced by viewing distance, in typical participants.

5.1.2 Hypotheses

For this chapter, it was determined whether viewing distance had an impact on either the accuracy and/or the precision of fixational eye movements, and whether there was a difference between the horizontal and vertical components during fixation. Also, in people with IN, the effects of ocular deviation and the dynamics of achieving and maintaining vergence was evaluated. Therefore, the null hypotheses are:

1. The accuracy and precision of fixational eye movements do not change at different viewing distances in people with IN and typical participants.

2. Only those participants with IN, and ocular deviation, can exhibit convergence dampening.
3. During vergence, people with IN use the quick phase of the nystagmus eye oscillation to take up fixation, or to move the eye under cover into its preferred position.
4. While vergence is maintained, i.e. when the cover is removed, conjugate oscillation is shown and the eyes drift away from the target while maintaining a vergence that matches what is being viewed.

5.2 Methods

5.2.1 Participants

For recruitment and pre-examination of these participants, see Section 2.3.1 of the general methods chapter.

5.2.2 Laboratory set up

The experiment reported for this chapter involved eye movement recording during a fixation task including simultaneous automated eye occlusion, at different distances. The same experiment was performed for those with IN and typical participants.

Automated occluder system, including IR pass occluders (Optolite®)

The automated eye occlusion unit, as the name implies, is instrumentation that was designed to automatically cover either of the participant's eyes during the experiment. It consists of two custom-made IR pass filters, each connected to a servo motor. The IR pass filters were necessary in order to occlude a participant's eye and prevent viewing of the target during the experiment, and at the same time allow eye tracking. As shown in Figure 5-1, each servo by means of wires connects to a junction box where information is relayed to the computer. Custom MATLAB code, written by Dr Dunn and thereafter modified by the author also using MATLAB (version R2016b; MathWorks, Natick, MA, USA), allowed simultaneous occlusion of a participant's eye in accordance with the experimental sequence and timing. In addition, a custom-made metallic holder was provided by staff of the School

of Engineering at Cardiff University. This holder was designed to not only fix the flippers in place, but also allow for easy positioning of the device around the head and chin rest of the SR Research head support.

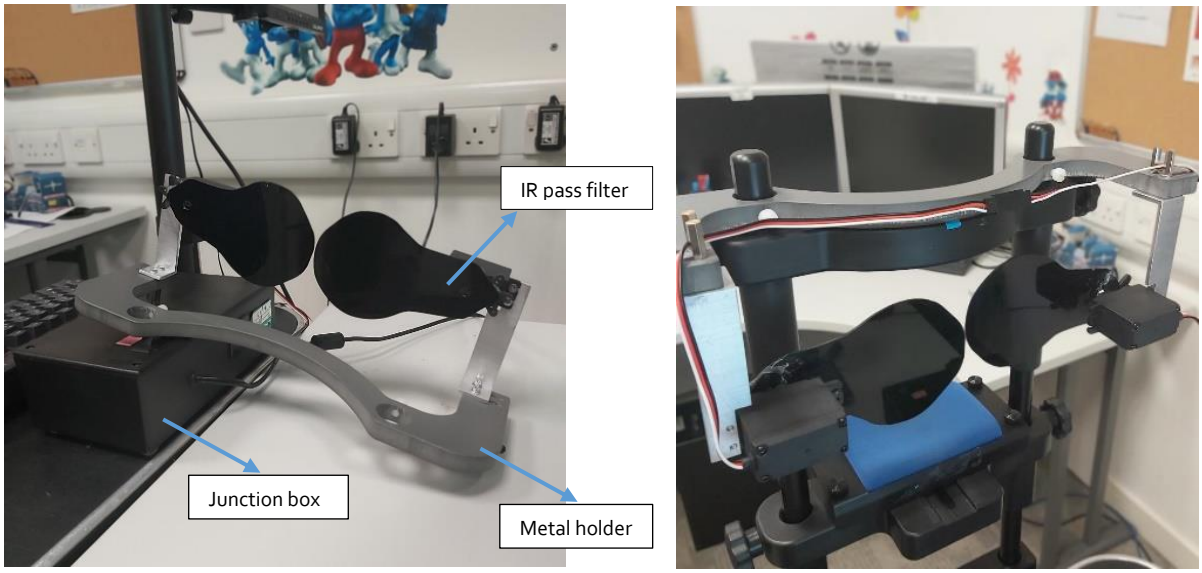

Figure 5-1: Instrumentation for automated eye occlusion
Photo on the left shows the occluder system resting on the junction box. Photo on the right is the occluder and metal holder firmly attached to the SR Research head support unit.

5.2.3 Procedure

Pilot experiment

In order to finetune the experimental design, a pilot study (Amiebenomo et al. 2021) was carried out at the initial stage of the PhD. The aim of this experiment was to determine the effect of change in viewing distance on fixational eye movements in typical participants.

Among 10 emmetropes (4 females), aged 22 to 37 years, eye movements were recorded while participants fixated a 0.5° white dot (on a black background) presented at the centre of the computer screens described in Section 2.4. None of the participants had a manifest ocular deviation or required correction for near work. For this experiment, the process of occlusion was also performed as would be seen in the diagram in Figure 5-2 but without the first 10 s of binocular viewing; the period before the flippers started to occlude each eye. This therefore meant that, the last ten seconds of binocular fixation was analysed to produce the accuracy and precision metrics for fixational eye movements.

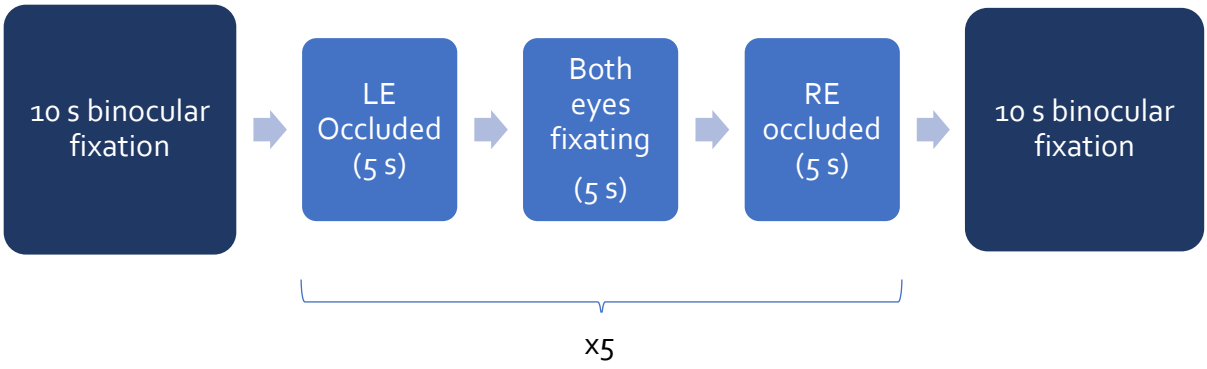

Figure 5-2: Schematic representation of the occlusion process during experiment.

The results (presented in Figure 5-3) show that there was no significant main effect of test distance and eye examined on the accuracy and precision of eye positions recorded. In other words, the experiment found no evidence that the test distance, and therefore convergence, influences the stability of fixation. However, at 25 cm, data for the RE were more imprecise than the LE .

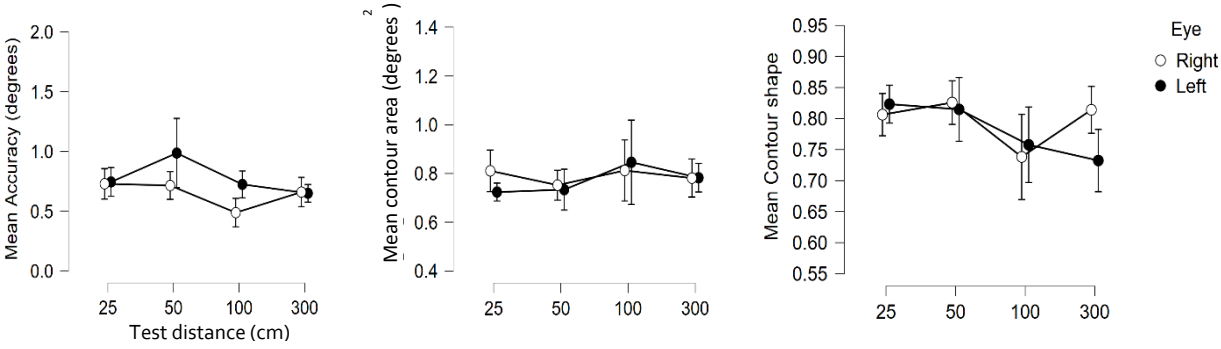

Test distance:
$F_{(1.69, 15.21)} = 0.94$, $p=0.40$, $\eta^2 = 0.05$ $F_{(3.00, 27.00)} = 0.29$, $p=0.83$, $\eta^2 = 0.02$ $F_{(3.00, 27.00)} = 0.64$, $p=0.60$, $\eta^2 = 0.05$

Eye examined:
$F_{(1.00, 9.00)} = 1.17$, $p=0.31$, $\eta^2 = 0.02$ $F_{(1.00, 9.00)} = 0.33$, $p=0.58$, $\eta^2 = 0.002$ $F_{(1.00, 9.00)} = 1.34$, $p=0.58$, $\eta^2 = 0.003$

Figure 5-3: Initial results for fixation at different distance in typical participants
Inset is results from statistical analysis

Considering that the eye which was last occluded (RE) may still be in motion, it was decided that only the last 5 s of binocular fixation should be included in the analysis. Moving

forward, it was important to ensure that the results obtained were not influenced by the fact that either eye could still be undergoing binocular recovery following dissociation (i.e. after the occluder was removed). Therefore, for the main experiment, the procedure was modified to include a period of fixation before the cover test sequence begins. It is expected that the fixational eye movement output, which will be obtained at the initial period of the experiment, will be free from any other eye movements that may happen as a result of a continuous binocular dissociation.

Main experiment

A single white 0.4° dot target (discussed in Section 2.5), on a black background, was presented at the centre of the computer screen, first at the farthest distance of 300 cm and then progressively to the nearest at 25 cm.

The automated cover test apparatus, as described in Section 5.2.2 comprised two IR pass filters otherwise known as flippers or occluders (one for each eye), and a control box which sent signals between the flippers and computer. A custom MATLAB® code programmed to synchronise with code required for the experimental target presentation ran during the experiment. The outcome was such that, while the flippers moved, the dot target continued to be presented on the monitor screen. The purpose of occluding each eye at intervals was to break fusion so that on refixation, how the eyes takes up convergence could be studied. Therefore, the sequence of the experiment (see Figure 5-2) included the 5 s window when both eyes were viewing simultaneously. This binocular fixation period was necessary in order to observe the eye movements while the cover was removed and reintroduced. This information was needed to study the dynamics of achieving and maintaining vergence in IN.

On activation, the automated occluders were programmed to stay open for 10 s followed by a 5 s occlusion of each eye in turn, with a 5 s interval during which both eyes were left open. This process was programmed to repeat for a total of five trials. During this process, participants were instructed to keep looking at the centre of the white dot presented at the centre of the display screen. Altogether, the experiment at each test distance lasted for about 2 minutes.

5.2.4 Validation of convergence accuracy

Similar to previous study (Dell'Osso et al. 2020), vergence eye movements were defined as the difference between left and right eye positions, while vergence induced by the target was calculated using the formula:

$$2[\tan^{-1}(x/y)]$$

Where:

IPD is the average IPD measured from all participants (see appendix) = 64.8 ± 3.15 mm
x , the distance between each eye and nose bridge = IPD/2 (mm)
y = viewing distance (mm)

The target viewed at 300 cm is expected to induce, in *each eye*, a vergence of:

$$[\tan^{-1}(\frac{32.4}{3000})]$$

$$= 0.62°$$

Therefore, the target vergence at 300 cm is = 1.24°

Table 5-1: Amount of vergence induced at each test distance
It is expected that the raw eye position trace produced for each eye, at all distances, should be at or near the respective expected converged position (°) when plotted.

Target distance (cm)	Approximate converged position for each eye (°)	Target vergence (°)
300	0.62	1.24
100	1.86	3.71
50	3.71	7.42
25	7.38	14.77

The expected amount of vergence induced by viewing the dot target at each distance is presented in Table 5-1. It can be seen that, at a distance of 50 cm, an approximate 3.71° vergence should be induced in each eye. This is almost equivalent to the value (4°) previously shown to sufficiently induce convergence dampening (Serra et al. 2006). Therefore, for a more complete evaluation of convergence dampening, results obtained from the 25 and 300 cm viewing distances were analysed. This is because at 25 and 300 cm, the maximum and minimum amount of convergence is induced, respectively. Therefore, both distances were evaluated for evidence of any dampening of the IN oscillation.

5.2.5 Analysis

Following a retrospective pursuit calibration (Section 2.6.1) and drift correction analysis (Section 2.7.2), eye movement recordings from this experiment were analysed in two parts. Firstly, the sections shaded light blue in Figure 5-2 were evaluated to determine the amount of ocular deviation and dynamics of eye movement, in each eye, as the flippers were automatically removed and then replaced. The second analysis involved an evaluation of the accuracy and precision of fixational eye movements using the initial section of binocular fixation (shaded dark blue) as represented in Figure 5-2 also.

Analysing these two parts produced results that are presented and discussed in the following three sections:

1. *Quantifying convergence dampening in IN and determining its relationship with ocular deviation*

The proportion of participants who have a convergence null was determined by comparing the results of the accuracy and precision of fixational eye movements obtained from the farthest and nearest measurement distance. The percentage change in values, obtained between these distance, were also noted. In addition to clinical measurements of ocular deviation, the amount of ocular deviation was objectively determined using methods similar to those described in a previous study by Sreenivasan and colleagues (Sreenivasan et al. 2016). For the experiment in this chapter, an objective amount of ocular deviation, for the eye under cover, was determined from the average eye position, just 1 s before the occluder was removed. To evaluate this eye position change on occlusion more reliably, the final amount of ocular deviation was obtained from a difference in mean eye position 1 s before the eye was covered and mean eye position 1 s before the cover is removed. At the same time, any amount of manifest deviation (tropia) was determined by evaluating the uncovered eye as it took up fixation from its previously deviated position.

The objective amount of ocular deviation (obtained while viewing at 25 cm only) was determined from the mean end point response amplitude for the first two trials when the occluder was introduced. Later trials were not included because it is assumed that there will be a systematic increase in ocular deviation with each occlusion, as a result of a continuous

disruption in the fusion mechanism. This amount of ocular deviation was first determined by extracting the centroid eye position value for the last second of occlusion time (1000 ms), just before the occluder is removed. This last second was chosen because at this point, it is expected that the eye was in its final position of rest. The values for the first two occlusion times were thereafter averaged to get one value for each eye. In a few cases where the required portion in trial one and two had missing data, trial three was evaluated. A sample portion of the eye position plot that was used to estimate ocular deviation is shown in Figure 5-4. To evaluate the relationship between convergence dampening and ocular deviation, the results for fixation performance and ocular deviation were correlated.

2. *Dynamics of achieving and maintaining vergence in IN*

In an individual with IN, where both eyes oscillate in the same direction, the mechanism by which they achieve the deconjugate eye movement of vergence was evaluated. For three participants, eye position data from the portion where the occluder was removed, i.e. when both eyes were fixating, were selected. These participants were chosen because they presented with characteristics typical of most people with IN, alongside an absence of a manifest ocular deviation. In addition, these participants were also selected because their eye position trace at the 25 cm viewing distance had minimal data loss. From the point where the occluder was removed, the eye movement response was noted. Eye position data for right and left eye, plotted against time, were qualitatively evaluated in order to determine which phase of the nystagmus waveform (slow or quick) was responsible for initiating the eye in convergence position.

3. *The effect of viewing distance on fixational eye stability in typical participants.*

For this, the bPDF method described in the methods chapter was utilised.

In order to determine the objective amount of ocular deviation, and evaluate the dynamics of eye movement during dissociation and re-fixation, eye movement recordings needed to be clearly differentiated into the relevant sections. For this, a MATLAB algorithm was used to indicate the exact time when the occluder was introduced and removed, and to display the eye movements happening in each eye during such periods. A sample eye position plot

(produced before drift correction) is presented in Figure 5-4. The output shows a replica of the experimental process described in Figure 5-2. In addition, the amount of vergence induced by fixating at the 25 cm near target is shown by the gap between the horizontal eye traces. Following categorization of eye movements in the recorded data, the next step was to analyse each component part. Data from participants with IN were evaluated and presented individually. All other bPDF and statistical analysis were performed as described in the methods chapter.

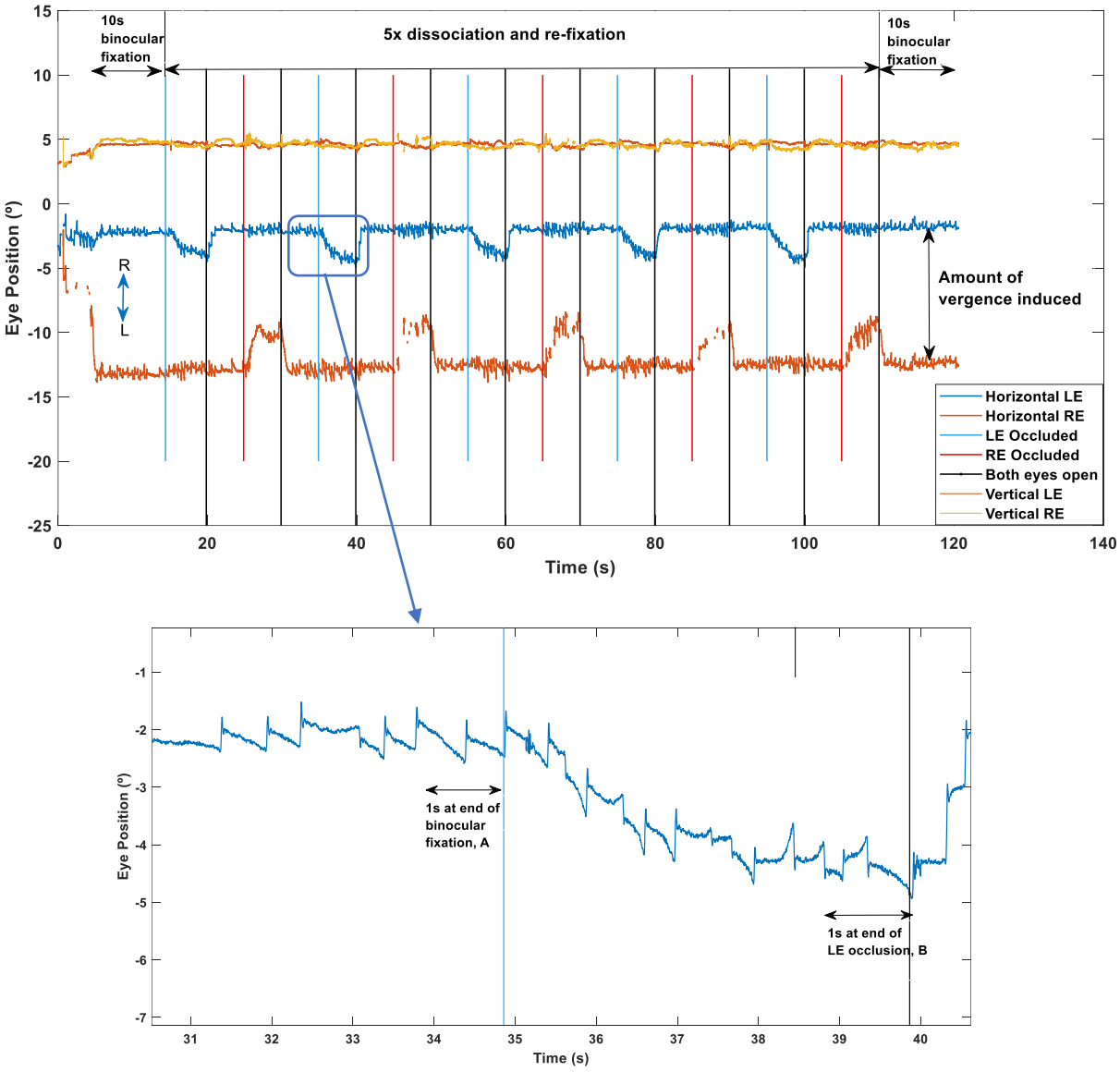

Figure 5-4: Horizontal and vertical eye position plot from participant IN16 while viewing at 25 cm.
Vertical lines indicate the start point where each eye was covered (blue and orange lines) or both eyes left open (black lines). The initial and last sections represent when both eyes were fixating for 10s. IN waveform oscillations can also be found in the eye movement trace during dissociation and re-fixation.
Eye traces are not 'Drift-corrected' and hence not in the exact midline position. However, notice the amount of vergence induced by the 25 cm viewing position. This is an expected value of about 13° between the

horizontal LE and RE trace. As shown by the blue double arrow, where the eye position trace moves downwards, this represents a leftward (L) deviation and where it moves upwards, it represents a rightward (R) deviation. For this participant, the LE moves leftward on dissociation (movement towards the temporal side), while the RE moves rightward on dissociation (movement towards the temporal side). Therefore, this participant has an outward (exo) deviation of the covered eye. The portion in a blue oval was zoomed-in to illustrate how the amount of ocular deviation was determined for one trial. In this case, it was the difference between mean eye position at A and B. To check for a deviation in the uncovered eye, differences in the other eye, at the same positions, was computed.

5.3 Results

5.3.1 Participants

Data from 17 participants with IN (9 females; aged 20 to 69 years; mean age, 47.8 years) and 14 typical participants (9 females; aged 20 to 39 years; mean age, 28 years) are reported for this experiment.

5.3.2 Quantifying convergence dampening in IN and determining its relationship with ocular deviation

Fixation performance at different viewing distances

Bivariate PDF analysis produces metrics that quantify the accuracy and precision of fixational eye movements. As described in section 2.8.2, these values were obtained from an analysis of the horizontal and vertical components of the eye movement.

Accuracy: Plots of normalised data representing the accuracy of eye movement while fixating at 300, 100, 50 and 25 cm are presented in Figure 5-5. Recall that the lower the value, the more accurate the eye position data points are with respect to the point of fixation, at the distance considered. The results indicate that, for most participants, measurements obtained at the nearest fixation distance were less accurate than at the farthest fixation distance. A repeated measures ANOVA showed that there was an effect of test distance on accuracy [$F_{(1.65, 26.37)} = 10.87$, **$p < 0.001$**, $\eta^2 = 0.21$], and an interaction between test distance and eye tested [$F_{(1.84, 29.45)} = 5.17$, **$p = 0.01$**, $\eta^2 = 0.07$]. Post Hoc comparison, using the t test with Bonferroni correction, indicated that the accuracy values at 100 (mean difference = 4.86; t = 5.31; $P_{bonf} = < 0.001$) and 300 cm (mean difference = 3.73; t = 4.07; $P_{bonf} = 0.001$) were significantly different from those done at the 25 cm test

distance. In addition, measures at 100 cm (mean difference = 3.00; t = 3.27; P_{bonf} = 0.012) were also significantly different from those done at the 50 cm test distance. In some cases, the accuracy of fixation differed between the right and left eye however, this difference was not statistically significant [$F_{(1, 16)}$ = 1.10, p = 0.31, η^2 = 0.01].

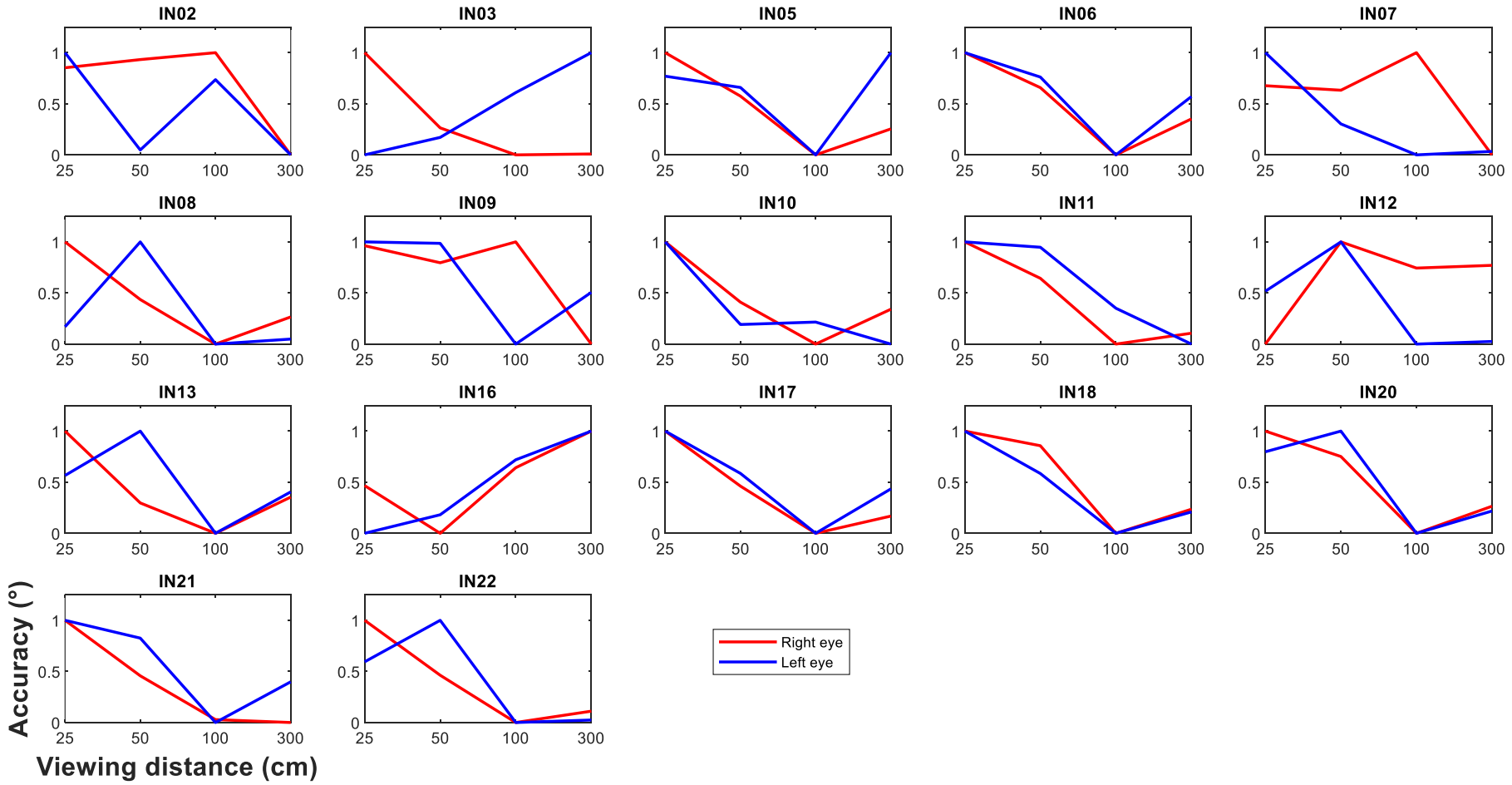

Figure 5-5: Accuracy at all viewing distances in participants with IN.

Data presented are **normalised** for values between 0 and 1.

The lowest point in each plot (0°, on the y scale) is the point of highest accuracy i.e. where the vector length from the isocontour centre to the target position is shortest.

Contour shape: Values representing the isocontour shape of eye movement positions, measured while fixating at 300, 100, 50 and 25 cm, are presented in Figure 5-6. Generally, results show that, for most participants, the derived isocontour shape was asymmetrical; slightly differing in each eye. Only in participants IN11, IN17 and IN22 do we find in one eye an equality between the major and minor axes spread, indicated by values close to or at 1. In a few participants (IN05, IN06, IN11, IN16 and IN22), eye position spread in both axes gradually became more symmetrical from the 300 cm to 25 cm viewing distance.

Recall that the isocontour shape is derived from a ratio of the minimum and maximum axes of the eye position isocontour. Since this parameter describes symmetry, it only gives a general overview of the equality of eye movement spread in both axes. Therefore, to fully represent both eye movement axes and determine in which IN eye movement component the eye moved more, the actual horizontal and vertical axis range of the isocontour was derived. See Section 2.7.3 for more details.

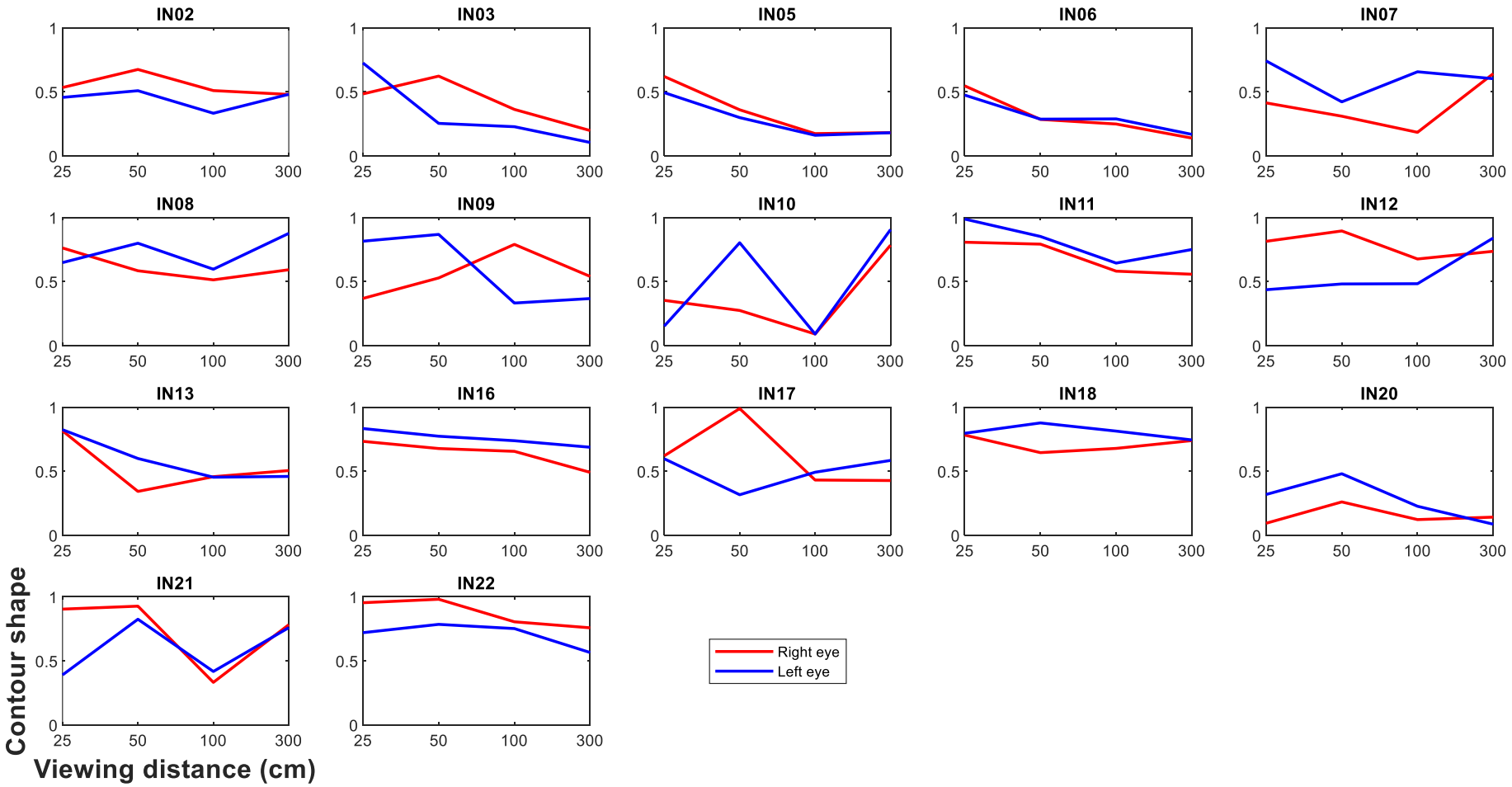

Figure 5-6: Contour shape at different distances in participants with IN

Each plot represents data obtained from the right and left eye. Since the shape factor is produced from a ratio, values fall within 0 and 1 therefore these were not normalised. The closer the value is to 1 the greater the symmetry between the minor and major isocontour axis. In other words the more uniformly spread data points are.

Contour area and the relationship between isocontour major and minor axis: The precision of eye movement was determined using the total area of the 68% isocontour. Plots for each participant are presented in Figure 5-7. Lower isocontour area values indicate a smaller spread of measured data point, suggesting a better precision at the viewing distance considered. In more than half of the participants (58.8%) (IN05, IN06, IN08, IN09, IN12, IN13, IN16, IN17, IN20 and IN22), fixation was more precise at 25 cm than at 300 cm for each eye. In three others (IN10, IN11 and IN21), a small reduction in isocontour area was only found in one eye; IN10 and IN21 – RE, IN11 – LE.

Using the real values, descriptive analysis showed that the mean and standard deviation of ocular precision decreased from 300 cm [RE = 5.75 ± 6.44 $(°)^2$ and LE = 4.25 ± 3.87 $(°)^2$], to 25 cm [RE = 3.20 ± 3.92 $(°)^2$ and LE = 2.87 ± 3.95 $(°)^2$]. However, statistical analysis using a repeated measures ANOVA showed that there was no significant main effect of test distance on precision [$F_{(1.6,\ 25.59)} = 2.02$, $p = 0.16$, $\eta^2 = 0.087$], and fixating eye, whether left or right [$F_{(1,\ 16)} = 1.64$, $p = 0.22$, $\eta^2 = 0.011$].

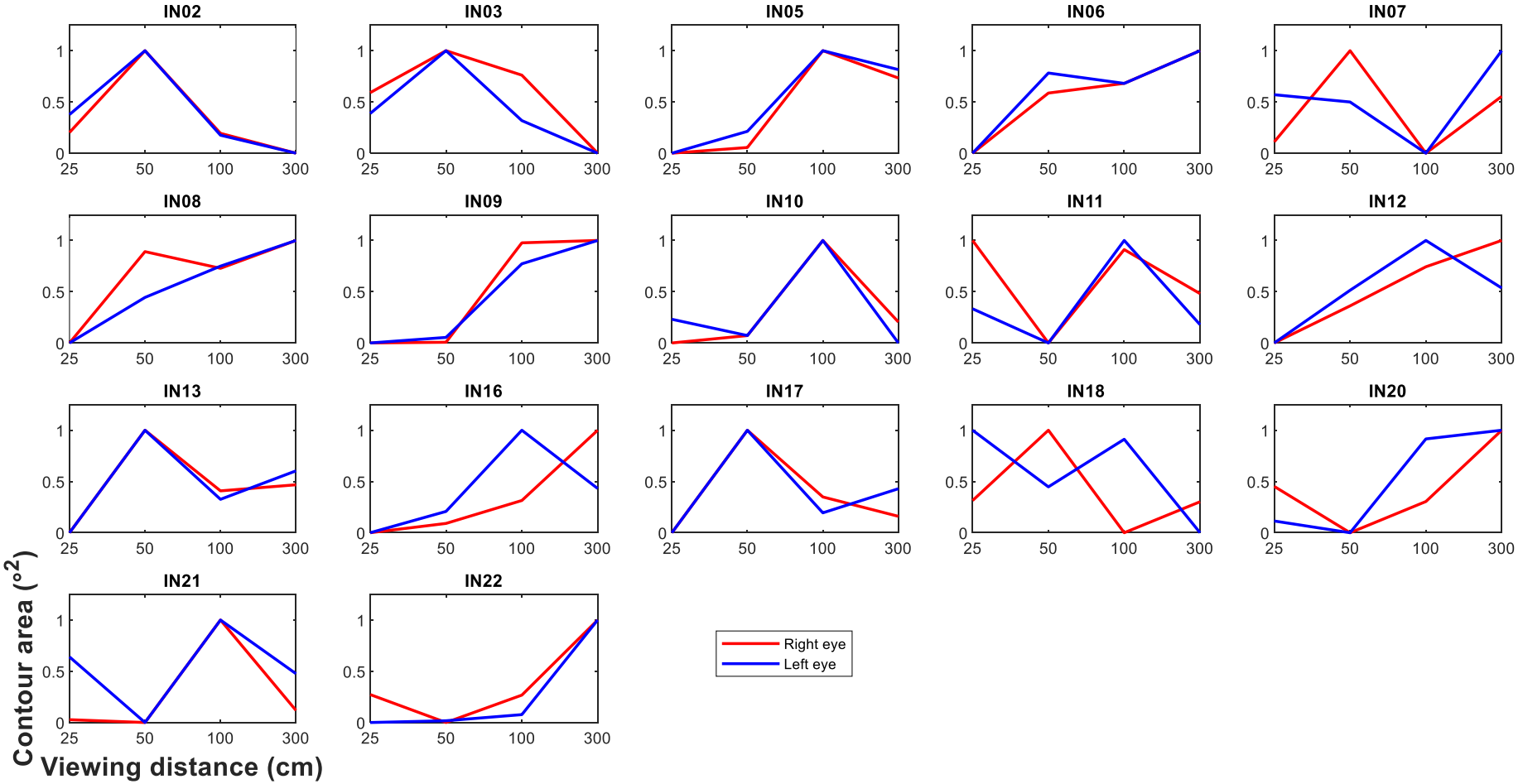

Figure 5-7: Contour area at different distances in participants with IN

Each plot represents data obtained from the right and left eye. Data presented are **normalised** for values between 0 and 1.

The lowest point in each plot (0°, on the Y scale) indicates the points of highest precision, or where the isocontour area is smallest.

Using derived values of contour shape and major axis orientation, the actual ranges of the isocontour major and minor axes were computed as described in Section 2.7.3. These normalised values (individually normalised for each parameter) are plotted in Figure 5-8 as the horizontal and vertical isocontour axis range, for each eye. It can be seen from the plots that, comparing change in precision from the 300 to 25 cm viewing distance, change in the horizontal axis, for example, does not guarantee an equal amount or same direction of precision change in the vertical axis. For example in participant IN03, precision in the horizontal axis improves at 25 cm but worsens for the vertical axis. It is only in participants IN05, IN08, IN09, IN13, IN16 and IN22 that the horizontal and vertical axis ranges, in both eyes, show an apparent decrease from 300 to 25 cm.

Considering the three factors of test distance, eye tested and isocontour axis range, a repeated measures ANOVA using the real values revealed a significant main effect of test distance [$F_{(2.35, 37.54)} = 3.80$, **$p = 0.03$**, $\eta^2 = 0.048$] and isocontour axis range [$F_{(1, 16)} = 12.59$, **$p = 0.003$**, $\eta^2 = 0.16$] on precision. Fixation was more precise at the nearer fixation distance, and the vertical isocontour axis range were lower, indicating less spread in the vertical component of the eye position trace. In addition, there was no significant main effect of the eye tested on precision [$F_{(1, 16)} = 1.58$, $p = 0.23$, $\eta^2 = 0.002$].

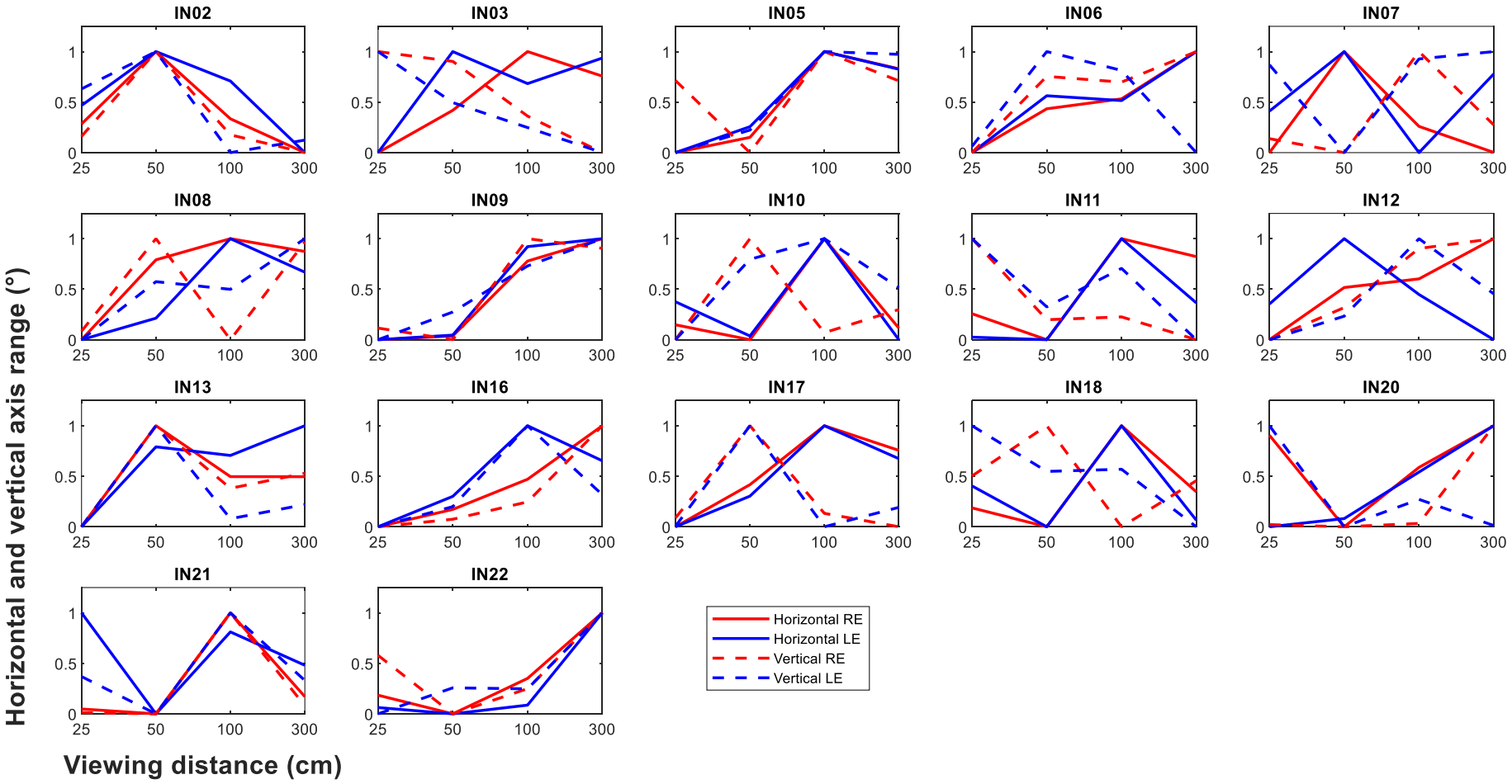

Figure 5-8: Horizontal and vertical axis range at different distances in people with IN

Each plot represents data obtained from the right (red traces) and left (blue traces) eye. Horizontal ranges are presented in continuous lines while the vertical ranges are shown as broken lines. Data presented for each eye and axes, are individually **normalised** for values between 0 and 1. The lowest point in each plot (0°, on the Y scale) indicates the points of highest precision, or where the isocontour area is smallest.

Change in accuracy and precision from distance to near

In order to address the first aim of this study, values for the percentage change in accuracy and precision values from 300 to 25 cm are presented in Table 5-2. A twofold change is represented by values of 100% or more. Where this value is negative, it indicates a decrease in isocontour area and hence more precision. Results show that more participants in Table 5-2 (b) and (c) i.e. those with a clinical phoria or without any deviation, were found to have a reduction in fixation precision from distance to near. A good number of them also had higher percentage changes than in the group with a clinical manifest deviation. For all participants, the mean and standard deviation percent reduction in fixation precision was -55.79 ± 23.32%

Table 5-2: Change in accuracy and precision from distance to near in people with IN

Table shows the change in each parameter at the farthest and nearest viewing position. Values in **bold** indicate where there was a percentage reduction in the measured parameter from distance to near. Participants are arranged by the magnitude of the increase in eye position precision, considering all parameters. Those indicated in **BLUE** were found to have a clinical convergence null. In (a), participants with a manifest deviation as measured clinically are presented, while data from those with a latent deviation or phoria are shown in (b). Those without any manifest or latent ocular deviation are presented in (c). R = Right, L = left

(a) These participants have a clinically manifest ocular deviation

Participant	Accuracy (°)				Contour area $(°)^2$			Horizontal axis range (°)			Vertical axis range (°)		
	Eye	300 cm	25 cm	% change	300 cm	25 cm	% change	300 cm	25 cm	% change	300 cm	25 cm	% change
IN05	R	6.39	15.33	139.81	6.63	2.03	**-69.44**	6.80	2.01	**-70.45**	1.32	1.32	0.08
	L	9.26	8.17	**-11.81**	6.34	1.45	**-77.13**	6.65	1.93	**-70.99**	1.36	0.97	**-28.89**
IN10	R	10.93	25.63	134.51	5.37	3.28	**-38.94**	2.80	3.20	14.41	2.50	1.76	**-29.91**
	L	1.47	10.04	582.66	1.56	4.32	177.41	1.38	6.02	337.5	1.45	0.93	**-35.48**
IN03	R	5.73	10.72	87.03	6.51	14.38	120.91	6.45	3.11	**-51.85**	1.36	6.09	348.64
	L	27.59	2.31	**-91.63**	10.61	17.39	63.87	11.35	4.47	**-60.67**	1.24	5.16	315.04
IN11	R	3.17	13.73	333.47	1.32	1.59	19.80	1.74	1.44	**-17.20**	0.97	1.44	47.94
	L	0.48	4.13	757.59	1.06	1.12	6.14	1.34	1.19	**-11.14**	1.01	1.20	19.23

(b) These participants have a clinically latent ocular deviation

Participant	Accuracy (°)				Contour area $(°)^2$			Horizontal axis range (°)			Vertical axis range (°)		
	Eye	300 cm	25 cm	% change	300 cm	25 cm	% change	300 cm	25 cm	% change	300 cm	25 cm	% change
IN16	R	0.46	0.33	**-27.71**	2.92	0.52	**-82.19**	2.28	0.95	**-58.28**	2.05	0.70	**-66.05**
	L	8.00	1.44	**-82.07**	0.81	0.45	**-44.35**	1.22	0.83	**-32.32**	0.84	0.69	**-17.88**
IN09	R	3.62	14.09	289.14	22.09	2.11	**-90.44**	6.39	1.03	**-83.84**	5.14	2.69	**-47.68**
	L	5.57	9.76	75.06	9.70	0.68	**-92.97**	5.78	0.98	**-83.06**	2.19	0.90	**-58.63**
IN22	R	4.59	5.70	24.05	1.765	1.06	**-39.77**	1.71	1.14	**-33.57**	1.32	1.19	**-9.84**
	L	2.58	5.38	108.41	1.42	0.72	**-49.44**	1.79	1.13	**-37.02**	1.01	0.81	**-19.94**
IN07	R	1.34	4.57	240.28	5.61	4.09	**-27.09**	3.32	3.32	**-0.12**	2.15	1.92	**-10.92**
	L	3.66	8.08	120.72	4.39	3.66	**-16.53**	2.97	2.49	**-16.09**	1.95	1.88	**-3.69**
IN06	R	9.64	15.87	64.69	5.56	1.59	**-71.43**	7.05	1.90	**-73.04**	1.42	1.09	**-23.47**
	L	9.61	11.96	24.43	4.74	1.51	**-68.10**	5.99	1.97	**-67.16**	1.04	1.05	1.06
IN20	R	5.84	16.91	189.54	21.80	12.02	**-44.89**	13.73	12.84	**-6.47**	3.45	1.20	**-65.25**
	L	2.20	5.52	150.50	14.13	4.04	**-71.41**	14.49	1.65	**-88.61**	1.33	3.88	192.47
IN12	R	7.09	5.42	**-23.51**	6.85	3.21	**-53.10**	2.59	1.98	**-23.49**	3.40	2.10	**-38.12**
	L	2.85	7.14	150.40	4.21	2.70	**-35.79**	2.52	2.78	10.19	2.13	1.29	**-39.25**
IN21	R	1.41	10.75	664.04	1.063	0.79	**-26.15**	1.27	1.05	**-17.18**	1.09	0.95	**-12.35**
	L	5.37	9.56	77.91	1.542	1.90	23.02	1.58	2.32	47.12	1.26	1.32	4.85

(c) These participants were orthophoric, clinically

Participant	Accuracy (°)				Contour area (°)^2			Horizontal axis range (°)			Vertical axis range (°)		
	Eye	300 cm	25 cm	% change	300 cm	25 cm	% change	300 cm	25 cm	% change	300 cm	25 cm	% change
IN19	R	1.29	9.09	606.29	5.77	0.69	**-87.99**	4.45	0.95	**-78.72**	1.71	0.95	**-44.37**
	L	1.75	1.63	**-6.81**	25.55	3.50	**-86.29**	8.38	2.81	**-66.49**	12.96	1.71	**-86.80**
IN13	R	4.45	9.16	105.84	2.70	0.70	**-73.91**	2.61	1.03	**-60.40**	1.32	0.87	**-33.71**
	L	7.68	8.38	9.18	3.14	0.98	**-68.98**	2.95	1.22	**-58.69**	1.36	1.02	**-24.72**
IN08	R	3.85	10.40	170.21	1.78	1.11	**-37.75**	1.89	1.33	**-29.61**	1.26	1.07	**-14.98**
	L	3.46	3.59	3.76	3.28	1.57	**-51.00**	2.10	1.62	**-23.01**	2.00	1.33	**-33.53**
IN17	R	3.39	14.92	340.31	1.99	1.67	**-16.02**	2.43	1.85	**-23.77**	1.05	1.15	9.13
	L	3.54	7.46	110.62	2.09	1.47	**-29.50**	2.01	1.77	**-11.94**	1.43	1.06	**-26.15**
IN18	R	2.45	9.34	282.13	1.23	1.23	0.24	1.22	1.18	**-3.77**	1.33	1.36	1.95
	L	3.20	5.85	82.63	0.68	1.10	62.22	1.02	1.10	7.65	0.87	1.29	48.05
IN02	R	3.23	5.33	64.92	2.52	3.06	21.64	2.56	2.70	5.63	1.30	1.45	11.39
	L	3.67	7.60	107.11	2.55	3.77	48.13	2.59	3.15	21.74	1.26	1.66	31.83

R = Right, L = left

Objectively determined ocular deviation and its relationship with convergence dampening

The mean amount of objective ocular deviation, measured for each participant at 25 cm is shown in Table 5-3. Clinically, the amount of ocular deviation present in an eye when it is covered represents the amount of latent deviation or phoria. In this case, the eye under cover deviates to a position of rest when it is not fixating (as seen in the zoomed portion of Figure 5-4). At the same time, if the fellow uncovered eye moves to take up fixation, the position it was before assuming a fixating role defines the amount of manifest deviation or tropia, clinically.

Table 5-3: Mean ocular deviation objectively measured in participants with IN
A + sign means eye moved up i.e. RIGHT. Therefore a + sign on the RE means RE moved out (Exo), while on the LE means it moved in (Eso). A - sign means eye moved down i.e. LEFT. Therefore, a - sign on the RE indicates that the eye moved in while if this was on the LE the eye moved out. 1° = 1.75 Δ dioptres

	Mean deviation of the covered eye			Mean deviation of the uncovered eye			
	RE °(Δ dioptre)	LE °(Δ dioptre)	Each eye moved	RE °(Δ dioptre)	Eye movement direction	LE °(Δ dioptre)	Eye movement direction
IN02	9.44 (5.39)	- (-)	Out	0.26 (0.15)	In	6.17 (3.53)	Out
IN03	-3.12 (1.78)	1.23 (0.70)	In	0.43 (0.25)	In	6.52 (3.73)	Out
IN05	1.06 (0.61)	-0.83 (0.47)	Out	-0.50 (0.29)	Out	-1.35 (0.77)	In
IN06	1.38 (0.79)	-0.56 (0.32)	Out	0.37 (0.21)	In	-0.23 (0.13)	In
IN07	2.35 (1.34)	-6.10 (3.49)	Out	-2.17 (1.24)	Out	-2.22 (1.27)	In
IN08	0.21 (0.12)	-0.63 (0.36)	Out	0.11 (0.06)	In	-0.12 (0.07)	In
IN09	4.77 (2.73)	-4.30 (2.46)	Out	1.60 (0.91)	In	0.94 (0.54)	Out
IN10	24.04 (13.74)	-16.84 (9.62)	Out	-25.61 (14.63)	Out	14.73 (8.42)	Out
IN11	4.67 (2.67)	-3.60 (2.06)	Out	-5.35 (3.06)	Out	0.24 (0.14)	Out
IN12	3.33 (1.90)	-3.18 (1.82)	Out	0.65 (0.37)	In	0.14 (0.08)	Out
IN13	-0.62 (0.35)	3.85 (2.20)	In	2.90 (1.66)	In	-0.33 (0.19)	In
IN16	3.33 (1.90)	-1.90 (1.09)	Out	0.40 (0.23)	In	0.24 (0.14)	Out
IN17	2.82 (1.61)	-4.83 (2.76)	Out	-0.24 (0.14)	Out	0.25 (0.14)	Out
IN18	4.89 (2.79)	-3.13 (1.79)	Out	-0.24 (0.14)	Out	-0.10 (0.06)	In
IN20	2.92 (1.67)	-2.72 (1.55)	Out	-3.57 (2.04)	Out	2.60 (1.49)	Out
IN21	2.01 (1.51)	-0.92 (0.53)	Out	-0.33 (0.19)	Out	3.16 (1.81)	Out
IN22	0.59 (0.34)	-3.63 (2.07)	Out	-1.00 (0.57)	Out	-0.48 (0.27)	In

RE= Right eye, LE = Left eye

The results indicate that an ocular displacement occurred in each eye when the cover was introduced. This amount of deviation was unequal in both eyes, in most cases. Considering the eye under cover, fifteen (88%) showed an outward deviation at near, which for most did not present clinically (see Table 8-1 in appendix). Clinically, values of about 3.5 Δ dioptres

phoria is expected at near (Hirsh, Alpern and Schultz 1948), and any value higher may become a manifest deviation if not compensated for. Results show that only four participants (IN02, IN03, IN10 and IN11) have values of ocular deviation which may be clinically significant.

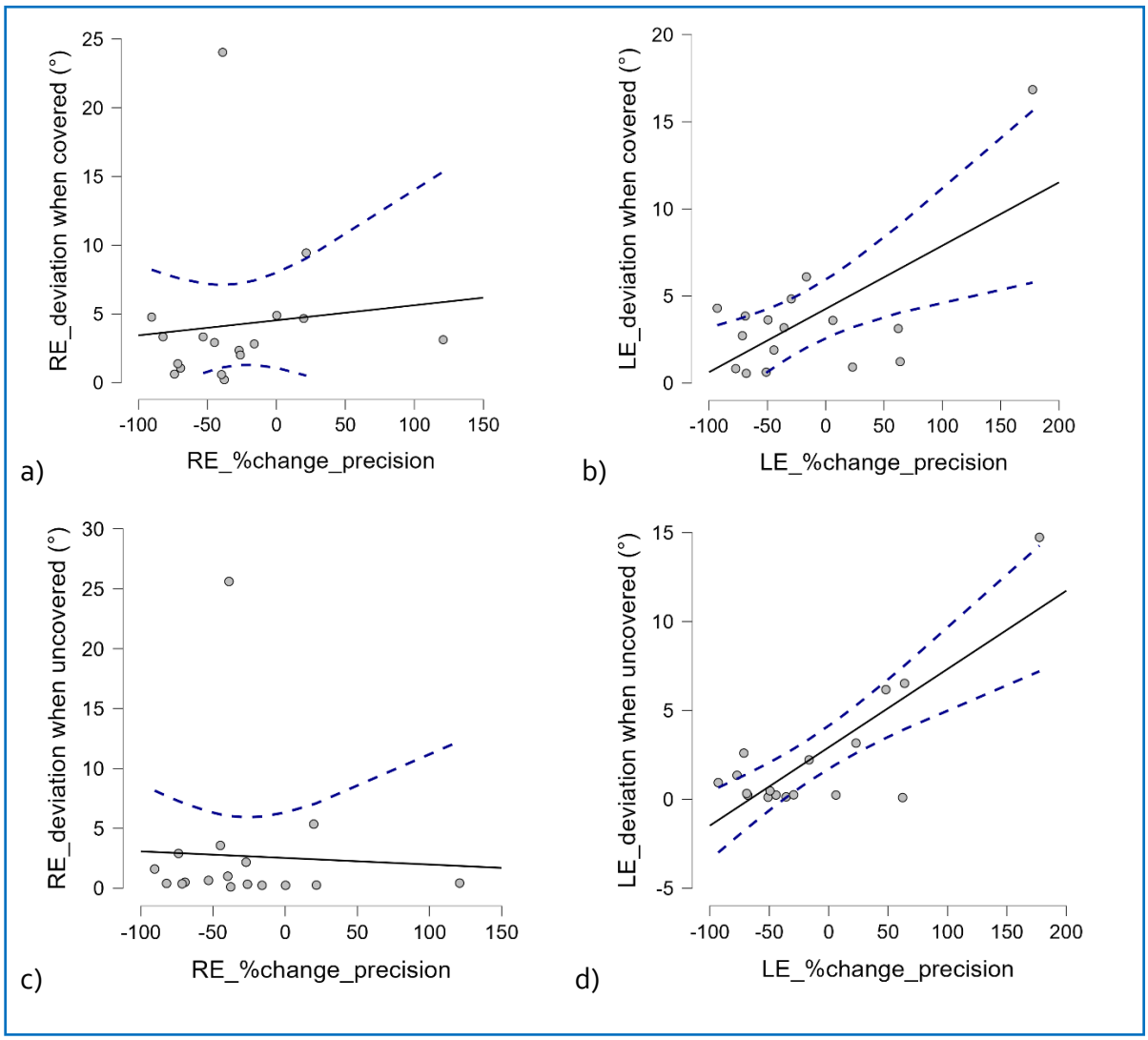

Figure 5-9: The relationship between ocular deviation and percentage change in fixation precision from 300 to 25 cm

Graphs are shown for derived values of covered eye deviation (a and b) and derived values of uncovered eye deviation (c and d). Negative percentage change values indicate a reduction in contour area size (i.e. fixation was more precise at 25 cm than at 300 cm). Values of ocular deviation were not assigned their signs because only the magnitude of deviation is relevant in this case.

Furthermore, correlation graphs were plotted to investigate any relationship between the mean amount of ocular deviation obtained from each eye and the change in precision from 300 to 25 cm. These are presented in Figure 5-9. Similar to findings in Table 5-2, results in

both left and right eye indicate that, the lower the amount of ocular deviation, the more the percentage reduction in fixation precision from distance to near. This relationship was however only significant in the left eye [r = 0.66, **p = 0.006**; (95% CI: 0.24, 0.87)], but not in the right eye [r = 0.10, p = 0.70; (95% CI: -0.4, 0.55)] for deviations of the covered eye, as well as in the left eye [r = 0.81, **p < 0.001**; (95% CI: 0.54, 0.93)] and not the right eye [r = -0.046, p = 0.86; (95% CI: -0.52, 0.44)] for deviations of the uncovered eye.

5.3.3 The dynamics of achieving and maintaining vergence in IN

The dynamics of convergence are demonstrated in three participants (IN08, IN13 and IN18) These participants had waveform amplitudes and frequencies ranging from 0.4 to 5.5° and 1.5 to 5.1 Hz, respectively, and typical ocular alignment (more details can be found in Table 8-1 of appendix). As seen in the 'zoomed in' eye position plot for each participant (Figure 5-10), the eye position traces end roughly in the same position while fixating binocularly. However, the IN oscillation is not completely similar in both eyes. This is reflected in the plots of absolute difference shown below for each participant. In all cases, the plot of absolute difference is not a straight line; particularly evident in participant IN18. This therefore indicates that there are very minimal differences in the waveform pattern between the right and left eye of these participants. Furthermore, a qualitative interpretation of the plots is that the quick phase contributes to moving the eye into the convergent (when fixing binocularly) and dissociated position (when the occluder was introduced), i.e. the quick phase does not fully compensate for the drift of the eye from the original position, but rather keeps facilitating the movement of the eye to the new ultimate position. This goal-oriented movement by the quick phase to achieve a new eye position, whether large or small, can also be seen in the zoomed-in plots in Figure 5-4.

In Figure 5-10a, eye position plots from participant IN08 show that there was little or no change in eye position when the occluder was introduced and removed. The IN waveform is seen to correspond in both eyes in the horizontal and vertical components. The small changes seen in the absolute difference plots may be attributed to instrument noise. In Figure 5-10b, there is a small change in eye position of about 1°, when the occluder was introduced and removed. IN oscillations are not present in the vertical component. During

the first trial of binocular fixation, a saccade of about 2° is present only in the LE. In plot c, the waveform oscillation is not conjugate. LE amplitude appears slightly higher than the right during binocular fixation. The period of latency before the eye moves into a convergence position is not obvious in the first two plots. However, in plot c this amount is shown to be about a quarter of a second.

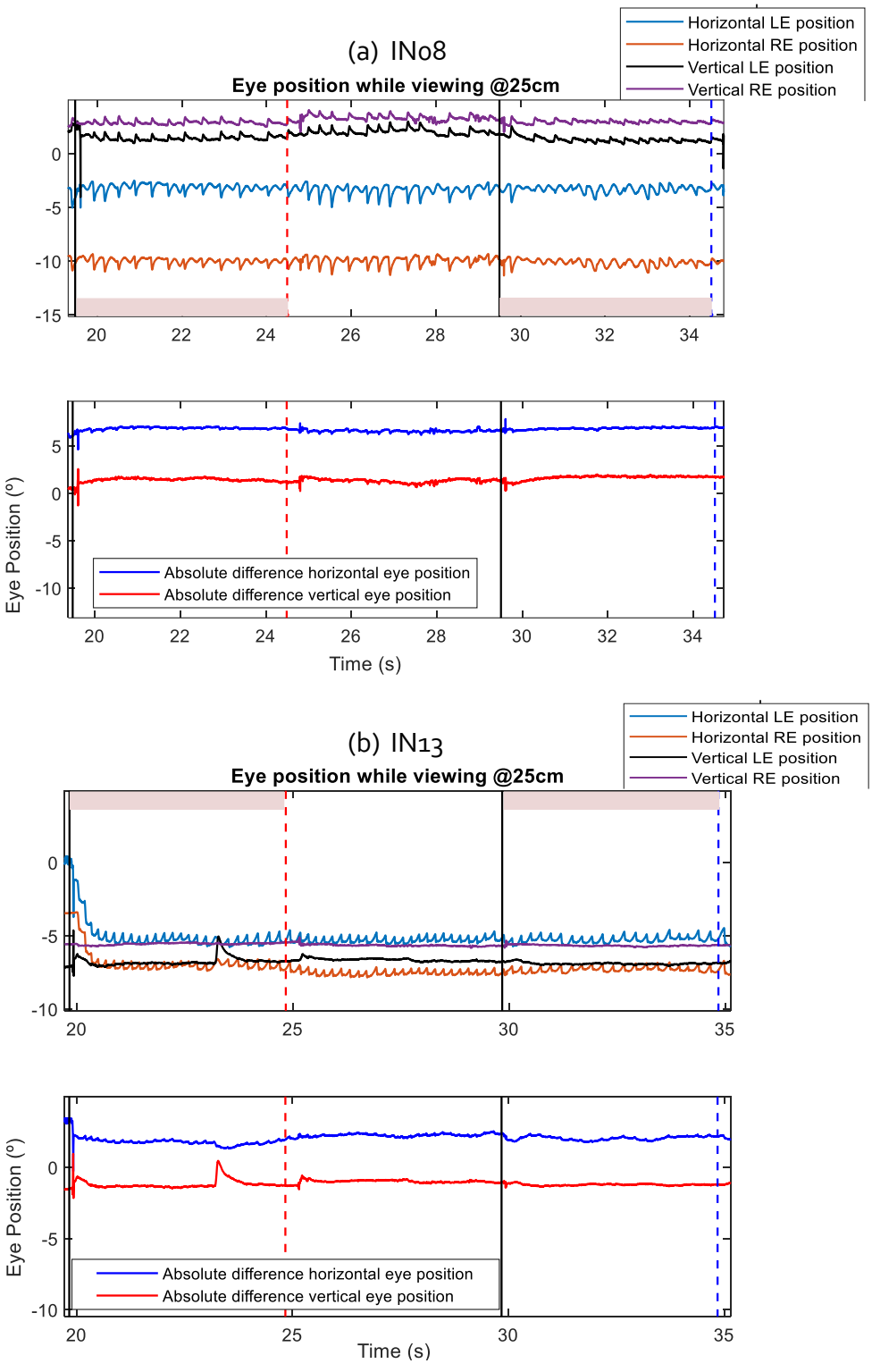

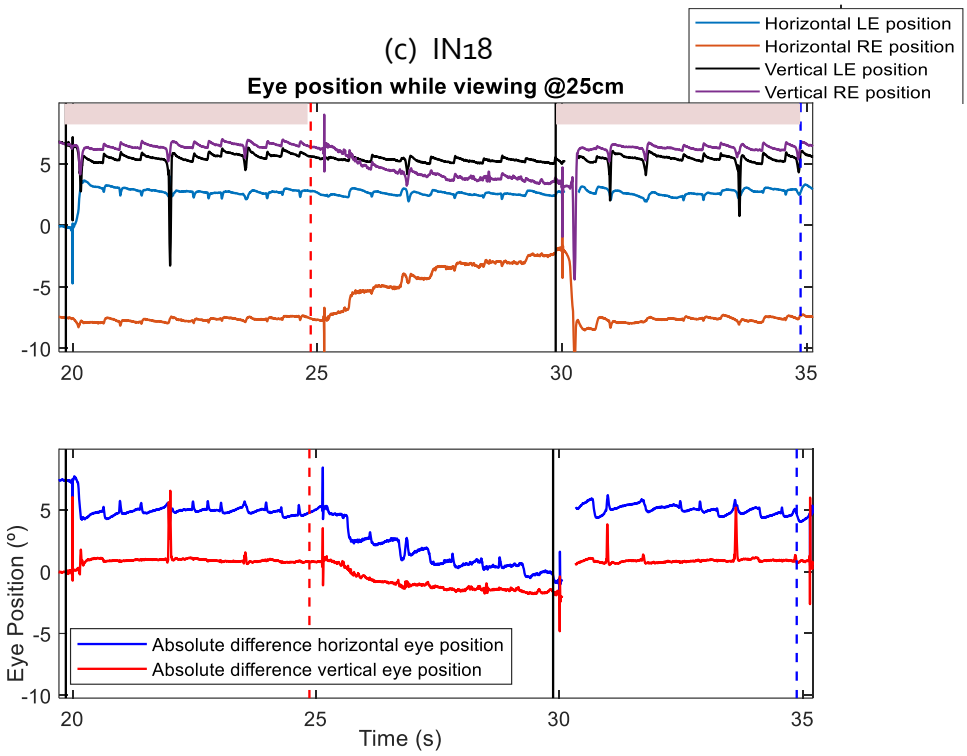

Figure 5-10: Sample plots for three participants showing the first two 5 s periods of binocular fixation
From the complete 120 ms of recorded data, the eye position plot is shown starting from the third trial where both eyes fixated binocularly (black vertical line marks the beginning). Each plot contains three complete trials represented by the vertical lines. The peach shaded portion is our main area of interest and marks the period during which the occluder was removed, and both eyes were fixating at the target. The middle portion beginning with a broken red vertical line, represents when the RE was covered, while the blue broken vertical line marks the beginning of when the LE was covered. Plots below represent the absolute difference in right and left eye position plots, for the horizontal and vertical eye position components.

5.3.4 The effect of viewing distance on fixation performance, in typical observers

For typical participants, bPDF plots were also produced to reflect the area of the eye movements while viewing at the four different distances. Using the 68% isocontour to account for the mean±1 SD of the observed data and exclude extreme values, the performance metrics representing accuracy and precision of eye movements were obtained and statistically analysed.

Accuracy: Results show that there was no significant main effect of test distance [$F_{(1.96, 25.48)} = 2.68$, $p = 0.09$] or eye examined [$F_{(1, 13)} = 1.99$, $p = 0.18$] on the accuracy of fixational eye movements at the four distances. However, there was a significant difference in values for the interaction between test distance and eye measured, [$F_{(3, 39)} = 3.43$, **$p = 0.03$**]. Data are presented in Figure 5-11. The dip in the plot at 25 and 100 cm (describing findings from

typical participants) appears to be a large difference in accuracy measures obtained at that distance and the adjacent ones, but note it only represents a small change in the Y value. In order to make this finding clearer, and at the same time show how data from the typical participants are much more precise than from those with IN, data obtained from those with IN were plotted in the same graph as typical participants (see Figure 5-11b).

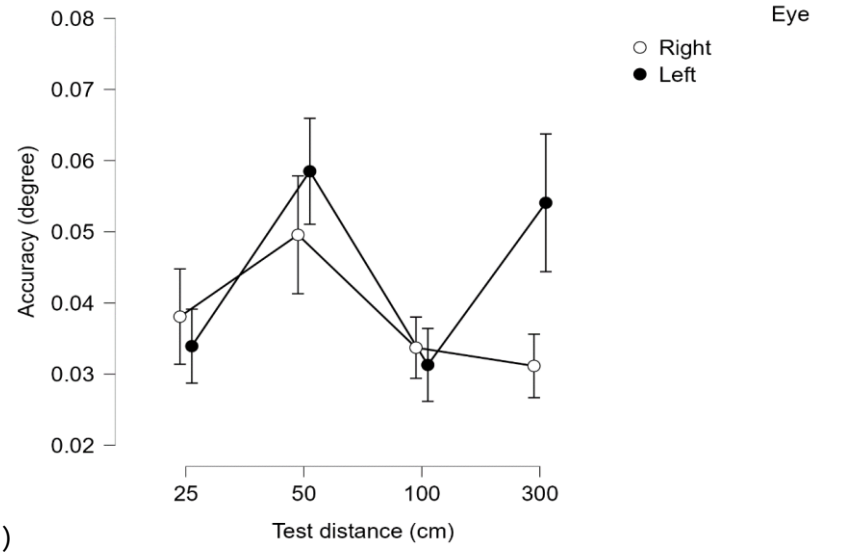

a)

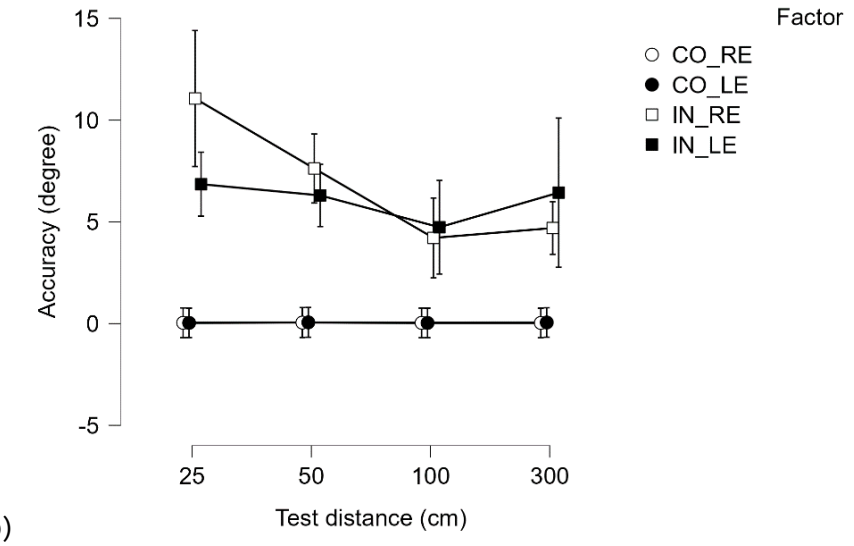

b)

Figure 5-11: Mean fixation accuracy at four distances.
Result from 14 typical participants are presented in (a) while the same data and data obtained from those with IN are plotted in (b). CO = control, IN = infantile nystagmus. RE and LE means right and left eye, respectively. Error bars = SE

Compared to typical participants, results from those with IN were much more inaccurate indicating that the centre points of the measured eye position data were further from the point of fixation.

Contour shape: Values obtained for isocontour symmetry are presented in Figure 5-12. These plots show an increase in shape factor from 300 to 25 cm, which means that the horizontal and vertical eye position range were more nearly equal at the closest distance. Analysis, however, revealed no significant main effect of test distance [$F_{(1.79, 23.29)} = 1.66$, $p = 0.21$], eye examined [$F_{(1, 13)} = 3.63$, $p=0.08$], or the interaction between both [$F_{(1.77, 23.02)} = 0.265$, $p = 0.74$].

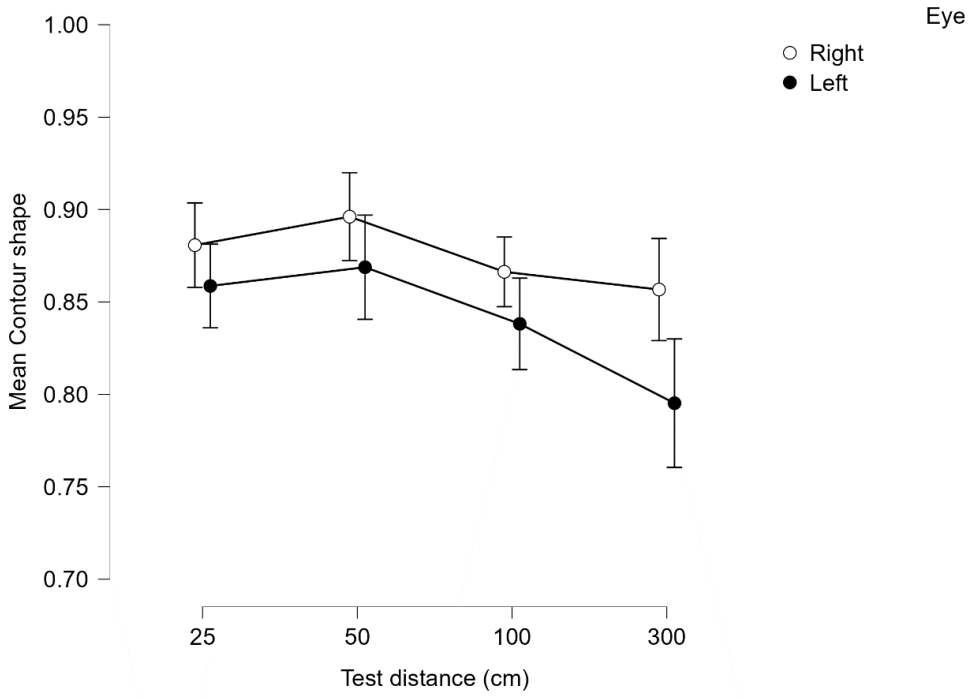

Figure 5-12: Mean contour shape at four distances for typical participants
Error bars = SE

Contour area including horizontal and vertical axis range: Values obtained for isocontour area are plotted in Figure 5-13. Results indicate that, although isocontour area was largest at 300 cm and became less at 25 cm, this change was not statistically significant [$F_{(3, 39)} = 2.39$, $p = 0.08$], nor did an interaction between test distance and eye examined signify any difference [$F_{(3, 39)} = 1.037$, $p = 0.39$]. Surprisingly, the right eye was more precise than the left eye [$F_{(1, 13)} = 4.83$, **$p=0.05$**], as reflected in the lower values obtained. But, this finding

was only marginal and not statistically significant for the horizontal [$F_{(1, 13)} = 3.70$, $p = 0.08$] or vertical [$F_{(1, 13)} = 1.74$, $p=0.21$] axis range, in both eyes.

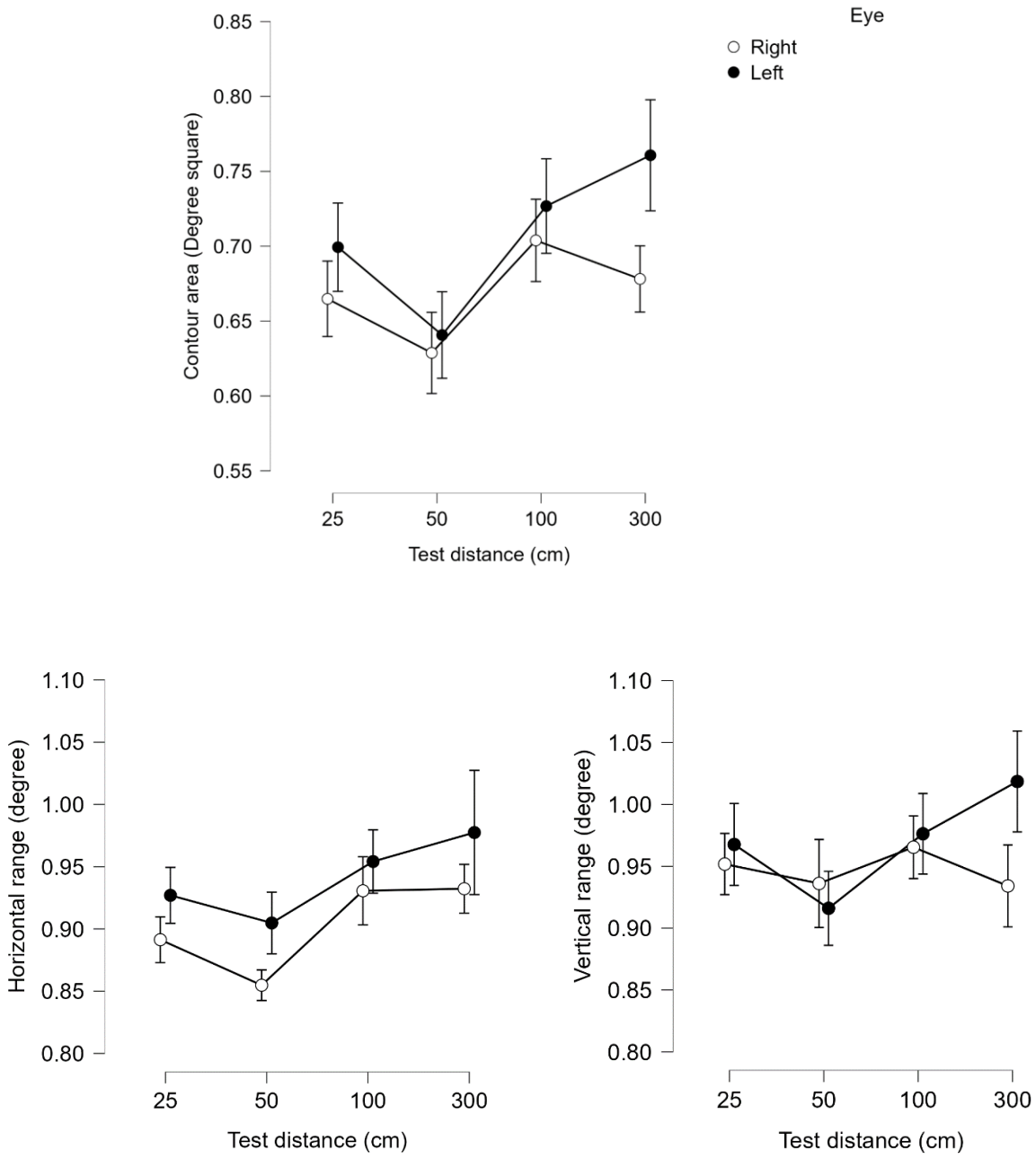

Figure 5-13: Mean contour area at four distances for typical participants
The values for fixation precision are plotted above while plots below are for the derived horizontal and vertical axis ranges. Error bars = SE

5.4 Discussion

The experiment was designed to evaluate convergence in all participants (IN and controls) and determine its relationship with ocular deviation in those with IN. In line with the first aim, the amount of convergence dampening in IN is quantified for the first time. A relatively high mean value of 56% reduction in fixation precision suggests that both components of the IN waveform reduces by more than half its original eye position spread, and further highlights the significance of convergence dampening, which is often used in IN management (Serra et al. 2006; Dell'Osso et al. 2020; Lee 2002). As seen in the data presented, convergence dampening may be present even when not found clinically. Therefore, the clinical diagnosis of convergence dampening alone may not be sufficient, since more participants were seen to have a reduction in the eye position spread (smaller isocontour areas); translating to a better precision at near. However, it becomes clearer that with the presence of a manifest ocular deviation, convergence dampening may not be achievable, and perhaps other binocular mechanisms may be interfering with the ability to fixate precisely at near.

In participants with IN, fixation accuracy was shown to reduce with convergence. This finding may not be considered significant because the accuracy metrics do not completely describe the fixation performance (as discussed in Section 2.7.3, page 53). However, for a few cases, this finding may be attributed to the presence of a deviation during binocular fixation, placing one eye a position away from the target. Most importantly, this finding may have also occurred as a result of a difference in beat direction in each participant's waveform oscillation. To illustrate further, where an oscillation in one eye happens to be in the opposite direction of fixation, one eye may be moving towards the nose and the other away from it therefore resulting in a wider spread of eye position data. The same can be said for those participants who were found to have poorer fixation precision at near.

The other findings concerning accuracy and precision of fixational eye movements are in no way different from those described in previous chapters, and highlights the idiosyncratic nature of IN (Ukwade and Bedell 1992). In line with previous chapters where variations in the horizontal and vertical axis range occurred with eccentric viewing, the variations seen in the horizontal and vertical axis range, with distance change, show that the IN waveform

within a participant can vary in the horizontal and vertical eye position components. Therefore, this demonstrates the importance of evaluating both components, and not just the waveform in the horizontal component.

In achieving and maintaining vergence, the evaluated waveforms show that, during vergence, conjugacy in IN waveform is relatively equal and may differ slightly in a few cases as a result of an intrusive saccade. For future studies, it may be important to quantify and statistically compare the corresponding slow phases and quick phases for each eye, and within given participants. The latency period could not be estimated because of the inherent issues encountered with determining latency in the IN waveform. At the positions where latency was needed to be objectively determined, most participants had incomplete data for which extrapolation gave erroneous findings. In addition, it was envisaged that 15 consecutive samples (Carl and Gellman 1987) or any other values chosen above the predetermined threshold could end up being a fast or slow phase and so the end point may not necessarily be uniform for all participants. Moreover, for the three participants described here, it was only in one of them that the eye movement delay was apparent. This may have occurred because of the participant's larger amount of phoric deviation.

In contrast to findings from participants with IN, in typical participants, fixation was more accurate at all distances, and at least in the LE more accurate at near than at the 300 cm viewing distance. Nevertheless, the poorer accuracy found in those with IN is expected owing to the IN waveform oscillations and subsequent larger spread of contour area in this group of participants. Participants with IN were seen to have an area of eye position ranging from 0.68 -25.55(°)^2, while for the typical participants contour area values were only at most about 0.8(°)^2. In general, considering all measures of accuracy and precision in typical participants, it can be concluded from this experiment that there is a tendency for fixation to be biased towards better performance at a close distance of up to 25 cm (although this may not necessarily be significant).

During this experiment, two main limitations were encountered. Firstly, because of the introduction of the flippers as an additional barrier during eye tracking, recording proved very difficult in participants with refractive correction. It has been shown that data quality can be reduced with any form of refractive correction in place (Holmqvist et al. 2011), more so when an additional barrier that could interfere with eye tracking is included. In addition,

a recent study (Wooding et al. 2023) has shown that with up to +7.00 DS of blur, individuals can maintain accurate and precise fixation. As a result, recordings were performed without participants spectacle correction (contact lenses used in a few cases). Nonetheless, because the target was large enough (0.4°) and scaled for each distance, target visibility was confirmed from each participant before recording began. Secondly, the mechanisms involved in moving the occluder system may have introduced a fair amount of noise in the output data especially for the left eye where, during the procedure, tiny twitching noises were heard at intervals. Attempts to reduce this twitching, suggested by the engineers who refurbished the instrument, by using foil paper around the wires and changing the servo at regular intervals were not fruitful. Participants were constantly reminded to ignore the slight noise and keep focusing on the target. Although findings may be tending towards slightly poorer fixation performance in the left eye (occurring because participants may have blinked in response to the distractions), these were not significant because of the precautions taken to avert an influence from the noise distraction. For further investigations, a quieter and more sophisticated motor system built to objectively work with the eye tracking apparatus will be necessary.

In summary, this chapter has provided novel findings on the objective amount of convergence dampening in IN and a general overview of the dynamics of achieving and maintaining convergence in IN, including a comparison of the fixation characteristics at distance and near in typical participants. In future it will also be necessary to evaluate further the IN oscillations and dynamics of achieving and maintain vergence using the horizontal and vertical components of the eye movements.

CHAPTER SIX

6 General conclusions and future work

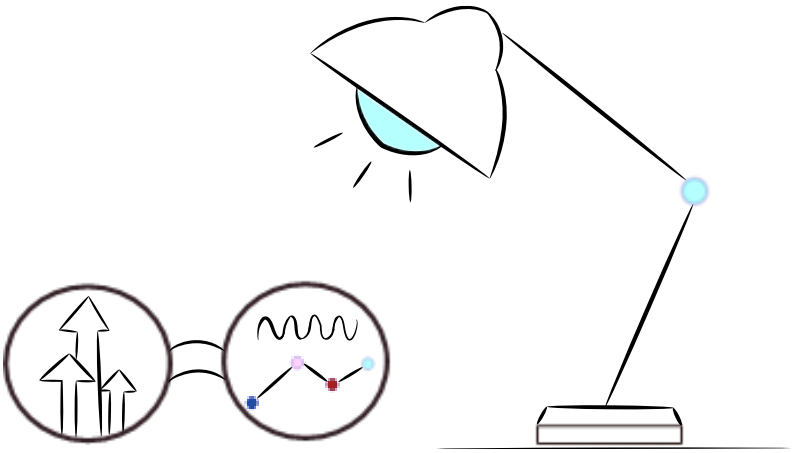

6.1 Overview

Fixation in the presence of IN was investigated as the main focus of this thesis. This final chapter summarises all of the findings concerning fixation performance and how this relates to eye-in-orbit position in those with IN and in typical participants. The overarching purpose of the experiments presented was to investigate, in detail, fixation performance and its implications at null positions (i.e. gaze angles and convergence positions), which is relevant for IN management. Novel findings of fixation performance as a function of horizontal gaze angles and convergence were presented using the bPDF analysis of eye positions. The contributions of the horizontal and vertical components, represented by the minimum and maximum axis range of the derived isocontour, were also investigated.

The objectives of experiments presented in this thesis were:

1. To determine any changes in fixation performance with eccentric viewing, taking into consideration the presence of an eccentric null zone in some people with IN. Fixation performance at different gaze angles, was also evaluated in typical participants.
2. To investigate any changes in visual performance at eccentric gaze positions. A psychophysical VA measurement task was included at the chosen gaze angles to evaluate any influence of eccentric gaze, and subsequently fixation performance, on VA threshold.
3. To evaluate fixation performance as a function of viewing distance. This was necessary to quantify the occurrence of convergence null in IN and to study its relationship with ocular deviation. The dynamics of achieving and maintaining vergence in those with IN was also described.

In Chapter one, a review of relevant literature was given as well as descriptions justifying why the bPDF method may provide a more comprehensive means of quantifying fixation performance. In Chapter two, details were provided about the materials used, participants recruited and an in-depth description of the bPDF method, as well as other methods used to analyse fixational eye movement data to produce quantitative measures of the accuracy and precision of fixation performance. In each experimental chapter that followed, a more detailed introductory section was included to highlight the rationale for each experiment.

The main findings from each experimental chapter (Chapters three to five), as well as the future work necessary to elaborate further on these research topics, are summarised in the following sections.

6.1.1 Chapter three

The aim of the experiment presented in Chapter three was solely to quantify fixation performance, from previously collected IN data, using the accuracy and precision of fixational eye movements at horizontal eccentric gaze positions up to ±20°. At the same time, the relationship between the derived horizontal and vertical bPDF isocontour range was evaluated to provide a possible explanation for why people with IN prefer to use their null zones. Given that it is common practice to analyse IN waveforms using only the horizontal components of recorded eye movements, the rationale behind analysing data obtained from this experiment stemmed from the need to provide a more comprehensive evaluation of the IN waveform (i.e. the horizontal and vertical components) that might better explain null zone preference.

The findings of variable isocontour symmetry (shape factor) and isocontour axis ranges, across gaze angles revealed that the horizontal and vertical waveform components, while fixating at different horizontal gaze positions, are often altered, and this change may contribute to fixation preference. The pattern by which horizontal and vertical components of the waveform change at eccentric gaze positions was however not uniformly defined and differed across participants. This is because it was seen that in more participants, a positive relationship existed between both variables such that as the horizontal axis range increases, the vertical increases as well. This finding has been observed clinically and is indeed similar to that found by Bedell, White and Abplanalp (1989), where the variability of eye positions in the horizontal and vertical components, from a group of 17 subjects (IN and controls), related positively ($r = 0.77$; $p < 0.01$). Results from a few of the other participants indicated that, as the vertical axis range increases, the horizontal decreases. It is possible that since the bPDF computation considers also the isocontour major axis of orientation to determine the horizontal and vertical axis range, this uncommon finding of a larger range in the vertical component may signify the need for a head tilt and explain how individuals with IN deal with this increase in the vertical component of the waveform. However, the

experiment was performed with the participant's head placed firmly on the head and chin rest to ensure that they could not tilt their head to a preferred position. Nonetheless, these results have highlighted the need for researchers to pay more attention to the vertical component of eye movements measured in a given visual plane of gaze angles.

The pattern of waveform variability across gaze angles can be said to be peculiar to each individual and may have been influenced by, among other factors, their emotional state, the presence of stress (Abadi and Dickinson 1986; Kraft and Irving 2004; Dunn et al. 2017; Jones et al. 2013), their null zones, and/or eccentricity of gaze. Since the subjectively estimated null zones and fixation performance do not completely correspond, it is imperative to explore further more objective measures of determining the null or abnormal head position, so that findings of fixation performance at eccentric gaze can be adequately determined.

Obtaining accurate null zones

In future, this research will include an objective measure of both head and eye position, using a device similar to that used for testing abnormal head postures (Kushner 2000; Hertle and Ahmad 2019). The aim would be to determine how each waveform component relates to gaze angle and its impact on head tilt, if any. Results could reveal how participants deal with either waveform component increasing/decreasing by adjusting their head position. The ability to keep the eyes fixating steadily on a target has been found to be similar with the degree of head stability (Shaikh et al. 2013) and due to the VOR, eye movement to maintain fixation will occur following a corresponding shift in head position. Therefore, determining the head position will have an influence on eye-in-orbit position.

For the proposed experiment, a device fabricated and programmed by Dr Lee McIlreavy (Adafruit bno55) to measure head position in the X, Y and Z planes can be validated and utilized. This IMU sensor (shown in Figure 6-1) measures head orientation at 100 Hz and has been attached to an adjustable head band easily put on by the participants. During the experiment, participants would be instructed to stay in their preferred head position, while reading a letter chart and eye movement simultaneously recorded. Results for head angle will then be cross correlated against fixational eye movements and gaze angle.

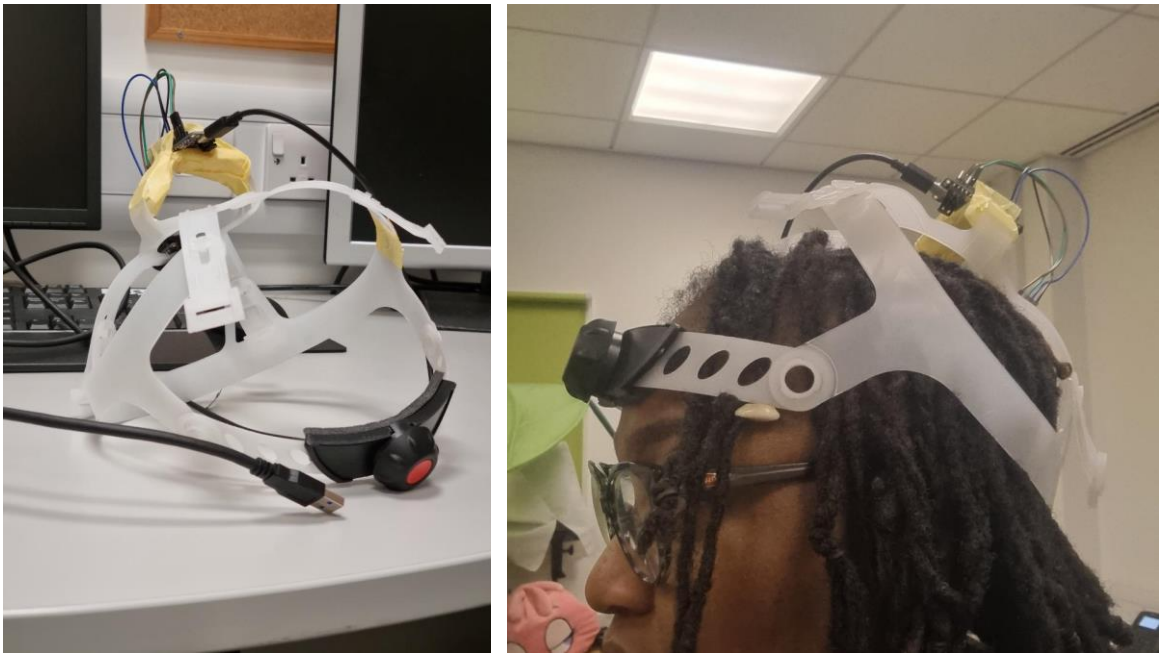

Figure 6-1: Device designed to measure head orientation
The device pictured here was programmed using Python, and has installed a USB reader for data recording. It can be connected to a computer to enable real time recording of head position. An adjustable red knob, seen in the picture on the left, is used to enable comfortable fit.

Another interesting finding from this chapter is the significant positive relationship between fixation precision and the VA measured clinically. The span of eye movement in the derived bPDF isocontour can be said to be the amplitude, and the degree of this eye movement excursion is what is judged clinically when doing a subjective null zone assessment. This relationship between fixation performance and VA highlights the need for early intervention, by way of educational support, in children who have been found to have high amplitude IN waveform that may be indicative of a higher degree of visual impairment. Given that IN eye movement is unlikely to change in adulthood, an intense IN eye movement in a child will most likely present, alongside underlying reduced vision that the clinician will need to attend to promptly by referring them to educational support services that could be of immense benefit.

6.1.2 Chapter four

The experiment in Chapter four was designed to investigate visual performance and its role in null zone preference. At seven evenly spaced eccentric gaze position up to ±45°, psychometric VA was measured and fixational eye movements recorded in participants

with IN as well as controls. The rationale for this study arose from an inability to find a definite visual reason for null zone preference in IN as explored in the previous chapter. In addition, given the existing literature reports only a marginal increase in VA in the null zone of those with IN, it was necessary to investigate further VA changes at eccentric gaze positions, while utilizing the bPDF method to investigate the relationship between the horizontal and vertical component parts of the eye movement trace at different horizontal gaze positions.

The results indicate that better VA is not defined by fixation at the null zone (or primary position in the case of typical participants). That only a quarter of participants with IN showed a correspondence of clinical null zone with best visual threshold was unexpected considering the existing literature. In addition, even though in two-third of the participants the gaze position of best fixation precision corresponded with that of best threshold VA, this gaze position did not correspond to the subjective eccentric null. This indicates that the use of a subjective means to determine null zones may be inadequate, and further highlights the need for an objective determination of the null zone.

With respect to fixation performance, a similar pattern is seen in those with IN and controls wherein better fixation performance does not always occur in the null zone or even the primary position. The relationships between the horizontal and vertical range of data spread (computed from the major and minor axis length, major axis orientation and shape factor of the derived 68% isocontour) were also seen to be variable among participants, and the values obtained differed in an undefined pattern. The degree of the entrainment behaviour between the horizontal and vertical component is not predictable and further buttresses the need to explore other factors that may produce a more definite answer to the observed null zone preference.

In light of these findings, assuming null zone/head positions is determined objectively, it remains unknown how fixation performance in the vertical plane might be influenced. Everyday visual scenes comprise gaze directions in vertical, horizontal and torsional/diagonal visual planes, and it has been found that about 5% of children with IN have a predominantly vertical or asymmetric horizontal waveform oscillation (Shawkat et al. 2000). The studies described in this thesis has investigated fixation only at different gaze directions in the horizontal visual plane. Perhaps further investigations into visual

performance along the vertical plane (in the first instance), and the contributions of the horizontal and vertical components of eye movements when viewing vertically may tease out more definitive results for the null zone preference. All of these findings put together could also improve our understanding of the implications of 'eccentric gaze' and its possible importance of gaze angles for those with IN when conducting clinical tests such as fundus photography, OCT scans or microperimetry.

Exploring fixation performance at vertical gaze angles

As a starting point, the existing results of eye movement recordings of fixation along the vertical plane, collected by Dr Matt Dunn, can also be analysed using the bPDF method. The aim of the experiment would be to determine if fixation performance changes as a function of vertical gaze angles. It is common knowledge that horizontal null zones exist, however information is lacking as to the existence of vertical null zones. Findings from this proposed analysis would provide additional novel information about null zones, and the relationships between the horizontal and vertical eye movement range along the vertical plane.

It is envisaged that eye movements may be more unstable at vertical rather than horizontal eccentricities, and the vertical neural integrator will have a tougher task in keeping gaze at primary/preferred position. This is because, in order to move the eyes vertically, more muscles (rectus and obliques: see Figure 1-8) are put to work, unlike horizontal gaze shifts where only rectus muscles are involved. In addition, the same neural integrator in the midbrain has been identified to control vertical and torsional eye movements (Sanchez and Rowe 2018). Therefore, this experiment might reveal additional findings related to the impact of head tilt in IN.

6.1.3 Chapter five

The experiment presented in chapter five was aimed at investigating the phenomenon of convergence null/dampening in IN and finding its relationship with ocular deviation. Also, in typical participants, fixation performance as a function of viewing distance (and convergence) was quantified using the bPDF method. Convergence null is a commonly reported occurrence in IN, however, the degree of eye movement reduction has not been

quantified. In addition, fixational eye movements have not been shown to vary with viewing distance in typical participants, and hence this is another motivation for this experiment.

From the results obtained, there was no evidence that fixation at a nearer viewing position guaranteed better fixation performance in typical participants, as occurs in some people with IN (Dell'Osso et al. 1972; Abadi and Bjerre 2002). It can therefore be concluded that, in typical participants, convergence does not influence the stability of fixation, and fixation may not have to be more precise for successful near work. The results also suggest that, where viewing distance varies, for example in a typical classroom, the ability of typical students to fixate adequately is unaffected.

In line with the existing literature, findings for this chapter show that more participants with IN had better fixation precision at the nearer fixation distance, and the vertical isocontour axis ranges were lower, indicating less spread in the vertical component of the eye position trace. It was also revealed for the first time that the mean percentage reduction in isocontour spread was a little over half (-55.79 ± 23.32%). In addition, the results revealed that participants with IN who have a latent ocular deviation or no deviation at all were more likely to exhibit a convergence null (represented by better fixation precision). This could imply that, at a closer working distance, an absence of or a minimal ocular deviation will enable the ocular mechanism to act by reducing IN oscillation perhaps to be able to improve the image (i.e. less image motion). In most cases, during the experiment, it was not feasible to use a patient's spectacle prescription together with the automated cover testing device because it interfered with data collection. However, in clinical settings and everyday situations, priority could be given to managing both latent and manifest ocular deviations in IN even though refractive errors may not be fully corrected.

Furthermore, because of the conjugacy of the IN oscillation and the mechanism of convergence which moves both eyes in a disconjugate manner to the point of fixation, it was necessary to understand the mechanism by which those with IN achieve convergence. Information about this is lacking in the literature, but as a starting point, a brief description of the eye movements taking place during the process of achieving and maintaining convergence was presented. Eye position plots, from fixation at 25 cm, indicated that the IN waveform while taking up fixation and during the fixation process appeared the same. In

addition, findings while taking up fixation points towards the fast phase as being responsible for achieving this. Whether this is the case more generally will require more work as this was only evaluated in three participants. Other factors that will need to be investigated will be the latency of the IN eye movements which occur prior to the eyes converging or diverging. Knowledge about the latency period could provide information regarding the relationship between each eye during vergence.

A brief description of future work is given as follows:

A) The dynamics of achieving and maintaining vergence

In order to thoroughly evaluate waveforms for any similarities or differences, it is crucial to quantify the IN waveform components and compare these values. This can be done using the data collected for this chapter. Recall that the Eyelink Data Viewer software was used initially to distinguish in the eye movement recording periods of blinks, saccades, and fixation. Blink events were removed and saccades were classed as quick phases, whereas all the other eye movement events not identified as blinks and saccades would for the purpose of this analysis be classified as slow phases. Corresponding slow phases and quick phases for each eye could then be compared within individual participants.

The latencies associated with vergence eye movements in IN were not particularly easy to estimate. This is because of the existence of the IN waveform parts (slow phase, fast phase and foveation periods) which may differ in length depending on the waveform type. Therefore, it may not always be clear what part of the waveform convergence is achieved, but quantifying the waveform components as described above will be helpful. Also, in most cases, participants had incomplete data at the position of presumed latency, and extrapolation gave erroneous findings. To investigate this issue of latency further, a modified method adapted from that used by Carl and Gellman (1987) could be utilized. For this, an average of the eye position during the 100 ms before occlusion will be taken as a baseline. The latency of the response could then be determined as the period when the eye position exceeded this baseline by three standard deviations (SD) of the regression line fit to the sample points 100 ms before the occlusion time. Since this threshold may be exceeded randomly by a saccade, there must also be at least 15 consecutive (1 ms) samples above it. Thus the period between when the occluder was removed and the time when the

amplitude of the eye position exceeds 3 SD from this regression line will be taken as the latency of response. It is envisaged that 15 consecutive samples chosen above the predetermined threshold could end up being a fast or slow phase, and so the end point may not necessarily be uniform for all participants.

In addition, given the conjugacy in IN eye oscillations, and the difference in latency period for esophoric and exophoric emmetropes (i.e. typical participants) in the delay in vergence initiation (Barnard and Thomson 1995), an investigation of any difference between eyes in IN will contribute significantly to our knowledge about the vergence dynamics in this condition.

B) The role of accommodation

The presence of an active accommodative system may not have influenced the results in this study because most participants were in the older age group, and with increasing age accommodation effort is reduced or completely absent. However, a future study involving children is being considered, and for this, accommodation is bound to play a big role, and the interplay between these two mechanisms (accommodation and convergence) may be significant. For this reason, a simultaneous measurement of accommodation alongside vergence tracking may be important.

In the initial stage of these PhD studies, attempts were made to investigate the off-axis performance of the PowerRef 3 (an instrument used to measure accommodative state, and hence refraction, in real time) in adult subjects (Amiebenomo et al. 2020). The aim was to determine the suitability of the instrument for recording in IN, given that during recording IN oscillations will continuously move the eyes to an eccentric gaze position (i.e. off the fixation target), and result in a change in accommodative state with a subsequent change in refractive error. To explain further, it is known that during refraction measurement, a shift off-axis could alter the measured refractive error (Seidemann et al. 2002; Fedtke, Ehrmann and Holden 2009; Radhakrishnan and Charman 2008). Therefore, it might be expected that IN oscillations will result in fluctuations in the measured refractive error, and the question was whether the instrument is robust to such fluctuations.

For the experiment, the PowerRef 3 (Plusoptix R09) was used to record refractive error and gaze angles, among six presbyopes without IN, at 1 m. Participants were aged between 43

and 70 years. Lens powers of +4, +3, +2 and +1 DS (for myopic defocus) as well as -2 and -4 DS (for hyperopic defocus) were used to induce defocus, to determine if a corresponding refraction reading will be obtained from the instrument. Figure 6-2 shows the experimental setup. Targets were sized 2 x 2 cm and presented at the chosen horizontal positions for convergence at 20, 25, 33.3, 50 and 100 cm (using an adult PD of 64 mm); targets were therefore spaced 3.2 cm apart, about 2° from each other. Measurements were obtained for at least 5 s at each gaze position.

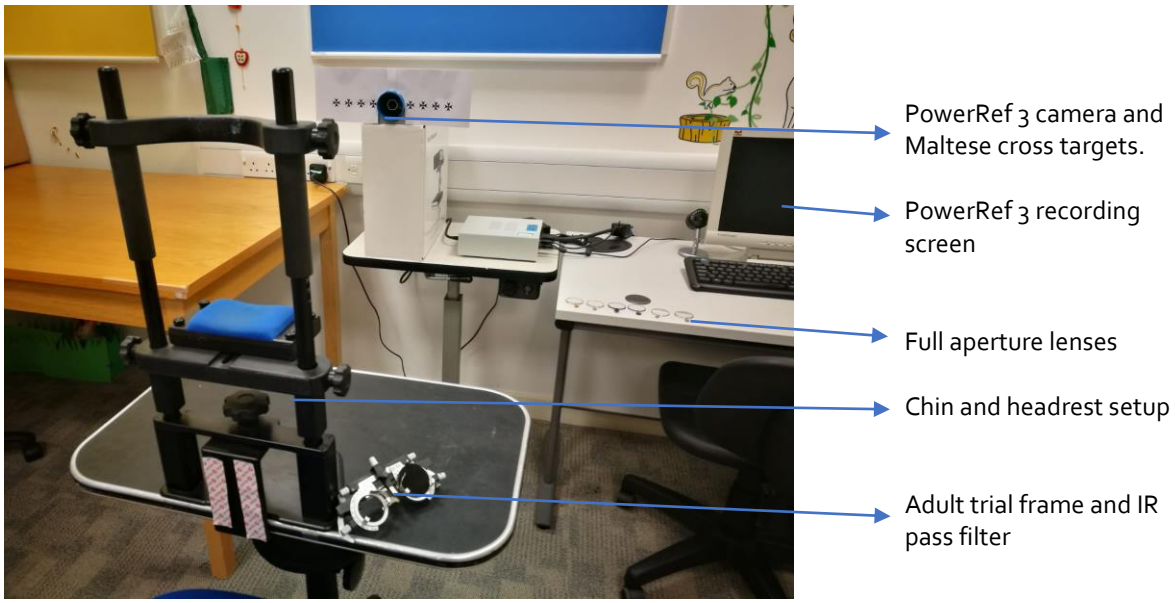

Figure 6-2: Experimental setup for off-gaze refraction measures

Results revealed that the lens-induced refractive changes were accurately measured both at the centre and off-axis positions (except for a -2D lens at 4°; P = 0.04). Also, for gaze positions up to 8°, the measured refraction was not significantly different from that at the central position. A diagram of the refractive findings at gaze positions is shown in Figure 6-3 while the relationship between measured and induced refraction (r^2 values ranging from 0.31 - 0.56) is presented in Figure 6-4.

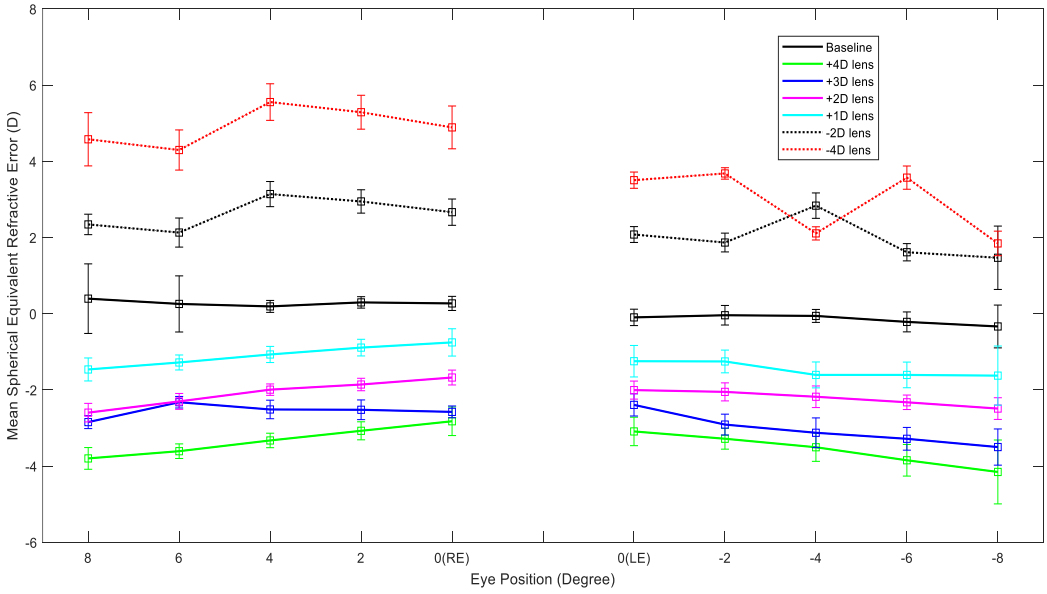

Figure 6-3: Mean refraction measured at different gaze positions, and with different lens induced.
The right eye (RE) refraction is represented on the left, while the left eye (LE) refraction is represented on the right.

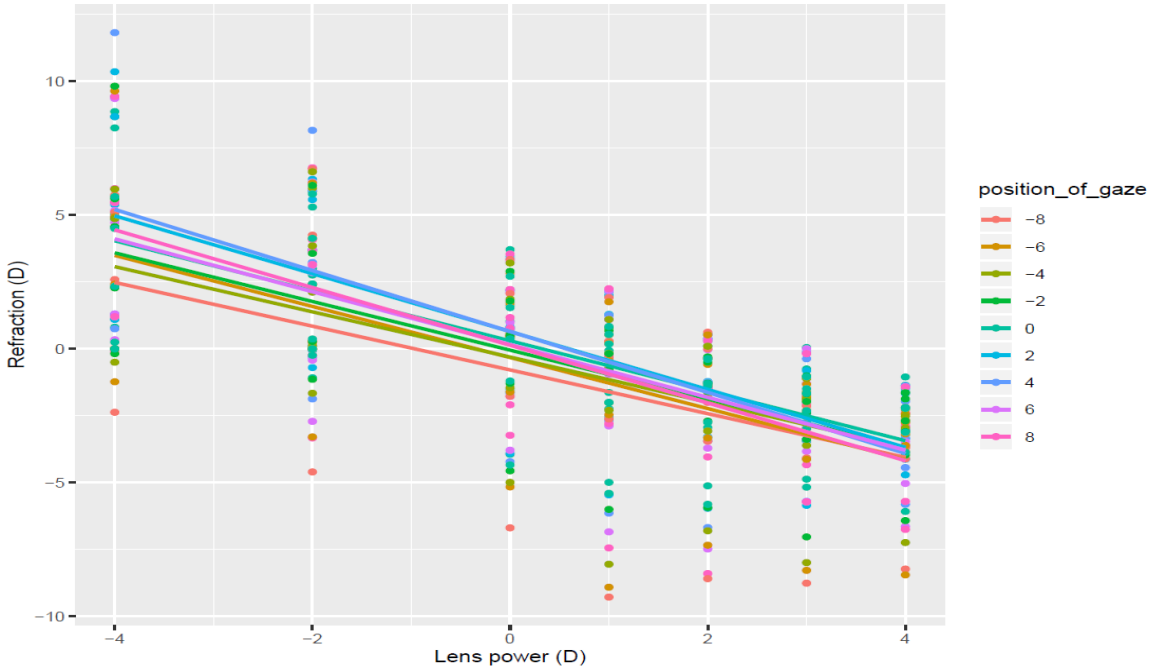

Figure 6-4: Relationship between measured refraction and induced lens power for all gaze positions.

Furthermore, IN eye movements were simulated using a moving grating stimulus which induced an OKN response. This OKN stimulus was presented on a smartphone at 30 cm. The PowerRef3 refraction and gaze angle recordings for a single 33 year old participant (emmetrope) are shown in Figure 6-5.

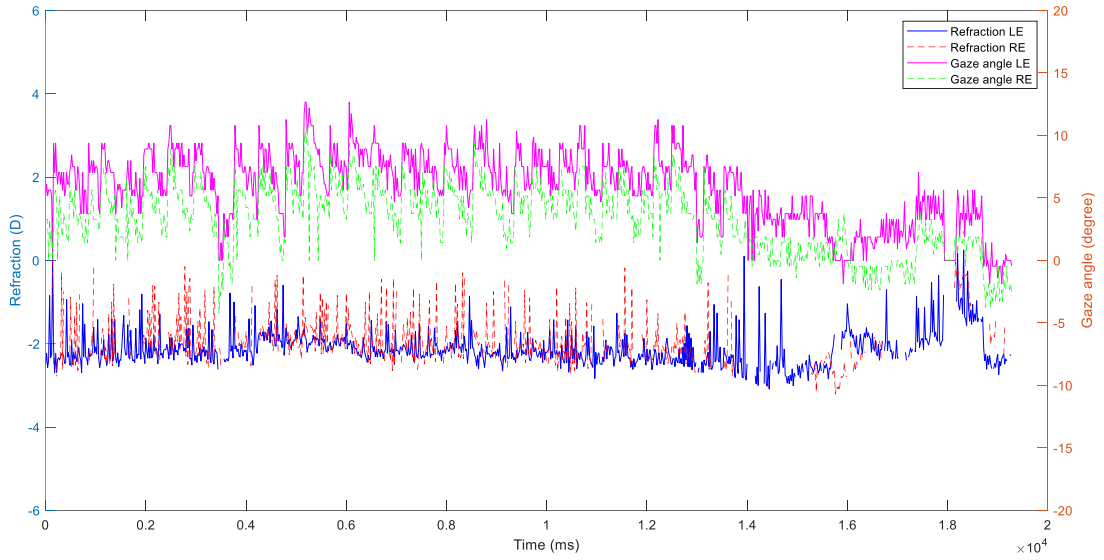

Figure 6-5: Simulated IN movement using OKN stimuli
LE = left eye, RE = right eye

Overall, the findings from these experiments have revealed that refraction off-axis can be measured using the PowerRef 3 and remains reliable for up to 8° eccentricity. This implies that any changes in the refractive state during IN eye movements can be adequately recorded. Data collection for this research is still in progress as there are methodological improvements that need to be made to this preliminary work. These include digitizing the target presentation on computer screens to allow for timestamping and accurate data evaluation, as well as synchronizing output measures with eye tracking measurements. To progress this research further, the prospects of simultaneously measuring accommodation and vergence in children with IN will be explored.

To simultaneously study accommodation and vergence an eye tracker and accommodation measuring device will need to be synchronised. Previous studies have attempted to design various types of instruments that can measure both physiological processes. However, the one that is most suitable for use in children due to its tolerance for head and eye movement, and its ability to obtain results quickly, is the video-based format fabricated by Suryakumar et al. (2007) (see Figure 6-6). In a similar fashion, attempts will be made to synchronise the PowerRef 3 and the EyeLink 1000 for the intended future studies.

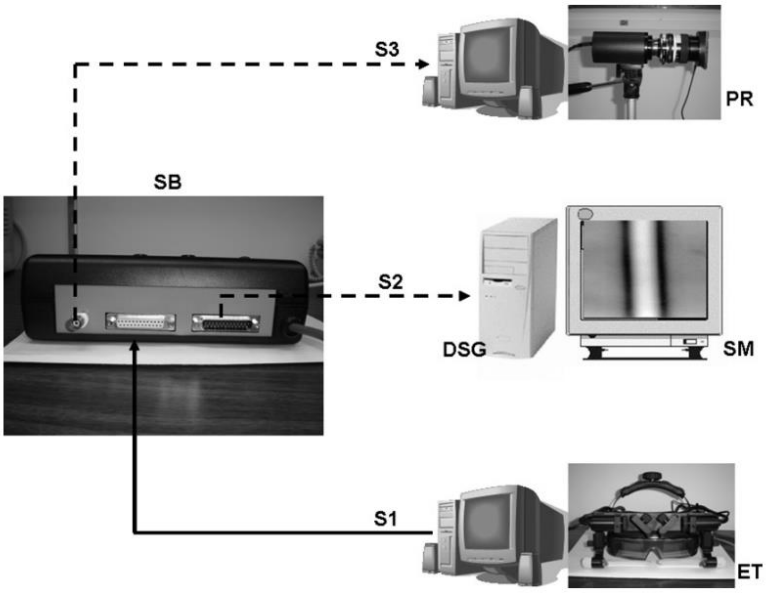

Figure 6-6: Measuring accommodation and vergence (Source: Suryakumar et al. 2007)
Diagram showing synchronization of a digital PhotoRefractor (PR) with a video-based stereo eye tracker (ET) to allow for simultaneous measurement and offline analysis of accommodation and vergence.
SB = synchronisation box; DSG = digital stimulus generator; S1, S2 and S3 represent the signals sent.

6.2 Summary

In summary, the experiments described in this thesis have provided additional information about fine foveal vision during fixation, in participants with IN and typical participants. The size of any changes with respect to gaze angles and viewing distance was quantified using the bPDF method. Of the hypotheses tested, the results indicate that, overall, best fixation and visual performance is not necessarily defined by the horizontal gaze angle corresponding to the null zone (or at primary position in the case of typical participants), or at the convergence null. Therefore, the fundamental reason that people with IN prefer to use their null cannot be fully explained on the basis of the results from this thesis. Nonetheless, the results highlight strongly a continuous variation in the horizontal and vertical range of eye movement components, at different fixation positions.

For the experiments presented in Chapters three and four, where fixation performance was quantified at different horizontal gaze angles, the results reveal a positive relationship between the derived horizontal and vertical isocontour axis range at gaze angles, in the majority of participants. However, for a few others, where the horizontal range increases alongside a vertical decrease, it is proposed that a need to adapt to these changes in the

horizontal and vertical components of the waveform could be the driving factor for using a head tilt. In addition, results from the experiment presented in Chapter three revealed that a poor fixation performance correlated with a reduced clinical VA . Furthermore, in Chapter four, which looked more specifically at visual performance, it was found that, although fixation performance remained the same across gaze angles, the gaze position of best fixation precision corresponded with that of best psychometric VA threshold, in the majority of participants. Surprisingly, however, most of these gaze positions did not correspond to the subjective eccentric null, and this finding further highlights the need for a more precise, objective means of determining null zones by quantifying head position.

As regards viewing distance, fixational eye stability may change with convergence (hence viewing distance) and has been reported to occur in those with IN, but not for typical participants. From the experiment performed in Chapter five, the typical reduction in IN waveform oscillation that occurred with convergence (convergence null/dampening) was quantified using a change in the span of eye position (fixation precision) from the farthest to the nearest distance. More than half of participants with IN exhibited a convergence null, and this was commonly found in participants with a clinically measured typical ocular alignment, as well as in those with a latent ocular deviation. This underlines the importance of prompt visual management in those with IN and a manifest deviation, in order to achieve a possible improvement in near viewing.

There is still a great deal that we do not understand about nystagmus and its impact on the way a person with IN sees. As this thesis vividly demonstrates, our understanding of IN is made difficult by the individual variations in its properties. Hopefully this work goes a little way towards increasing our understanding of the fixational eye movements as well as the fixation and visual performance, at gaze positions and different viewing distances, in those with IN.

Finally, we cannot completely ignore the interaction that could exist between viewing at different gaze angles and at different distances. One question that remains is how varied the null is with distance, which may be implied by people having a convergence null. The experiments described here looked at these individual aspects, but given that the null zone has been reported to vary for different viewing distances (Kraft and Irving 2004), exploring

both together, including the extent the vertical component of eye movement at each plane relate, may be crucial.

REFERENCES

7

Abadi R V. (2002) Mechanisms underlying nystagmus. *Journal of the Royal Society of Medicine* **95**: 231–234.

Abadi R V. and Bjerre A (2002) Motor and sensory characteristics of infantile nystagmus. *British Journal of Ophthalmology* **86**: 1152–1160.

Abadi R V. and Pascal E (1995) Eye movement behaviour in human albinos. In: *Studies in Visual Information Processing*. Elsevier Masson SAS, pp. 255–268.

Abadi R V. and Pascal E (1994) Periodic alternating nystagmus in humans with albinism. *Investigative Ophthalmology and Visual Science* **35**: 4080–4086.

Abadi R V. and Pascal E (1991) Visual resolution limits in human albinism. *Vision Research* **31**: 1445–1447.

Abadi R V., Pascal E, Whittle J and Worfolk R (1989) Retinal fixation behavior in human albinos. *Optometry and Vision Science* **66**: 276–280.

Abadi R V. and Whittle J (1991) The nature of head postures in congenital nystagmus. *Archives of Ophthalmology* **109**: 216–220.

Abadi R V and Dickinson CM (1986) Waveform characteristics in congenital nystagmus. *Documenta Ophthalmologica* **64**: 153–167.

Abel LA, Parker L, Daroff RB and Osso LFD (1978) End-point nystagmus. *Investigative Ophthalmology and Visual Science* **17**: 539–544.

Del Águila-Carrasco AJ, Esteve-Taboada JJ, Papadatou E, Ferrer-Blasco T and Montés-Micó R (2017a) Amplitude, latency, and peak velocity in accommodation and disaccommodation dynamics. *BioMed Research International* 1–8.

Del Águila-Carrasco AJ, Marín-Franch I, Bernal-Molina P, Esteve-Taboada JJ, Kruger PB, Montés-Micó R and López-Gil N (2017b) Accommodation responds to optical vergence and not defocus blur alone. *Investigative Ophthalmology and Visual Science* **58**: 1758–1763.

Alexiev K and Vakarelski T (2023) Can microsaccades be used for biometrics? *Sensors* **23**: 1–22.

Amiebenomo OM-A, McIlreavy L, Erichsen JT and Woodhouse JM (2021) Effect of viewing distance on fixation characteristics in typical observers. *Investigative Ophthalmology and Visual Science* **62**: 3334–3334.

Amiebenomo OM-A, McIlreavy L, Erichsen JT and Woodhouse JM (2020) The potential off-axis performance and accuracy of the PowerRef 3 for measurements in Nystagmus: AVA Christmas Meeting, Cardiff University, December 16, 2019. *Perception* **49**: 700–726.

Anantrasirichai N, Gilchrist ID and Bull DR (2016) Fixation identification for low-sample-rate mobile eye trackers. In: *Proceedings - International Conference on Image Processing, ICIP*. IEEE Computer Society, pp. 3126–3130.

Anderson AG, Ratnam K, Roorda A and Olshausen BA (2020) High-acuity vision from retinal image motion. *Journal of Vision* **20**: 34–34.

Anderson HA, Manny RE, Glasser A and Stuebing KK (2011) Static and dynamic

measurements of accommodation in individuals with Down syndrome. *Investigative Ophthalmology and Visual Science* **52**: 310–317.

Anderson RS and Ennis FA (1999) Foveal and peripheral thresholds for detection and resolution of vanishing optotype tumbling E's. *Vision Research* **39**: 4141–4144.

Averbuch-Heller L, Dell'Osso LF, Leigh RJ, Jacobs JB and Stahl JS (2002) The torsional component of 'horizontal' congenital nystagmus. *Journal of Neuro-Ophthalmology* **22**: 22–32.

Barnard SNA and Thomson DW (1995) A quantitative analysis of eye movements during cover test - a preliminary report. *Ophthalmic and Physiological Optics* **15**: 413–419.

Bedell HE, White JM and Abplanalp PL (1989) Variability of foveations in congenital nystagmus. *Clinical Vision Sciences* **4**: 247–252.

Bertsch M, Floyd M, Kehoe T, Pfeifer W and Drack A V. (2017) The clinical evaluation of infantile nystagmus: What to do first and why. *Ophthalmic Genetics* **38**: 22–33.

Bharadwaj SR (2017) Accomodation mechanism. In: Artal P ed. *Handbook of Visual Optics, Volume One: Fundamentals and Eye Optics*. Boca Raton:Taylor & Francis: CRC Press, pp. 363–376.

Bharadwaj SR and Candy TR (2008) Cues for the control of ocular accommodation and vergence during postnatal human development. *Journal of Vision* **8**: 1–16.

Bhattarai D, Suheimat M, Lambert AJ and Atchison DA (2019) Fixation stability with Bessel beams. *Optometry and Vision Science* **96**: 95–102.

Bifulco P, Cesarelli M, Loffredo L, Sansone M and Bracale M (2003) Eye movement baseline oscillation and variability of eye position during foveation in congenital nystagmus. *Documenta Ophthalmologica* **107**: 131–136.

Blignaut P (2017) Using smooth pursuit calibration for difficult-to-calibrate participants. *Journal of Eye Movement Research* **10**: 1–13.

Botev ZI (2015) *kernel density estimation - File Exchange - MATLAB Central* [Online]. Available at: https://uk.mathworks.com/matlabcentral/fileexchange/17204-kernel-density-estimation?s_tid=srchtitle [Accessed: 21 May 2023].

Botev ZI, Grotowski JF and Kroese DP (2010) Kernel density estimation via diffusion. *Annals of Statistics* **38**: 2916–2957.

Bowers NR, Gautier J, Lin S and Roorda A (2021) Fixational eye movements in passive versus active sustained fixation tasks. *Journal of Vision* **21**: 1–16.

Brodsky MC and Fray KJ (1997) The prevalence of strabismus in congenital nystagmus: The influence of anterior visual pathway disease. *Journal of American Association for Pediatric Ophthalmology and Strabismus* **1**: 16–19.

Butterworth S (1930) On the theory of filter amplifiers. *Experimental Wireless and the Wireless Engineer* 536–541.

Büttner U and Büttner-Ennever JA (2006) Present concepts of oculomotor organization.

Progress in Brain Research **151**: 1–42.

Carl JR and Gellman RS (1987) Human smooth pursuit: Stimulus-dependent responses. *Journal of Neurophysiology* **57**: 1446–1463.

Castet E and Crossland M (2012) Quantifying eye stability during a fixation task: A review of definitions and methods. *Seeing and Perceiving* **25**: 449–469.

Cesarelli M, Bifulco P, Loffredo L and Bracale M (2000) Relationship between visual acuity and eye position variability during foveations in congenital nystagmus. *Documenta Ophthalmologica* **101**: 59–72.

Chang MY, Binenbaum G, Heidary G, Cavuoto KM, Morrison DG, Trivedi RH, Kim SJ and Pineles SL (2023) Surgical treatments to improve visual acuity in infantile nystagmus syndrome: A report by the American Academy of Ophthalmology. *Ophthalmology* **130**: 331–344.

Cherici C, Kuang X, Poletti M and Rucci M (2012) Precision of sustained fixation in trained and untrained observers. *Journal of Vision* **12**: 1–16.

Chung STL and Bedell HE (1996) Velocity criteria for 'foveation periods' determined from image motions simulating congenital nystagmus. *Optometry and Vision Science* **73**: 92–103.

Clark AM, Intoy J, Rucci M and Poletti M (2022) Eye drift during fixation predicts visual acuity. *Psychological and Cognitive Sciences* **119**: 1–10.

Clark R, Blundell J, Dunn MJ, Erichsen JT, Giardini ME, Gottlob I, Harris C, Lee H, McIlreavy L, Olson A, Jay SE, Valldeflors V-N, Waddington J, Woodhouse JM, Gilchrist ID and Williams C (2019) The potential and value of objective eye tracking in the ophthalmology clinic. *Eye* 1–3.

Collewijn H, Apkarian P and Spekreijse H (1985) The oculomotor behaviour of human albinos. *Brain* **108**: 1–28.

Collewijn H and Kowler E (2008) The significance of microsaccades for vision and oculomotor control. *Journal of Vision* **8**: 1–21.

Crossland MD, Culham LE and Rubin GS (2004) Fixation stability and reading speed in patients with newly developed macular disease. *Ophthalmic and Physiological Optics* **24**: 327–333.

Crossland MD and Rubin GS (2002) The use of an infrared eyetracker to measure fixation stability. *Optometry and Vision Science* **79**: 735–739.

Dai B, Cham KM and Abel LA (2021) Velocity viscrimination in infantile nystagmus syndrome. *Investigative Ophthalmology and Visual Science* **62**: 1–9.

Davies JR and Freeman TCA (2011) Simultaneous adaptation to non-collinear retinal motion and smooth pursuit eye movement. *Vision Research* **51**: 1637–1647.

Dell'Osso L, Gauthier G, Liberman G and I LS (1972) Eye movement recording as a diagnostic tool in a case of congenital nystagmus. *American Journal of Optometry and Archives of American Academy of Optometry* **49**: 3–13.

Dell'osso LF (2002) Development of new treatments for congenital nystagmus. *Annals of the New York Academy of Sciences* **956**: 361–379.

Dell'Osso LF (1973) Fixation characteristics in hereditary congenital nystagmus. *American Journal of Optometry and Archives of American Academy of Optometry* **50**: 85–90.

Dell'osso LF and Daroff RB (1975) Congenital nystagmus waveforms and foveation stratergy. *Documenta Ophthalmolgica* **39**: 155–182.

Dell'osso LF and Daroff RB (1990) Eye movement characteristics and recording techniques. In: Glasser JS ed. *Neuro-ophthalmology*. 3rd ed. Philadelphia: Lippincott Williams and Wilkins, pp. 327–343.

Dell'osso LF and Daroff RB (1974) Functional organization of the ocular motor system. *Aerospace Medicine* **45**: 873–875.

Dell'Osso LF and Flynn JT (1979) Congenital Nystagmus surgery. A quantitative evalaution of the effects. *Archives of Ophthalmology* **97**: 462–469.

Dell'Osso LF, Flynn JT and Daroff RB (1974) Hereditary congenital nystagmus. An intrafamilial study. *Archives of Disease in Childhood* **92**: 366–374.

Dell'Osso LF and Jacobs JB (2002) An expanded nystagmus acuity function: Intra- and intersubject prediction of best-corrected visual acuity. *Documenta Ophthalmologica* **104**: 249–276.

Dell'Osso LF, van der Steen H, Steinman RM and Collewijn H (1992a) Foveation dynamics in congenital nystagmus. II: Smooth pursuit. *Documenta Ophthalmolgica* **79**: 25–49.

Dell'Osso LF, Van Der Steen J, Steinman RM and Collewijn H (1992b) Foveation dynamics in congenital nystagmus I: Fixation. *Documenta Ophthalmologica* **79**: 1–23.

Dell'Osso LF, Van Der Steen J, Steinman RM and Collewijn H (2020) Foveation dynamics in congenital nystagmus IV: vergence. *Documenta Ophthalmologica* **140**: 221–232.

Ditchburn RW and Ginsborg BL (1953) Eye movements during fixation. *The Journal of Physiology* **119**: 1–17.

Dunn MJ, Harris CM, Ennis FA, Margrain TH, Woodhouse JM, McIlreavy L and Erichsen JT (2019) An automated segmentation approach to calibrating infantile nystagmus waveforms. *Behaviour Research Methods* 1–11.

Dunn MJ, Margrain TH, Woodhouse JM, Ennis FA, Harris CM and Erichsen JT (2014) Grating visual acuity in infantile nystagmus in the absence of image motion. *Investigative Ophthalmology and Visual Science* **55**: 2682–2686.

Dunn MJ, Wiggins D, Woodhouse JM, Margrain TH, Harris CM and Erichsen JT (2017) The effect of gaze angle on visual acuity in infantile nystagmus. *Investigative Ophthalmology and Visual Science* **58**: 642–650.

Eizenman M, Hallett PE and Frecker RC (1985) Power spectra for ocular drift and tremor. *Vision Research* **25**: 1635–1640.

Fadzil NM, Mohammed Z, Shahimin MM and Saliman NH (2019) Reading performance and

compensatory head posture in infantile nystagmus after null zone training. *International Journal of Environmental Research and Public Health* **16**: 1–7.

Faraway JJ and Jhun M (1990) Bootstrap choice of bandwidth for density estimation. *Journal of the American Statistical Association* **85**: 1119–1122.

Fedtke C, Ehrmann K and Holden BA (2009) A review of peripheral refraction techniques. *Optometry and Vision Science* **86**: 429–446.

Felius J, Fu VLN, Birch EE, Hertle RW, Jost RM and Subramanian V (2011) Quantifying nystagmus in infants and young children: Relation between foveation and visual acuity deficit. *Investigative Ophthalmology and Visual Science* **52**: 8724–8731.

Fitzmaurice K and Lesley T (1987) Visual acuity is not the bottom line: some techniques of visual rehabilitation. *Australian Orthoptic Journal* **24**: 23–25.

Fogt N, Toole AJ and Rogers DL (2016) A review of proximal inputs to the near response. *Clinical and Experimental Optometry* **99**: 30–38.

Galvez-Ruiz A, Galindo-Ferreiro A and Lehner A (2021) A new gene mutation in a family with idiopathic infantile nystagmus. *Saudi Journal of Ophthalmology* **35**: 61–65.

Glasser A (2011) Accommodation. In: *Adler's physiology of the eye*. 11th ed. Edingburg: Saunders/Elsevier, p. 795.

González EG, Teichman J, Lillakas L, Markowitz SN and Steinbach MJ (2006) Fixation stability using radial gratings in patients with age-related macular degeneration. *Canadian Journal of Ophthalmology* **41**: 333–339.

González EG, Wong AMF, Niechwiej-Szwedo E, Tarita-Nistor L and Steinbach MJ (2012) Eye position stability in amblyopia and in normal binocular vision. *Investigative Ophthalmology and Visual Science* **53**: 5386–5394.

Gottlob I and Proudlock FA (2014) Aetiology of infantile nystagmus. *Current Opinion in Neurology* **27**: 83–91.

Gradstein L, Reinecke RD, Wizov SS, Goldstein HP and Repka MX (1997) Congenital periodic alternating nystagmus: Diagnosis and management. *Ophthalmology* **104**: 918–929.

Gresty M, Page N and Barratt H (1984) The differential diagnosis of congenital nystagmus. *Journal of Neurology, Neurosurgery and Psychiatry* **47**: 936–942.

Han SJ, Guo Y, Granger-Donetti B, Vicci VR and Alvarez TL (2010) Quantification of heterophoria and phoria adaptation using an automated objective system compared to clinical methods. *Ophthalmic and Physiological Optics* **30**: 95–107.

Hanselman D (2012) *Extract contour data from contour matrix C - File Exchange - MATLAB Central* [Online]. Available at: https://uk.mathworks.com/matlabcentral/fileexchange/38863-extract-contour-data-from-contour-matrix-c [Accessed: 21 May 2023].

Harrar V, Le Trung WL, Malienko A and Khan AZ (2018) A nonvisual eye tracker calibration method for video-based tracking. *Journal of Vision* **18**: 1–11.

Harris CM (1995) Problems in modelling congenital nystagmus: Towards a new model. In: *Studies in visual information processing*. Elsevier Masson SAS, pp. 239–253.

Harris CM, Waddington J and Erichsen JT (2012) 'Infantile nystagmus: an adaptationist approach' in The Challenge of Nystagmus. In: Harris C, Gottlob I, and Sanders J eds. *Nystagmus Network Research Workshop, Abingdon, UK*. The Nystagmus Network: Cardiff, UK, pp. 27–48.

Harrison JJ, Sumner P, Dunn MJ, Erichsen JT and Freeman TCA (2015) Quick phases of infantile nystagmus show the saccadic inhibition effect. *Investigative Ophthalmology and Visual Science* **56**: 1594–1600.

Hertle RW and Ahmad A (2019) Clinical and electrophysiological results of eye muscle surgery in 17 patients with downbeat nystagmus. *Indian Journal of Ophthalmology* **67**: 109–115.

Hertle RW and Dell'Osso LF (1999) Clinical and ocular motor analysis of congenital nystagmus in infancy. *Journal of the American Association for Pediatric Ophthalmology and Strabismus* **3**: 70–79.

Hertle RW, Dell'Osso LF, FitzGibbon EJ, Thompson D, Yang D and Mellow SD (2003) Horizontal rectus tenotomy in patients with congenital nystagmus: Results in 10 adults. *Ophthalmology* **110**: 2097–2105.

Hertle RW, Maldanado VK, Maybodi M and Yang D (2002) Clinical and ocular motor analysis of the infantile nystagmus syndrome in the first 6 months of life. *The British Journal of Ophthalmology* **86**: 670–675.

Hessels RS and Hooge ITC (2019) Eye tracking in developmental cognitive neuroscience – The good, the bad and the ugly. *Developmental Cognitive Neuroscience* **40**: 1–11.

Hirsh M, Alpern M and Schultz H (1948) The variation of phoria with age. *American Journal of Optometry and Archives of American Academy of Optometry* **25**: 535–541.

Holmqvist K and Blignaut P (2020) Small eye movements cannot be reliably measured by video-based P-CR eye-trackers. *Behavior Research Methods* **52**: 2098–2121.

Holmqvist K, Nyström M, Andersson R, Dewhurst R, Jarodzka H and van de Weijer J (2011) *Eye tracking: A comprehensive guide to methods and measures*. Oxford: Oxford University Press, UK.

Holmqvist K, Örbom SL, Hooge ITC, Niehorster DC, Alexander RG, Andersson R, Benjamins JS, Blignaut P, Brouwer AM, Chuang LL, Dalrymple KA, Drieghe D, Dunn MJ, Ettinger U, Fiedler S, Foulsham T, van der Geest JN, Hansen DW, Hutton SB, Kasneci E, Kingstone A, Knox PC, Kok EM, Lee H, Lee JY, Leppänen JM, Macknik S, Majaranta P, Martinez-Conde S, Nuthmann A, Nyström M, Orquin JL, Otero-Millan J, Park SY, Popelka S, Proudlock F, Renkewitz F, Roorda A, Schulte-Mecklenbeck M, Sharif B, Shic F, Shovman M, Thomas MG, Venrooij W, Zemblys R and Hessels RS (2022) Eye tracking: empirical foundations for a minimal reporting guideline. *Behavior Research Methods 2022* **32**: 1–53.

Horwood AM and Riddell PM (2008) The use of cues to convergence and accommodation in naïve, uninstructed participants. *Vision Research* **48**: 1613–1624.

Hung GK and Semmlow JL (1980) Static behavior of accommodation and vergence: Computer simulation of an interactive dual-feedback system. *IEEE Transactions on Biomedical Engineering* **BME-27**: 439–447.

Hung GK, Zhu H and Ciuffreda KJ (1997) Convergence and divergence exhibit different response characteristics to symmetric stimuli. *Vision Research* **37**: 1197–1205.

Hvid K, Nissen KR, Bayat A, Roos L, Grønskov K and Kessel L (2020) Prevalence and causes of infantile nystagmus in a large population-based Danish cohort. *Acta Ophthalmologica* **98**: 506–513.

Jones P (2011) The impact of stress on visual function in nystagmus. PhD thesis, Cardiff University.

Jones PH, Harris CM, Margaret Woodhouse J, Margrain TH, Ennis FA and Erichsen JT (2013) Stress and visual function in infantile nystagmus syndrome. *Investigative Ophthalmology and Visual Science* **54**: 7943–7951.

Kasthurirangan S and Glasser A (2005) Characteristics of pupil responses during far-to-near and near-to-far accommodation. *Ophthalmic and Physiological Optics* **25**: 328–339.

Klier EM, Meng H and Angelaki DE (2011) Revealing the kinematics of the oculomotor plant with tertiary eye positions and ocular counterroll. *Journal of Neurophysiology* **105**: 640–649.

Ko HK, Poletti M and Rucci M (2010) Microsaccades precisely relocate gaze in a high visual acuity task. *Nature Neuroscience* **13**: 1549–1553.

Kraft SP and Irving EL (2004) A case of different null zones for distance and near fixation. *American Orthoptic Journal* **54**: 102–111.

Krauzlis RJ (2013) Eye movements. In: *Fundamental Neuroscience*. 4th ed. Elsevier, pp. 697–714.

Krishnan V., Farazian F and Stark L (1973) An analysis of latencies and prediction in the fusional vergence system. *American Journal of Optometry and Archives of American Academy of Optometry* **50**: 933–939.

Kulke L (2015) Cortical mechanisms of visual attention in typically developing infants and adults. Doctoral thesis: University College London.

Kumar A, Gottlob I, Mclean RJ, Thomas S, Thomas MG and Proudlock FA (2011) Clinical and oculomotor characteristics of albinism compared to FRMD7 associated infantile nystagmus. *Investigative Ophthalmology and Visual Science* **52**: 2306–2313.

Kumar G and Chung STL (2014) Characteristics of fixational eye movements in people with macular disease. *Investigative Ophthalmology and Visual Science* **55**: 5125–5133.

Kushner BJ (2000) The usefulness of the cervical range of motion device in the ocular motility examination. *Archives of Ophthalmology* **118**: 946–950.

Labhishetty V, Bobier WR and Lakshminarayanan V (2019) Is 25 Hz enough to accurately measure a dynamic change in the ocular accommodation? *Journal of Optometry* **12**: 22–29.

Lee J (2002) Surgical management of nystagmus. *Journal of the Royal Society of Medicine*

95: 238–241.

Leek MR (2001) Origins of adaptive psychophysical procedures. *Perception and Psychophysics* **63**: 1279–1292.

Leigh RJ and Zee DS (2015) *The Neurology of eye movements*. Oxford University Press.

Levitt H (1971) Transformed up-down methods in psychoacoustics. *The Journal of the Acoustical Society of America* **49**: 467–477.

Li J, Lam CSY, Yu M, Hess RF, Chan LYL, Maehara G, Woo GC and Thompson B (2010) Quantifying sensory eye dominance in the normal visual system: A new technique and insights into variation across traditional tests. *Investigative Ophthalmology and Visual Science* **51**: 6875–6881.

Liu B, Zhao QC, Ren YY, Wang QJ and Zheng XL (2018) An elaborate algorithm for automatic processing of eye movement data and identifying fixations in eye-tracking experiments. *Advances in Mechanical Engineering* **10**: 1–15.

Love J, Selker R, Marsman M, Jamil T, Dropmann D, Verhagen J, Ly A, Gronau QF, Šmíra M, Epskamp S, Matzke D, Wild A, Knight P, Rouder JN, Morey RD and Wagenmakers EJ (2019) JASP: Graphical statistical software for common statistical designs. *Journal of Statistical Software* **88**: 1–17.

Mack DJ, Belfanti S and Schwarz U (2017) The effect of sampling rate and lowpass filters on saccades – A modeling approach. *Behavior Research Methods* **49**: 2146–2162.

Martinez-Conde S, Macknik SL, Troncoso XG and Dyar TA (2006) Microsaccades counteract visual fading during fixation. *Neuron* **49**: 297–305.

Maybodi M (2003) Infantile-onset nystagmus. *Current Opinion in Ophthalmology* **14**: 276–285.

McIlreavy L (2016) Fixational and pursuit eye movements in infantile nystagmus: oculomotor control and perception. PhD thesis, Cardiff University.

McIlreavy L, Freeman TCA and Erichsen JT (2020) Two-dimensional analysis of horizontal and vertical pursuit in infantile nystagmus reveals quantitative deficits in accuracy and precision. *Investigative Ophthalmology and Visual Science* **61**: 1–12.

McIlreavy L, Freeman TCA and Erichsen JT (2019) Two-dimensional analysis of smooth pursuit eye movements reveals quantitative deficits in precision and accuracy. *Translational Vision Science and Technology* **8**: 1–17.

McIlreavy L, Nedelchev VV and Ennis FA (2022) Two-dimensional eye velocity distributions of foveal fixation at different gaze angles. *Investigative Ophthalmology and Visual Science* **63**: 2774–A0309.

McLean R, Proudlock F, Thomas S, Degg C and Gottlob I (2007) Congenital nystagmus: Randomized, controlled, double-masked trial of memantine/gabapentin. *Annals of Neurology* **61**: 130–138.

McSorley E, Gilchrist ID and McCloy R (2019a) The programming of sequences of saccades. *Experimental Brain Research* **237**: 1009–1018.

McSorley E, Gilchrist ID and McCloy R (2019b) The role of fixation disengagement in the parallel programming of sequences of saccades. *Experimental Brain Research* **237**: 3033–3045.

Meiusi RS, Lavoie JD and Summers CG (1993) The effect of grating orientation on resolution acuity in patients with nystagmus. *Journal of Pediatric Ophthalmology and Strabismus* **30**: 259–261.

Mestre C, Otero C, Díaz-Doutón F, Gautier J and Pujol J (2018) An automated and objective cover test to measure heterophoria. *PLoS ONE* **13**: 1–21.

Mordi JA and Ciuffreda KJ (1998) Static aspects of accommodation: age and presbyopia. *Vision Research* **38**: 1643–1653.

Morgan MW (1980) The maddox classification of vergence eye movements. *Optometry and Vision Science* **57**: 537–539.

Murphy WK and Laskin DM (1990) Intercanthal and interpupillary distance in the black population. *Oral Surgery, Oral Medicine, Oral Pathology* **69**: 676–680.

Nash DL, Diehl NN and Mohney BG (2017) Incidence and types of pediatric nystagmus. *American Journal of Ophthalmology* **182**: 31–34.

von Noorden GK and Campos EC (2002) *Binocular vision and ocular motility: Theory and management of strabimus*. 6th ed. St. Louis, Missouri: Mosby, Inc USA.

Della Osso L, Gauthier G, Liberman G and Stark L (1972) Eye movement recordings as a diagnostic tool in a case of congenital nystagmus. *Optometry and Vision Science* **49**: 3–13.

Otero-Millan J, Macknik SL and Martinez-Conde S (2014) Fixational eye movements and binocular vision. *Frontiers in Integrative Neuroscience* **8**: 1–10.

Papageorgiou E, McLean RJ and Gottlob I (2014) Nystagmus in childhood. *Pediatrics and Neonatology* **55**: 341–351.

Pfeuffer K, Vidal M, Turner J, Bulling A and Gellersen H (2013) Pursuit calibration: Making gaze calibration less tedious and more flexible. *UIST 2013 - Proceedings of the 26th Annual ACM Symposium on User Interface Software and Technology* 261–269.

Poletti M, Listorti C and Rucci M (2013) Microscopic eye movements compensate for nonhomogeneous vision within the fovea. *Current Biology* **23**: 1691–1695.

Radhakrishnan H and Charman WN (2008) Peripheral refraction measurement: does it matter if one turns the eye or the head? *Ophthalmic and Physiological Optics* **28**: 73–82.

Ratnam K, Domdei N, Harmening WM and Roorda A (2017) Benefits of retinal image motion at the limits of spatial vision. *Journal of Vision* **17**: 1–11.

Raveendran RN, Bobier WR and Thompson B (2019) Binocular vision and fixational eye movements. *Journal of Vision* **19**: 1–15.

Raveendran RN, Krishnan AK, Thompson B and Raveendran. RN (2020) Reduced fixation stability induced by peripheral viewing does not contribute to crowding. *Journal of Vision* **20**: 1–13.

Rice ML, Leske DA, Smestad CE and Holmes JM (2008) Results of ocular dominance testing depend on assessment method. *Journal of the American Association for Pediatric Ophthalmology and Strabismus* **12**: 365–369.

Robb RM (1972) Periodic alternation of null point in congenital nystagmus. *Archives of Ophthalmology* **87**: 169–173.

Robinson DA (1981) The use of control systems analysis in the neurophysiology of eye movements. *Annals Review in Neuroscience* **4**: 463–503.

Rucci M (2008) Fixational eye movements, natural image statistics, and fine spatial vision. *Network: Computation in Neural Systems* **19**: 253–285.

Rucci M, Iovin R, Poletti M and Santini F (2007) Miniature eye movements enhance fine spatial detail. *Nature* **447**: 851–855.

Rucci M and Poletti M (2015) Control and functions of fixational eye movements. *Annual Review of Vision Science* **1**: 499–518.

Sanchez K and Rowe FJ (2018) Role of neural integrators in oculomotor systems: a systematic narrative literature review. *Acta Ophthalmologica* **96**: e111–e118.

Sarvananthan N, Surendran M, Roberts EO, Jain S, Thomas S, Shah N, Proudlock FA, Thompson JR, Mclean RJ, Degg C, Woodruff G and Gottlob I (2009) The prevalence of nystagmus: The Leicestershire nystagmus survey. *Investigative Ophthalmology and Visual Science* **50**: 5201–5206.

Schlauch RS and Rose RM (1990) Two-, three-, and four-interval forced-choice staircase procedures: Estimator bias and efficiency. *The Journal of the Acoustical Society of America* **88**: 732–740.

Schor CM (1992) A dynamic model of cross-coupling between accomodation and convergence: Simulations of step and frequency responses. *Optometry and Vision Science* **69**: 258–269.

Seidemann A, Schaeffel F, Guirao A, Lopez-Gil N and Artal P (2002) Peripheral refractive errors in myopic, emmetropic, and hyperopic young subjects. *Journal of the Optical Society of America A* **19**: 2363–2373.

Self JE, Dunn MJ, Erichsen JT, Gottlob I, Griffiths HJ, Harris C, Lee H, Owen J, Sanders J, Shawkat F, Theodorou M, Whittle JP, Arblaster GE, Bjerre A, Dunn MJ, Erichsen JT, Gottlob I, Griffiths HJ, Harris C, Lee H, McIlreavy L, Owen J, Sanders J, Self JE, Shawkat F, Theodorou M, Whittle JP, Osborne D, Ranger M, Norman C, MacKenzie K, Venturi N, Tailor V, Proudlock F, McLean R, Thomas M, Sheth V and Carter P (2020) Management of nystagmus in children: a review of the literature and current practice in UK specialist services. *Eye* **34**: 1515–1534.

Semmlow J and Wetzel P (1979) Dynamic contributions of the components of binocular vergence. *Journal of the Optical Society of America* **69**: 639–645.

Serra A, Dell'Osso LF, Jacobs JB and Burnstine RA (2006) Combined gaze-angle and vergence variation in infantile nystagmus: Two therapies that improve the high-visual-acuity field and methods to measure it. *Investigative Ophthalmology and Visual Science* **47**:

2451–2460.

Shah N, Dakin SC, Redmond T and Anderson RS (2011) Vanishing optotype acuity: Repeatability and effect of the number of alternatives. *Ophthalmic and Physiological Optics* **31**: 17–22.

Shaikh AG, Wong AL, Zee DS and Jinnah HA (2013) Keeping your head on target. *Journal of Neuroscience* **33**: 11281–11295.

Shallo-Hoffmann J, Faldon M and Tusa RJ (1999) The incidence and waveform characteristics of periodic alternating nystagmus in congenital nystagmus. *Investigative Ophthalmology and Visual Science* **40**: 2546–2553.

Shallo-Hoffmann J and Riordan-Eva P (2001) Recognizing periodic alternating nystagmus. *Strabismus* **9**: 203–215.

Shaunak S, O'Sullivan E and Kennard C (1995) Eye Movements. *Journal of Neurology Neurosurgery and Psychiatry* **59**: 115–125.

Shawkat FS, Kriss A, Thompson D, Russell-Eggitt I, Taylor D and Harris C (2000) Vertical or asymmetric nystagmus need not imply neurological disease. *British Journal of Ophthalmology* **84**: 175–180.

Shirama A, Kanai C, Kato N and Kashino M (2016) Ocular fixation abnormality in patients with autism spectrum disorder. *Journal of Autism and Developmental Disorders* **46**: 1613–1622.

Simmers AJ, Gray LS and Winn B (1999) The effect of abnormal fixational eye movements upon visual acuity in congenital nystagmus. *Current Eye Research* **18**: 194–202.

Simonsz HJ and Den Tonkelaar I (1990) 19th Century mechanical models of eye movements, Donders' law, Listing's law and Helmholtz' direction circles. *Documenta Ophthalmologica* **74**: 95–112.

Skavenski AA and Steinman RM (1970) Control of eye position in the dark. *Vision Research* **10**: 193–198.

Southall JPC and von Helmholts H (1925) Helmholtz's treatise on physiological optics, translated from the third German edition. Vol. I by James P. C. Southall and Helmholtz. *The American Journal of Psychology* **36**: 305.

Spauschus A, Marsden J, Halliday DM, Rosenberg JR and Brown P (1999) The origin of ocular microtremor in man. *Experimental Brain Research* **126**: 556–562.

SR Research Ltd. (2014) *EyeLink ® 1000 Plus User Manual 1.0.12*.

Sreenivasan V, Babinsky EE, Wu Y and Candy TR (2016) Objective measurement of fusional vergence ranges and heterophoria in infants and preschool children. *Investigative Ophthalmology and Visual Science* **57**: 2678–2688.

Steinman RM (1965) Effect of target Size, luminance and color on monocular fixation. *Journal of the Optical Society of America* **55**: 1159–1165.

Steinman RM, Haddad GM, Skavenski AA and Wyman D (1973) Miniature eye movement.

Science **181**: 810–819.

Suppiej A, Ceccato C, Lonardi V and Reffo ME (2022) Infantile nystagmus without overt eye abnormality: Early features and neuro-ophthalmological diagnosis. *Developmental Medicine & Child Neurology* **00**: 1–7.

Suryakumar R, Meyers JP, Irving EL and Bobier WR (2007) Application of video-based technology for the simultaneous measurement of accommodation and vergence. *Vision Research* **47**: 260–268.

Tarpey P, Thomas S, Sarvananthan N, Mallya U, Lisgo S, Talbot CJ, Roberts EO, Awan M, Surendran M, McLean RJ, Reinecke RD, Langmann A, Lindner S, Koch M, Jain S, Woodruff G, Gale RP, Degg C, Droutsas K, Asproudis I, Zubcov AA, Pieh C, Veal CD, MacHado RD, Backhouse OC, Baumber L, Constantinescu CS, Brodsky MC, Hunter DG, Hertle RW, Read RJ, Edkins S, O'Meara S, Parker A, Stevens C, Teague J, Wooster R, Futreal PA, Trembath RC, Stratton MR, Raymond FL and Gottlob I (2006) Mutations in a novel member of the FERM family, FRMD7 cause X-linked idiopathic congenital nystagmus (NYS1). *Nature Genetics* **38**: 1242–1244.

Thaler L, Schütz AC, Goodale MA and Gegenfurtner KR (2013) What is the best fixation target? The effect of target shape on stability of fixational eye movements. *Vision Research* **76**: 31–42.

Theodorou M and Clement R (2016) Classification of infantile nystagmus waveforms. *Vision Research* **123**: 20–25.

Thomas MG, Gottlob I, McLean RJ, Maconachie G, Kumar A and Proudlock FA (2011) Reading strategies in infantile nystagmus syndrome. *Investigative Ophthalmology and Visual Science* **52**: 8156–8165.

Thurtell MJ and Leigh RJ (2012) Treatment of nystagmus. *Current Treatment Options in Neurology* **14**: 60–72.

Ukwade MT and Bedell HE (1992) Variation of congenital nystagmus with viewing distance. *Optometry and Vision Science* **69**: 976–985.

Vancleef K, Read JCA, Herbert W, Goodship N, Woodhouse M and Serrano-Pedraza I (2018) Two choices good, four choices better: For measuring stereoacuity in children, a four-alternative forced-choice paradigm is more efficient than two. *PLoS ONE* **13**: 1–15.

Vieira da Costa ACR, Lopes MCB and Nakanami CR (2014) Influence of head posture on the visual acuity of children with nystagmus. *Arquivos Brasileiros de Oftalmologia* **77**: 8–11.

Wang ZI and Dell'Osso LF (2007) Being 'slow to see' is a dynamic visual function consequence of infantile nystagmus syndrome: Model predictions and patient data identify stimulus timing as its cause. *Vision Research* **47**: 1550–1560.

Wetherill GB and Levitt H (1965) Sequential estimation of points on a psychometric function. *British Journal of Mathematical and Statistical Psychology* **18**: 1–10.

Whittaker SG, Budd J and Cummings RW (1988) Eccentric fixation with macular scotoma. *Investigative Ophthalmology and Visual Science* **29**: 268–278.

Wiggins D, Woodhouse JM, Margrain TH, Harris CM and Erichsen JT (2007) Infantile nystagmus adapts to visual demand. *Investigative Ophthalmology and Visual Science* **48**: 2089–2094.

Wooding S, Byford J, Nedelchev V, Ennis FA and McIlreavy L (2023) Optical defocus and viewing condition reduce the precision of fixational eye movements. *ARVO Abstract*

Yang Q, Bucci MP and Kapoula Z (2002) The latency of saccades, vergence, and combined eye movements in children and in adults. *Investigative Ophthalmology and Visual Science* **43**: 2939–2949.

Yang Q, Le T-T and Kapoula Z (2009) Aging effects on the visually driven part of vergence movements. *Investigative Opthalmology and Visual Science* **50**: 1145.

Zahidi AAA (2019) Characteristics and impact of nystagmus on visual acuity and eye movements in children with and without Down's syndrome. PhD Thesis, Cardiff University.

8

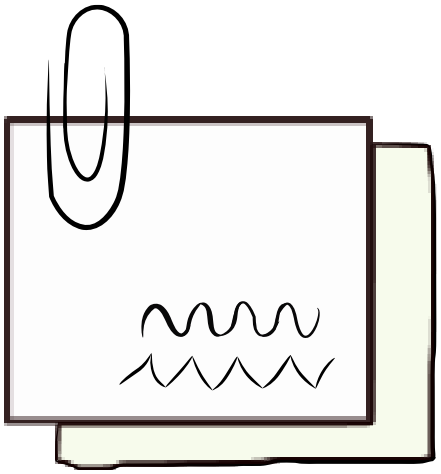

8.1 Participant details

Table 8-1: Clinical details from 18 participants with IN

ID	Associations	Age/Sex	VA (logMAR)	Ocular alignment @near	Ocular dominance	IPD (mm)	Null zone	Convergence null?	Lens prescription	VA with prescription	Prescription used for: Gaze angle experiement-1, Convergence experiment-2
IN02	Idiopathic	65/M	RE: LE: 1.08	Ortho	LE	68	Right gaze	False	RE: -14.50/-2.25 x 65 LE: -11.25/-3.25 x 90 Add: +4.00 DS	RE: 0.16 LE: 0.12	False
IN03	Idiopathic	69/M	RE: 0.74 LE: 0.86	Alt SOT	RE	68	Left gaze	False	RE: -3.00/-1.25 x 150 LE: -3.75/-1.50 x 160 Add: +8.25 DS	RE: 0.76 LE: 0.76	False
IN05	Idiopathic	37/M	RE: 0.38 LE: 0.48	L SOT	RE	66	PP, up gaze	False	RE: +3.50/-3.25 x 155 LE: +3.50/-3.25 x 30	RE: 0.32 LE: 0.42	False
IN06	Idiopathic	30/F	RE: 0.26 LE: 0.52	XOP	RE	62	Right gaze	False	RE: -1.75/-0.50 x 140 LE: -2.75/-1.50 x 10	RE: 0.04 LE: 0.12	False
IN07	Idiopathic	57/F	RE: 0.68 LE: 0.60	XOP	LE	64	Right gaze	False	RE: +6.00-3.50 x 172 LE: +6.25-3.25 x 15 Add: + 1.75 DS	RE: 0.66 LE: 0.44	False
IN08	Idiopathic	26/F	RE: 0.10 LE: 0.12	Ortho	RE	62	Left gaze	True	RE: -0.25-0.25 x 20 LE: +0.50-0.75 x 50	RE: 0.10 LE: 0.12	False
IN09	Mild ocular albinism	26/M	RE: 1.04 LE: 1.22	XOP	RE	66	Right gaze	True	RE: -4.25 LE: -5.25	RE: 0.26 LE: 0.30	True, 2 CL

ID	Associations	Age/Sex	VA (logMAR)	Ocular alignment	Ocular dominance	IPD (mm)	Null zone	Convergence null?	Lens prescription	VA with prescription	Prescription used for: Gaze angle experiement-1, Convergence experiment-2
IN10	Congenital	29/M	RE: 1.04 LE: 0.90	Alt XOT	Equal	66	Right gaze, RE Left gaze, LE	True	RE: -4.00/-2.75 x 77 LE:-3.75/-4.00 x 95	RE: 0.34 LE: 0.34	False
IN11	Congenital, rotatory	63/M	RE: 1.02 LE: 1.30	Alt XOT	RE	65	PP	True	RE: -7.50-1.00 x 35 LE: -10.75-1.25 x 25 Add:+3.50	RE: 0.52 LE: 0.63	Spectacles, 2
IN12	Congenital	61/F	RE: 1.38 LE: 1.38	XOP	RE	70	PP	False	RE:-2.75 DS LE: -4.00/-1.00 x 90	RE: 1.06 LE: 1.06	False
IN13	Oculocutaneous albinism	66/F	RE: 1.08 LE: 0.86	Ortho	LE	67	PP	False	RE: -5.00/-1.50 x 25 LE: -4.50/-2.50 x 180 Add: +4.00 DS	RE: 0.74 LE: 0.64	False
IN16	Idiopathic	64/F	RE: 1.04 LE: 1.00	XOP	LE	57	PP; R=L	False	RE: -3.50/-1.50 x 40 LE: -1.25/-5.00 x 70 2ΔBO Add: +3.00 DS	RE: 0.74 LE: 0.70	False
IN17	Idiopathic. Movement appears more in LE than RE	58/F	RE: 0.62 LE: 0.22	Ortho	LE	65	PP, broad RE: PP and right gaze LE: PP, R=L	False	RE: -2.00/-1.00 x 85 LE: +0.25/-1.50 x 75 Add: +2.25 DS	RE: 0.20 LE: 0.16	False

ID	Associations	Age/Sex	VA (logMAR)	Ocular alignment	Ocular dominance	IPD (mm)	Null zone	Convergence null?	Lens prescription	VA with prescription	Prescription used for: Gaze angle experiement-1, Convergence experiment-2
IN18	Congenital	35/M	RE: 0.60 LE: 0.44	Ortho	LE	68	PP, broad. RE: R>L LE: L>R	False	RE: +0.50 DS LE: ∞	RE: 0.54 LE: 0.44	False
IN19	Congenital	57/M	RE: 0.52 LE: 1.00	Ortho	LE	65	LE: slightly R of PP RE: R>L	True	RE: +12.00 DS LE: +5.00 DS	RE: 0.46 LE: 0.44	CL, 1 and 2
IN20	OCA2	49/F	RE: 0.64 LE: 0.42	SOP	LE	68	PP	True	RE: -1.00-1.75 x 90 LE: -0.75-1.75 x 90	RE: 0.48 LE: 0.42	CL, 2
IN21	OCA2	58/M	RE: 0.50 LE: 0.46	SOP	RE	65	Slightly in L. R>L	False	RE: +3.25/-1.00 x 180 LE: +2.00/-1.00 x 180 Add: +3.00 DS	RE: 0.34 LE: 0.34	False
IN22	Ocular albinism	20/F	RE: 0.66 LE: 0.52	SOP	LE	64	Central to L, broad. R>L	False	RE: +3.25/-3.50 x 20 LE: +0.75/-2.75 x 175	RE: 0.64 LE: 0.42	False

R = right gaze, L = left gaze, RE = right eye, LE = left eye, Alt = alternating, SOT = Esotropia, XOT = Exotropia, SOP = Esophoria, XOP = Exophoria, Ortho = Orthophoria, CL = contact lens, OCA = Oculocutaneous albinism, PP = primary position.

Table 8-2: Clinical details from 14 typical participants

ID	Age/Sex	VA (logMAR)	Ocular alignment	Ocular dominance	IPD (mm)	Lens prescription	VA with prescription	Prescription used for: Gaze angle experiement-1, Convergence experiment-2
C01	25/F	RE: -0.30 LE: -0.30	Ortho	RE	67	RE: - LE: -	RE: - LE: -	False
C02	27/F	RE: -0.12 LE: -0.14	Ortho	LE	62	RE: - LE: -	RE: - LE: -	False
C03	24/F	RE: 1.04 LE: 1.04	Ortho	LE	62	RE: -5.75 DS LE: -5.75 DS	RE: -0.14 LE: -0.16	CL, 2
C04	24/F	RE: -0.18 LE: 0.00	Ortho	LE	65	RE: - LE: -	RE: - LE: -	False
C05	29/F	RE: -0.26 LE: -0.26	Ortho	LE	62	RE: - LE: -	RE: - LE: -	False
C06	26/F	RE: -0.24 LE: -0.20	Ortho	RE	58	RE: - LE: -	RE: - LE: -	False
C08	25/M	RE: 0.50 LE: 0.50	Ortho	LE	65	RE: -2.25 DS LE: -2.50 DS spectacles	RE: -0.3 LE: -0.3	False
C09	26/F	RE: 0.10 LE: 0.10	Ortho	RE	62	RE: -0.75 DS LE: -0.75 DS spectacles	RE: -0.16 LE: -0.16	False
C10	25/M	RE: 0.92 LE: 0.92	XOP	RE	62	RE: -6.50/-0.50 x 170 LE: -5.75/-0.75 x 170 spectacles	RE: -0.22 LE: -0.22	False

ID	Age/Sex	VA (logMAR)	Ocular alignment	Ocular dominance	IPD (mm)	Lens prescription	VA with prescription	Prescription used for: Gaze angle experiement-1, Convergence experiment-2
C11	30/M	RE: 1.08 LE: 1.08	XOP	RE	67	RE: -5.50/-1.00 x 15 LE: -5.50/-0.50 x 10	RE: -0.1 LE: 0.04	CL, 2
C12	33/F	RE: -0.10 LE: -0.10	Ortho	RE	63	RE: - LE: -	RE: - LE: -	False
C13	20/M	RE: -0.16 LE: -0.26	Ortho	RE	67	RE: - LE: -	RE: - LE: -	False
C14	39/M	RE: -0.20 LE: -0.20	Ortho	RE	71	RE: - LE: -	RE: - LE: -	False
C15	39/F	RE: -0.10 LE: -0.10	Ortho	RE	66	RE: - LE: -	RE: - LE: -	False

R = right gaze, L = left gaze, RE = right eye, LE = left eye, Alt = alternating, SOP = Esophoria, XOP = Exophoria, Ortho = Orthophoria, CL = contact lens.

8.2 Additional results

a) Individual plots for insignificant correlations between the isocontour horizontal and vertical axis range - Chapter three. Patient identity can be found on the axes of each plot. H = horizontal, V = vertical

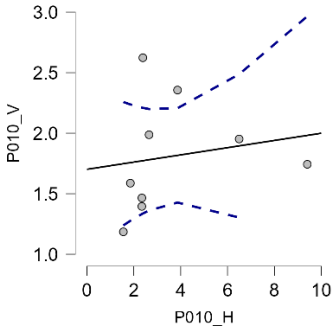

r = 0.167

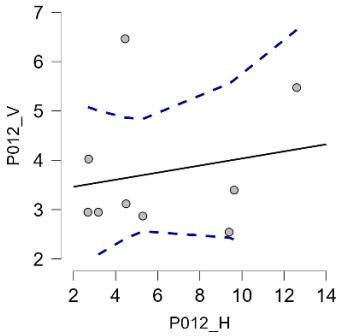

r = 0.191

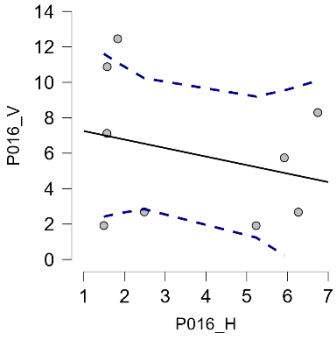

r = -0.276

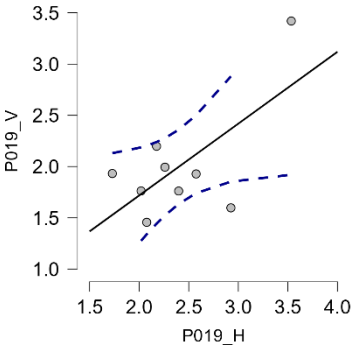

r = 0.663

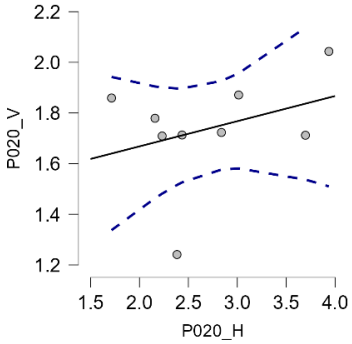

r = 0.336

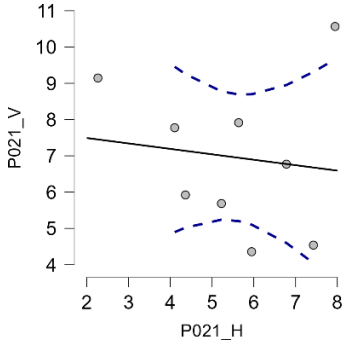

r = -0.128

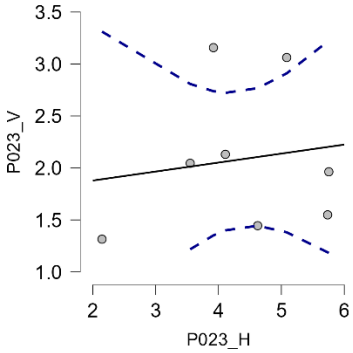

$r = 0.150$

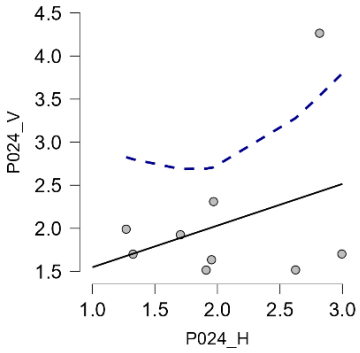

$r = 0.348$

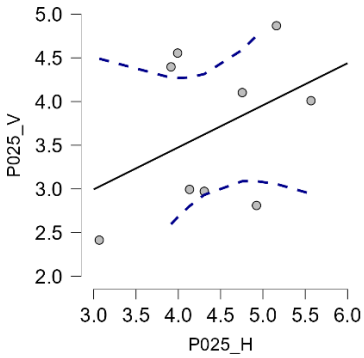

$r = 0.411$

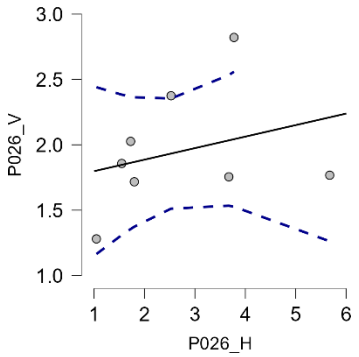

$r = 0.292$

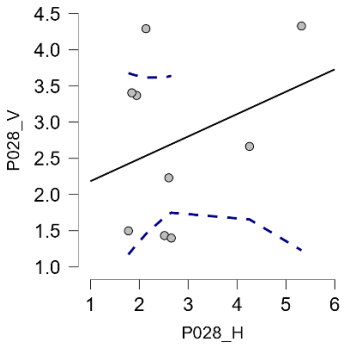

$r = 0.318$

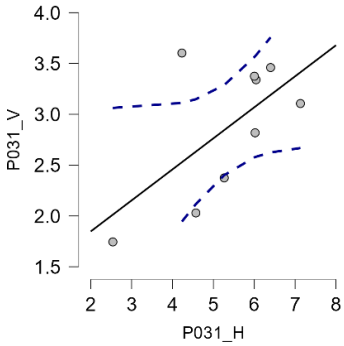

$r = 0.628$

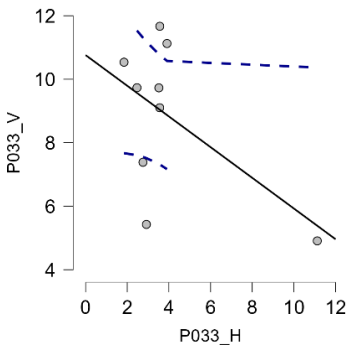

$r = -0.551$

b) Individual plots for insignificant correlations between the isocontour horizontal and vertical axis range - Chapter four. Patient identity can be found on the axes of each plot. H = horizontal, V = vertical

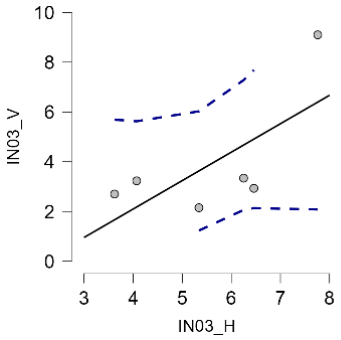

$r = 0.691$

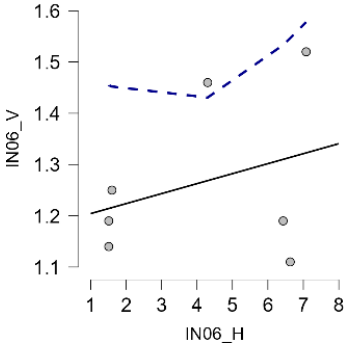

$r = 0.315$

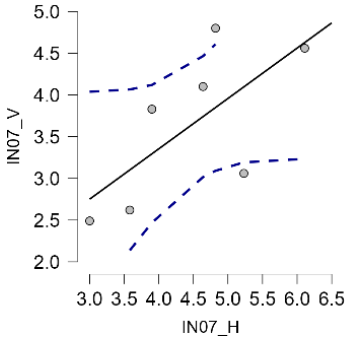

$r = 0.689$

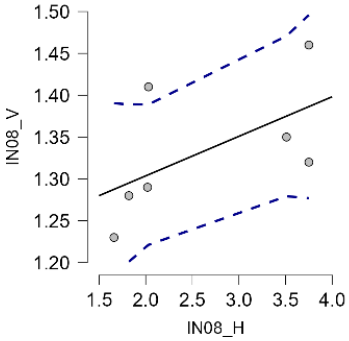

$r = 0.576$

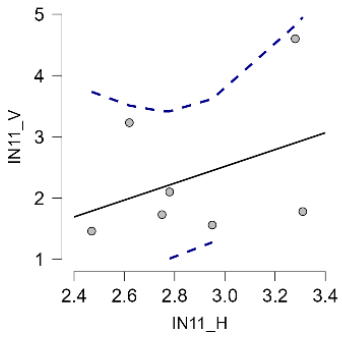

$r = 0.380$

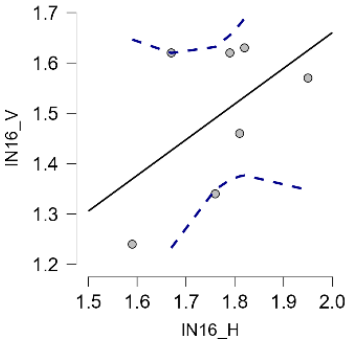

$r = 0.524$

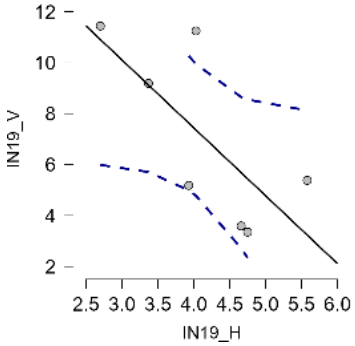

$r = -0.726$

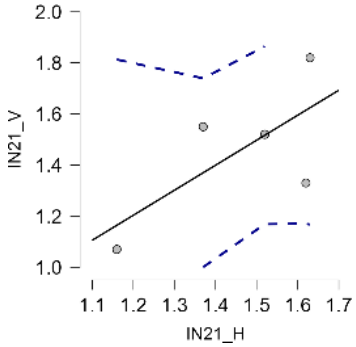

$r = 0.695$

8.3 Research output

Paper

Dunn MJ, Alexander RG, Amiebenomo OM, Arblaster G, Atan G, Erichsen JT, Ettinger U, Giardini ME, Gilchrist ID, Hamilton R, Hessels RS, Hodgins S, Hooge ITC, Jackson BS, Lee H, Macknik SL, Martinez-Conde S, McIlreavy L, Muratori LM, Niehorster DC, Nyström M, Otero-Millan J, Self JE, Singh T, Smyrnis N and Sprenger A (2023). Minimal reporting guideline for research involving eye tracking (2023 edition) *Behaviour Research Methods.* https://doi.org/10.3758/s13428-023-02187-1.

Oral presentations

1. Amiebenomo OM, McIlreavy L, Erichsen JT and Woodhouse JM (2023) Probability Density Function analysis for infantile nystagmus eye movement data. Presented at ResMeet'23, India Vision Institute's 3rd virtual Optometry and Vision Science Research meeting, 22 July.

2. Amiebenomo OM, McIlreavy L, Erichsen JT and Woodhouse JM (2022) Fixation as a function of eye in orbit position. Presented at the Nystagmus Network virtual open day 2022, 1 Oct.

3. Amiebenomo OM, McIlreavy L, Erichsen JT and Woodhouse JM (2022) Fixation performance as a function of convergence and eccentric gaze positions. Presented at the Nystagmus Network research workshop 2022 (virtual), 30 Sept.

4. Amiebenomo OM, McIlreavy L, Erichsen JT and Woodhouse JM (2022) Accuracy and precision of fixation is correlated with gaze angle. Presented at the 21st European Conference on Eye Movement (ECEM), University of Leicester, Leicester, UK, 21 – 25 Aug, 2022.
   Book of abstracts: https://bop.unibe.ch/JEMR/article/view/8878/11862

Poster presentations

1. Amiebenomo OM, McIlreavy L, Erichsen JT and Woodhouse JM (2021) Fixation characteristics at off-gaze positions in typical observers. Presented at the American Academy of Optometrists (AAO) annual meeting, Academy 2021, Boston, USA, 3 – 6 Nov, 2021.
   Abstract: https://aaopt.org/past-meeting-abstract-archives/
   Grant award: The Johnson and Johnson Vision Student Travel Fellowship, $750.

2. Amiebenomo OM, McIlreavy L, Erichsen JT and Woodhouse JM (2021) Effect of viewing distance on fixation characteristics in typical observers. Presented at the Association for Research in Vision and Ophthalmology (ARVO) annual meeting (virtual), 1 – 7 May, 2021.
   Abstract: https://iovs.arvojournals.org/article.aspx?articleid=2776161

3. Amiebenomo OM, McIlreavy L, Erichsen JT and Woodhouse JM (2019) The potential off-axis performance and accuracy of the PowerRef 3 for measurements in nystagmus. Presented at the 28th British Ocular Motor Group (BOMG) meeting and the 24th Applied Vision Association (AVA) Christmas Meeting, Cardiff University, UK, 16 – 17 Dec, 2019.
   Abstract: https://journals.sagepub.com/doi/10.1177/0301006620921389